

AD _____

Award Number: DAMD17-94-J-4417

TITLE: Identifying and Isolating Breast Cancer-Associated Genes on Chromosomes

PRINCIPAL INVESTIGATOR: Thomas B. Shows, Ph.D.

CONTRACTING ORGANIZATION: Health Research, Incorporated
Buffalo, New York 14263

REPORT DATE: October 1999

TYPE OF REPORT: Final

PREPARED FOR: U.S. Army Medical Research and Materiel Command
Fort Detrick, Maryland 21702-5012

DISTRIBUTION STATEMENT: Approved for public release
distribution unlimited

The views, opinions and/or findings contained in this report are those of the author(s) and should not be construed as an official Department of the Army position, policy or decision unless so designated by other documentation.

DTIC QUALITY INSPECTED 8

20010109 070

REPORT DOCUMENTATION PAGE			Form Approved OMB No. 074-0188	
Public reporting burden for this collection of information is estimated to average 1 hour per response, including the time for reviewing instructions, searching existing data sources, gathering and maintaining the data needed, and completing and reviewing this collection of information. Send comments regarding this burden estimate or any other aspect of this collection of information, including suggestions for reducing this burden to Washington Headquarters Services, Directorate for Information Operations and Reports, 1215 Jefferson Davis Highway, Suite 1204, Arlington, VA 22202-4302, and to the Office of Management and Budget, Paperwork Reduction Project (0704-0188), Washington, DC 20503				
1. AGENCY USE ONLY (Leave blank)	2. REPORT DATE October 1999	3. REPORT TYPE AND DATES COVERED Final (01 Oct 94 - 30 Sep 99)		
4. TITLE AND SUBTITLE Identifying and Isolating Breast Cancer-Associated Genes on Chromosomes		5. FUNDING NUMBERS DAMD17-94-J-4417		
6. AUTHOR(S) Thomas B. Shows, Ph.D.				
7. PERFORMING ORGANIZATION NAME(S) AND ADDRESS(ES) Health Research, Incorporated Buffalo, New York 14263 e-mail: tbs@shows.med.buffalo.edu		8. PERFORMING ORGANIZATION REPORT NUMBER		
9. SPONSORING / MONITORING AGENCY NAME(S) AND ADDRESS(ES) U.S. Army Medical Research and Materiel Command Fort Detrick, Maryland 21702-5012		10. SPONSORING / MONITORING AGENCY REPORT NUMBER		
11. SUPPLEMENTARY NOTES				
12a. DISTRIBUTION / AVAILABILITY STATEMENT Approved for public release distribution unlimited			12b. DISTRIBUTION CODE	
13. ABSTRACT (Maximum 200 Words) A region on human chromosome 11 at p15.5 is associated with breast cancer. Metastasis and poor outcome are the cancer phenotypes associated with this region. This is a study to identify the gene(s) responsible in 11p15.5. We have constructed a detailed physical map across the region, participated in sequencing the region, generated a transcript map across the region and have analyzed most of the genes in the region as candidates for tumor suppressor genes. Recently, we reduced the candidate region to 400 kb and found that it contained about 4-6 potential genes. We have cloned and characterized the region. Interestingly, this small 11p15.5 region has now been shown to be associated with at least eight different tumors and the overgrowth Beckwith-Wiedemann syndrome. To complicate this region further, it is also imprinted. We have evidence suggesting preferential 11p15.5 maternal loss in breast tumors demonstrating that breast cancer in this region has an imprinting component. We could not find mutations in a tumor suppressor gene; however, we reported mutations in an imprinting center in this region which likely is the locus responsible for the tumors associated with this chromosomal region. We have cloned the homologous imprinted region from the mouse and are testing for imprinted expression in fetal and adult tissues including mammary gland for breast cancer studies.				
14. SUBJECT TERMS Breast Cancer, Growth Control, Gene Markers, Chromosome 11, Gene Cloning, Diagnosis,			15. NUMBER OF PAGES 90	
			16. PRICE CODE	
17. SECURITY CLASSIFICATION OF REPORT Unclassified	18. SECURITY CLASSIFICATION OF THIS PAGE Unclassified	19. SECURITY CLASSIFICATION OF ABSTRACT Unclassified	20. LIMITATION OF ABSTRACT Limited	

FOREWORD

Opinions, interpretations, conclusions and recommendations are those of the author and are not necessarily endorsed by the U.S. Army.

_____ Where copyrighted material is quoted, permission has been obtained to use such material.

_____ Where material from documents designated for limited distribution is quoted, permission has been obtained to use the material.

_____ Citations of commercial organizations and trade names in this report do not constitute an official Department of Army endorsement or approval of the products or services of these organizations.

_____ In conducting research using animals, the investigator(s) adhered to the "Guide for the Care and Use of Laboratory Animals," prepared by the Committee on Care and use of Laboratory Animals of the Institute of Laboratory Resources, national Research Council (NIH Publication No. 86-23, Revised 1985).

___✓___ For the protection of human subjects, the investigator(s) adhered to policies of applicable Federal Law 45 CFR 46.

___✓___ In conducting research utilizing recombinant DNA technology, the investigator(s) adhered to current guidelines promulgated by the National Institutes of Health.

___✓___ In the conduct of research utilizing recombinant DNA, the investigator(s) adhered to the NIH Guidelines for Research Involving Recombinant DNA Molecules.

_____ In the conduct of research involving hazardous organisms, the investigator(s) adhered to the CDC-NIH Guide for Biosafety in Microbiological and Biomedical Laboratories.



PI - Signature Date 1/18/00

**IDENTIFYING AND ISOLATING BREAST CANCER-ASSOCIATED
GENES ON CHROMOSOME 11**

Table of Contents

Front Cover	1
SF298	2
Foreword	3
Table of Contents	4
Introduction and Rationale	5
Statement of Work	6
Progress Achieved	6-7
Personnel on Grant	8
List of Publications	8-10
Conclusion	11
Report of Inventions and Subcontracts	12
Attachments: Appendices 1-17	

Please Note: Information presented in this Progress Report contains proprietary or unpublished data and should be considered *confidential*.

INTRODUCTION AND RATIONALE

The 11p15.5 chromosomal region was associated with breast cancer by loss of heterozygosity (LOH) studies which involved losing, in tumor tissue, one copy of biallelic genetic markers mapped to the 11p15.5 region. We have reduced this region in 11p15.5 to less than 400 kb between the markers D11S1318 and D11S4088 by examining a larger population of tumor tissues and looking for the smallest LOH region. Our hypothesis was that a single gene in this region, when mutated, would cause breast cancer. We performed the usual genomic experiments and physically mapped the region, constructed both BAC and PAC contigs through the region, generated a transcription map through the region, sequenced the region, identified all the genes in the region and have been analyzing candidate genes for mutations specific to breast cancer. See Appendices for references, results and methodology.

During this exercise, there were published reports outside the breast cancer field that had to be addressed in order to understand the involvement of breast cancer with the 11p15.5 region. It was reported that several additional cancers and the Beckwith-Wiedemann syndrome (BWS; an abnormal growth disorder) were mapped to the identical region by different genetic procedures including LOH. The other tumors mapping to this region were Wilms' tumor, rhabdomyosarcoma, hepatoblastoma, adrenocortical carcinoma, gastric cancer, malignant glioma, bladder carcinoma and ovarian carcinoma. In addition, there was increased risk of breast cancer in mothers of children with rhabdomyosarcoma and BWS. This evidence suggested a single gene associated with all tumors mapping to this region or several genes closely linked, each specific for a different tumor. This second possibility was not considered likely and has been set aside temporarily.

In addition and during this study, this identical region was associated with imprinting and this added complexity has significantly changed the thinking and approaches to explaining the genetics of breast cancer associated with 11p15.5, as well as, the other tumors in this multi-tumor imprinted region.

Abnormalities in an imprinting center and development in this region could very well explain the multitude of tumors and abnormal growth phenotypes associated with this region. For this reason, we have turned our attention to understanding imprinting in 11p15.5. Therefore, we have added another task (Task 7) to this study. That new task was to investigate imprinting in this region and identify an imprinting center in the smallest candidate region. We have found an imprinting center in this region and have shown that mutation does occur at this locus. We are in the process of examining breast tumors to determine if this imprinting center is associated with breast cancer (for references, See Appendices 1-8).

STATEMENT OF WORK

- Task 1. Refining and narrowing the human chromosome 11 region associated with the breast cancer phenotype between genes CALCA and HBB.
- Task 2. Complete a contig across this region.
- Task 3. Identify genes in the implicated region.
- Task 4. Analyze candidate genes for mutations associated with breast cancer.
- Task 5. Examine candidate tumor suppressor genes.
- Task 6. Identify gene markers that can be used for diagnosis.
- Task 7. Investigate the involvement of imprinting in breast cancer and the identification of an imprinting center in the smallest candidate region.

PROGRESS ACHIEVED

- Task 1. Project completed. The region between genes CALCA and HBB (referred to as the original larger region) on human chromosome 11p15.5 has been defined and, in fact, narrowed to only 400 kb (the smaller region defined by LOH). This task was presented in a previous year's progress report and involves physical mapping across the region and determining the smallest region of overlap by loss of heterozygosity (LOH) studies in breast cancer samples (see Figs. 1 & 2 and Appendices 1, 2, 3 and 9 for methodology and maps).
- Task 2. Project completed. A physical map across the 11p15.5 original larger region has been completed and analyzed for verification and integrity. A PAC (P1 artificial chromosome) cloned contig of 700 kb between DNA markers D11S517 and H19 (including the 400 kb smaller candidate region) in the multiple tumor associated region will allow the identification and localization of all genes in the region. See Appendix 1 for methodology and Fig. 1 in Appendix 1 for the mapped contig.
- Task 3. Project completed. Identification of 18 genes in the original larger region has been carried out by cDNA selection and DNA sequencing. This was facilitated by developing a comprehensive transcript map from a large-insert bacterial clone (BAC) contig between markers D11S601 and D11S1318. The transcript map has been published and presented previously. See Appendices 3, 4 and 10 for methodology and maps. Also, see Fig. 1 of Appendix 4 and Fig. 1 of Appendix 3 in that order.

- Task 4. Project completed. Genes in the original larger region have been identified such as CARS, NAP2, IPL, ORCTL2, p57^{KIP2}, KVLQT1, ASCL2, H19, IGF2 and TAPA. See Appendices 2, 3 and 11 for the methodology, maps and genes identified.
- Task 5. Project nearing completion. We continue to analyze genes identified in the candidate region for mutations in breast cancer tissue. No mutations in breast cancer have been found in the above listed genes. We have evidence for 18 genes in the original larger region and are progressing through the remaining few genes. See Appendices 1, 2, 5, 6, and 11 for details and methodologies.
- Task 6. Develop gene markers for diagnosis. This project is nearing completion. We have narrowed the candidate region by LOH studies of breast tumor (See Task 1 and Fig. 1). This region has been reduced to less than 400 kb (the smaller LOH region) located between markers D11S4088 and D11S1318 in the p15.5 region of chromosome 11. The region contains 4-6 transcripts, one of which may act as a tumor suppressor gene. Studies are underway to isolate and characterize these genes. This localization places the chromosomal region associated with breast cancer directly in an imprinting region suggesting an altered imprinting component associated with the breast cancer phenotype rather than a specific tumor suppressor gene defect. While we continue to look for mutations in a specific breast cancer tumor suppressor gene, we have turned our attention to a likely mutation in an imprinting center which we have described in this region that is suggested to be involved in several cancers, including breast. See Appendices 2, 3 and 12 for details and methodology.
- Task 7. Imprinting and breast cancer. Project nearing completion. Our evidence has demonstrated that there is a component of breast cancer that is located on chromosome 11 in the 11p15.5 region, between markers D11S4088 and D11S1318, that is imprinted. Our LOH evidence suggested a preferential maternal loss in tumors which implies that a 11p.15.5 breast cancer tumor suppressor gene is imprinted. This evidence was presented in the last report and also in Appendices 3, 7, 8, 13, 14, 15 and 16. Our evidence indicates that there is an imprinting center in an intron between the 10th and 11th exon of the KVLQT1 gene which appears to regulate this DNA region encoding a breast cancer associated phenotype. Mutants of this imprinting center have been observed, so far, in the Beckwith-Weidemann syndrome (an overgrowth syndrome associated with cancer including breast cancer). Breast cancer patients are being analyzed for mutations at this locus (See Fig. 1 of Appendix 3).

We have turned to the mouse to test this imprinted region further in mammary glands and under experimental conditions. A PAC contig was generated across the homologous chromosomal candidate region on mouse distal chromosome 7.

We have published this map (Fig. 1 of Appendix 8). This homologous mouse region was shown to be imprinted previously and we have confirmed this (Fig. 2 of Appendix 3). Having this region cloned in the mouse gives us the reagents for sequencing, mutagenic studies and analyzing these genes in the mammary gland and studying imprinting and its involvement in breast cancer. These mouse studies are in progress.

LIST OF PERSONNEL RECEIVING PAY

Conroy, Jeffrey
Day, Colleen
Frame, Nancy
Haley, Linda
Henry, W. Michael
Higgins, Michael, J., Ph.D.
Karpenko, Matthew
Kuhn, Nancy
Mayers, Peter
Nowak, Norma J., Ph.D.
Ovak, Donna
Qin, Shizhen, Ph.D.
Shows, Thomas B., Ph.D.
Simpson, Stacey
Zhang, Jialu

PUBLICATIONS

- Appendix 1: Reid, L.H., Davies, C., Cooper, P.R., Crider-Miller, S.J., Sait, S.N.J., Nowak, N.J., Evans, G., Stanbridge, E.J., de Jong, P., Shows, T.B., Weissman, B.E. and Higgins, M.J. 1997. A 1-Mb physical map and PAC contig of the imprinted domain in 11p15.5 that contains the TAPA1 and the BWSCR1/WT2 region. *Genomics* 43: 366-375.
- Appendix 2: Cooper, P.R., Smilnich, N.J., Day, C.D., Nowak, N.J., Reid, L.H., Pearsall, R.S., Reece, M., Prawitt, D., Landers, J., Housman, D.E., Winterpacht, A., Zabel, B.U., Pelletier, J., Weissman, B.E., Shows, T.B. and Higgins, M.J. 1998. Divergently transcribed overlapping genes expressed in liver and kidney and located in the 11p15.5 imprinted domain. *Genomics* 49: 38-51.
- Appendix 3: Smilnich, N.J., Day, C.D., Fitzpatrick, G.V., Caldwell, G.M., Lossie, A.C., Cooper, P.R., Smallwood, A.C., Joyce, J.A., Schofield, P.N., Reik, W., Nicholls,

- R.D., Weksberg, R., Driscoll, D.J., Maher, E.R., Shows, T.B. and Higgins, M.J. 1999. A maternally methylated CpG-island in KvLQT1 is associated with an antisense paternal transcript and loss of imprinting in Beckwith-Wiedemann syndrome. *Proc. Natl. Acad. Sci., USA* 96: 8064-8069.
- Appendix 4: Crider-Miller, S.J., Reid, L.H., Higgins, M.J., Nowak, N.J., Shows, T.B., Futreal, P.A. and Weissman, B.E. 1997. Novel transcript sequences within the BWS/WT2 region in 11p15.5: Tissue-specific expression correlates with cancer type. *Genomics* 46: 355-363.
- Appendix 5: Rodriguez, P., Munroe, D., Prawitt, D., Chu, L.L., Bric, E., Kim, J., Reid, L.H., Davis, C., Nakagama, H., Loebbert, R., Winterpacht, A., Petruzzi, M.J., Higgins, M.J., Nowak, N., Evans, G., Shows, T., Weissman, B.E., Zabel, B., Housman, D.E. and Pelletier, J. 1997. Functional characterization of human nucleosome assembly protein-2 (NAP1L4) suggests a role as a histone chaperone. *Genomics* 44: 253-265.
- Appendix 6: Banki, K., Eddy, R.L., Shows, T.B., Halladay, D.L., Bullrich, F., Croce, C.M., Jurecic, V., Baldini, A. and Perl, A. 1997. The human transaldolase gene (TALDO1) is located on chromosome 11 at p15.4-p15.5. *Genomics* 45: 233-238.
- Appendix 7: Gabriel, J.M., Higgins, M.J., Gebuhr, T.C., Shows, T.B., Saitoh, S. and Nicholls, R.D. 1998. A model system to study genomic imprinting of human genes. *Proc. Natl. Acad. Sci., USA* 95: 14857-14862.
- Appendix 8: Day, C.D., Smilnich, N.J., Fitzpatrick, G.V., de Jong, P.J., Shows, T.B. and Higgins, M.J. 1999. The imprinted domain in mouse distal chromosome 7: Reagents for mutagenesis and sequencing. *Mammalian Genome* 10: 182-185.
- Appendix 9: Shows, T.B., Higgins, M.J. and Nowak, N.J. 1997. Identifying and isolating breast cancer-associated genes on chromosome 11. Department of Defense, U.S. Army Breast Cancer Meeting, An Era of Hope, October 30-November 3, Washington, D.C.
- Appendix 10: Higgins, M.J., Reid, L.H., Cooper, P.R., Weissman, B.E., Stanbridge, E.J., Sait, S.N.J., Nowak, N.J., de Jong, P.J., Gabriel, J.M., Nicholls, R.D., Davis, C., Evans, G.A., Gross, K., Rommens, J., Pelletier, J., Landers, J., Zabel, B. and Shows, T.B. 1997. A 1 mb transcription map of the imprinted BWSCR1/tumor suppressor region in 11p15.5. HGM '97 Meeting, March 6-8, Toronto, Ontario, Canada.
- Appendix 11: Prawitt, D., Gaertner, B., Higgins, M., Shows, T.B., Landers, J., Housman, D.E., Pelletier, J., Winterpacht, A. and Zabel, B. 1997. Characterization of transcripts expressed in kidney and derived from 11p15.5, a region linked to Beckwith-

Wiedemann-syndrome and Wilms' tumor formation. ASHG Meeting, October 28-November 2, Baltimore, MD. *Amer. J. Hum. Genet.* 61: A78 (Abstract #428).

- Appendix 12: Shows, T.B., Higgins, M.J. and Nowak, N.J. 1998. Identifying breast cancer-associated genes on human chromosome 11. AACR Annual Mtg., March 28-April 1, New Orleans, LA.
- Appendix 13: Higgins, M.J., Cooper, P.R., Nowak, N.J., Reid, L.H., Crider-Miller, S.J., Davies, C., Gabriel, J.M., Nicholls, R.D., de Jong, P., Evans, G., Weissman, B.E. and Shows, T.B. 1997. Loss of imprinting at IGF2 and a novel CpG-island in a BWS fetus with an inversion chromosome 11. Gordon Research Conference on Epigenetics, Plymouth, NH, August 10-15.
- Appendix 14: Preisinger, E., Higgins, M., Morgenbesser, S., Reid, L., Dasgupta, S., Landers, J., Shows, T., Weissman, B. and Housman, D. 1997. Loss of replicative asynchrony at the imprinted region on 11p15.5 in embryonal rhabdomyosarcoma. ASHG Meeting, October 28-November 2, Baltimore, MD. *Amer. J. Hum. Genet.* 61: A78 (Abstract #429).
- Appendix 15: Higgins, M.J., Smilnich, N.J., Day, C.D., Smallwood, A.V., Lossie, A., Cooper, P.R., Caldwell, G.M., Discoll, D.J., Maher, E.R. and Shows, T.B. 1998. A maternally methylated CpG-island in KvLQT1 is associated with a paternally expressed transcript and loss of imprinting in Beckwith-Wiedemann syndrome. American Society of Human Genetics Annual Meeting, October 28 - November 2, Denver, CO. *Amer. J. Hum. Genet.* 63: A328 (Abstract #1898).
- Appendix 16: Cooper, P.R., Reid, L.H., Crider-Miller, S.J., Pelletier, J., Pearsall, R.S., Zabel, B.U., Weissman, B.E., Shows, T.B. and Higgins, M.J. 1998. Towards the molecular dissection of the imprinted domains in human chromosome band 11p15.5 and mouse distal chromosome 7. 18th Annual Samuel Lunenfeld Research Institute, Mount Sinai Hospital, Toronto, Ontario, Canada.
- Appendix 17: Day, C.D., Smilnich, N.J., Fitzpatrick, G.V., Diaz-Myer, N., Titus, R.L., Caldwell, G.M., Lossie, A.C., Smallwood, A.C., Joyce, J.A., Schofield, P.N., Reik, W., Nicholls, R.D., Weksberg, R., Driscoll, D.J., Mayer, E.R., Cooper, P.R., Shows, T.B., and Higgins, M.J. 1999. A putative imprinting control region in 11p15.5 and its loss of methylation in Beckwith-Wiedemann syndrome. *Amer. J. Human Genet.* 65: A104 (Abstract #549).

CONCLUSION

Originally, our goals were to describe a tumor suppressor gene in the 11p15.5 region specific for breast cancer. After a genomic characterization of the region, we could not identify a tumor suppressor gene; however, we did find an imprinting center in the region that demonstrated mutations associated with one of the 8-10 growth disorders and tumors that have been mapped to this region. We are currently examining breast cancer samples for mutations in this imprinting center.

REPORT OF INVENTIONS AND SUBCONTRACTS

(Pursuant to "Patent Rights" Contract Clause) (See Instructions on Reverse Side.)

Form Approved
OMB No. 0704-0297
Expires Jun 30, 1992

Public reporting burden for this collection of information is estimated to average 5 minutes per response, including the time for reviewing instructions, searching existing data sources, gathering and maintaining the data needed, and completing and reviewing the collection of information. Send comments regarding this burden estimate or any other aspect of this collection of information, including suggestions for reducing this burden, to Washington Headquarters Services, Directorate for Information Operations and Reports, 1215 Jefferson Davis Highway, Suite 1204, Arlington, VA 22202-4302, and to the Office of Management and Budget, Paperwork Reduction Project (0704-0297), Washington, DC 20503.

1a. NAME OF CONTRACTOR/SUBCONTRACTOR Thomas B. Shows, Ph.D.		2a. NAME OF GOVERNMENT PRIME CONTRACTOR		3. TYPE OF REPORT (X one) a. INTERIM <input type="checkbox"/> b. FINAL <input type="checkbox"/>	
b. ADDRESS (include ZIP Code) Health Research, Inc. RP Division, Buffalo, NY		b. ADDRESS (include ZIP Code) Final Report November 1999		4. REPORTING PERIOD (YYMMDD) a. FROM <input type="checkbox"/> b. TO <input type="checkbox"/>	
c. CONTRACT NUMBER DAND17-94-J-4417		c. CONTRACT NUMBER		d. AWARD DATE (YYMMDD)	

SECTION I - SUBJECT INVENTIONS

14263

5. "SUBJECT INVENTIONS" REQUIRED TO BE REPORTED BY CONTRACTOR/SUBCONTRACTOR (If "None," so state)

a. NAMES OF INVENTIONS (Last, First, MI)	b. TITLE OF INVENTION(S)	c. DISCLOSURE NO., PATENT APPLICATION SERIAL NO. OR PATENT NO.	d. ELECTION TO FILE PATENT APPLICATIONS				e. CONFIRMATORY INSTRUMENT OR ASSIGNMENT FORWARDED TO CONTRACTING OFFICER	
			(1) United States		(2) Foreign			
None.	None.		(a) Yes <input type="checkbox"/>	(b) No <input type="checkbox"/>	(a) Yes <input type="checkbox"/>	(b) No <input type="checkbox"/>	(1) Yes <input type="checkbox"/>	(2) No <input type="checkbox"/>


1. EMPLOYER OF INVENTIONS NOT EMPLOYED BY CONTRACTOR/SUBCONTRACTOR		9. ELECTED FOREIGN COUNTRIES IN WHICH A PATENT APPLICATION WILL BE FILED	
(1) (a) Name of Inventor (Last, First, MI)	(2) (a) Name of Inventor (Last, First, MI)	(2) Foreign Countries of Patent Application	
(b) Name of Employer	(b) Name of Employer		
(c) Address of Employer (include ZIP Code)	(c) Address of Employer (include ZIP Code)		

SECTION II - SUBCONTRACTS (Containing a "Patent Rights" clause)

6. SUBCONTRACTS AWARDED BY CONTRACTOR/SUBCONTRACTOR (If "None," so state)

a. NAME OF SUBCONTRACTOR(S)	b. ADDRESS (include ZIP Code)	c. SUBCONTRACT NO.(S)	d. DFAR "PATENT RIGHTS"	e. DESCRIPTION OF WORK TO BE PERFORMED UNDER SUBCONTRACT(S)	f. SUBCONTRACT DATES (YYMMDD)	
			(1) Clause Number		(1) Award	(2) Estimated Completion
			(2) Date (YYMM)			

SECTION III - CERTIFICATION

7. CERTIFICATION OF REPORT BY CONTRACTOR/SUBCONTRACTOR		Non-Profit Organization (If appropriate box)	
a. NAME OF AUTHORIZED CONTRACTOR/SUBCONTRACTOR OFFICIAL (Last, First, MI) Shows, Thomas B., Ph.D.	Not required if Small Business or	c. I certify that the reporting party has procedures for prompt identification and timely disclosure of "Subject Inventions," that such procedures have been followed and that all "Subject Inventions" have been reported.	
b. TITLE Member, Cancer Genetics	d. SIGNATURE 	e. DATE SIGNED 1/18/00	

DD Form 882, OCT 89

Previous editions are obsolete.

9/1/284

A 1-Mb Physical Map and PAC Contig of the Imprinted Domain in 11p15.5 That Contains TAPA1 and the BWSCR1/WT2 Region

Laura H. Reid,^{*,1} Chris Davies,[†] Paul R. Cooper,[‡] Shyra J. Crider-Miller,^{*} Sheila N. J. Sait,[§] Norma J. Nowak,[‡] Glen Evans,[†] Eric J. Stanbridge,[¶] Pieter deJong,[†] Thomas B. Shows,[‡] Bernard E. Weissman,^{*} and Michael J. Higgins^{‡,1}

^{*}Department of Pathology and Lineberger Comprehensive Cancer Center, University of North Carolina, Chapel Hill, North Carolina 27599; [†]McDermott Center for Human Growth and Development, University of Texas Southwestern Medical Center, Dallas, Texas 75235; [‡]Department of Human Genetics and [§]Department of Cytogenetics, Roswell Park Cancer Institute, Buffalo, New York 14263; and [¶]Department of Microbiology and Molecular Genetics, University of California, Irvine, California 92717

Received December 24, 1996; accepted May 27, 1997

We have constructed a 1-Mb contig in human chromosomal band 11p15.5, a region implicated in the etiology of several embryonal tumors, including Wilms tumor, and in Beckwith–Wiedemann syndrome. Cosmid, P1, PAC, and BAC clones were characterized by *NotI*/*SalI* digestion and hybridized to a variety of probes to generate a detailed physical map that extends from D11S517 to L23MRP. Included in the map are the CARS, NAP2, p57/KIP2, KVLQT1, ASCL2, TH, INS, IGF2, H19, and L23MRP genes as well as end probes isolated from PACs. The TAPA1 gene, whose protein product can transmit an antiproliferative signal, was also localized in the contig. However, Northern blot analysis demonstrated that its expression did not correlate with tumorigenicity in G401 Wilms tumor hybrids, suggesting that TAPA1 is not responsible for the tumor suppression associated with 11p15.5. Genomic clones were used as probes in FISH analysis to map the breakpoints from three Beckwith–Wiedemann syndrome patients and a rhabdoid tumor. Interestingly, each of the breakpoints disrupts the KVLQT1 gene, which is spread over a 400-kb region of the contig. Since 11p15.5 contains several genes with imprinted expression and one or more tumor suppressor genes, our contig and map provide a framework for characterizing this intriguing genetic environment.

© 1997 Academic Press

INTRODUCTION

Several lines of evidence suggest that human chromosomal band 11p15.5 contains genes involved in tumor suppression and embryonic growth. First, rare

chromosomal breakpoints in Beckwith–Wiedemann syndrome (BWS) patients and pediatric tumors map to 11p15.5 (Mannens *et al.*, 1994; Sait *et al.*, 1994). These breakpoints cluster in three regions of 11p15.5, most often in the BWSCR1 domain between D11S648 and D11S551 (Hoovers *et al.*, 1995). Since BWS patients suffer from a variety of overgrowth disorders and predisposition to embryonic tumors including Wilms tumor (WT) and rhabdomyosarcoma, the breakpoints may disrupt developmental genes or their regulation. Second, loss of heterozygosity (LOH) in 11p15.5 has been detected in BWS and sporadic WT cases (Mannens *et al.*, 1988; Reeve *et al.*, 1989; Wadey *et al.*, 1989). LOH in the same region of 11p15.5 is also observed in a variety of adult tumors (Seizinger *et al.*, 1991), suggesting the presence of a common tumor suppressor gene or a cluster of cancer-related genes. Third, 11p15.5 contains at least three imprinted genes (H19, IGF2,² and p57/KIP2) that are normally expressed from one, parent-specific allele. Loss of imprinting (LOI) mutations have been detected at H19, IGF2, and to a lesser extent p57/KIP2 in WT and BWS patients (Moulton *et al.*, 1994; Ogawa *et al.*, 1993; Rainier *et al.*, 1993; Steenman *et al.*, 1994; Weksberg *et al.*, 1993a). The resulting abnormal expression of these genes may contribute to tumor development. Finally, we and others have transferred regions of 11p15.5 into mammalian cells to demonstrate tumor suppressor activity in the G401 WT cell line (Dowdy *et al.*, 1991; Reid *et al.*, 1996b; Weissman *et al.*, 1987) and growth arrest in the RD rhabdomyosarcoma cell line (Koi *et al.*, 1993; Loh *et al.*, 1992). These functional experiments confirm the existence of at least one suppressor gene in 11p15.5, sometimes referred to as WT2.

¹ To whom correspondence may be addressed. (L.H.R.) Telephone: (919) 966-1350. Fax: (919) 966-3015. E-mail: lhr@med.unc.edu. (M.J.H.) Telephone: (716) 845-3582. Fax: (716) 845-8449. E-mail: higgins@shows.med.buffalo.edu.

² Abbreviations used: ASCL2, achaete-scute homolog-2; CARS, cysteinyl-tRNA synthetase; HBB, β -globin; IGF2, insulin-like growth factor II; INS, insulin; NAP2, nucleosome assembly protein II; TAPA1, target of an antiproliferative antibody; TH, tyrosine hydroxylase.

As part of an ongoing effort to characterize 11p15.5, we have constructed a detailed physical map and a 1-Mb contig of cosmid, P1, BAC, and PAC clones. The contig extends from D11S517 to L23MRP and includes the region with tumor and growth suppressor activity. Using fluorescence *in situ* hybridization (FISH), we have mapped the chromosomal breakpoint in three BWS patients and one rhabdoid tumor within the contig. Interestingly, these chromosome rearrangements each disrupted the KVLQT1 gene, a potassium channel protein associated with the development of long QT (LQT) cardiac disorder. In addition, the contig has allowed the precise mapping of several genes, including TAPA1. This gene, along with other members of the transmembrane four superfamily (TMSF), has been implicated in the regulation of cell growth. However, Northern blot analysis suggests that TAPA1 is not the operative tumor suppressor gene in our G401 WT assay.

MATERIAL AND METHODS

Isolation of genomic clones. PCR primers have been previously published: D11S517 (Koi *et al.*, 1993); p57/KIP2 (Reid *et al.*, 1996a); KVLQT1 (Wang *et al.*, 1996); TAPA1/WI-9248 (GDB Accession No. 678191); D11S1318/Afm218xe1 (GDB Accession No. 199331); L23MRP (Tsang *et al.*, 1995); D11S601, D11S648, D11S679, and D11S1 (Reid *et al.*, 1996b). D11S724 primers are 5'-CTT CTC AGT GTA TCA CAT CC-3' and 5'-TCC CCC GAT TGT TTA TTG GTT G-3'. ASCL2 primers are 5'-CGT GAA GCT GGT GAA CTT G-3' and 5'-GAT GTA CTC CAC GGC TGA G-3'. Cosmids c19A2, c43D7, and c54B1 were identified in the Los Alamos human chromosome 11 cosmid library by hybridization with the D11S517 PCR product. Cosmids c14F5 (Reid *et al.*, 1996a) and cH19 were isolated from the same library using human p57/KIP2 and H19 cDNA probes, respectively. Cosmids c565, c395, c469, and c555 were previously identified in a different chromosome 11 cosmid library (Tanigami *et al.*, 1992). They contain markers D11S601, D11S648, D11S679, and D11S724, respectively.

P1 clones were isolated by PCR screening in the DuPont Merck Pharmaceutical Human Foreskin Fibroblast (Shepherd *et al.*, 1994) with the assistance of Genome Systems. Well positions for each P1 clone are as follows: P1-1429, HFF1 0434-9E; P1-1430, HFF1 0713-6A; P1-3314, HFF1 0252-D10; P1-3315, HFF1 0789-G8; P1-3316, HFF1 1093-E5; P1-6959, HFF1 0086-A9; P1-6960, HFF1 0549-F1. BAC clones (Shizuya *et al.*, 1992) were identified by STS-based PCR using DNA pools obtained from Research Genetics followed by hybridization of 384-clone filters corresponding to positive plates. One PAC was isolated from RPCI-1 by PCR screening with the assistance of Genome Systems. Other PAC clones were identified in libraries RPCI-1, 3, 4, and 5, constructed as described (Ioannou *et al.*, 1994) but in the pCYPAC2 vector. Two PAC clones were derived from the RPCI-6 library constructed in the pPAC4 vector. Pools of radiolabeled probes were hybridized to high-density filters each containing approximately 18,000 unique PAC clones. Positive clones were grown in 96-well plates, transferred to filter replicates, and hybridized to individual probes as described (Ioannou *et al.*, 1994). A variety of probes were used to detect 11p15.5 clones, including PCR products generated from sequence tagged sites (STSs), intact YACs excised from low-melting-point CHEF gels, *Alu* PCR products derived from YACs (Qin *et al.*, 1996), and end fragments isolated from PACs (see below). All probes were labeled by random-priming (Feinberg and Vogelstein, 1983) and hybridized as described (Church and Gilbert, 1984).

Isolation of end-fragment probes from PAC clones. End fragments were recovered from PAC clones using a modified ligation-mediated

technique (Kere *et al.*, 1992; Wu *et al.*, 1996). Approximately 100 ng of PAC DNA was digested with *Rsa*I and ligated to a double-stranded linker. An aliquot (1 μ l) of the ligation reaction was amplified in a 30- μ l PCR containing primers corresponding to the linker (Kere *et al.*, 1992) and to the sequence immediately adjacent to either side of the *Bam*HI cloning site (Wu *et al.*, 1996) (T7 side, 5'-GCC GCT AAT ACG ACT CAC TAT AGG GAG AG-3'; SP6 side, 5'-GGC CGC CTG GCC GTC GAC ATT TAG GTG ACA CTA TAG-3'). Cycling conditions were 94°C for 5 min followed by 35 cycles of 94°C for 10 s; 65°C for 20 s; 72°C for 1 min and a final extension at 72°C for 10 min. End fragments were isolated in low-melting-point gels. Approximately 75% of the PAC ends were recovered using the *Rsa*I restriction enzyme. The remaining ends were usually isolated using *Alu*I or *Eco*RV.

Construction of the contig and physical map. Cosmid and BAC DNA was isolated using anion-exchange columns (Qiagen). P1 and PAC DNA was isolated using an alkaline lysis protocol followed by phenol-chloroform extraction and isopropanol precipitation as recommended by Genome Systems. For PAC end-fragment mapping, cloned DNA was digested with *Not*I and *Eco*RI (New England Biolabs), electrophoresed in 0.8% agarose gels and blotted onto Hybond-N+ (Amersham) according to the manufacturer's instructions. For restriction mapping, DNA was digested with *Not*I and/or *Sal*I, separated in 0.4% agarose/1 \times TAE gels, and nicked in 0.25 M HCl prior to denaturation and transfer in a 1.5 M NaCl/0.5 M NaOH solution to positively charged membranes (Boehringer-Mannheim). Alternatively, high-molecular-weight fragments were separated in 1% Seakem LE agarose (FMC Bioproducts)/0.5 \times TBE gels using a FIGE apparatus (Bio-Rad) and nicked with 60 mJ of ultraviolet light before transfer. Southern blots were hybridized with gel-purified DNA fragments, PCR products, end fragments, and intact clones using either the nonradioactive Genius system (Boehringer-Mannheim) at 65°C or ³²P-labeled probes at 42°C. Repetitive sequences in probes were blocked by preannealing with *Cot*I DNA according to the manufacturer's directions (Gibco-BRL).

Patient material and FISH analysis. Chromosome spreads were prepared by standard procedures from the following patient samples: (1) primary cells from an aborted fetus with clinical features indicative of BWS and a 46,XY,inv(11)(p13p15.5),mat karyotype (Christian *et al.*, 1993); (2) lymphoblastoid cell lines from two unrelated BWS patients, one with t(11;16) and the other carrying t(11;22) (Weksberg *et al.*, 1993b); and (3) the TM87-16 cell line derived from a patient with a malignant rhabdoid tumor and 46,XY,t(11;22)(p15.5;q11.23) karyotype (Karnes *et al.*, 1991). FISH was carried out essentially as described (Sait *et al.*, 1994). Approximately 200 ng of PAC or BAC DNA was labeled with digoxigenin-11-dUTP (Boehringer-Mannheim) by random priming, preannealed with *Cot*I DNA, hybridized to metaphase chromosomes, and detected with FITC.

Northern blot analysis. G401.6TG.c6 is an *hprt*-deficient derivative of the G401 cell line. It was originally classified as a Wilms tumor (Peebles *et al.*, 1978), although many of its properties are more consistent with a rhabdoid tumor (Garvin *et al.*, 1993). MCH 486.1, MCH 486.2G, MCH 486.2J, MCH 486.2L and MCH 486.5 are G401 hybrid lines that contain the radiation-reduced t(X;11) chromosome from XMCH 708.25 and do not form tumors when injected into nude mice (Reid *et al.*, 1996b). MCH 369.18 and MCH 485.2A, are G401 hybrid lines that contain the radiation-reduced t(X;11) chromosomes from XMCH 708.24 or XMCH 708.26 (Dowdy *et al.*, 1991; Reid *et al.*, 1996b). These cell lines do form tumors after mouse inoculation. Polyadenylated RNA (2 μ g) was isolated using an oligo(dT) kit (Collaborative Research), separated on 1% agarose-formaldehyde/MOPS gels, transferred to nylon membranes (Boehringer Mannheim), and hybridized to ³²P-labeled DNA probes at 42°C in a 50% formamide solution. The TAPA1 probe was the 1.5-kb *Bam*HI-*Xho*I insert from the human cDNA clone.

RESULTS

Isolation of Genomic Clones in 11p15.5

Our previous cytogenetic and PFGE experiments had localized 11p15.5 breakpoints in three BWS patients

and one rhabdoid tumor between D11S679 and IGF2 (Sait *et al.*, 1994). In addition, functional experiments had detected tumor suppressor activity distal to D11S601 (Reid *et al.*, 1996b). Therefore, we concentrated our efforts on identifying large-insert genomic clones between D11S601 and IGF2.

Four cosmids had been previously isolated from 11p15.5 (Tanigami *et al.*, 1992) and mapped to our region of interest by pulsed-field gel electrophoresis (Higgins *et al.*, 1994; Redeker *et al.*, 1994): c565 (D11S601), c395 (D11S648), c469 (D11S679), and c555 (D11S724). Five additional clones were identified by screening the chromosome 11 cosmid library with a D11S517 PCR product, a p57/KIP2 cDNA fragment, and an H19 probe. Using both PCR- and hybridization-based techniques, several YAC libraries (CEPH-A, ICI, St. Louis, RPCI chromosome 11) were screened with probes generated from the cosmids. These efforts identified only a few small and sometimes rearranged YAC clones (unpublished data). Attempts to "walk" from these initial clones by *Alu* PCR hybridization techniques (Qin *et al.*, 1996) met with only limited success, suggesting that this interval would be difficult to clone in yeast-based vectors.

To circumvent this problem, we shifted our efforts to large-insert, bacteria-based cloning systems. Due to limited library size (approximately three genome equivalents), initial screens utilized three different libraries: the P1 library of Shepard *et al.* (1994), the BAC library of Shizuya *et al.* (1992), and the RPCI-1 PAC library (P. deJong, unpublished results). Seven P1 clones, five BACs, and one PAC were identified by PCR-based screening with D11S517, D11S648, D11S679, D11S1, D11S724, and H19 primers. Four additional PAC clones were detected by hybridization with *Alu* PCR products amplified from YACs containing D11S601 and D11S724. Later work focused on expanded PAC libraries (RPCI-3, 4, 5 and 6; P. deJong, unpublished results). Hybridization to RPCI-4 PAC filters with an intact, gel-isolated YAC containing D11S724 led to the recovery of 11 clones, while a D11S724 PCR product identified 4 clones. D11S1318, IGF2, and H19 probes each detected 2 PAC clones. Five additional clones were recovered by hybridizing with end fragments isolated from PACs that contained IGF2 or D11S1318. Later hybridizations of the RPCI-6 library to D11S1318, ASCL2, and IGF2 probes identified 2 clones. In total, 45 large-insert clones were identified between D11S517 and L23MRP (Table 1 and Fig. 1). The size of each insert was determined by FIGE. They ranged from 70 to 180 kb, with a mean PAC insert size of 130 kb. The 11p15.5 location of several of these clones was confirmed by FISH analysis (data not shown).

Contig and Physical Map Construction

Overlaps between clones were established by STS content, restriction mapping, and end-fragment hy-

bridizations. Previous cytogenetic and molecular experiments had mapped several STSs and known genes to this region of 11p15.5, including CARS (Cruzen *et al.*, 1993); p57/KIP2 (Matsuoka *et al.*, 1995); TAPA1 (Virtaneva *et al.*, 1994); ASCL2 (Alders *et al.*, 1997; Miyamoto *et al.*, 1996); L23MRP (Tsang *et al.*, 1995), and the TH/INS/IGF2/H19 cluster. In addition, the KVLQT1 (Wang *et al.*, 1996) and NAP2 (D. Munroe and J. Pelletier, unpublished data; Hu *et al.*, 1996) genes have been isolated with genomic clones from the area. To localize these markers in the contig, PCR products and cDNA clones were hybridized to Southern blots of the constituent clones. These experiments detected physical linkage between several of the large-insert clones, as shown in Table 1.

Most of the 11p15.5 loci were localized to relatively small, contiguous regions of DNA. However, detailed analysis detected fragments of the KVLQT1 gene in several, distant 11p15.5 clones (represented as solid circles in Fig. 1B). For example, KVLQT1 cDNA hybridized to multiple restriction fragments in BAC-70I6, and preliminary sequence data (C. Davies and G. Evans, unpublished data) identified downstream exons in PAC-74K15 and PAC-23N20. In addition, upstream coding sequence recently cloned by us (S. J. Crider-Miller, L. H. Reid and B. E. Weissman, unpublished data) and others (Lee *et al.*, 1997; Sanguinetti *et al.*, 1996) is contained in PAC-5K6. These results suggest that KVLQT1 is a large gene spread over 400 kb.

To generate a physical map, each 11p15.5 clone was characterized by *NotI* and *SalI* digestion (Fig. 1C). Overlaps suggested by common bands in adjacent clones were confirmed by Southern blot hybridizations using gel-purified fragments or intact clones as probes. Frequently, the number or position of restriction sites was insufficient to verify physical contiguity. In these cases, overlap was detected by Southern blots hybridized with end fragments isolated from individual PACs by ligation-mediated PCR. For example, restriction maps of PAC-698D9 and PAC-915F1 did not detect common *NotI/SalI* fragments with PAC-1075F20. However, end-fragment probes from the former two clones hybridized to PAC-1075F20, thereby establishing overlap (Table 1). Restriction mapping and end-fragment hybridization experiments failed to detect overlap between clones containing D11S1318/ASCL2 and those containing TH/INS/IGF2. To bridge this gap, the T7-end of PAC-861M13 was used to rescreen the library. Two new PACs were identified, and the SP6 end of one of these (PAC-592M15) hybridized to the IGF2-containing PACs, thus bridging the gap.

By aligning the overlapping large-insert clones, we constructed a contiguous, 1-Mb physical map of genomic DNA between D11S517 and L23MRP (Fig. 1B). This contig has sufficient depth so that the size of each *NotI* and *SalI* fragment rarely relies on the analysis of individual clones. The restriction sites were generally consistent between clones. Only three rearranged clones were detected. BAC-87F5 and BAC-47G8, both

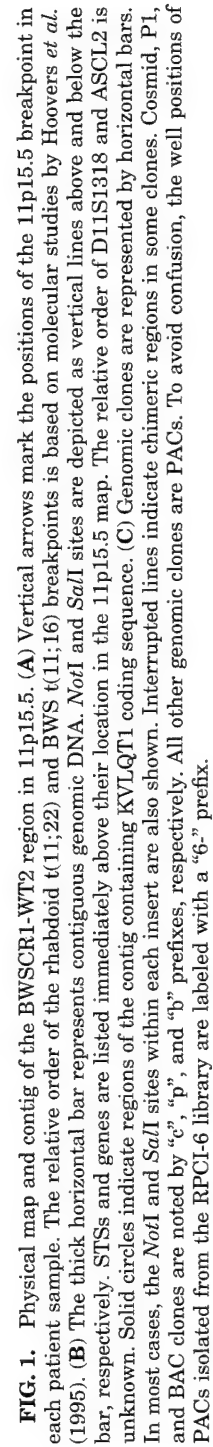


TABLE 1
STS Content in 11p15.5 P1, BAC, and PAC Clones

Contig Clone	11p15.5 probe																									
	D11S517	D11S601	D11S648	p57/KIP2	D11S679	D11S1	74K15-T7	608B4-SP6	74K15-SP6	D11S724	552A16-SP6	5K6-SP6	698D9-SP6	TAPA-1	915F1-T7	698D9-T7	861M13-SP6	ASCL2	D11S1318	861M13-T7	592M15-SP6	TH	INS	IGF2	H19	L23MRP
P1-3314	+	+																								
P1-3315	+	+																								
P1-3316	+	+																								
PAC-192M22	+	+																								
PAC-47G3	+	+	+																							
P1-1429			+																							
P1-1430			+																							
PAC-23N20			+	+	+																					
PAC-695C12					+	+	+																			
P1-6959					+	+	+																			
P1-6960						+	+																			
PAC-74K15							+	+	+																	
PAC-552A16								+	+	+	+															
PAC-608B4								+	+	+	+															
BAC-47G8						+	+	+	+	+	+															
BAC-7016										+	+															
BAC-87F5										+	+															
PAC-5K6												+														
PAC-915F1												+	+	+	+											
PAC-698D9												+	+	+	+	+										
PAC-1075F20													+	+	+	+	+	+	+							
PAC-861M13																	+	+	+	+						
PAC-739A23																		+	+	+	+					
PAC-592M15																			+	+	+	+				
PAC-532K15																				+	+	+	+			
PAC-416J1																					+	+	+	+		
PAC-6-103P2																						+	+	+	+	
PAC-895K23																							+	+	+	
PAC-998N23																								+	+	
BAC-148C3																									+	+
PAC-1096G20																									+	+
BAC-142F11																									+	+

Clones were tested for 11p15.5 genes, STSs, and PAC end-fragments by PCR and Southern blot experiments.

Blank spaces indicate that the presence of the marker in that clone was negative or not determined. Not all clones in the 11p15.5 contig are included in this table.

located near D11S724, apparently have internal deletions. PAC-539G11 contains part of chromosome 2 as determined by FISH analysis (data not shown).

Identification of Chromosome Breakpoints

Using a combination of FISH and PFGE, we had previously mapped a BWS t(11;22) between D11S679 and D11S724, a BWS inv(11) at D11S724, and the breakpoints of a BWS t(11;16) and a rhabdoid tumor t(11;22) to a region between D11S724 and IGF2 (Sait *et al.*, 1994). To map these four breakpoints within the large-insert bacterial clone contig, several of the genomic clones shown in Fig. 1 were used as probes in FISH analysis of metaphase chromosomes from these patient cell lines. Clones P1-6959 and P1-6960 were shown to span the BWS t(11;22) translocation by their hybridization to both the der(11) and the der(22) chromosomes (Fig. 2A). FISH experiments with PAC-608B4 to metaphase chromosomes derived from a BWS abortus with a paracentric inversion involving the distal short arm of chromosome 11 resulted in signals on the normal chromosome 11 at 11p15.5 and two signals on the inverted chromosome 11, one at 11p15.5 and one at

11p13 (Fig. 2B). Similar results were obtained with BAC-87F5 and BAC-47G8 (data not shown) and had been previously observed with c555 (Sait *et al.*, 1994), suggesting that the distal inversion breakpoint of the rearrangement is contained in these clones. When chromosome spreads from a BWS t(11;16) and a rhabdoid tumor t(11;22) cell line were hybridized with PAC-915F1, signals were observed, in each case, on both derivative chromosomes and the normal chromosome 11 (Fig. 2C). These results demonstrate that PAC-915F1 spans the chromosome 11 breakpoint region in both of these cell lines.

TAPA1 Expression

We have used somatic cell hybrids in a functional assay to identify regions of chromosome 11 that suppress tumorigenicity in the G401 Wilms tumor cell line (Dowdy *et al.*, 1991; Reid *et al.*, 1996b; Weissman *et al.*, 1987). This assay has enabled us to localize a tumor suppressor gene to a region of 11p15.5 telomeric to the D11S601 locus (Reid *et al.*, 1996b). Because TAPA1 maps to the same region, we investigated whether its expression might contribute to the tumor suppression

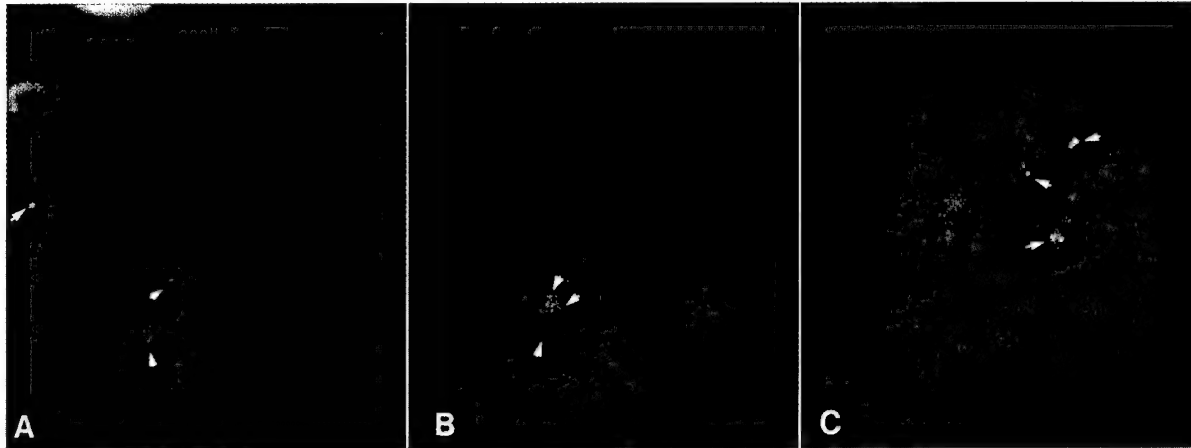


FIG. 2. FISH analysis of 11p15.5 chromosome rearrangements. Propidium iodide-stained metaphase spreads are shown hybridized with P1 and PAC probes. (A) The BWS t(11;22) hybridized with P1-6959 showing signals on the normal chromosome 11 (center arrow), the der(22) (left arrow), and the der(11) (bottom arrow). (B) Metaphase chromosomes from a BWS inv(11) abortus showing hybridization of PAC-608B4 to a single site (11p15.5) on the normal chromosome 11 (bottom arrow) and to two places (p15.5 and p13) on the inv(11) chromosome (top arrows). (C) Hybridization signals using PAC-915F1 are observed in cells from a rhabdoid tumor t(11;22) on the normal chromosome 11 (top arrow), the der(11) (center arrow), and the der(22) (bottom arrow).

observed in our assay. Previous experiments demonstrated that five G401 hybrid lines, MCH 486.1, MCH 486.2G, MCH 486.2J, MCH 486.2L, and MCH 486.5 were suppressed for tumorigenicity (Reid *et al.*, 1996b). Two other G401 hybrid lines, MCH 369.18 and MCH 485.2A, were tumorigenic (Dowdy *et al.*, 1991; Reid *et al.*, 1996b). Each of these G401 hybrid lines contains an introduced t(X;11) chromosome with an intact TAPA1 gene. To determine the level of TAPA1 expression in G401 and the microcell hybrid lines, Northern blots containing polyadenylated RNA isolated from the G401, MCH 369, MCH 485, and MCH 486 cell lines were hybridized to a TAPA1 cDNA probe. As shown in Fig. 3, the intact 1.6-kb transcript was detected in G401 and each of the hybrid lines. These results indicate that TAPA1 expression does not correlate with tumor suppression in the G401 hybrid lines.

DISCUSSION

As part of our work to isolate novel genes in human chromosome band 11p15.5, we have constructed a 1-Mb contig of cosmid, P1, PAC, and BAC clones that extends from D11S517 to L23MRP. Functional studies have demonstrated that this region contains genes involved in tumor suppression and *in vitro* growth. For example, introduction of a radiation-reduced t(X;11) chromosome that contains 11p15.5 DNA telomeric to D11S601 suppressed tumorigenicity in the G401 WT cell line (Reid *et al.*, 1996b). Analogous experiments using the RD rhabdomyosarcoma cell line showed growth suppression after transferring a 3-Mb subchromosomal fragment that maps between HBB and IGF2 (Koi *et al.*, 1993). Detailed PFGE experiments demonstrated that the subchromosomal fragment extends at most 365 kb telomeric to D11S724 and that the 11p15.5 breakpoint in the t(X;11) chromosome maps 30 kb centromeric to D11S648. Therefore, an approximately 700-kb region of 11p15.5 DNA is contained in both the subchromosomal fragment and the t(X;11) chromosome. Assuming the same genetic element suppresses both the RD and the G401 cell lines, then one can limit its location to this smallest region of overlap, all of which is contained in the PAC contig. This area of 11p15.5 undergoes frequent LOH in a variety of pediatric and adult tumors (Seizinger *et al.*, 1991) and contains rearrangement breakpoints from a rhabdoid tumor and BWS patients (Hoovers *et al.*, 1995; Mannens *et al.*, 1994; Sait *et al.*, 1994). Therefore, the genomic clones and restriction map presented in this paper should assist in the isolation and characterization of new tumor suppressor genes in 11p15.5.

Large-insert clones in our contig have been well characterized by *NotI* and *SalI* restriction mapping. The *NotI* map is in good agreement with pulsed-field gel

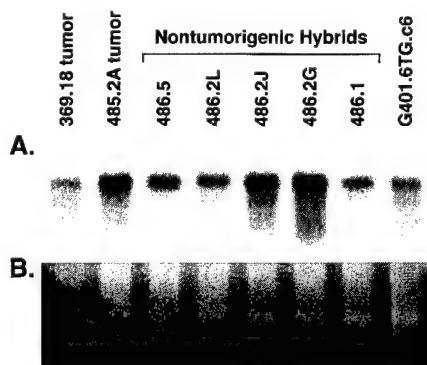


FIG. 3. TAPA1 expression in the G401 hybrid lines. (A) Northern blot hybridized with a human cDNA TAPA1 probe. Each lane contains 2 μ g of polyadenylated RNA isolated from the G401.6TG.c6 parental cell line, the G401 hybrid lines that were suppressed for tumorigenicity, or mouse tumors arising after inoculations with G401 hybrid lines that were not suppressed. (B) The same Northern blot stained with ethidium bromide to indicate relative RNA loading.

maps of 11p15.5 (Higgins *et al.*, 1994; Redeker *et al.*, 1994) and reveals potential CpG islands which are often associated with promoter sequences. As shown in Fig. 1, *NotI* sites were frequently observed in the centromeric end of the contig. However, telomeric clones contained relatively few *NotI* sites. This reduced restriction site frequency may correlate with a reduced gene density in these areas. Overlap between adjacent clones was confirmed by hybridization experiments. STS markers and known genes were localized to individual restriction fragments, rather than generally mapped to clones. Such detailed restriction maps were not available in previous cosmid (Hoovers *et al.*, 1995) and P1 (Wang *et al.*, 1996) contigs of this region of 11p15.5. Moreover, other contigs have been unable to close the gap between clones containing D11S1318/ASCL2 and those containing TH/INS/IGF2. The present contig is composed mainly of PAC clones with an average insert size of 130 kb. These clones can be transfected into mammalian cells and tested for their influence on tumorigenicity. Similar experiments assisted in the localization of a 3p21 tumor suppressor gene (Todd *et al.*, 1996).

The contig has allowed the precise localization of several previously isolated genes. The CARS gene had been mapped to c19A2 (Cruzen *et al.*, 1993), which we isolated using a D11S517 PCR product. The ASCL2 gene, which encodes a transcription factor that is essential for extraembryonic development (Guillemot *et al.*, 1994), had been mapped near the IGF2/H19 complex (Alders *et al.*, 1997; Miyamoto *et al.*, 1996). We detected ASCL2 on PAC-861M13 and PAC-1075F20 by PCR and hybridization experiments. KVLQT1 is a potassium channel gene that was isolated by exon amplification with P1 clones between D11S679 and D11S551 (Wang *et al.*, 1996). Our PCR and Southern blot experiments mapped much of its coding sequence to BAC-70I6. However, additional data identified the KVLQT1 start site in PAC-5K6 and downstream exons in PAC-74K15 and PAC-23N20. After the submission of this paper, similar results were reported by Lee *et al.* (1997). These data indicate that KVLQT1 is a large gene spread over 400 kb that contains several smaller genes within its introns (unpublished data). Such a genomic structure is unusual for potassium channel genes, which tend to be small and sometimes lack introns (Salkoff *et al.*, 1992; Strong *et al.*, 1993).

The TAPA1 gene (CD81), a 26-kDa membrane protein, is localized in our contig between D11S724 and D11S1318. This gene had been previously mapped to 11p15.5 using somatic cell hybrids (Virtaneva *et al.*, 1994), but its location within the band was unknown. TAPA1 was identified by its ability to transmit an antiproliferative signal in a human B-cell lymphoma line (Oren *et al.*, 1990). Further analysis revealed that this protein is part of a signal transducing complex in B cells that responds to activated complement (Fearon and Carter, 1995) and has a critical role in early T-cell development (Boismenu *et al.*, 1996). The TAPA1

protein contains four transmembrane domains and so belongs to the TMSF of genes. Inactivation of some TMSF proteins has been shown to enable tumor progression. For example, CD9 expression coincides with reduced metastatic potential in melanomas (Si and Hersey, 1993), while KAI1 expression correlates with metastasis suppression in the rat AT6.1 prostate cancer cell line (Dong *et al.*, 1995). In addition, KAI1 expression is reduced during human prostatic cancer development (Dong *et al.*, 1996) and in some metastatic breast cancer lines (A. White and K. Phillips, unpublished results). To determine whether TAPA1 expression was responsible for the tumor suppression observed in our functional assay, we hybridized a TAPA1 cDNA probe to Northern blots containing mRNA from G401 and hybrid cell lines. TAPA1 expression was observed in all lines regardless of their tumorigenic phenotype, suggesting that this gene was not the 11p15.5 tumor suppressor gene.

Our contig predicts the following gene order: centromere – CARS – NAP2 – p57/KIP2 – KVLQT1 – TAPA1 – ASCL2 – TH – INS – IGF2 – H19 – L23MRP – telomere. Several of these genes have been localized to the syntenic region of mouse chromosome 7 (Mouse Genome Database; <http://www.informatics.jax.org>) and have imprinted gene expression. Some isoforms of IGF2 are exclusively expressed from the paternal allele (Gianoukakis *et al.*, 1993; Ohlsson *et al.*, 1993). H19 and p57/KIP2 are predominantly expressed from the maternal allele (Chung *et al.*, 1996; Hatada *et al.*, 1996; Kondo *et al.*, 1996; Matsuoka *et al.*, 1996; Zhang and Tycko 1992). The ASCL2 gene is also likely to be imprinted in humans, since the mouse homolog is expressed exclusively from the maternal allele (Guillemot *et al.*, 1995) and human ASCL2 is not expressed in hydatidiform moles that contain two sets of paternal genes (Alders *et al.*, 1997). Recently, Lee *et al.* (1997) demonstrated tissue-specific imprinting at the human KVLQT1 gene. These investigators found that one isoform of KVLQT1 is predominantly expressed in cardiac tissues from both parental alleles, while another isoform is expressed in most tissues, but exclusively from the maternal allele. Interestingly, our contig appears to be flanked by nonimprinted genes, including NAP2 on the centromeric boundary (Hu *et al.*, 1996) and L23MRP on the telomeric boundary (Tsang *et al.*, 1995). It will be interesting to determine whether the TAPA1 gene has imprinted expression. If not, then human chromosome band 11p15.5 may contain at least one nonimprinted gene interspersed within an imprinted domain.

FISH analysis mapped the breakpoints from three BWS patients and one rhabdoid tumor to a 220- to 320-kb region between D11S679 and TAPA1. The location of these breakpoints is consistent with other analyses (Hoovers *et al.*, 1995; Mannens *et al.*, 1994; Sait *et al.*, 1994), although a more telomeric site for the rhabdoid t(11;22) breakpoint has been reported (Newsham *et al.*, 1994). Surprisingly, each of the breakpoints disrupts

the KVLQT1 gene. Mutations in KVLQT1 have been detected in the LQT syndrome as well as in the Jervell and Lange-Nielsen (JLN) disorder, both of which are characterized by abnormal cardiac repolarization patterns and an increased risk of arrhythmia. Yet BWS patients in general and rearrangement patients in particular do not suffer from this type of heart disease. This discrepancy may be explained by the different types of mutations responsible for each disorder. Recent studies have shown that the cardiac IKs potassium channel is a coassembly of KVLQT1 and minK (IsK) proteins (Barhanin *et al.*, 1996; Sanguinetti *et al.*, 1996). The JLN syndrome is an autosomal recessive disorder caused by frameshift mutations in both KVLQT1 alleles, preventing production of any functional potassium channels (Neyroud *et al.*, 1997). LQT is an autosomal dominant disease attributed to missense mutations in one KVLQT1 allele (Russell *et al.*, 1996; Wang *et al.*, 1996). The mutant proteins in these patients may have a dominant-negative effect when complexed with the wildtype KVLQT1 proteins. Therefore, although LQT patients retain one wildtype KVLQT1 allele, they may produce enough defective potassium channels to develop abnormal repolarization. On the other hand, the chromosome rearrangements that disrupt the maternal KVLQT1 allele in some BWS patients would result in drastically truncated KVLQT1 polypeptides incapable of taking part in IKs potassium channel assembly. The paternal allele, however, would produce intact KVLQT1 protein and form presumably normal IKs potassium channels. In this way, the BWS rearrangement patients would not experience arrhythmia symptoms. Furthermore, since KVLQT1 is not imprinted in the heart (Lee *et al.*, 1997), the expression of this gene in cardiac tissue is unlikely to be affected by the domain wide disruptions of imprinting thought to be important in the etiology of BWS (Weksberg and Squire, 1996).

Since BWS patients frequently have paternal 11p15.5 duplications (Junien 1992) and because LOH studies detect maternal loss in Wilms tumors (Manens *et al.*, 1988; Schroeder *et al.*, 1987; Williams *et al.*, 1989), it seems likely that this region of DNA contains both a paternally expressed growth factor and a maternally expressed tumor suppressor gene. Expression at these and other imprinted loci may be regulated by a common imprinting center analogous to that found in the Prader-Willi/Angelman syndrome region in 15q (Dittrich *et al.*, 1996). Disruptions in the 11p15.5 imprinting center could produce biallelic expression at the paternally expressed IGF2 locus, and loss of expression at maternally expressed genes, including p57/KIP2, KVLQT1, ASCL2, and H19. LOI has been detected in Wilms tumors at the p57/KIP2, H19, and IGF2 loci (Moulton *et al.*, 1994; Ogawa *et al.*, 1993; Rainier *et al.*, 1993; Steenman *et al.*, 1994) and in BWS patients without chromosome rearrangements at the IGF2 locus (Weksberg *et al.*, 1993a). It seems likely that the rearrangements described in this study have similar LOI

effects. Indeed, we (M. J. Higgins, unpublished data) and others (Brown *et al.*, 1996) have detected biallelic expression at the IGF2 locus in two (inv)11 BWS patients. Therefore, the chromosome rearrangements in 11p15.5 may influence the expression of multiple, nearby loci by disrupting an imprinting center, or by "classical" position effects. Our contig and physical map should assist in the characterization of this intriguing domain and in the isolation of new genes involved in BWS and tumor development.

ACKNOWLEDGMENTS

We thank Karen Smith, Tina Dennis, Eleanor Leigh Briley, Nancy Smilinc, Colleen Day, and Linda Haley for excellent technical assistance; Ande West, Kevin Kelleher, David McElligott, and Licia Salleri for assistance in screening YAC and cosmid libraries; Genome Systems for isolating P1 clones and one PAC; the Japanese Cancer Research Resource Bank for cosmids; Chenyan Wu for PAC vector primers; Jin-Tang Dong for the TAPA1 cDNA probe; KAC Phillips and Alicia White for unpublished TAPA1 data; and Jerry Pelletier and David Munroe for unpublished NAP2 data. This research is supported by NIH grants to B.E.W. (CA63176), E.J.S. (CA19104), and T.B.S. (HG00359, HG00333, CA63333) as well as by an ACS grant to T.B.S. (PDT445K) and an ACS fellowship to L.H.R.

REFERENCES

- Alders, M., Hodgess, M., Postmus, J., van Wijk, I., Blik, J., de Meulemeester, J., Westerveld, A., Oudejans, C., Little, P., and Manens, M. (1997). Human MASH2 maps to chromosome 11p15 close to IGF2 and is expressed in extravillous trophoblast. *Hum. Molec. Genet.* **6**: 859-867.
- Barhanin, J., Lesage, F., Guillemare, E., Fink, M., Lazdunski, M., and Romey, G. (1996). K_vLQT1 and IsK (mink) proteins associate to form the I_{ks} cardiac potassium current. *Nature* **384**: 78-80.
- Boismenu, R., Rhein, M., Fischer, W. H., and Havran, W. L. (1996). A role for CD81 in early T cell development. *Science* **271**: 198-200.
- Brown, K. W., Villar, A. J., Bickmore, W., Clayton-Smith, J., Catchpoole, D., Maher, E. R., and Reik, W. (1996). Imprinting mutation in the Beckwith-Wiedemann syndrome leads to biallelic IGF2 expression through an H19-independent pathway. *Hum. Mol. Genet.* **5**: 2027-2032.
- Christian, C. L., Liner, R. I., Abu Bak'r, S., McCallum, W. D., and Conte, W. J. (1993). Genomic imprinting and the Beckwith-Wiedemann syndrome associated with a familial chromosome #11 inversion. *Am. J. Hum. Genet. Suppl.* **53**: 533.
- Chung, W. Y., Yuan, L., Feng, L., Hensle, T., and Tycko, B. (1996). Chromosome 11p15.5 regional imprinting: Comparative analysis of KIP2 and H19 in human tissues and Wilms' tumors. *Hum. Mol. Genet.* **5**(8): 1101-1108.
- Church, G. M., and Gilbert, W. (1984). Genomic sequencing. *Proc. Natl. Acad. Sci. USA* **81**: 1991-1995.
- Cruzen, M. E., Bengtsson, U., McMahon, J., Wasmuth, J. J., and Arfin, S. M. (1993). Assignment of the cysteinyl-tRNA synthetase gene (CARS) to 11p15.5. *Genomics* **15**: 692-693.
- Dittrich, B., Buiting, K., Korn, B., Rickard, S., Buxton, J., Saitoh, S., Nicholls, R., Poustka, A., A., W., Zabel, B., and Horsthemke, B. (1996). Imprint switching on human chromosome 15 may involve alternative transcripts of the SNRPN gene. *Nature Genet.* **14**: 163-170.
- Dong, J.-T., Suzuki, H., S.S., P., Bova, S., Schalken, J. A., Isaacs, W. B., Barrett, J. C., and Isaacs, J. T. (1996). Down-regulation of the KAI1 metastasis suppressor gene during the progression of

- human prostatic cancer infrequently involves gene mutation or allelic loss. *Cancer Res.* **56**: 4387–4390.
- Dong, J. T., Lamg, P. W., Rinker-Schaeffer, C. W., Vukanovic, J., Ichikawa, T., Isaacs, J. T., and Barrett, J. C. (1995). KAI1, a metastasis suppressor gene for prostate cancer on human chromosome 11p11.2. *Science* **268**: 884–886.
- Dowdy, S. F., Fasching, C. L., Scanlon, D. J., Araujo, D., Livanos, E., Lai, K.-M., Weissman, B. E., and Stanbridge, E. J. (1991). Suppression of tumorigenicity in Wilms' tumor by the p14:p15 region of chromosome 11. *Science* **254**: 293–295.
- Fearon, D. T., and Carter, R. H. (1995). The CD19/CR2/TAPA-1 complex of B lymphocytes: Linking natural to acquired immunity. *Annu. Rev. Immunol.* **13**: 127–149.
- Feinberg, A. P., and Vogelstein, B. (1983). A technique for radiolabelling DNA fragments to high specific activity. *Anal. Biochem.* **132**: 6–13.
- Garvin, A. J., Re, G. G., Tarnowski, B. I., Hazen-Martin, D. J., and Sens, D. A. (1993). The G401 cell line, utilized for studies of chromosomal changes in Wilms' tumor, is derived from a rhabdoid tumor of the kidney. *Am. J. Pathol.* **142**(2): 375–380.
- Giannoukakis, N., Deal, C., Pacquette, J., Goodyer, C., and Polychronakos, C. (1993). Parental genomic imprinting of the human IGF2. *Nature Genet.* **4**: 98–101.
- Guillemot, F., Caspari, T., Tilghman, S. M., Copeland, N. G., Gilbert, D. J., Jenkins, N. A., Anderson, D. J., Joyner, A. L., Rossant, J., and Nagy, A. (1995). Genomic imprinting of Mash2, a mouse gene required for trophoblast development. *Nature* **9**: 235–242.
- Guillemot, F., Nagy, A., Auerbach, A., Rossant, J., and Joyner, A. (1994). Essential role of Mash-2 in extraembryonic development. *Nature* **371**: 333–336.
- Hatada, I., Inazawa, J., Abe, T., Nakayama, M., Kaneko, Y., Jinno, Y., Niikawa, N., Ohashi, H., Fukushima, Y., Iida, K., Yutani, C., Takahashi, S. I., Chiba, Y., Ohishi, S., and Mukai, T. (1996). Genomic imprinting of human p57/KIP2 and its reduced expression in Wilms' tumors. *Hum. Mol. Genet.* **5**(6): 783–788.
- Higgins, M. J., Smilnich, N. J., Sait, S., Koenig, A., Pongratz, J., Gessler, M., Richard, C. W., III, James, M. R., Sanford, J. P., Kim, B.-W., Cattellane, J., Nowak, N. J., Winterpacht, A., Zabel, B. U., Munroe, D. J., Bric, E., Housman, D. E., Jones, C., Nakamura, Y., Gerhard, D. S., and Shows, T. B. (1994). An ordered *NotI* fragment map of human chromosome band 11p15. *Genomics* **23**: 211–222.
- Hoovers, J. M. N., Kalikin, L. M., Johnson, L. A., Alders, M., Redeker, B., Law, D. J., Blied, J., Steenman, M., Benedict, M., Wiegant, J., Lengauer, C., Taillon-Miller, P., Schlessinger, D., Edwards, M. C., Elledge, S. J., Ivens, A., Westerveld, A., Little, P., Mannens, M., and Feinberg, A. P. (1995). Multiple genetic loci within 11p15 defined by Beckwith-Wiedemann syndrome rearrangement breakpoints and subchromosomal transferable fragments. *Proc. Natl. Acad. Sci. USA* **92**: 12456–12460.
- Hu, R.-J., Lee, M. P., Johnson, L. A., and Feinberg, A. P. (1996). A novel human homologue of yeast nucleosome assembly protein, 65 kb centromeric to the p57/KIP2 gene is biallelically expressed in fetal and adult tissues. *Hum. Mol. Genet.* **5**(11): 1743–1748.
- Ioannou, P. A., Amemiya, C. T., Garnes, J., Kroisel, P. M., Shizuya, H., Chen, C., Batzer, M. A., and De Jong, P. J. (1994). A new bacteriophage P1-derived vector for the propagation of large human DNA fragments. *Nature Genet.* **6**: 84–89.
- Junien, C. (1992). Beckwith-Wiedemann syndrome, tumorigenesis and imprinting. *Curr. Opin. Genet. Dev.* **2**: 431–438.
- Karnes, P. S., Tran, T. N., Cui, M. Y., Bogenmann, E., Shimada, H., and Ying, K. L. (1991). Establishment of a rhabdoid tumor cell line with a specific chromosomal abnormality, 46, XY,t(11;22)(p15.5;q11.23). *Cancer Genet. Cytogenet.* **56**: 31–38.
- Kere, J., Nagaraja, R., Mimm, S., Ciccodicola, A., D'Urso, M., and Schlessinger, D. (1992). Mapping human chromosomes by walking with sequence-tagged sites from end fragments of yeast artificial chromosome inserts. *Genomics* **14**: 241–248.
- Koi, M., Johnson, L. A., Kalikin, L. M., Little, P. F. R., Nakamura, Y., and Feinberg, A. P. (1993). Tumor cell growth arrest caused by subchromosomal transferable DNA fragments from chromosome 11. *Science* **260**: 361–364.
- Kondo, M., Matsuoka, S., Uchida, K., Osada, H., Nagatake, M., Takagi, K., Harper, J. W., Takahashi, T., Elledge, S. J., and Takahashi, T. (1996). Selective maternal-allele loss in human lung cancers of the maternally expressed p57/KIP2 gene at 11p15.5. *Oncogene* **12**: 1365–1368.
- Lee, M. P., Hu, R.-H., Johnson, L. A., and Feinberg, A. P. (1997). Human KVLQT1 gene shows tissue-specific imprinting and encompasses Beckwith-Wiedemann syndrome chromosomal rearrangements. *Nature Genet.* **15**: 181–185.
- Loh, W. E., Scrabble, H. J., Livanos, E., Arboleda, M. J., Cavenee, W. K., Oshimura, M., and Weissman, B. E. (1992). Human chromosome 11 contains two different growth suppressor genes for embryonal rhabdomyosarcoma. *Proc. Natl. Acad. Sci. USA* **89**: 1755–1759.
- Mannens, M., Hoovers, J. M. N., Redeker, E., Verjaal, M., Feinberg, A. P., Little, P., Boavida, M., Coad, N., Steenman, M., Blied, J., Niikawa, N., Tonoki, H., Nakamura, Y., de Boer, E. G., Slater, R. M., John, R., Cowell, J. K., Junien, C., Henry, I., Tommerup, N., Weksberg, R., Puschel, S. M., Leschot, N. J., and Westerveld, A. (1994). Parental imprinting of human chromosome region 11p15.3-pter involved in the Beckwith-Wiedemann syndrome and various human neoplasia. *Eur. J. Hum. Genet.* **2**: 3–23.
- Mannens, M., Slater, R. M., Heyting, C., Blied, J., de Kraker, J., Coad, N., de Pagter-Holthuisen, P., and Pearson, P. L. (1988). Molecular nature of genetic changes resulting in loss of heterozygosity of chromosome 11 in Wilms' tumors. *Hum. Genet.* **81**: 41–48.
- Matsuoka, S., M.C., E., Bai, C., Parker, S., Zhang, P., Baldini, A., Harper, J. W., and Elledge, S. J. (1995). p57/KIP2, a structurally distinct member of the p21/CIP1 Cdk inhibitor family, is a candidate tumor suppressor gene. *Genes Dev.* **9**: 650–662.
- Matsuoka, S., Thompson, J. S., Edwards, M. C., Barletta, J. M., Grundy, P., Kalikin, L. M., Harper, J. W., Elledge, S. J., and Feinberg, A. P. (1996). Imprinting of the gene encoding a human cyclin-dependent kinase inhibitor, p57/KIP2, on chromosome 11p15. *Proc. Natl. Acad. Sci. USA* **93**: 3026–3030.
- Miyamoto, T., Jinno, Y., T., S., Ikeda, Y., Masuzaki, H., Niikawa, N., and Ishikawa, M. (1996). Genomic cloning and localization to chromosome 11p15.5 of the human achaete-scute homolog 2 (ASCL2). *Cytogenet. Cell. Genet.* **73**: 312–314.
- Moulton, T., Crenshaw, T., Hao, Y., Moosikasuwan, J., Lin, N., Dembitzer, F., Hensle, T., Weiss, L., McMorro, L., Loew, T., Kraus, W., Gerald, W., and Tycko, B. (1994). Epigenetic lesions at the H19 locus in Wilms' tumor patients. *Nature Genet.* **7**: 440–447.
- Newsham, I., Daub, D., Besnard-Guerin, C., and Cavenee, W. (1994). Molecular sublocalization and characterization of the 11;22 translocation breakpoint in a malignant rhabdoid tumor. *Genomics* **19**: 433–440.
- Neyroud, N., Tesson, F., Denjoy, I., Leibovici, M., Donger, C., Barhanin, J., Fauré, S., Gary, F., Coumel, P., Petit, D., Schwartz, K., and Guicheney, P. (1997). A novel mutation in the potassium channel gene KVLQT1 causes the Jervell and Lange-Nielsen cardioauditory syndrome. *Nature Genet.* **15**: 186–189.
- Ogawa, O., Eccles, M. R., Szeto, J., McNoe, L. A., Yun, K., Maw, M. A., Smith, P. J., and Reeve, A. E. (1993). Relaxation of insulin-like growth factor II gene imprinting implicated in Wilms' tumor. *Nature* **362**: 749–751.
- Ohlsson, R., Nystrom, A., Pfeifer-Ohlsson, S., Tohonen, V., Hedberg, F., Schofield, P., Flam, F., and Ekstrom, T. J. (1993). IGF2 is parentally imprinted during human embryogenesis and in the Beckwith-Wiedemann syndrome. *Nature Genet.* **4**: 94–97.
- Oren, R., Takahashi, S., Doss, C., Levy, R., and Levy, S. (1990). TAPA-1, the target of an antiproliferative antibody, defines a new family of transmembrane proteins. *Mol. Cell. Biol.* **10**(8): 4007–4015.

- Peebles, P. T., Trisch, T., and Papageorge, A. G. (1978). Isolation of four unusual pediatric solid tumor cell lines. *Pediatr. Res.* **12**: 485.
- Qin, S., Nowak, N. J., Zhang, J., Sait, S., Mayers, P. G., Higgins, M. J., Cheng, Y. J., Munroe, D. J., Gerhard, D. S., Weber, B. H., Bric, E., Housman, D. E., Evans, G. A., and Shows, T. B. (1996). A high-resolution physical map of human chromosome 11. *Proc. Natl. Acad. Sci. USA* **93**: 3149–3154.
- Rainier, S., Johnson, L. A., Dobry, C. J., Ping, A. J., Grundy, P. E., and Feinberg, A. P. (1993). Relaxation of imprinted genes in human cancer. *Nature* **362**: 747–749.
- Redeker, E., Hoovers, J. M. N., Alders, M., van Moorsel, C. J. A., Ivens, A. C., Gregory, S., Kalikin, L., Blik, J., De Galan, L., van den Bogaard, R., Visser, J., van der Voort, R., Feinberg, A. P., Little, P. F. R., Westerveld, A., and Mannens, M. (1994). An integrated physical map of 210 markers assigned to the short arm of human chromosome 11. *Genomics* **21**: 538–550.
- Reeve, A. E., Sih, S. A., Raizis, A. M., and Feinberg, A. P. (1989). Loss of allelic heterozygosity at a second locus on chromosome 11 in sporadic Wilms' tumor cells. *Mol. Cell. Biol.* **9**: 1799–1803.
- Reid, L. H., Crider-Miller, S. J., West, A., Lee, M., Massague, J., and Weissman, B. E. (1996a). Genomic organization of the human p57/KIP2 gene and its analysis in the G401 Wilms' tumor assay. *Cancer Res.* **56**: 1214–1218.
- Reid, L. H., West, A., Gioeli, D. G., Phillips, K., Kelleher, K. F., Araujo, D., Stanbridge, E. J., Dowdy, S. F., and Gerhard, D. S. (1996b). Localization of a tumor suppressor gene in 11p15.5 using the G401 Wilms' tumor assay. *Hum. Mol. Genet.* **5**(2): 239–247.
- Russell, M. W., Dick, M., Collins, F. S., and Brody, L. C. (1996). KVLQT1 mutations in three families with familial or sporadic long QT syndrome. *Hum. Mol. Genet.* **5**(9): 1319–1324.
- Sait, S. N. J., Nowak, N. J., Singh-Kahlon, P., Weksberg, R., Squire, J., Shows, T. B., and Higgins, M. J. (1994). Localization of Beckwith-Wiedemann and rhabdoid tumor chromosome rearrangements to a defined interval in chromosome band 11p15.5. *Genes Chromosome Cancer* **11**: 97–105.
- Salkoff, L., Baker, K., Butler, A., Covarrubias, M., Pak, M. D., and Wei, A. (1992). An essential set of K⁺ channels conserved in flies, mice and humans. *Trends Neurosci.* **15**: 161–166.
- Sanguinetti, M. C., Curran, M. E., Zou, A., Shen, J., Spector, P. S., Atkinson, D. L., and Keating, M. T. (1996). Coassembly of K_vLQT1 and mink (IsK) proteins to form cardiac I_{Ks} potassium channel. *Nature* **384**: 80–83.
- Schroeder, W. T., Chao, L. Y., Dao, D. D., Strong, L. C., Pathak, S., Riccardi, V., Lewis, W. H., and Saunders, G. F. (1987). Nonrandom loss of maternal chromosome 11 alleles in Wilms tumors. *Am. J. Hum. Genet.* **40**(5): 413–420.
- Seizinger, B. R., Klinger, H. P., Junien, C., Nakamura, Y., Le Beau, M., Cavenee, W., Emanuel, B., Ponder, B., Naylor, S., Mitelman, F., Louis, D., Menon, A., Newsham, I., Decker, J., Kaelbling, M., Henry, I., and Deimling, A. v. (1991). Report of the committee on chromosome and gene loss in human neoplasia. *Cytogenet. Cell Genet.* **58**: 1080–1096.
- Shepherd, N. S., Pfrogner, B. D., Coulby, J. N., Ackerman, S. L., Vaidyanathan, G., Sauer, R. H., Balkenhol, T. C., and Sternberg, N. (1994). Preparation and screening of an arrayed human genomic library generated with the P1 cloning system. *Proc. Natl. Acad. Sci. USA* **91**: 2629–2633.
- Shizuya, H., Birren, B., Kim, U. J., Mancino, V., Slepak, T., Tachiiri, Y., and Simon, M. (1992). Cloning and stable maintenance of 300-kilobase-pair fragments of human DNA in *Escherichia coli* using an F-factor-based vector. *Proc. Natl. Acad. Sci. USA* **89**(18): 8794–8797.
- Si, Z., and Hersey, P. (1993). Expression of the neuroendocrine antigen and analogues in melanoma. CD9 expression appears inversely related to metastatic potential of melanoma. *Int. J. Cancer* **54**: 37–43.
- Steenman, M. J. C., Rainier, S., Dobry, C. J., Grundy, P., Horon, I. L., and Feinberg, A. P. (1994). Loss of imprinting of IGF2 is linked to reduced expression and abnormal methylation of H19 in Wilms' tumor. *Nature Genet.* **7**: 433–439.
- Strong, M., Chandy, K. G., and Gutman, G. A. (1993). Molecular evolution of voltage-sensitive ion channel genes: On the origins of electrical excitability. *Mol. Biol. Evol.* **10**: 221–242.
- Tanigami, A., Tokino, T., Takiguchi, S., Mori, M., Glaser, T., Park, J. W., Jones, C., and Nakamura, Y. (1992). Mapping of 262 DNA markers into 24 intervals on human chromosome 11. *Am. J. Hum. Genet.* **50**: 56–64.
- Todd, M. C., Xiang, R.-H., Garcia, D. K., Kerbacher, K. E., Moore, S. L., Hensel, C. H., Liu, P., Siciliano, M. J., Kok, K., Berg, A. v. d., Veldhuis, P., Buys, C. H. C. M., Killary, A. M., and Naylor, S. L. (1996). An 80 kb P1 clone from chromosome 3p21.2 suppresses tumor growth in vivo. *Oncogene* **13**: 2387–2396.
- Tsang, P., Gilles, F., Yuan, L., Kuo, Y.-H., Lupu, F., Samara, G., Moosikasuwan, J., Goy, A., Zelenetz, A. D., Salleri, L., and Tycko, B. (1995). A novel L23-related gene 40 kb downstream of the imprinted H19 gene is biallelically expressed in mid-fetal and adult human tissues. *Hum. Mol. Genet.* **4**: 1499–1507.
- Virtaneva, K. I., Emi, N., Marken, J. S., Aruffo, A., Jones, C., Spurr, N., and Schroder, J. P. (1994). Chromosomal localization of three human genes coding for A15, L6, and S5.7 (TAPA1): All members of the transmembrane 4 superfamily of proteins. *Immunogenetics* **39**: 329–334.
- Wadey, R. B., Pal, N., Buckle, B., Yeomans, E., Pritchard, J., and Cowell, J. K. (1989). Mapping of regions of loss of heterozygosity in Wilms' tumors. *Cytogenet. Cell Genet.* **51**: 1100.
- Wang, Q., Curran, M. E., Splawski, I., Burn, T. C., Millholland, J. M., VanRaay, T. J., Shen, J., Timothy, K. W., Vincent, G. M., de Jager, T., Schwartz, P. J., Towbin, J. A., Moss, A. J., Atkinson, D. L., Landes, G. M., Connors, T. D., and Keating, M. T. (1996). Positional cloning of a novel potassium channel gene: KVLQT1 mutations cause cardiac arrhythmias. *Nature Genet.* **12**: 17–23.
- Weissman, B. E., Saxon, P. J., Pasquale, S. R., Jones, G. R., Geiser, A. G., and Stanbridge, E. J. (1987). Introduction of a normal human chromosome 11 into a Wilms' tumor cell line controls its tumorigenic expression. *Science* **236**: 175–180.
- Weksberg, R., Shen, D. R., Fei, Y. L., Song, Q. L., and Squire, J. (1993a). Disruption of insulin-like growth factor 2 imprinting in Beckwith-Wiedemann syndrome. *Nature Genet.* **5**: 143–150.
- Weksberg, R., and Squire, J. S. (1996). Molecular biology of Beckwith-Wiedemann syndrome. *Med. Ped. Oncol.* **27**: 464–469.
- Weksberg, R., Teshima, I., Williams, B. R. G., Greenberg, C. R., Pueschel, S. M., Chernos, J. E., Fowlow, S. B., Hoyme, E., Anderson, I. J., Whiteman, D. A. H., Fisher, N., and Squire, J. (1993b). Molecular characterization of cytogenetic alterations associated with the Beckwith-Wiedemann syndrome (BWS) phenotype refines the localization and suggests the gene for BWS is imprinted. *Hum. Mol. Genet.* **2**(5): 549–556.
- Williams, J. C., Brown, K. W., Mott, M. G., and Maitland, N. J. (1989). Maternal allele loss in Wilms' tumour. *Lancet* **1**: 283–284.
- Wu, C., Zhu, S., Simpson, S., and de Jong, P. J. (1996). DOP-vector PCR: A method for rapid isolation and sequencing of insert termini from PAC clones. *Nucleic Acids Res.* **24**: 2614–2615.
- Zhang, Y., and Tycko, B. (1992). Monoallelic expression of the human H19 gene. *Nature Genet.* **1**: 40–44.

Divergently Transcribed Overlapping Genes Expressed in Liver and Kidney and Located in the 11p15.5 Imprinted Domain

Paul R. Cooper,* Nancy J. Smilnich,* Colleen D. Day,* Norma J. Nowak,* Laura H. Reid,†
R. Scott Pearsall,‡ Mark Reece,§ Dirk Prawitt,[¶] John Landers,|| David E. Housman,||
Andreas Winterpacht,[¶] Bernhard U. Zabel,[¶] Jerry Pelletier,§ Bernard E. Weissman,†
Thomas B. Shows,* and Michael J. Higgins*,[¶]

*Department of Human Genetics and ‡Department of Cellular & Molecular Biology, Roswell Park Cancer Institute, Buffalo, New York 14263; †Department of Pathology and Lineberger Comprehensive Cancer Center, University of North Carolina, Chapel Hill, North Carolina 27599; §McGill Cancer Center, McGill University, Montreal, Quebec, Canada;

[¶]Department of Pediatrics, University of Mainz, Mainz, Germany; and ||Center for Cancer Research, Massachusetts Institute of Technology, Cambridge, Massachusetts 02139

Received November 28, 1997; accepted January 15, 1998

Human chromosomal band 11p15.5 has been shown to contain genes involved in the development of several pediatric and adult tumors and in Beckwith–Wiedemann syndrome (BWS). Overlapping P1 artificial chromosome clones from this region have been used as templates for genomic sequencing in an effort to identify candidate genes for these disorders. PowerBLAST identified several matches with expressed sequence tags (ESTs) from fetal brain and liver cDNA libraries. Northern blot analysis indicated that two of the genes identified by these ESTs encode transcripts of 1–1.5 kb with predominant expression in fetal and adult liver and kidney. With RT-PCR and RACE, full-length transcripts were isolated for these two genes, with the largest open reading frames encoding putative proteins of 253 and 424 amino acids. Database comparison of the predicted amino acid sequence of the larger transcript indicated homology to integral membrane organic cation transporters; hence, we designate this gene *ORCTL2* (organic cation transporter-like 2). An expressed sequence polymorphism provided evidence that the *ORCTL2* gene exhibits “leaky” imprinting in both human fetal kidney and human fetal liver. The mouse orthologue (*Orctl2*) was identified, and a similar polymorphism was used to demonstrate maternal-specific expression of this gene in fetal liver from interspecific F1 mice. The predicted protein of the smaller gene showed no significant similarity in the database. Northern and RACE analyses suggest

that this gene may have multiple transcription start sites. Determination of the genomic structure in humans indicated that the 5'-end of this transcript overlaps in divergent orientation with the first two exons of *ORCTL2*, suggesting a possible role for antisense regulation of one gene by the other. We, therefore, provisionally name this second transcript *ORCTL2S* (*ORCTL2*-antisense). The expression patterns of these genes and the imprinted expression of *ORCTL2* are suggestive of a possible role in the development of Wilms tumor (WT) and hepatoblastoma. Although SSCP analysis of 62 WT samples and 10 BWS patients did not result in the identification of any mutations in *ORCTL2* or *ORCTL2S*, it will be important to examine their expression pattern in tumors and BWS patients, since epigenetic alteration at these loci may play a role in the etiology of these diseases. © 1998 Academic Press

INTRODUCTION

Beckwith–Wiedemann syndrome (BWS) is characterized by numerous growth abnormalities and a 1000-fold increase in the predisposition to childhood tumors, including Wilms tumor (WT), rhabdomyosarcoma (RD), adrenocortical carcinoma, and hepatoblastoma. The gene(s) for BWS has been localized to the 11p15.5 region by linkage analysis of autosomal dominant pedigrees (Ping *et al.*, 1989; Koufos *et al.*, 1989) and also by the identification of chromosomal breakpoints in this region in BWS patients (Mannens *et al.*, 1994; Sait *et al.*, 1994; Hoovers *et al.*, 1995). BWS occurs with an incidence of 1 in 13,700 births, with 15% of these cases being familial and transmitted from maternal carriers, suggestive of an involvement of genomic imprinting. Further support for a role of genomic imprinting comes from the complex inheritance of this condition, with subclasses of patients showing paternal uniparental

Further discussion with the HUGO/GDB Nomenclature Committee indicates that *ORCTL2*, *ORCTL2S*, and *Orctl2* will eventually be renamed using the root *SLC22A* to designate it as a member of the SLC (solute carrier) superfamily.

[¶]To whom correspondence and reprint requests should be addressed at the Department of Human Genetics, Roswell Park Cancer Institute, Elm & Carlton Streets, Buffalo, NY 14263. Telephone: (716) 845-3582. Fax: (716) 845-8449. E-mail: higgins@show.med.buffalo.edu.

disomy (UPD), paternal duplication, or maternal translocations and inversions affecting 11p15.5 (Hoovers *et al.*, 1995; Junien, 1992; Weksberg and Squire, 1996).

Loss of heterozygosity (LOH) at 11p15.5 has been observed in a variety of adult and childhood cancers, including those associated with BWS, suggesting the existence of one or more tumor suppressor genes in this region. Specific loss of maternal 11p15 alleles provides evidence for the involvement of genomic imprinting (Seizinger *et al.*, 1991; Schroeder *et al.*, 1987; Pal *et al.*, 1990; Scrable *et al.*, 1989). Subchromosomal fragment transfer experiments into a G401 rhabdoid tumor cell line and the RD cell line using regions of 11p15.5 have also demonstrated the region's tumor suppressor activity (Koi *et al.*, 1993; Reid *et al.*, 1996a).

Genomic imprinting remains a partially understood mechanism that results in the modification of the genome in the gamete or zygote, generally leading to parental-specific monoallelic or differential allelic expression in somatic tissues of the offspring. Thus far the 11p15.5 region has been shown to contain several genes known to undergo this phenomenon, including *IGF2*, *H19*, *KIP2* (CDKN1C), *IPL*, and *KVLQT1* (Neumann and Barlow, 1996; John and Surani, 1996; Hatada *et al.*, 1996; Matsuoka *et al.*, 1996; Lee *et al.*, 1997a; Qian *et al.*, 1997). Loss of imprinting (LOI) at *H19* and *IGF2* has been detected in BWS patients, and coding mutations in *KIP2* have been identified in a small proportion of cases (Weksberg *et al.*, 1993; Hatada *et al.*, 1996; Joyce *et al.*, 1997; Lee *et al.*, 1997b; O'Keefe *et al.*, 1997). Mouse models that either overexpress *Igf2* (Leighton *et al.*, 1995; Sun *et al.*, 1997) or are *Kip2* knockouts (Zhang *et al.*, 1997; Yan *et al.*, 1997) exhibit most, but not all, phenotypic characteristics typical of BWS. Significantly, none of these mice developed tumors. It has been suggested that combining the defects of these mutant mice might yield a mouse model that recapitulates a more complete range of the BWS phenotypes seen in humans (Reik and Maher, 1997; Hopkin, 1997). These data support the argument that more than one gene contributes to the BWS phenotype, and although *IGF2* and *KIP2* appear to be major contributors, it remains to be determined whether other imprinted 11p15.5 loci are involved in BWS. Disruption of imprinting control, as a result of the BWS-associated rearrangement breakpoints or some other epigenetic modification, could cause aberrant expression of a number of genes in this region.

The identity of imprinted genes in 11p15.5 that contribute to the development of WT (and other tumors) is even less clear (reviewed in Moulton *et al.*, 1996; O'Keefe *et al.*, 1997). LOI at *H19*, *IGF2*, and, to a lesser extent, *KIP2* has been detected in WT (Moulton *et al.*, 1994; Ogawa *et al.*, 1993; Rainier *et al.*, 1993; Steenman *et al.*, 1994). The *IGF2* gene encodes a potent fetal mitogen, and the closely linked *H19* gene may promote tumorigenesis either directly by a loss of tumor suppressor activity (Hao *et al.*, 1993) or by affecting the expression of *IGF2*. However, neither of these loci is included

in the chromosome fragment shown to elicit growth arrest in RD cells (Koi *et al.*, 1993). Considering the proposed function of the *KIP2* protein as a cell cycle regulator (Lee *et al.*, 1995; Matsuoka *et al.*, 1995), its imprinted expression, and its involvement in BWS, one might consider this gene a strong candidate for the elusive 11p15 tumor suppressor gene, *WT2*. Arguing against the involvement of *KIP2* in Wilms tumor is the lack of correlation found between its expression and suppressor activity in the G401 tumorigenicity assay (Reid *et al.*, 1996b). Although *KIP2* has been shown to be down-regulated in most Wilms tumors (Hatada *et al.*, 1996; Thompson *et al.*, 1996), the more direct proof of inactivating mutations in expressing tumors has not been found (Orlow *et al.*, 1996; Overall *et al.*, 1996; O'Keefe *et al.*, 1997). Furthermore, another maternally expressed gene, *H19*, is also repressed in a majority of Wilms tumors (Rainier *et al.*, 1993; Moulton *et al.*, 1994; Steenman *et al.*, 1994). Perhaps this reflects a regional dysregulation and repression of maternally expressed genes in Wilms tumor. In this regard, it is significant that, of all the genetic subclasses of BWS, patients with UPD may have the greatest incidence of tumors (Henry *et al.*, 1991). In principle, these patients would have biallelic expression of all paternally expressed imprinted genes and full or partial null mutations in all maternally expressed genes in 11p15. Loss of imprinting control could have similar consequences affecting multiple genes distributed over several hundred kilobases of DNA.

The BWS and WT phenotypes may, therefore, be attributable to the altered expression of a number of genes in this region. The observation that most imprinted genes are involved at some level in cellular growth argues for the continued exploration of 11p15 for novel imprinted genes whose deregulated expression (or in some cases mutation) can contribute to tumor development and overgrowth syndromes. It is, therefore, important to define the limits of this imprinting domain and to characterize all the genes that lie within it. These studies should yield further imprinted genes and/or tumor suppressors. We generated a detailed physical map in the form of a 1-Mb P1 artificial chromosome (PAC) contig to define the set of genes involved (Reid *et al.*, 1997). Clones from this contig have been used to generate high-throughput genomic sequence (HTGS). PowerBLAST analysis of this sequence identified several homologies with expressed sequence tags (ESTs) from fetal brain or liver in the database that mapped between the imprinted genes *IPL* and *KIP2*, suggesting the possibility that these ESTs represent novel imprinted genes. We report here the isolation of the full-length sequences of the human and mouse genes identified by EST clone 161420 and also that of the human gene identified by EST clone 272021. We present the characterization of these newly identified genes with respect to their expression patterns, sequence homologies, allelic expression patterns, and mutational analysis in BWS and WT.

MATERIALS AND METHODS

Rapid amplification of cDNA ends (RACE) analysis. RACE-ready human and mouse kidney cDNAs (Clontech) were used in amplification experiments with gene-specific primers in a nested PCR strategy in conjunction with the AP1 and AP2 primers (Clontech). The first primer listed for each experiment is regarded as the remote primer. Following primary amplification, a 1000-fold dilution of the reaction was made, and the nested primer was used. Primer sequences for *ORCTL2* 3' RACE were (5'–3') 161D (AGGCAGCCAGGAAGGAGAGCGTGAGCG), then 161Brev (CAGGAGATCCAAGCAGGAGGC). For mouse, *Orctl2* primers were (5'–3') 5' RACE, m161Dr (TCTTGCCCCGCACTGGTTTGGCA), followed by m161BDr (TTTGCGAACCTGCCGAACAC); 3' RACE, m161Bf (GTGTCTCTTCATGCAGTTCTCCATC), then m161Bdf (TATCTGTCTCGGACACTGG). For human *ORCTL2S*, primers used for 5' RACE were (5'–3') 3-272 (CATTCCAGGCGGTACAGTCCGAGCTGC), then either 5-272 (CTGAGGCATCACCTCCTCTGAGAAGCC) or 272B5 (AATCCAGTTCCCAACAGTTGGAG). Typical conditions were 35 cycles with annealing temperatures between 55 and 60°C with extensions of 2 min, in either 5× TNK50 (Blanchard *et al.*, 1993) or 10× PCR Buffer 3 (Boehringer).

Reverse transcriptase-coupled PCR (RT-PCR). RNA from human adult kidney was purchased from Clontech. Total RNA was isolated from cell lines, fetal tissues (obtained from the Brain and Tissue Banks for Developmental Disorders, University of Maryland), and fetal (E17.5) mouse tissues using RNeasy Mini Kits (Qiagen). Approximately 6 µg RNA was digested with RNase-free DNase (GIBCO BRL). Half of the treated RNA was used for first-strand cDNA synthesis with Superscript (GIBCO BRL) reverse transcriptase, and the remainder was incubated in a similar manner without reverse transcriptase. Primer sequences used for amplification between 161420 EST sequence and GRAIL-predicted exons were (5'–3') 161A (CGCTCACCCACCGGCACCCGTGC) and 161L (GATAGCAACCTGCACGTGGCCGAAGAC). Amplification of mouse oligo(dT)-primed kidney cDNA was performed using human *ORCTL2* gene-specific primers 161B (5'–3') (TCGGTCATCTTGCTTACCTACGTGCTG) and 161D (5'–3') (AGGCAGCCAGGAAGGAGAGCTGAGCG).

Mutational analysis in Wilms tumor and BWS patients. Single-stranded conformation polymorphism (SSCP) analysis was carried out as described (Bardeesy *et al.*, 1994) using 8% nondenaturing polyacrylamide gels run at 30 W for 4–5 h. Fourteen sets of primers designed to amplify the entire putative protein coding sequences of *ORCTL2* and *ORCTL2S* were used in this analysis. All primers used for *ORCTL2* except D7.Bf were located in introns near the exon-intron boundaries. Because of the larger exons making up *ORCTL2S*, all but primers 272-4 and 272-5 were from exonic sequence. The primers used for the *ORCTL2* gene were (5'–3') D7.Bf (CCCTGCTGCGCCTTGTCCA) and D7.Br (AGGGGCTGGGGTGTGTGA), D7.Cf (CCTGCAGTCTTTCCAGC) and D7.Cr (GGCCTGGGTACCTGTGGG), D7.Df (GGTCCGACCCGCCCTC) and D7.Dr (CACCTGACTCCAGTCCC), D7.Ef (CTTTCCGCTCAGCTCC) and D7.Er (GTCCTGACCCACAGACTC), D7.Ff (TGCAGCCGAGGCTGTGTGC) and D7.Fr (TCTGGGCAGGGTGTACCT), D7.Gf (GGCCTGAATGGCCTCTCC) and D7.Gr (CTGGCCGCTGTTGGGGCA), D7.Hf (GGTACTCACCCCTGTTC) and D7.Hr (CAGCAGGCCCTGTGTGCC), D7.If (CCACTTCTACCCTCTCTG) and D7.Ir (GAGTGGGCCCCAAGCGG), and D7.Jf (GCCCCACTCAGCTCGG) and D7.Jr (GGCTGCTCCACTCGCTGG). Primers used for the *ORCTL2S* gene were (5'–3') 272-1 (TTTGTCTATGAACAGGCTC) and 272-2 (TCTGAAGCGGTGAATGCC), 272-3 (CCAGCGAGCCTGTGCGTC) and 272-4 (CATACCCAAACAATCCGTGC), 272-5 (TATTCTTTGTGCCAACAC) and 272-6 (GACCCGTTTGGCCGGGAA), 272-7 (CGTTCCTGACACAACGTTC) and 272-8 (GTTCCGGGCCCTTGTGT), and 272-9 (ATGACAGGACGTGAACAT) and 272-10 (AGGAACAATATTGTACTCT). Thirty-five cycles of PCR were carried out at an annealing temperature between 55 and 60°C.

Identification of expressed polymorphisms in human and mouse *ORCTL2*. PCR products amplified with D7.Bf and D7.Br from human DNA samples and exhibiting apparent polymorphisms by SSCP

were cloned into pCR-Script (Stratagene), and six clones from each sample were sequenced by manual cycle sequencing (GIBCO BRL). Sequence variants that resulted in changes of restriction recognition sites were confirmed by digestion of the purified PCR product (Boehringer Mannheim PCR Product Purification Kit) with the appropriate restriction endonuclease. Electrophoresis of PCR products was in 4–5% Nusieve gels (FMC). DNA samples from various cell lines and fetal livers were tested by PCR and subsequent restriction digestion to identify heterozygous samples. For the mouse gene (*Orctl2*), primers (5'–3') m161.UT3 (CAGAATCAACAGGACTTTTGC) and m161.UT2 (GATATGGTAGGATGGAGAAC) were used to amplify a portion of presumptive exon B from DNA of C57BL/6J and PWK mouse strains. SSCP differences were a result of a polymorphic *MspI* site.

Analysis of allelic expression patterns. Allele expression bias of *ORCTL2* in humans was assessed by RT-PCR and direct sequencing with RNA from samples shown to be heterozygous for characterized polymorphisms. To amplify across an intron, a primer was designed from *ORCTL2* exon C (161b-c.r, 5'-CAAACACCGCCCCGCCAG-3') and paired with D7.Bf for RT-PCR. A "touchdown" cycling program consisting of 2 cycles for each 1-degree interval between annealing temperatures of 67 and 62°C and 5 cycles at 61°C, followed by 30 cycles at 60°C was used. RT-PCR products were purified as above, digested for a minimum of 5 h with *AvaI*, *HinfI*, or *BsrFI*, and separated in 5% Nusieve gels. For the mouse *Orctl2* gene, RNA was prepared from (C57BL/6J × PWK)F1 and (PWK × C57BL/6J)F1 fetal liver and kidney, and RT-PCR was carried out using the Superscript OneStep RT-PCR Kit (GIBCO BRL) with primers m161.UT3 and m161.6 (AGGAAGGAGAGTGAGAGTG). After purification, PCR products were digested with *MspI*. Direct sequencing of PCR products was performed on an ABI373A automatic sequencer using primer 161b-c.r for cDNA amplification products and D7.Br for genomic DNA PCR products.

Northern blot analysis. Multiple tissue Northern blots were purchased from Clontech. Hybridizations and washes were carried out as described (Church and Gilbert, 1984). To control for differences in lane loading, EST cDNA clone 645081 (GenBank AA205888), which showed identity to human glyceraldehyde-3-phosphate dehydrogenase (GAPDH) mRNA (GenBank M33197), was hybridized to the same blots.

Computational methods. DNA sequencing of several PAC clones encompassing the BWS/WT2 region (Reid *et al.*, 1997) was carried out at the McDermott Center for Human Growth and Development, University of Texas, Southwestern Medical Center at Dallas (<http://mcdermott.swmed.edu>). Genomic sequence was assessed for coding potential using the client program PowerBLAST (<http://ncbi.nlm.nih.gov/pub/sim2/PowerBLAST>) and a network version of GRAIL (<http://avalon.emp.ornl.gov/GRAIL-bin/EmptyGrailForm>). Database and sequence analyses were performed using the GCG software package, Geneworks, MacVector, and the BLAST network service from the National Center for Biotechnology Information. Transmembrane α -helix prediction was performed at the TMPred—Prediction of Transmembrane Regions and Orientation website (http://ulrec3.unil.ch/software/TMPRED_form.html) using standard criteria (Hofmann and Stoffel, 1993).

RESULTS

Identification and Characterization of the Human *ORCTL2* and *ORCTL2S* Genes

Clones comprising a 1-Mb PAC contig across the imprinted BWS/WT2 region in 11p15.5 (Reid *et al.*, 1997) were used as templates for the determination of the genomic sequence of this region (McDermott Center). We have subjected the sequence (GenBank Accession No. AC001228) obtained from several clones to PowerBLAST analysis (Zhang and Madden, 1997) using

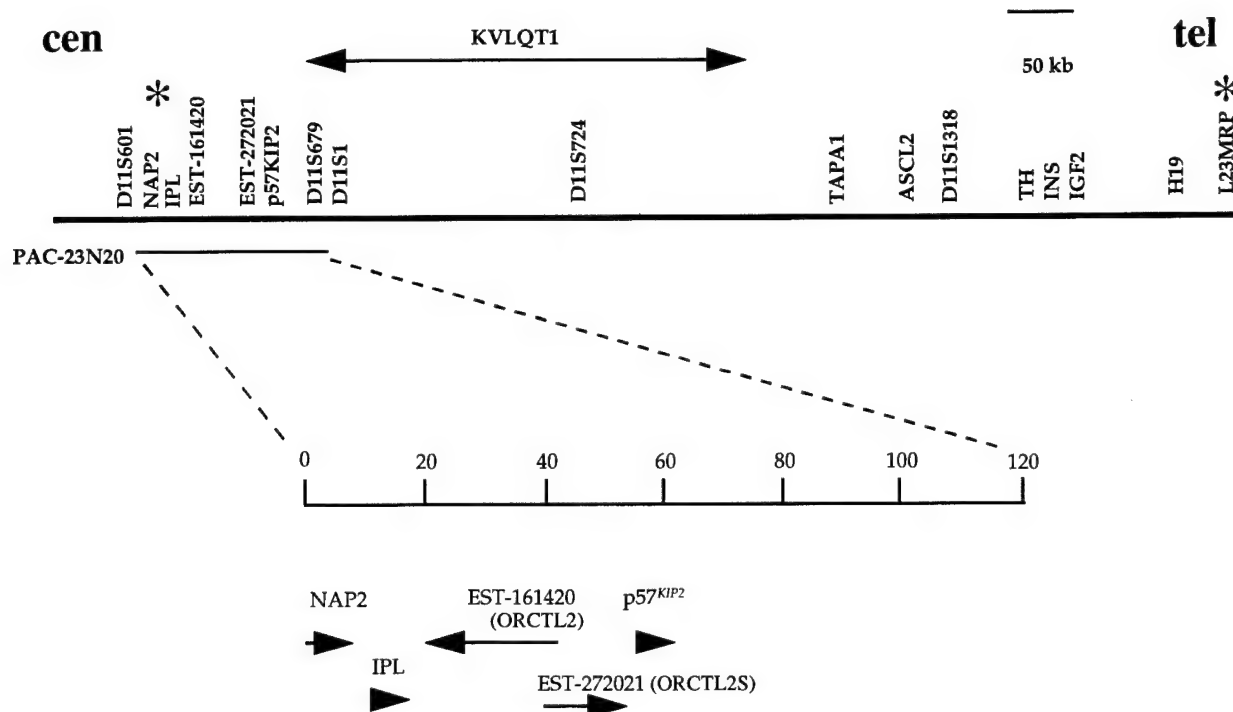


FIG. 1. Map of the 11p15.5 imprinted domain. Asterisks above *NAP2* and *L23MRP* genes mark the proposed centromeric and telomeric boundaries, respectively, of the imprinted region based on their apparent lack of imprinting (Tsang *et al.*, 1996; Hu *et al.*, 1996). The multiple exons of *KVLQT1*, which are spread over 300–350 kb (Lee *et al.*, 1997; Reid *et al.*, 1997), are indicated as the horizontal line above the map. An enlargement of PAC 23N20 is shown below, indicating the location of the 161420 and 272021 ESTs with respect to the imprinted genes *IPL* and *KIP2*. Arrows represent the direction of transcription.

the nonredundant (nr) and expressed-sequence tags (dbEST) databases (Crider-Miller *et al.*, 1997). This analysis resulted in the identification of the previously characterized genes *NAP2* (Hu *et al.*, 1996; Rodriguez *et al.*, 1997), *IPL* (Qian *et al.*, 1997), *KIP2* (Lee *et al.*, 1995; Matsuoka *et al.*, 1995), and *KVLQT1* (Wang *et al.*, 1996). In addition to known genes, a number of EST matches were found, suggesting the presence of several novel 11p15.5 genes. Two of the EST clones (161420 [Accession No. H25530] and 272021 [Accession No. N35348] in Fig. 1) identified in the sequence of PAC clone 23N20, apparently representing different genes, were obtained (IMAGE Consortium) and sequenced in their entirety. The expression pattern of these two transcripts was determined using the cDNA inserts as probes onto multiple tissue Northern blots. These data indicated that the genes identified by these ESTs were predominantly expressed in fetal and adult liver and kidney and adult colon (Fig. 2A). The Northern analysis also indicated that neither of the cDNA clones represented the full-length transcript. GRAIL analysis was performed on the genomic sequence surrounding these genes, resulting in the prediction of several exons of "excellent quality" in the correct orientation 3' to the sequence obtained from cDNA clone 161420 (unlike most EST clones, 161420 is the 5'-end of the gene and was cloned because of an internal *NotI* site in the cDNA). To determine whether these predicted exons were part of the same transcript as identi-

fied by EST 161420, we performed RT-PCR from human kidney RNA using primers 161A and 161L, designed from the EST- and the GRAIL-predicted exon sequences, respectively. Sequencing of the amplification products indicated that six of the seven predicted exons were indeed part of the same gene identified by EST 161420.

To complete the 5'-ends for these two genes, we performed RACE (Chenchik *et al.*, 1995) using RACE-ready kidney cDNA (Clontech). The sequence of the 5' RACE products was compared to that of the genomic DNA obtained from PAC clone 23N20. This allowed verification of the RACE products and determination of each gene's exon-intron structure. The 5' RACE product generated using a primer located 155–177 bp from the 5'-end of EST 161420 co-mapped with the 5'-terminus of this cDNA clone, suggesting that, at least in kidney RNA, clone 161420 contains the 5'-end of the transcript. Comparison of the cDNA sequence to that of the genomic clone demonstrated that the gene associated with the EST 161420 gene is encoded in 11 exons distributed over approximately 23 kb (Fig. 3). 5' RACE using a primer located 85–111 bp from the 5'-end of EST 272021 resulted in three discrete PCR products of 250, 450, and 950 bp (data not shown). The sequence of the 950-bp product combined with that of cDNA clone 272021 indicated that the associated gene comprises four exons spread over about 12 kb (Fig. 3). All of the presumed splice junctions for both genes conformed to

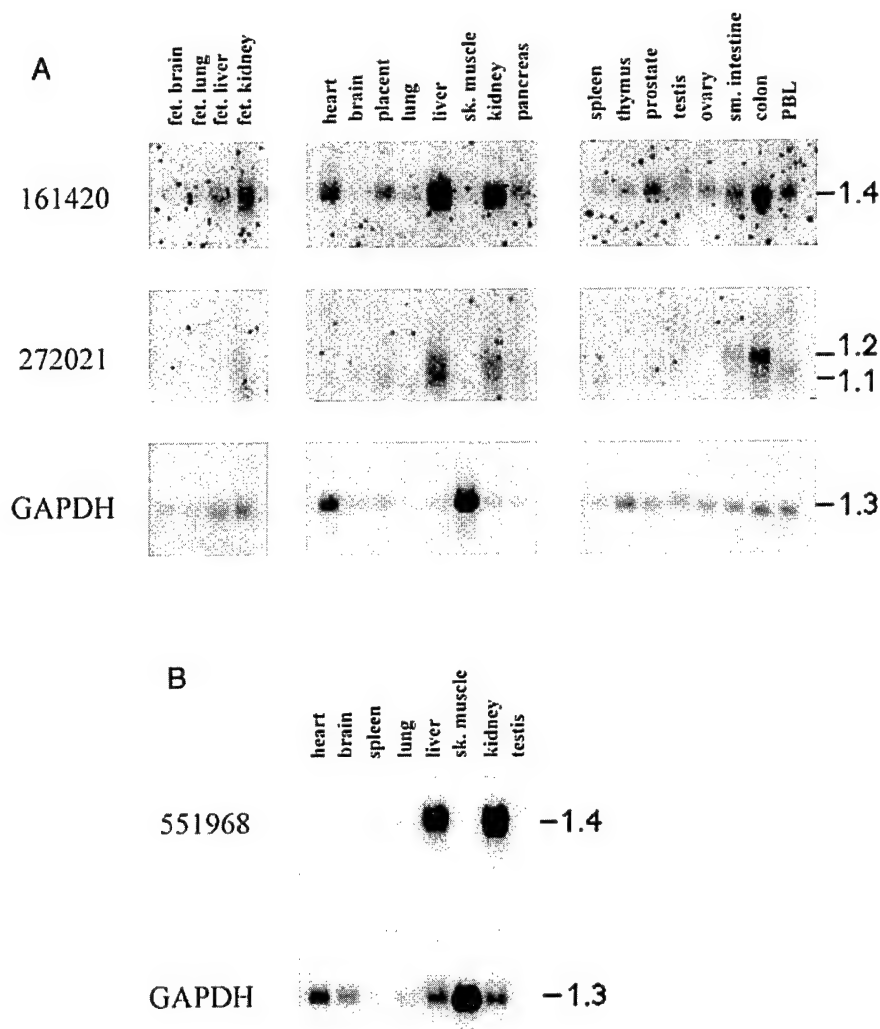


FIG. 2. (A) Northern blot analysis of the 161420 and 272021 ESTs. Inserts from the 161420 and 272021 ESTs were hybridized to multiple tissue Northern blots (Clontech). To control for differences in loading between lanes, the same filters were hybridized with the insert from EST clone 645081 corresponding to the GAPDH gene. (B) Mouse Northern blot analysis using the mouse homolog of the human 161420 EST (EST 551968) and the human GAPDH EST clone 645081 as hybridization probes. Sizes are in kilobases.

the GT-AG rule. This analysis also indicated that the 161420 and 272021 genes are divergently expressed. The transcriptional orientation of the 272021 gene is centromere to telomere, the same direction as the closely linked *KIP2* gene (Reid *et al.*, 1996b), which lies just 2.5 kb downstream. The 161420 gene is transcribed in the telomeric to centromeric direction in the orientation opposite to that of 272021 and the *IPL* gene, which is located approximately 3 kb centromeric to the most 3' exon of the 161420 gene (Figs. 1 and 3). Interestingly, it was also found that exon A of the 272021 transcript overlapped by 31 bp with exon B of the 161420 gene, suggesting a possible role for attenuation between these two genes (Fig. 3). The sequence of the 250-bp 5' RACE product generated from EST 272021 terminated within exon C of this gene (Fig 3). Although the 450-bp 5' RACE product of 272021 was not sequenced, its size is not consistent with it resulting from alternative splicing. These results, combined with the detection on Northern blots (Fig. 2) of more than one

transcript size, suggest that the gene corresponding to the 272021 EST may have multiple transcription start sites or promoters.

Analysis of the 272021 gene sequence indicated that its largest open reading frame (ORF) was 759 bp, capable of coding a protein of 253 amino acids. The predicted protein showed no homology with entries in the databases. Furthermore, no initiation codons that approximated well with that of the Kozak (1991) consensus sequence could be found, and despite the presence of a poly(A) tail, a characteristic polyadenylation signal was absent. The largest potential open reading frame of the 161420 gene identified was 1272 bp, capable of encoding a protein of 424 amino acids. The predicted amino acid sequence of the 161420 ORF was used to search the public databases, resulting in similarities being detected between this protein sequence and several similarly sized integral membrane drug resistance proteins from lower eukaryotic and prokaryotic organisms (Fig. 4). Hydropathy analyses suggested a topol-

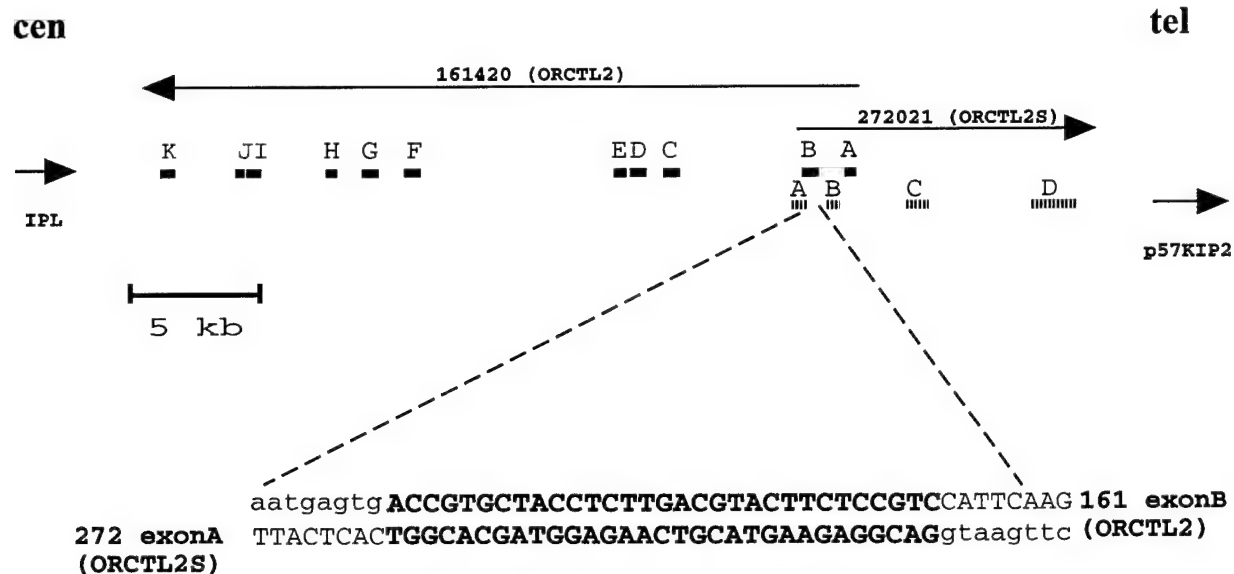


FIG. 3. Exon-intron structure of the genes encoding the 161420 (ORCTL2) and 272021 (ORCTL2S) ESTs. Comparison of the cDNA and genomic DNA sequences allowed the determination of the exon-intron boundaries. The two genes overlap in divergent orientation (arrows represent the direction of transcription). The first exon of the 272021 shares 31 bp (in the antisense direction) with the second exon of the 161420 gene. Uppercase letters represent exonic sequences, lowercase intronic sequences. Shared nucleotides are boldface.

ogy of nine major hydrophobic regions for the 161420 gene that may represent membrane-spanning α -helices. These predicted regions consistently aligned with the positions of the transmembrane regions of the *Escherichia Coli* tetracycline-resistance protein, class E, and with those for the *Bacillus subtilis* multidrug-resistance protein 2 (Allard and Bertrand, 1993; Ahmed *et al.*, 1995). This observation is consistent with the notion that the protein encoded by the 161420 gene is a novel integral membrane pump involved in cellular detoxification. Due to the sequence similarity with drug-resistance proteins and organic cation transporters, we propose that the gene encoding the 161420 cDNA clone be called organic cation transporter-like 2 (ORCTL2, HUGO/GDB Nomenclature Committee). Due to the lack of detectable sequence homology and its overlap and divergent orientation with respect to ORCTL2, the transcription unit coding for the 272021 EST clone is provisionally termed ORCTL2S for ORCTL2-antisense transcript.

Isolation of the Mouse Homolog of the Human ORCTL2 Gene

Initially, RT-PCR was performed with primers designed from the human sequence (161-B and 161-D) using RNA from mouse kidney. This resulted in the generation of a PCR fragment of the predicted size. Comparison of the amplification product's sequence with that of the human sequence verified this PCR product as the likely mouse homolog. Primers were designed from the mouse sequence, and RACE was carried out to obtain the 5'- and 3'-ends of the gene. Subsequent database searches revealed that the sequence of EST clone 551968 (corresponding to the apparent

mouse homolog of the ORCTL2 gene) had recently been deposited. The EST clone and the RACE products were sequenced, resulting in an exact match between the two sequences. Alignment of the human and mouse cDNA sequences showed approximately 75% identity through the ORF. Compared to mouse, the conceptual human protein of the largest ORF contained an additional 12 residues at the amino-terminus (Fig. 4). However, in the cases of both the human and the mouse sequences, the context of the second ATG more closely resembles the Kozak consensus sequence, suggesting that translation may actually begin at this position. The remainder of the two predicted proteins showed greater than 80% sequence identity and 86% amino acid similarity (Fig. 4). Northern blot analysis to adult mouse tissue RNAs using the mouse ORCTL2 homologue cDNA (EST 551968, Accession No. AA087428) gave an expression pattern very similar to that of the human gene, except the murine gene exhibited more restricted expression, primarily in liver and kidney (Figs. 2A and 2B). As would be predicted from the sequence alignments (Fig. 4), hydropathy analysis of Orctl2 indicated membrane-spanning α -helices at approximately the same positions as those predicted for the human ORCTL2 gene.

Mapping by hybridization of the putative mouse gene (Orctl2) to PAC clones from the syntenic region on chromosome 7 added further evidence that the sequence we describe here is the true orthologue of the human gene (M.J.H., unpublished results).

Genomic Imprinting of ORCTL2 in Human and Mouse

The location of ORCTL2 and ORCTL2S between the two imprinted genes IPL and KIP2 (Figs. 1 and 3) sug-

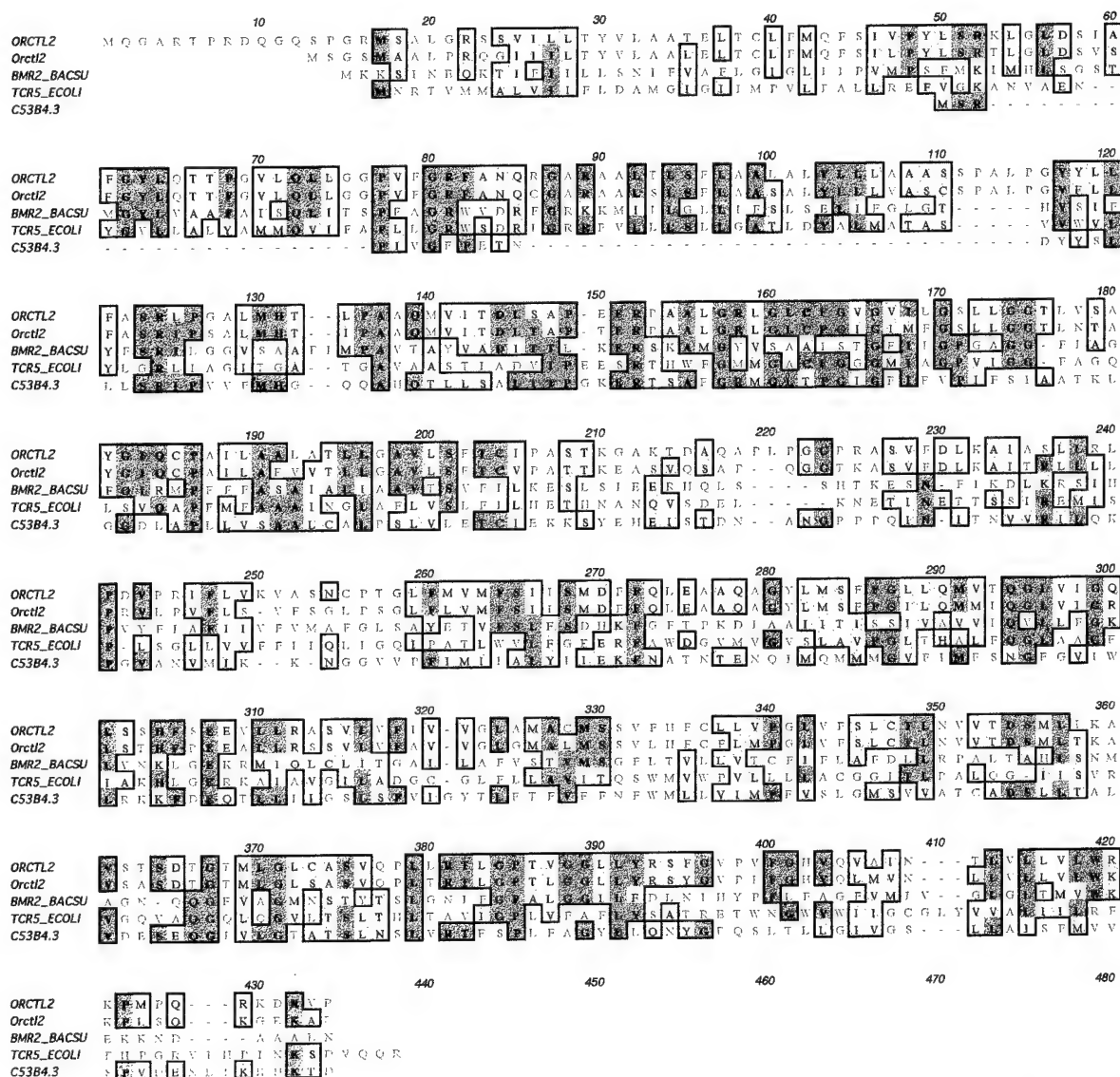


FIG. 4. Multiple sequence alignment using standard parameters of the Clustal W algorithm. Protein sequences that showed a statistically significant sequence similarity to the human and mouse *ORCTL2* proteins as determined by BlastX analysis were used in the alignment. *ORCTL2* and *Orctl2* refer to the human and mouse protein sequences, respectively. *TCR5_ECOLI* refers to the *E. coli* tetracycline-resistance class E protein, *C53B4.3* refers to a *Caenorhabditis elegans* predicted ORF, and *BMR2_BACSU* refers to the *B. subtilis* multidrug-resistance protein 2.

gested that these genes may also be regulated by genomic imprinting. To analyze the imprinting status of the human *ORCTL2* gene, polymorphisms identified by SSCP in exon B (see Fig. 5A for position of PCR primers) were characterized by sequencing. Two sequence differences were identified 13 and 32 bp downstream of the first ATG start codon or 14 and 33 bp upstream of the second ATG codon. These polymorphisms are detectable by *Ava*I or *Hin*FI in one case (*Ava*I and *Hin*FI detect the same polymorphism but recognize opposite alleles) and by *Bsr*FI in the other and, if included in an ORF, would result in conservative amino acid changes (i.e., alanine to threonine at codon 6 and arginine to glutamine at codon 12). Initially, DNA from various cell lines and tissues was tested by PCR for heterozygosity at these two sites. Only one of

six fetal fibroblast cell lines carried both alleles at the *Ava*I/*Hin*FI site, while four were heterozygous at the *Bsr*FI polymorphism. Of 10 human fetal liver DNAs, 4 and 5 showed heterozygosity at the *Ava*I/*Hin*FI and *Bsr*FI sites, respectively (Fig. 5A). These expressed sequence polymorphisms were then used to determine the allelic expression pattern of the *ORCTL2* gene by restriction enzyme digestion of RT-PCR products. To preclude the amplification of genomic DNA contaminating RNA samples, a PCR primer was designed in exon C so that the RT-PCR product would span an intron (Fig. 5A). RT-PCR analysis of liver RNA from four heterozygous fetuses showed varying degrees of preferential expression from one allele (Fig. 5A). For example, liver RNA from fetal sample 9 exhibited nearly exclusive expression of the uncut (258 bp) allele

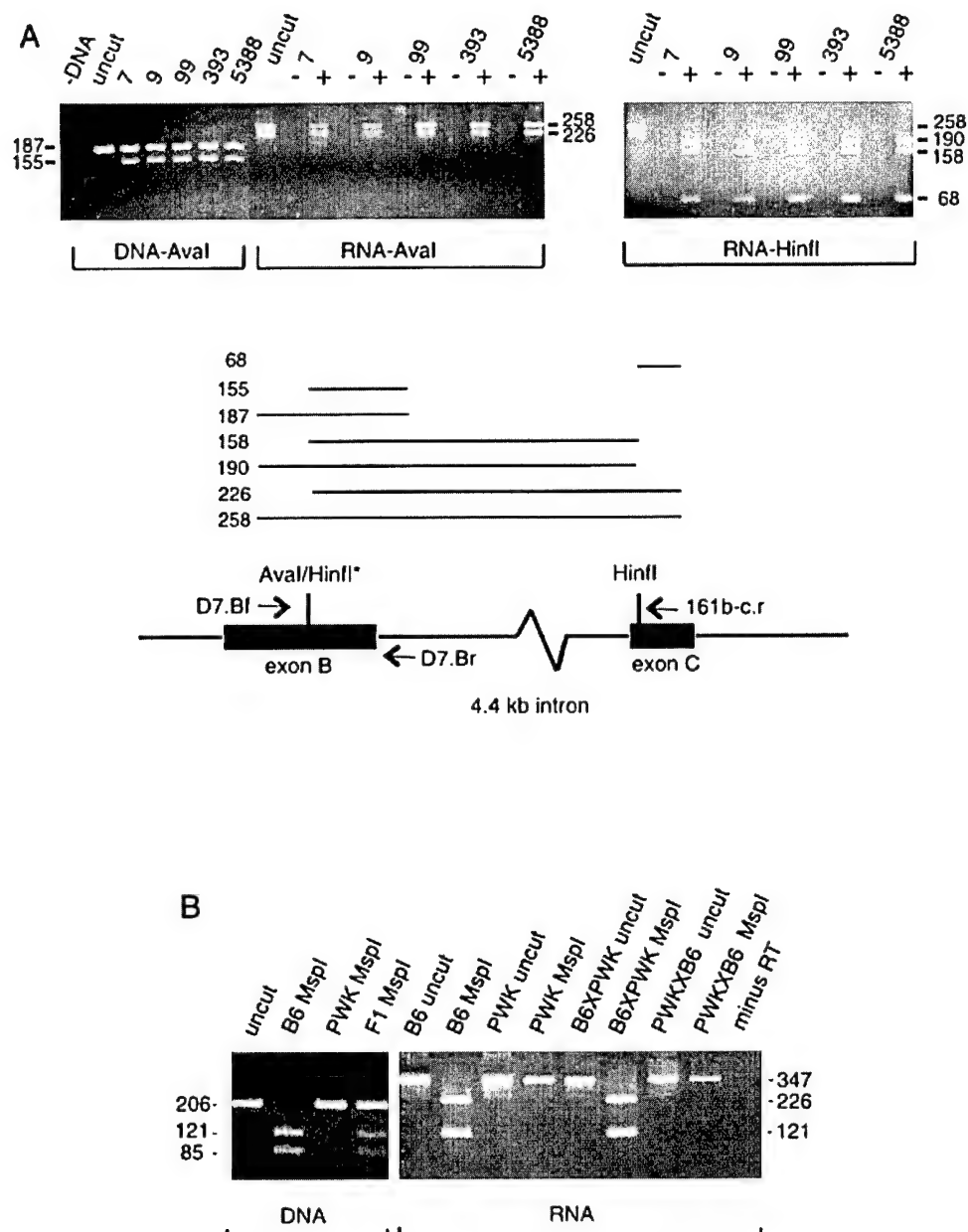


FIG. 5. Allelic expression analysis of the human and mouse *ORCTL2/Orctl2* genes. (A) Primers D7.Bf and D7.Br (see partial exon-intron map below) were used to amplify human genomic DNA samples which were subsequently screened by restriction enzyme digestion for heterozygosity at the *AvaI/Hinfl* polymorphism (*) in exon B. The approximately threefold higher intensity of the 187-bp band compared to the 155-bp band is likely due to the formation of heteroduplexes during PCR (for the *AvaI/Hinfl* site) that are also resistant to cleavage by the restriction enzymes. Five human fetal samples were heterozygous (DNA-*AvaI*). Liver RNA from four of the fetuses and fetal fibroblast line (5388) RNA was subjected to RT-PCR using the D7.Bf and 161b-c.r primers and digested with *AvaI* (RNA-*AvaI*) or *Hinfl* (RNA-*Hinfl*). The map locations of the various restriction fragments observed in the gels are shown schematically above the partial exon-intron map. Fragments that cross the 4.4-kb intron are not drawn to scale. (B) Primers m161.UT2 and m161.UT3 were used to amplify liver genomic DNA from C57BL/6J (B6), PWK, and PWK \times B6 F1 mice. PCR products were then digested with *MspI*, demonstrating that PWK \times B6 F1 offspring are heterozygous for the *MspI* site in (presumptive) exon B of *Orctl2*. RT-PCR was carried out using primers m161.UT3 and m161.6 (in presumptive exon D), resulting in a 347-bp cDNA product that spans two introns. *MspI* digestion of F1 liver RT-PCR products from reciprocal interspecific crosses showed that the maternally derived *Orctl2* allele was exclusively expressed. Sizes are in basepairs.

in *AvaI* digests and predominant expression of the digested (158 bp) allele when *Hinfl* was used. Similarly, RFLP analysis of RT-PCR products from fetal liver sample 7 demonstrated significant bias toward monoallelic expression, but with the smaller (226 bp) allele predominating following digestion with *AvaI* and the

larger (190 bp) allele after *Hinfl* digestion. Fetal liver samples 99 and 393 exhibited observable but less marked bias in allelic expression (Fig. 5A), and kidney samples from the same fetuses showed allelic expression bias similar to that of their liver counterpart (data not shown). In contrast, the fetal skin fibroblast cell

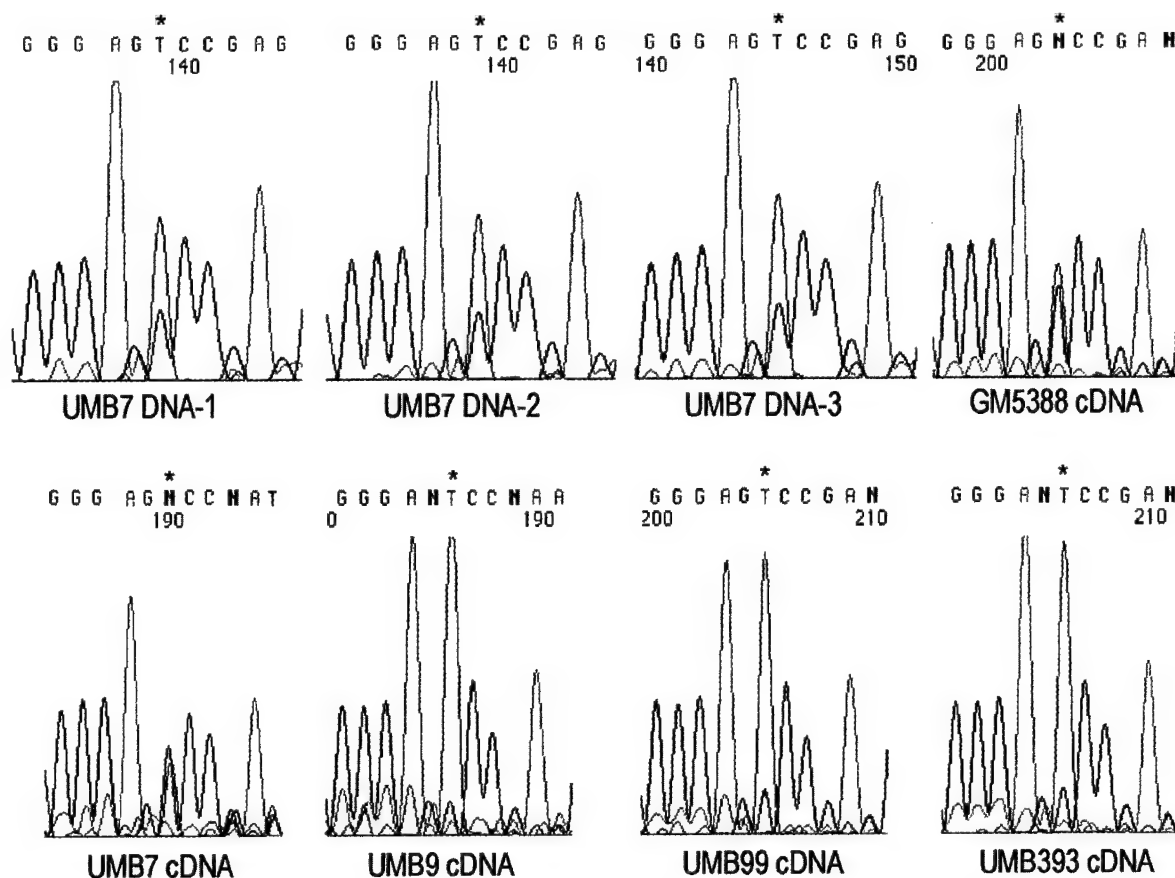


FIG. 6. Electropherograms of direct fluorescence sequencing of genomic DNA PCR and RT-PCR products. The first three panels represent the sequence encompassing the polymorphic *AvaI/HinfI* site in independently amplified PCR products from the heterozygous sample UMB7 using primers D7.Bf and D7.Br. Despite the expectation of roughly equal signals, integration of the separate C and T peaks indicated a 2.5-fold greater signal in the T peak. A factor of 2.5 was therefore used to normalize the C and T peaks in the cDNA samples. An asterisk marks the position of the polymorphic site.

line GM05388 showed what appeared to be nearly biallelic expression of *ORCTL2* (Fig. 5). This apparent biallelic expression was also observed in other fetal fibroblast cell lines as well as in lymphoblast cell lines (data not shown).

Preferential expression of one allele was confirmed by direct fluorescence sequencing of RT-PCR products (Fig. 6). To correct for unequal signal intensity of fluorescent dideoxy-terminators, three independently amplified samples of DNA from UMB7 liver were sequenced directly. Since this sample is known to be heterozygous at the *AvaI/HinfI* polymorphism (Fig. 5A), one might expect similar-sized peaks representing the two alleles. However, as can be seen in Fig. 6, the T peak is consistently greater in area by approximately 2.5-fold compared to the C peak. Using this value to normalize the weaker C signal, direct sequencing of cDNA from four fetal liver samples demonstrated preferential expression from one allele. For example, cDNA from UMB9 had a normalized C peak that was only 22% of the T peak. The underrepresented allele in the remaining fetal liver cDNA samples was estimated to be one-third of the preferentially expressed allele. Thus, this assay demonstrated that, in fetal liver, one

allele contributed an average of 4.5 times as much mRNA to the steady-state RNA levels than did the lower expressed allele. Surprisingly, in fibroblast line GM05388, direct sequencing suggested a weak allelic bias, with the less abundant allele representing approximately 65% of the more predominant allele.

Because parental DNA for the fetal samples described above was not available, the direction of imprinting (i.e., maternal or paternal) was determined in the mouse, since in all previous examples of imprinted genes, the direction of imprinting in mouse and human is the same. A polymorphism between the inbred strains C57BL/6J (B6) and PWK for an *MspI* site was identified in presumptive exon B of the *Orctl2* gene. B6 mice were homozygous for the presence of the *MspI* site, PWK homozygous for the absence of this site, and F1 offspring heterozygous for the polymorphism (Fig. 5B). When RT-PCR products from (B6 female \times PWK male)F1 fetal liver was digested with *MspI*, only the digested allele was present, with virtually no trace of the undigested allele (on some gels a faint undigested band was visible resulting from either incomplete digestion or very low level expression from the paternal allele). On the other hand, F1 fetal liver RT-PCR prod-

ucts from the reciprocal cross (i.e., PWK female \times B6 male) showed only the undigested band. This result suggests that, in contrast to humans, preferential allelic expression of *Orctl2* is tightly regulated in mouse fetal liver. Furthermore, since in both crosses the expressed allele in F1 fetal liver was derived from the mother, *Orctl2* and, presumably, the human gene (*ORCTL2*) are expressed primarily from the maternal allele.

Mutational Analysis of the *ORCTL2* and *ORCTL2S* Genes

The predominant expression in fetal liver and kidney and map location of these two genes made them good candidates for genes mutated in WT, other embryonal tumors such as hepatoblastoma, and/or BWS. Furthermore, the finding that *ORCTL2* is imprinted in these tissues strengthens the position of this gene as a candidate disease locus. To assess whether these genes contribute to WT or BWS, we analyzed DNA from 62 WTs and 10 BWS patients using SSCP analysis on the putative protein coding exons of both the 161420 and the 272 genes. However, the only SSCP shifts observed were also seen in normal controls and thus represent sequence polymorphisms in the normal population.

DISCUSSION

Our results indicate that *ORCTL2* is imprinted, albeit with varying degrees of "leakiness," in fetal liver and kidney, such that one allele (paternal) is expressed at 20–30% the level of the preferentially expressed allele (maternal) (Figs. 5A and 6). On the other hand, *ORCTL2* is only weakly imprinted, if at all, in fetal fibroblast and lymphoblast cell lines. This apparent lack of imprinting of the *ORCTL2* gene was also observed in other tissues (heart, brain, spleen, thymus) derived from a single fetus (N.J.S., unpublished results). Except for lymphoblast cell lines, adult tissues have not yet been assessed for imprinting. However, preliminary analysis of liver from newborn F1 mice suggests that the strength of imprinting is diminished following fetal development (C.D.D., unpublished results). Leakiness of imprinting or incomplete repression of one allele for genes in this region is not unprecedented, with allelic expression biases of less than 100% being detected for both *KIP2* and *IPL* (Hatada *et al.*, 1996; Matsuoka *et al.*, 1996; Qian *et al.*, 1997).

It is conceivable that this leakiness of imprinting of the *ORCTL2* gene in human fetal liver and kidney could be due to a cellular heterogeneity, with certain populations of cells exhibiting complete repression of one allele and others with biallelic expression. This question will only be answered by the examination of the allelic expression at the single-cell level. However, considering that repression of the paternal mouse allele is virtually complete (Fig. 5B), it seems more likely that some relaxation of imprinting at this locus has

occurred during mammalian evolution. The different allelic expression bias detected between the individual fetuses tested here may also suggest that a polymorphism for imprinting strength exists in the population in general (Fig. 5A).

Although based on its location in a cluster of imprinted genes, one might expect *ORCTL2S* to also show preferential expression of one allele, the imprinted status of this locus remains to be determined due to the lack of useable informative polymorphisms in the human transcript and the inability to identify the mouse orthologue. Direct sequencing of fetal liver and kidney RT-PCR products encompassing a rare *AciI* polymorphism in exon C from a single individual suggested biallelic expression of this transcript (N.J.S., unpublished). However, as mentioned above, 5' RACE experiments suggest the possibility of multiple transcription start sites in *ORCTL2S*, one of which may be located near the 5'-end of exon C and would initiate an RNA that would contain the *AciI* polymorphism. Thus, it is possible that the putative promoter initiating in exon C may not be imprinted, whereas additional upstream promoters may, in fact, direct monoallelic expression. This situation would be somewhat analogous to the differential imprinting observed at the multiple promoters of the *IGF2* gene (Vu and Hoffman, 1994).

The proximity of *ORCTL2* and *ORCTL2S* and the fact that these two genes are known to be expressed in a similar spatial and temporal way raise the possibility that the proteins encoded by these genes are involved in different steps of the same pathway, interact directly, or share regulatory mechanisms. Precedents for divergently transcribed genes involved in the same biochemical pathway include the *GPAT* and *AIRC* genes involved in purine nucleotide synthesis (Gavalas and Zalkin, 1995), for genes transcribing proteins that are part of the same complex include collagen $\alpha 1(\text{IV})$ and $\alpha 2(\text{IV})$ (Heikkilä *et al.*, 1993), and for genes divergently transcribed and linked in the same process include *TAP1* and *LMP2* in antigen processing (Wright *et al.*, 1995). Genes that are found in physical proximity can contribute to the same phenotype when mutated. Such genes include the *SMN* and *NAIP* genes in spinal muscular atrophy (Lefebvre *et al.*, 1995; Roy *et al.*, 1995) and *RAG-1* and *RAG-2*, involved in V(D)J recombination (Oettinger *et al.*, 1990). Pertinently and intriguingly, the sequence overlap of the human *ORCTL2* and *ORCTL2S* genes is reminiscent of that seen in the *WT1* and *Wit-1* genes in 11p13 (Campbell *et al.*, 1994; Eccles *et al.*, 1994). The *WT1* gene encodes a zinc finger protein that acts as a transcription factor, and mutations in this gene have been found in sporadic Wilms tumor cases, Wilms tumor associated with WAGR, and Denys-Drash syndrome (Haber *et al.*, 1991; Little *et al.*, 1992; Pelletier *et al.*, 1991a, b; Baird *et al.*, 1992a, b). *WT1* and *Wit-1* are transcribed in a spatial and temporal pattern that is very similar to that of the *ORCTL2* and *ORCTL2S* genes, and *Wit-1* expression is less abundant than *WT1* expression

(Yeger *et al.*, 1992), as is that of *ORCTL2S* compared to *ORCTL2*. *ORCTL2S* has no homologs in the nucleic acid or protein databases and has no good match to the Kozak consensus sequence or to a consensus polyadenylation signal (although EST clone 272021 did contain a poly[A] tail). These characteristics suggest that *ORCTL2S* may not be translated, as is also thought to be the case for *Wit-1* (Huang *et al.*, 1990). Due to the identification of overlapping transcription start sites of *WT1* and *Wit-1*, Eccles *et al.* (1994) postulated that RNA transcription from the *Wit-1* gene may result in heteroduplex formation with the RNA from the *WT1* gene, with a consequent decrease in translation of the *WT1* protein. It is conceivable that a similar mechanism may occur for the regulation of translation of *ORCTL2* by *ORCTL2S*.

Although we have yet to show imprinted expression of the *ORCTL2S* locus, its divergent orientation and overlap with respect to *ORCTL2* are reminiscent of the *Igf2r/AS-RNA* gene pair in the mouse, of which the proper imprinted expression of *Igf2r* is dependent on the transcription of an oppositely imprinted, divergently oriented, antisense RNA originating from a CpG island in the second intron of *Igf2r* (Barlow, 1997; Wutz *et al.*, 1997). If this analogy were true, one would predict that upstream promoters of *ORCTL2S* might be imprinted on the maternal allele to allow exclusive or preferential expression of the paternal allele. The *ORCTL2/ORCTL2S* gene pair may, therefore, represent an additional example of imprinted genes regulated by an "expression-competition" mechanism, perhaps due to the existence of shared regulatory elements (Bartolomei *et al.*, 1993; Barlow, 1997). Another possibility is that the *ORCTL2S* gene serves more than one function, one involved in the regulation of *ORCTL2* at the level of transcription or translation and the other coding for a polypeptide. The selective use of multiple promoters may dictate in which function an *ORCTL2S* transcript is involved.

The location, expression pattern, and imprinting status of the *ORCTL2* and *ORCTL2S* genes make these loci good candidates for involvement in BWS and WT. Although no mutations were found in patients, the potential contributions of these genes to these disorders cannot be excluded, since the possibility remains that they could be subject to epigenetic alterations. A regional disruption of imprinting could affect a number of genes in 11p15.5, resulting in an up- or down-modulation of their expression levels, as has been previously described for *IGF2*, *H19*, and *KIP2* in WT (Ogawa *et al.*, 1993; Rainier *et al.*, 1993; Moulton *et al.*, 1996; Steenman *et al.*, 1994; Hatada *et al.*, 1996; Thompson *et al.*, 1996). Therefore, their analysis with respect to expression levels in WT is warranted. Evidence thus far suggests BWS and WT could be contiguous gene syndromes with certain genes contributing more to the phenotype than others (Hopkin, 1997; O'Keefe *et al.*, 1997; Reik and Maher, 1997). Hydrophathy analysis and the protein sequence homology detected for the human

and mouse *ORCTL2* predict this gene to encode an integral membrane protein possibly involved in drug or other organic cation transport in or out of the cell. How the *ORCTL2* gene could contribute to BWS or WT when aberrantly expressed or mutated is as yet unclear.

Interestingly, in comparison to other imprinted genes, *ORCTL2* is one of the largest in terms of genomic size (23kb) and, apart from *Igf2r* of mouse and human KVLQT, contains the largest number of exons (Hurst *et al.*, 1996; Lee *et al.*, 1997a). This observation is relevant with respect to the controversy regarding whether imprinted genes have few and small introns and to the associated evolutionary theories (Haig, 1996). However, the isolation of additional genes from 11p15.5 and other imprinted regions is necessary to resolve this debate.

Defining the telomeric and centromeric limits of the 11p15.5 imprinted domain is important toward understanding the mechanism of imprinting, but even more important for the study of tumors that show exclusive maternal LOH in this region. Results so far would suggest that *NAP2* and *L23MRP* define the centromeric and telomeric limits (Hu *et al.*, 1996; Tsang *et al.*, 1995), respectively. Therefore, genes that lie within these boundaries are good candidates for tumor suppressors. The conventional approach of positional cloning coupled with the analysis of HTGS will allow a better understanding of the mechanisms of imprinting and the genes that are under its control. The rapidly expanding database of HTGS provides an unprecedented resource that will enable more efficient gene identification and characterization along with expediting the search for the 11p15.5 imprinting center(s) (Reik and Maher, 1997). Analysis of the HTGS in this region has enabled us to identify other genes that show intriguing expression patterns and are potentially imprinted.

Here we supply the information and reagents for the further characterization and analysis of these two intriguing genes, which will allow determination of their contributions to the BWS and WT phenotypes.

ACKNOWLEDGMENTS

We thank Dr. Glen Evans for genomic sequences, Mr. G. Kohler for computer assistance, the University of Maryland Brain and Tissue Banks for Developmental Disorders, and Mrs. D. Ovak for typing and preparation of the manuscript. This research was supported by NIH Grants HG00333 and CA63333, U.S. Army Grant DAMD-17-94-J-4417, and an AROCC Foundation Grant to T.B.S. as well as NIH Grant CA63176 to B.E.W.

REFERENCES

- Allard, J. D., and Bertrand, K. P. (1993). Sequence of a class E tetracycline resistance gene from *Escherichia coli* and comparison of related tetracycline efflux proteins. *J. Bacteriol.* **175**: 4554-4560.
- Ahmed, M., Lyass, L., Markham, P. N., Taylor, S. S., Vazquez-Laslop, N., and Neyfakh, A. A. (1995). Two highly similar multidrug transporters of *Bacillus subtilis* whose expression is differentially regulated. *J. Bacteriol.* **177**: 3904-3910.

- Baird, P. N., Groves, N., Haber, D. A., Housman, D. E., and Cowell, J. K. (1992a). Identification of mutations in the WT1 gene in tumours from patients with the WAGR syndrome. *Oncogene* **7**: 2141–2149.
- Baird, P. N., Santos, A., Groves, N., Jadresic, L., and Cowell, J. K. (1992b). Constitutional mutations in the WT1 gene in patients with Denys-Drash syndrome. *Hum. Mol. Genet.* **1**: 301–305.
- Bardeesy, N., Falkoff, D., Petruzzi, M. J., Nowak, N., Zabel, B., Adam, M., Aguiar, M. C., Grundy, P., Shows, T. B., and Pelletier, J. (1994). Anaplastic Wilms' tumour, a subtype displaying poor prognosis, harbours p53 gene mutations. *Nature Genet.* **7**: 91–97.
- Barlow, D. P. (1997). Competition—A common motif for the imprinting mechanism? *EMBO J.* **16**: 6899–6905.
- Bartolomei, M. S., Webber, A. L., Brunkow, M. E., and Tilghman, S. M. (1993). Epigenetic mechanisms underlying the imprinting of the mouse *H19* gene. *Genes Dev.* **7**: 1663–1673.
- Blanchard, M. M., Taillon-Miller, P., and Nowotny, P. (1993). PCR buffer optimization with uniform temperature regimen to facilitate automation. *PCR Methods Appl.* **2**: 234–240.
- Campbell, C. E., Huang, A., Gurney, A. L., Kessler, P. M., Hewitt, J. A., and Williams, B. R. G. (1994). Antisense transcripts and protein binding motifs within the Wilms tumour (WT1) locus. *Oncogene* **9**: 583–595.
- Chenchik, A., Moqadam, F., and Siebert, P. (1995). Marathon cDNA amplification: A new method for cloning full length cDNAs. *CLON-TECHNIQUES* **X**: 5–8.
- Church, G. M., and Gilbert, W. (1984). Genomic sequencing. *Proc. Natl. Acad. Sci. USA* **81**: 1991–1995.
- Crider-Miller, S. J., Reid, L. H., Higgins, M. J., Nowak, N. J., Shows, T. B., Futreal, P. A., and Weissman, B. E. (1997). Novel transcribed sequences within the BWS/WT2 region in 11p15.5: Tissue-specific expression correlates with cancer type. *Genomics* **46**: 355–363.
- Eccles, M. R., Grubb, G., Ogawa, O., Szeto, J., and Reeve, A. E. (1994). Cloning of novel Wilms tumor gene (WT1) cDNAs: Evidence for antisense transcription of WT1. *Oncogene* **9**: 2059–2063.
- Gavalas, A., and Zalkin, H. (1995). Analysis of the chicken GPAT/AIRC bidirectional promoter for *de novo* purine nucleotide synthesis. *J. Biol. Chem.* **270**: 2403–2410.
- Haber, D. A., Sohn, R. L., Buckler, A. J., Pelletier, J., Call, K. M., and Housman, D. E. (1991). Alternative splicing and genomic structure of the Wilms tumor gene WT1. *Proc. Natl. Acad. Sci. USA* **86**: 9618–9622.
- Haig, D. (1996). Do imprinted genes have few and small introns? *Bioessays* **18**: 351–353.
- Hao, Y., Crenshaw, T., Moulton, T., Newcomb, E., and Tycko, B. (1993). Tumor-suppressor activity of H19 RNA. *Nature* **365**: 764–767.
- Hatada, I., Inazawa, J., Abe, T., Nakayama, M., Kaneko, Y., Jinno, Y., Niikawa, N., Ohashi, H., Fukushima, Y., Iida, K., Yutani, C., Takahashi, S., Chiba, Y., Ohishi, S., and Mukai, T. (1996). Genomic imprinting of human *KIP2* and its reduced expression in Wilms' tumors. *Hum. Mol. Genet.* **5**: 783–788.
- Heikkilä, P., Soininen, R., and Tryggvason, K. (1993). Directional regulatory activity of cis-acting elements in the bidirectional $\alpha 1(IV)$ and $\alpha 2(IV)$ collagen gene promoter. *J. Biol. Chem.* **268**: 24677–24682.
- Henry, I., Bonaiti-Pellie, C., Chehensse, V., Beldjord, C., Schwartz, C., Utermann, G., and Junien, C. (1991). Uniparental paternal disomy in a genetic cancer-predisposing syndrome. *Nature* **351**: 665–667.
- Hofmann, K., and Stoffel, W. (1993). TMbase—A database of membrane spanning protein segments. *Biol. Chem. Hoppe-Seyler* **347**: 166.
- Hoovers, J. M., Kalikin, L. M., Johnson, L. A., Alders, M., Redeker, B., Law, D. J., Blik, J., Steenman, M., Benedict, M., Wiegant, J., Lengauer, C., Taillonmiller, P., Schlessinger, D., Edwards, M. C., Elledge, S. J., Ivens, A., Westerveld, A., Little, P., Mannens, M., and Feinberg, A. P. (1995). Multiple genetic loci within 11p15 defined by Beckwith-Wiedemann syndrome rearrangement breakpoints and subchromosomal transferable fragments. *Proc. Natl. Acad. Sci. USA* **92**: 12456–12460.
- Hopkin, K. (1997). Beckwith-Wiedemann syndrome: Lone gunman or genetic mob? *J. NIH Res.* **9**: 27–29.
- Hu, R.-J., Lee, M. P., Johnson, L. A., and Feinberg, A. P. (1996). A novel human homologue of yeast nucleosome assembly protein, 65kb centromeric to p57^{KIP2} gene, is biallelically expressed in fetal and adult tissues. *Hum. Mol. Genet.* **5**: 1743–1748.
- Huang, A., Campbell, C., Bonetta, L., McAndrews-Hill, M. S., Chilton-McNeill, S., Coppes, M. J., Law, D. J., Feinberg, A. P., Yeger, H., and Williams, B. R. G. (1990). Tissue, developmental, and tumor specific expression of divergent transcripts in Wilms tumor. *Science* **250**: 991–994.
- Hurst, L. D., McVean, G., and Moore, T. (1996). Imprinted genes have few and small introns. *Nature Genet.* **12**: 234–237.
- John, R. M., and Surani, M. A. (1996). Imprinted genes and regulation of gene expression by epigenetic inheritance. *Curr. Opin. Genet. Dev.* **8**: 348–353.
- Joyce, J. A., Lam, W. K., Catchpoole, D. J., Jenks, P., Reik, W., Maher, E. R., and Schofield, P. N. (1997). Imprinting of *IGF2* and *H19*: Lack of reciprocity in sporadic Beckwith-Wiedemann syndrome. *Hum. Mol. Genet.* **6**: 1543–1548.
- Junien, C. (1992). Beckwith-Wiedemann syndrome, tumorigenesis and imprinting. *Curr. Opin. Genet. Dev.* **2**: 431–438.
- Koi, M., Johnson, L. A., Kalikin, L. M., Little, P. F. R., Nakamura, Y., and Feinberg, A. P. (1993). Tumor cell growth arrest caused by subchromosomal transferable DNA fragments from chromosome 11. *Science* **260**: 361–364.
- Koufos, A., Grundy, P., Morgan, K., Aleck, K. A., Hadro, T., Lampkin, B. C., Kalbakji, A., and Cavenee, W. K. (1989). Familial Wiedemann-Beckwith syndrome and a second Wilms' tumour locus both map to 11p15.5. *Am. J. Hum. Genet.* **44**: 711–719.
- Kozak, M. (1991). Structural features in eukaryotic mRNAs that modulate the initiation of translation. *J. Biol. Chem.* **266**: 19867–19870.
- Lee, M. P., Hu, R.-H., Johnson, L. A., and Feinberg, A. P. (1997a). Human *KVLQT1* gene shows tissue specific imprinting and encompasses Beckwith Wiedemann syndrome chromosomal rearrangements. *Nature Genet.* **15**: 181–185.
- Lee, M. P., DeBaun, M., Randhawa, G., Reichard, B. A., Elledge, S. J., and Feinberg, A. P. (1997b). Low frequency of p57^{KIP2} mutation in Beckwith-Wiedemann syndrome. *Am. J. Hum. Genet.* **61**: 304–309.
- Lee, M.-H., Reynisdottir, I., and Massague, J. (1995). Cloning of p57^{KIP2}, a cyclin-dependent kinase inhibitor with unique domain structure and tissue distribution. *Genes Dev.* **9**: 639–649.
- Lefebvre, S., Burglen, L., Reboullet, S., Clermont, O., Bulet, P., Viollet, L., Benichou, B., Cruaud, C., Millasseau, P., Zeviani, M., Le Paslier, D., Frezal, J., Cohen, D., Weissenbach, J., Munnich, A., and Melki, J. (1995). Identification and characterization of a spinal muscular atrophy-determining gene. *Cell* **80**: 155–166.
- Leighton, P. A., Ingram, R. S., Eggenschwiler, J., Efstratiadis, A., and Tilghman, S. M. (1995). Disruption of imprinting caused by deletion of the *H19* gene region in mice. *Nature* **375**: 34–39.
- Little, M. H., Prosser, J., Condie, A., Smith, P. J., van Heyningen, V., and Hastie, N. D. (1992). Zinc finger point mutations within the WT1 gene in Wilms tumor patients. *Proc. Natl. Acad. Sci. USA* **89**: 4791–4795.
- Mannens, M., Hoovers, J. M. N., Redeker, E., Verjaal, M., Feinberg, A. P., Little, P., Boavida, M., Coad, N., Steenman, M., Blik, J., Niikawa, N., Tonoki, H., Nakamura, Y., de Boer, E. G., Slater, R. M., John, R., Cowell, J. K., Junien, C., Henry, I., Tommerup, N., Weksberg, R., Puschel, S. M., Leschot, N. J., and Westerveld, A. (1994). Parental imprinting of human chromosomal region 11p15.3-pter involved in the Beckwith-Wiedemann syndrome and various human neoplasia. *Eur. J. Hum. Genet.* **2**: 3–23.

- Matsuoka, S., Edwards, M. C., Bai, C., Parker, S., Zhang, P., Baldini, A., Harper, J. W., and Elledge, S. J. (1995). p57KIP2, a structurally distinct member of the p21CIP1 Cdk inhibitor family, is a candidate tumor suppressor gene. *Genes Dev.* **9**: 650–662.
- Matsuoka, S., Thompson, J. S., Edwards, M. C., Barlett, J. M., Grundy, P., Kalikin, L. M., Harper, J. W., Elledge, S. J., and Feinberg, A. P. (1996). Imprinting of the gene encoding a human cyclin-dependent kinase inhibitor, p57(KIP2), on chromosome 11p15. *Proc. Natl. Acad. Sci. USA* **93**: 3026–3030.
- Moulton, T., Crenshaw, T., Hao, Y., Moosikasuwan, J., Lin, N., Dembitzer, F., Hensle T., Weiss, L., McMorrow, L., Loew, T., Kraus, W., Gerald, W., and Tycko, B. (1994). Epigenetic lesions at the *H19* locus in Wilms' tumor patients. *Nature Genet.* **7**: 440–447.
- Moulton, T., Chung, W.-Y., Yuan, L., Hensle, T., Waber, P., Nisen, P., and Tycko, B. (1996). Genomic imprinting and Wilms' tumor. *Med. Pediatr. Oncol.* **27**: 476–483.
- Neumann, B., and Barlow, D. P. (1996). Multiple roles for DNA methylation in gametic imprinting. *Curr. Opin. Genet. Dev.* **6**: 159–163.
- Oettinger, M. A., Schatz, D. G., Gorka, C., and Baltimore, D. (1990). RAG-1 and RAG-2, adjacent genes that synergistically activate V(D)J recombination. *Science* **248**: 1517–1523.
- Ogawa, O., Eccles, M. R., Szeto, J., McNoe, L. A., Yun, K., Maw, M. A., Smith, P. J., and Reeve, A. E. (1993). Relaxation of insulin like growth factor II gene imprinting implicated in Wilms' tumor. *Nature* **362**: 749–751.
- O'Keefe, D., Dao, D., Zhao, L., Sanderson, R., Warburton, D., Weiss, L., Anyane-Yeboah, W., and Tycko, B. (1997). Coding mutations in p57^{KIP2} are present in some cases of Beckwith–Wiedemann syndrome but are rare or absent in Wilms' tumors. *Am. J. Hum. Genet.* **61**: 295–303.
- Orlow, I., Iavarone, A., Crider-Miller, S. J., Bonilla, F., Latres, E., Lee, M.-H., Gerald, W. L., Massagué, J., Weissman, B. E., and Cordón-Cardó, C. (1996). Cyclin-dependent kinase inhibitor p57^{KIP2} in soft tissue sarcomas and Wilms' tumors. *Cancer Res.* **56**: 1219–1221.
- Overall, M. L., Spencer, J., Bakker, M., Dziadek, M., and Smith, P. J. (1996). p57^{KIP2} is expressed in Wilms' tumor with LOH of 11p15.5. *Genes Chromosomes Cancer* **17**: 56–59.
- Pal, N., Wade, R. B., Buckle, B., Yeomans, E., Pritchard, J., and Cowell, J. K. (1990). Preferential loss of maternal alleles in sporadic Wilms' tumour. *Oncogene* **5**: 1665–1668.
- Pelletier, J., Bruening, W., Li, F. P., Haber, D. A., Glaser, T., and Housman, D. E. (1991a). WT1 mutations contribute to abnormal genital system development and hereditary Wilms' tumour. *Nature* **353**: 431–434.
- Pelletier, J., Bruening, W., Kashtan, C. E., Mauer, S. M., Manivel, J. C., Striegel, J. E., Houghton, D. C., Junien, C., Habib, R., Fouser, L., Fine, R. N., Silverman, B. L., Haber, D. A., and Housman, D. (1991b). Germline mutations in the Wilms' tumor suppressor gene are associated with abnormal urogenital development in Denys–Drash syndrome. *Cell* **67**: 437–447.
- Ping, A. J., Reeve, A. F., Law, D. J., Young, M. R., Boehnke, M., and Feinberg, A. P. (1989). Genetic linkage of Beckwith–Wiedemann syndrome to 11p15. *Am. J. Hum. Genet.* **44**: 720–723.
- Qian, N., Frank, D., O'Keefe, D., Dao, D., Zhao, L., Yuan, L., Wang, Q., Keating, M. T., Walsh, C., and Tycko, B. (1997). The *IPL* gene on chromosome 11p15.5 is imprinted in humans and mice and is similar to *TDAG51*, implicated in Fas expression and apoptosis. *Hum. Mol. Genet.* **6**: 2021–2029.
- Rainier, S., Johnson, L. A., Dobry, C. J., Ping, A. J., Grundy, P. E., and Feinberg, A. P. (1993). Relaxation of imprinted genes in human cancer. *Nature* **362**: 747–749.
- Reid, L. H., West, A., Gioeli, D. G., Phillips, K. K., Kelleher, K. F., Araujo, D., Stanbridge, E. J., Dowdy, S. F., Gerhard, D. S., and Weissman, B. E. (1996a). Localization of a tumor suppressor gene to 11p15.5 using the G401 Wilms' tumor assay. *Hum. Mol. Genet.* **5**: 239–247.
- Reid, L. H., Crider-Miller, S. J., West, A., Lee, M. H., Massague, J., and Weissman, B. E. (1996b). Genomic organization of the human p57KIP2 gene and its analysis in the G401 Wilms' tumor assay. *Cancer Res.* **56**: 1214–1218.
- Reid, L. H., Davies, C., Cooper, P. R., Crider-Miller, S. J., Sait, S. N. J., Nowak, N. J., Evans, G., Stanbridge, E. J., de Jong, P., Shows, T. B., Weissman, B. E., and Higgins, M. J. (1997). A 1-Mb physical map and PAC contig of the imprinted domain in 11p15.5 that contains TAPA1 and the BWSCR1/WT2 region. *Genomics* **43**: 366–375.
- Reik, W., and Maher, E. R. (1997). Imprinting in clusters: Lessons from Beckwith–Wiedemann syndrome. *Trends Genet.* **13**: 330–334.
- Rodriguez, P., Munroe, D., Prawitt, D., Chu, L. L., Bric, E., Kim, J., Reid, L. H., Davies, C., Nakagama, H., Loebbert, R., Winterpacht, A., Petrucci, M. J., Higgins, M. J., Nowak, N., Evans, G., Shows, T., Weissman, B. E., Zabel, B., Housman, D. E., and Pelletier, J. (1997). Functional characterization of human nucleosome assembly protein 1 (NAPIL4) suggests a role as a histone chaperone. *Genomics* **44**: 365–367.
- Roy, N., Mahadevan, M. S., McLean, M., Shutler, G., Yaraghi, Z., Farahani, R., Baird, S., Besner-Johnston, A., Lefebvre, C., Kang, X., Salih, M., Aubry, H., Tamai, K., Guan, X., Ioannou, P., Crawford, T. O., de Jong, P. J., Surh, L., Ikeda, J. E., Korneluk, R. G., and MacKenzie, A. (1995). The gene for neuronal apoptosis inhibitory protein is partially deleted in individuals with spinal muscular atrophy. *Cell* **80**: 167–178.
- Sait, S. N. J., Nowak, N. J., Singh-Kahlon, P., Weksberg, R., Squire, J., Shows, T. B., and Higgins, M. J. (1994). Localization of Beckwith–Wiedemann and rhabdoid tumor chromosome rearrangements to a defined interval in chromosome band 11p15.5. *Genes Chromosomes Cancer* **11**: 97–105.
- Scrabble, H., Cavenee, W., Ghavimi, F., Lovell, M., Morgan, K., and Sapienza, C. (1989). A model for embryonal rhabdomyosarcoma tumorigenesis that involves genomic imprinting. *Proc. Natl. Acad. Sci. USA* **86**: 7480–7484.
- Seizinger, B., Klinger, H. P. J., Junien, C., Nakamura, Y., LeBeau, M., Cavenee, W., Emmanueal, B., Ponder, B., Naylor, S., Louis, D., Menon, A., Newsham, I., Decker, J., Knebling, M., Henry, I., and Deimling, A. V. (1991). Report of the Committee on Chromosome and Gene Loss in Human Neoplasia. *Cytogenet. Cell. Genet.* **58**: 1080–1096.
- Schroeder, W. T., Chao, L. Y., Dao, D. D., Strong, L. C., Pathak, S., Riccardi, V., Lewis, W. H., and Saunders, G. F. (1987). Non-random loss of maternal chromosome 11 alleles in Wilms tumors. *Am. J. Hum. Genet.* **40**: 413–420.
- Steenman, M. J., Rainier, S., Dobry, C. J., Grundy, P., Horon, I. L., and Feinberg, A. P. (1994). Loss of imprinting of *IGF2* is linked to reduced expression and abnormal methylation of *H19* in Wilms' tumour. *Nature Genet.* **7**: 433–439.
- Sun, F.-L., Dean, W. L., Kelsey, G., Allen, N. D., and Reik, W. (1997). Transactivation of *IGF2* in a mouse model of Beckwith–Wiedemann syndrome. *Nature* **389**: 809–815.
- Thompson, J. S., Reese, K. J., DeBaun, M. R., Perlman, M., and Feinberg, A. P. (1996). Reduced expression of the cyclin dependent kinase inhibitor p57^{KIP2} in Wilms' tumor. *Cancer Res.* **56**: 5723–5727.
- Tsang, P., Gilles, F., Yuan, L., Kuo, Y. H., Lupu, F., Samara, G., Moosikasuwan, J., Goye, A., Zelenetz, A. D., Selleri, L., and Tycko, B. (1995). A novel L23-related gene 40 kb downstream of the imprinted *H19* gene is biallelically expressed in mid-fetal and adult human tissues. *Hum. Mol. Genet.* **4**: 1499–1507.
- Vu, T. H., and Hoffman, A. R. (1994). Promoter-specific imprinting of the human insulin-like growth factor-II gene. *Nature* **371**: 714–717.
- Wang, Q., Curran, M. E., Splawski, I., Burn, T. C., Millholland, J. M., Van Raay, T. J., Shen, J., Timothy, K. W., Vincent, G. M., de Jager, T., Schwartz, P. J., Toubin, J. A., Moss, A. J., Atkinson, D. L.,

- Landes, G. M., Connors, T. D., and Keating, M. T. (1996). Positional cloning of a novel potassium channel gene: KVLQT1 mutations cause cardiac arrhythmias. *Nature Genet.* **12**: 17–23.
- Weksberg, R., Shen, D. R., Fei, Y. L., Song, Q. L., and Squire, J. (1993). Disruption of insulin-like growth factor 2 imprinting in Beckwith–Wiedemann syndrome. *Nature Genet.* **5**: 143–150.
- Weksberg, R., and Squire, J. A. (1996). Molecular biology of Beckwith–Wiedemann syndrome. *Med. Pediatr. Oncol.* **27**: 462–469.
- Wright, K. L., White, L. C., Kelly, A., Beck, S., Trowsdale, J., and Ting, J. P.-Y. (1995). Coordinate regulation of the human TAP1 and LMP2 genes from a shared bidirectional promoter. *J. Exp. Med.* **181**: 1459–1471.
- Wutz, A., Smrka, O. W., Schwelfer, N., Schellander, K., Wagner, E. F., and Barlow, D. P. (1997). Imprinted expression of the *Igf2r* gene depends on an intronic CpG island. *Nature* **389**: 745–749.
- Yan, Y., Frisen, J., Lee, M. H., Massague, J., and Barbacid, M. (1997). Ablation of the CDK inhibitor p57^{KIP2} results in increased apoptosis and delayed differentiation during mouse development. *Genes Dev.* **11**: 973–983.
- Yeger, H., Cullinane, C., Flenniken, A., Huang, A., Chilton-McNeil, S., Bonetta, L., Campbell, C., McGrews-Hill, M., Coppes, M., Greenberg, M., Thorner, P., and Williams, B. R. G. (1992). Coordinate expression of Wilms' tumor genes correlates with Wilms' tumor phenotypes. *Cell Growth Differ.* **3**: 855–864.
- Zhang, P., Liegeois, N. J., Wong, C., Finegold, M., Hou, H., Thompson, J. C., Silverman, A., Harper, J. W., DePinho, R. A., and Elledge, S. J. (1997). Altered cell differentiation and proliferation in mice lacking p57^{KIP2} indicates a role in Beckwith–Wiedemann syndrome. *Nature* **387**: 151–158.
- Zhang, J., and Madden, T. L. (1997). PowerBLAST: A new network BLAST application for interactive or automated sequence analysis and annotation. *Genome Res.* **7**: 649–656.

A maternally methylated CpG island in *KvLQT1* is associated with an antisense paternal transcript and loss of imprinting in Beckwith–Wiedemann syndrome

NANCY J. SMILINICH*, COLLEEN D. DAY*, GALINA V. FITZPATRICK*, GERMAINE M. CALDWELL*, AMY C. LOSSIE†, P. R. COOPER*, ALLAN C. SMALLWOOD‡, JOHANNA A. JOYCE§, PAUL N. SCHOFIELD§, WOLF REIK¶, ROBERT D. NICHOLLS||**, ROSANNA WEKSBERG††, D. J. DRISCOLL†, EAMONN R. MAHER‡, THOMAS B. SHOWS*, AND MICHAEL J. HIGGINS*‡‡

*Department of Cancer Genetics, Roswell Park Cancer Institute, Elm and Carlton Streets, Buffalo, NY 14263; †Division of Genetics, Department of Pediatrics, University of Florida College of Medicine, Gainesville, FL 32610; ‡Section of Medical and Molecular Genetics, Department of Paediatrics and Child Health, University of Birmingham, The Medical School, Birmingham B15 2TT, United Kingdom; §Laboratory of Stem Cell Biology, Department of Anatomy, University of Cambridge, Cambridge CB2 3DY, United Kingdom; ¶Laboratory of Developmental Genetics and Imprinting, The Babraham Institute, Cambridge CB2 4AT, United Kingdom; ||Department of Genetics, Case Western Reserve University School of Medicine, Cleveland, OH 44106; **Center for Human Genetics, University Hospitals of Cleveland, Cleveland, OH 44106; and ‡‡Department of Genetics, Hospital for Sick Children, Toronto, ON M5G 1X8, Canada

Edited by Stuart H. Orkin, Harvard Medical School, Boston, MA, and approved May 17, 1999 (received for review March 5, 1999)

ABSTRACT Loss of imprinting at *IGF2*, generally through an *H19*-independent mechanism, is associated with a large percentage of patients with the overgrowth and cancer predisposition condition Beckwith–Wiedemann syndrome (BWS). Imprinting control elements are proposed to exist within the *KvLQT1* locus, because multiple BWS-associated chromosome rearrangements disrupt this gene. We have identified an evolutionarily conserved, maternally methylated CpG island (*KvDMR1*) in an intron of the *KvLQT1* gene. Among 12 cases of BWS with normal *H19* methylation, 5 showed demethylation of *KvDMR1* in fibroblast or lymphocyte DNA; whereas, in 4 cases of BWS with *H19* hypermethylation, methylation at *KvDMR1* was normal. Thus, inactivation of *H19* and hypomethylation at *KvDMR1* (or an associated phenomenon) represent distinct epigenetic anomalies associated with biallelic expression of *IGF2*. Reverse transcription–PCR analysis of the human and syntenic mouse loci identified the presence of a *KvDMR1*-associated RNA transcribed exclusively from the paternal allele and in the opposite orientation with respect to the maternally expressed *KvLQT1* gene. We propose that *KvDMR1* and/or its associated antisense RNA (*KvLQT1-AS*) represents an additional imprinting control element or center in the human 11p15.5 and mouse distal 7 imprinted domains.

Genomic imprinting describes the process by which a subset of mammalian genes is “marked” during gametogenesis such that they are expressed differentially in somatic cells depending on their parental origin (1–3). This mark may be differential methylation, because DNA methylation is necessary for the proper regulation of imprinted genes (4). Furthermore, some differentially methylated regions (DMRs) are thought to represent gametic imprints, because they are differentially methylated in male and female germ cells and remain so throughout development (5–10). Nevertheless, the mechanism by which the primary information in these DMRs is used to regulate genomic imprinting is understood only partially. The DMRs of most imprinted genes are associated with short, G-rich, direct repeat sequences (11, 12), which have been postulated to facilitate heterochromatinization and gene silencing at imprinted loci (11). A more recently identified characteristic of imprinted genes is their association, in some cases, with imprinted antisense RNA transcripts. At the paternally ex-

pressed mouse *Igf2* and *Zpf127* (and human homologue) loci, antisense transcripts that are also expressed paternally have been identified and overlap with the protein coding gene (13–15). For the maternally expressed *Igf2r* and *UBE3A* genes, overlapping antisense transcripts have been found and are oppositely imprinted with respect to the protein coding gene (16, 17). It has been proposed that antisense transcripts serve to regulate overlapping genes by promoter or transcript occlusion or by competing with these loci for regulatory elements such as transcription factors or enhancers (18). An allele-specific competitive advantage for each transcript on the respective alleles would lead to imprinted gene expression (19).

Normal mammalian development requires the correct parental contribution of imprinted genes. A lack of biparental contribution or aberrant expression of imprinted genes leads to a variety of developmental abnormalities in the mouse (20–22) and humans (22–27). Human chromosome 11p15.5 contains at least seven imprinted genes (Fig. 1), six of which are preferentially or exclusively expressed from the maternally derived chromosome and one (*IGF2*) of which is expressed primarily from the paternal allele (22). BWS, an overgrowth and cancer predisposition condition that maps to this region, results from the aberrant expression of one or more of these imprinted loci. BWS has a complex genetic etiology and can arise from paternal uniparental disomy (UPD), paternal duplication of 11p15.5, maternally inherited coding mutations in the *p57^{KIP2}* gene, or maternal chromosome rearrangements (26, 28). However, the most common mechanism resulting in BWS is the loss of imprinting (LOI) of *IGF2* without apparent chromosomal abnormalities (26, 29–32). In contrast to Wilms’ tumors where LOI at *IGF2* is usually accompanied by hypermethylation and silencing of the *H19* gene (33, 34), biallelic expression of *IGF2* in BWS usually occurs independently of changes in methylation or expression at *H19* (32).

The identification of an *H19*-independent pathway for LOI at *IGF2* in patients with BWS suggests that at least one additional imprinting control region exists in chromosome band 11p15.5 (31, 32, 35). The existence of additional imprinting control elements is supported by the finding that, although

This paper was submitted directly (Track II) to the *Proceedings* office. Abbreviations: BWS, Beckwith–Wiedemann syndrome; DMR, differentially methylated region; EST, expressed sequence tag; LOI, loss of imprinting; LOH, loss of heterozygosity; RT-PCR, reverse transcription–PCR; RT, reverse transcriptase; UPD, uniparental disomy. Data deposition: The sequence reported in this paper has been deposited in the GenBank database (accession no. AF119385).

‡‡To whom reprint requests should be addressed. e-mail: higgins@shows.med.buffalo.edu.

The publication costs of this article were defrayed in part by page charge payment. This article must therefore be hereby marked “advertisement” in accordance with 18 U.S.C. §1734 solely to indicate this fact.

PNAS is available online at www.pnas.org.

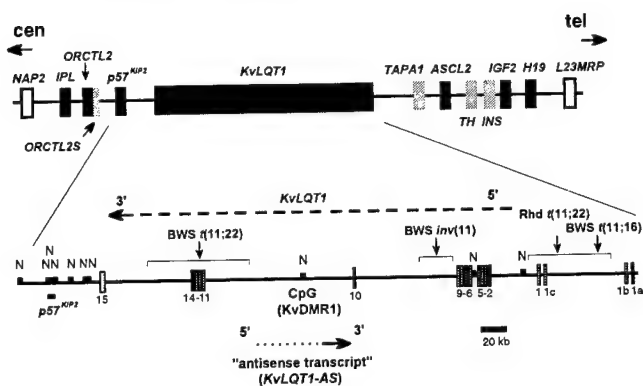


FIG. 1. Map of the 1,000-kb 11p15.5 imprinted domain. The relative location and sizes of genes are drawn approximately to scale, with genes shown to be regulated by genomic imprinting as solid black boxes. Imprinted expression of *ORCTL2S*, *TAPA1*(*CD81*), *TH*, and *INS* (gray boxes) has not yet been established, although *Tapa1* and *Ins* have restricted allele-specific expression in the mouse (22). Presented below the map is an enlargement of the *KvLQT1* locus showing its exon-intron structure (nomenclature from Lee *et al.*; ref. 38) as determined by comparison of the mRNA (GenBank accession no. U89364) and genomic sequences (GenBank accession nos. AC001228, AC003675, U90095, AC002403, AC000377, and AC003693), and the position of the intronic, differentially methylated CpG island *KvDMR1* and *NotI* (N) sites. The direction of transcription of the maternally expressed *KvLQT1* gene and the paternally expressed antisense transcript (*KvLQT1-AS*) are indicated. The approximate locations of the Beckwith-Wiedemann syndrome (BWS) and rhabdoid tumor (Rhd) 11p15.5 rearrangement breakpoints are shown. cen, centromere; tel, telomere.

targeted deletion of *H19* affects the imprinting of *Igf2* and *Ins2* (36), the more distant *Mash2*, *Kvlt1*, and *p57KIP2* genes are unaffected (37). Although effects at more removed loci cannot be excluded, the disruption of the *KvLQT1* gene in multiple cases of BWS patients with chromosome rearrangements suggests that the *KvLQT1* locus may harbor imprinting control elements (38, 39). This report describes the identification and characterization of a region within the human and mouse *KvLQT1* genes that has characteristics of an imprinting control element. We find that the imprinted methylation at this locus is disrupted in a majority of patients with BWS lacking other known genetic defects, and we suggest that this loss of methylation may be causally related to the disease phenotype.

MATERIALS AND METHODS

Cell Lines, Patient Samples, and Mice. Cell lines with names containing the prefix "GM-" were obtained from the NIGMS Human Genetic Mutant Cell Repository. Peripheral blood lymphocytes were obtained from laboratory staff. Wilms' tumor samples were provided by the National Wilms' Tumor Study Group Tissue Bank. Cell lines from patients with BWS carrying the *inv*(11), *t*(11;16), and *t*(11;22) rearrangements as well as a cell line from the rhabdoid tumor with the *t*(11;22) rearrangement have been described by Sait *et al.* (40). Fibroblast or lymphocyte DNA samples from nonrearrangement BWS cases were from patients who have been described (31, 32). Human testis, sperm, and ovaries were obtained as described by Driscoll and Migeon (41). Other fetal tissues were acquired from the Brain and Tissues Banks for Developmental Disorders (University of Maryland). C57BL/6J and PWK inbred mouse strains were provided by Rosemary Elliott (Roswell Park Cancer Institute).

DNA Preparation and Southern Hybridization. Genomic DNA was prepared from cell lines and most tissues by standard proteinase K digestion and phenol extraction. Sperm DNA was isolated from semen as described (41). Probes BX2 and DMRP

were generated by PCR from PAC clone pdJ-74K15 (39) by using primers BX2f (5'-TCCATGCAGGGGATCGG-3') plus BX2r (5'-GCAGTCCACATGGAAGGGCCAAACG-3') and DMRP2f (5'-TCCTGGGGAGGTAGAAATG-3') plus DMRP2r (5'-TGTCTGCCTGCTTCCTCTG-3'), respectively. PCR products were cloned into pCRII-TOPO (Invitrogen). Southern hybridizations were generally carried out as described (40) with two final washes of 0.2× SSC/0.5% SDS at 65°C. Hybridization signal was detected by using a Storm PhosphorImager (Molecular Dynamics). Quantitation of band intensity was done by using National Institutes of Health IMAGE software (rsb.info.nih.gov/nih-image/).

Isolation and Characterization of the Mouse Locus. A portion (subclone 34; sc34) of the corresponding mouse locus was isolated by low-stringency (final washes: 2× SSC/0.5% SDS at 55°C) hybridization of the human locus to a *PsI* subclone library of a murine PAC clone known to span the syntenic region on mouse distal chromosome 7 (42). The locus was expanded by rescreeing the subclone library with a probe generated from the mouse PAC by using a linker-mediated PCR method (39) and a unique primer (sc34.3: 5'-GGTCCTGAATATACTAGAAACCC-3') designed from the sequence of sc34.

Reverse Transcription-PCR (RT-PCR). Total RNA was isolated from cell lines and tissues by using RNeasy Mini Kits (Qiagen, Chatsworth, CA), and ~6 µg of RNA was treated with RNase-free DNase (GIBCO/BRL). Half of the treated RNA was used for first-strand cDNA synthesis with Superscript II (GIBCO/BRL) reverse transcriptase (+RT) by using either oligo(dT) or an antisense strand-specific (sense with respect to *KvLQT1* mRNA) primer. The remainder of the treated RNA was incubated in a similar manner but without reverse transcriptase (-RT). The sequence of primers used for expressed sequence tag (EST) "connection," "transcript sampling," and expression analysis in single chromosome 11 hybrids (see Fig. 2 for primer positions) as well as those used for strand-specific reverse transcription are available on request from the authors.

Analysis of Allelic Expression Patterns in the Mouse. An expressed polymorphism in the mouse antisense transcript was detected between C57BL/6J and PWK mice by single-strand conformation polymorphism analysis by using genomic DNA and primers sc34.1 (5'-TTGCCTGAGGATGGCTGTG-3') and sc34.2 (5'-CTTCCGCTGTAACTTTCTG-3') with 0.5× MDE gels (FMC; 32 W; 3.5 h; 4°C). Cloning into pCRII-TOPO and sequencing identified a single base pair (A-G) polymorphism (position 4,231 in GenBank accession no. AF119385) between C57BL/6J and PWK mice, respectively. Allelic expression analysis was performed by using the same primers but with cDNA made from F₁ fetal tissue RNA. Polymorphism characterization and assessment of imprinting at *Kvlt1* were carried out as described above but with primers *Kvlt1*5.5 (5'-GGGTAGAGCCTGACTCCTTCATTC-3') and *Kvlt1*6 (5'-TAGGGTGGACAGTGGACAATCC-3'). Two polymorphisms between C57BL/6J and PWK mice were found: a dinucleotide substitution, GC/CA in C57BL/6J and PWK, respectively, at position 2,460-2,461 in the 3' untranslated region of the *Kvlt1* mRNA (GenBank accession no. U70068) and an insertion-deletion polymorphism (C) at position 2,481.

Bioinformatics. CpG islands were located by using GRAIL (avalon.epn.ornl.gov/Grail-bin/EmptyGrailForm). Database searches were performed by using BLAST at the National Center for Biotechnology Information web site (www.nlm.nih.gov/cgi-bin/BLAST/nph-blast?Jform=0). Direct repeat structures (see Fig. 2 for locations) were identified by dot matrix analysis by using the PUSTELL DNA MATRIX module (window = 40 min; percentage score = 57) in MACVECTOR (Oxford Molecular Group, Campbell, CA).

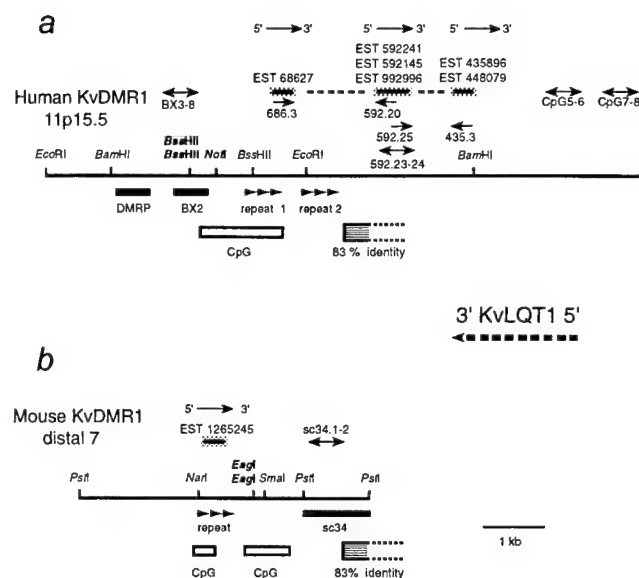


FIG. 2. The human and mouse *KvDMR1* loci. (a) Physical map of the human locus showing restriction sites with respect to hybridization probes DMRP and BX2 (solid black boxes), the *KvDMR1* CpG island, the position of two direct repeat structures, and several ESTs transcribed in the opposite (antisense) direction compared with *KvLQT1*. The dashed line connecting these cDNA fragments indicates that amplification products joining these cDNA fragments could be obtained by RT-PCR by using EST-specific primers. The bidirectional arrows (primer names indicated above) correspond to positive RT-PCR assays used to "sample" the genomic DNA sequence for expressed sequences. (b) Physical map of the syntenic mouse locus (same symbols as in a). A region of homology (83% identity over 437 bp) between the mouse and human loci is indicated by the striped box (the open end indicates that the downstream extent of homology is unknown, as the mouse sequence is not complete).

RESULTS

Maternal-Specific Methylation at *KvDMR1*. One-third (>325 kb) of the 1-Mb imprinted domain in 11p15.5 is occupied by the *KvLQT1* gene, in which protein-coding mutations result in Romano-Ward and Jervell and Lange-Nielsen syndromes (43). The human and mouse (*KvLqt1*) genes are regulated by genomic imprinting in a developmental and tissue-specific manner (37, 38, 44–46); however, features characteristic of imprinted genes, such as differentially methylated CpG-rich regions (DMRs) and short direct tandem repeat structures (11, 12), have not been reported. Large-scale sequencing of PAC clone pdJ-74K15 (GenBank accession no. U90058; ref. 39) and computer analysis identified a *NotI*-site-containing CpG island (designated *KvDMR1*) in intron 10 of *KvLQT1*, which also contained two direct repeat sequence motifs (Figs. 1 and 2a). Two probes, DMRP and BX2 (Fig. 2a), were developed by PCR and hybridized to Southern blots of normal human DNA digested with the methylation-sensitive enzymes *NotI* or *BssHII* and either *EcoRI* or *BamHI*. The 4.2-kb *EcoRI* and 6.0-kb *BamHI* fragments detected by these probes were digested only partially with *NotI* or *BssHII*, presumably because of differential methylation (Fig. 3a and data not shown). A similar experiment with DNA from Wilms' tumors that had LOH in 11p15 showed that the uncut 6.0-kb *BamHI* fragments were absent or greatly reduced (Fig. 3b). Because virtually all 11p15 LOH observed in Wilms' tumors involves the maternal chromosome, these results suggest that the observed differential methylation was likely due to complete methylation on the maternally derived chromosome.

To confirm the parental origin of the methylated *KvDMR1* allele and to show that this methylation was regulated by genomic imprinting, the mouse locus was identified and used

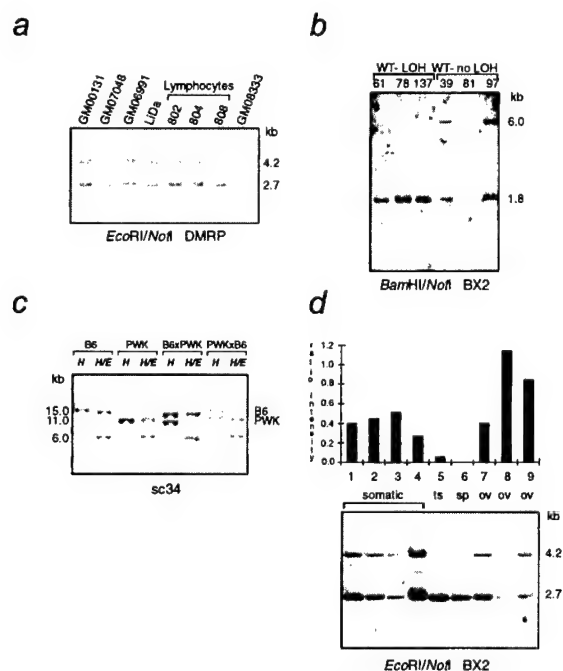


FIG. 3. Differential methylation of *KvDMR1*. (a) DNA isolated from normal lymphoblastoid (GM00131, GM07048, and GM06991), peripheral blood lymphocyte (802, 804, and 808), or fibroblast (GM08333) cells was digested with *EcoRI* and *NotI* and hybridized with DMRP (see Fig. 2a). (b) Southern blot of *BamHI/NotI*-digested DNA from Wilms' tumors (WT) with loss of heterozygosity (LOH) or without LOH (no LOH) in 11p15 and hybridized with the BX2 probe (Fig. 2a). (c) Hybridization of sc34 to *HindIII* (H) and *HindIII/EagI* (H/E) double digests of adult kidney DNA from reciprocal [C57BL/6J (B6) x PWK]F₁ animals (for F₁ hybrids, the maternal parent is specified first). (d) The BX2 probe was hybridized to *EcoRI/NotI* digests of human DNA from somatic tissues (peripheral blood lymphocytes or brain), testes (ts), sperm (sp), and fetal ovaries (ov). The ratio of the intensity of the upper and lower bands is shown in the accompanying histogram. The faint band at 3–3.5 kb present in all lanes is a cross-hybridizing locus observed when experiments are done at reduced stringency. The additional band seen in the sperm lane is likely due to a heterogeneous methylation at this cross-reacting locus.

to analyze DNA isolated from adult kidney. sc34 (Fig. 2b) detected a *HindIII* restriction fragment length polymorphism between C57BL/6J and PWK mice. In (C57BL/6J x PWK)F₁ interspecific animals, only the 11.0-kb PWK (paternal) allele was cleaved by the methylation-sensitive restriction enzyme *EagI*, whereas, in F₁ DNA from the reciprocal cross, the paternally derived 15.0-kb C57BL/6J allele was cut by *EagI* (Fig. 3c). The observed allele-specific methylation illustrates that *KvLQT1* has a DNA methylation imprint typically associated with imprinted genes (11, 12), providing evidence for maternal-specific methylation in the human 11p15.5/mouse distal 7 imprinted domain.

To determine whether the methylation at *KvDMR1* represents an imprinting mark established in the germ line, BX2 was hybridized to *EcoRI/NotI* digests of human somatic and germ-line DNA samples (Fig. 3d). In this experiment, the average ratio of the intensity of the uncut (methylated) to cut (unmethylated) band for somatic cell DNA was 0.4. Methylation at this locus was virtually absent in sperm DNA but enriched in two (ratio = 0.8 and 1.1) of three fetal ovary DNA samples. Because ovary samples typically contain 70% somatic cells (41), these results are consistent with the *NotI* site being completely methylated in human oocytes. The lack of enrichment in one ovarian specimen may reflect a larger than average contribution of somatic tissue in this dissection. Although definitive proof of maternal methylation during gametogenesis awaits analysis of purified oocytes, these results are consistent

with maternal-specific methylation at *KvDMR1* and, together with the finding of differential methylation at this site in murine embryonic stem cells (data not shown), suggest that this epigenetic difference represents a true gametic imprinting mark.

Identification of Human (*KvLQT1*) and Mouse (*Kvlqt1*) Antisense Transcripts. Further characterization of the mouse locus (GenBank accession no. AF119385) located the differentially methylated *EagI* site(s) within a CpG island and identified a direct repeat sequence (Fig. 2b) in a position analogous to the human CpG island. Sequence alignment uncovered a region of 83% identity over >400 bp between human and mouse loci (see Fig. 2); however, no consensus splice sites could be found. BLAST analysis of *KvDMR1* and flanking sequences identified several ESTs in human and one in mouse representing sequences transcribed in the opposite orientation with respect to *KvLQT1* (Fig. 2). RT-PCR analysis with oligo(dT)-primed cDNA from human fetal liver RNA suggested that these cDNAs represented fragments of the same transcript (Fig. 4a). All EST and RT-PCR sequences were continuous with genomic DNA and showed no evidence of exon-intron boundaries. For each RT-PCR experiment, identical results were obtained when cDNA synthesis was

carried out with primers specific for transcripts from the antisense strand (with respect to the direction of transcription of *KvLQT1*). Although RT-PCR detected transcripts in all human fetal tissues tested (Fig. 4a), corresponding transcripts were not detectable on Northern blots (CLONTECH) made from fetal or adult RNAs. Mouse EST 1265245 and human EST 68627 contained potential ORFs (150–400 bp) but are unlikely to reflect protein-coding potential, considering that no homology (at the nucleotide or amino acid level) exists between them. Although its length and potential overlap with *KvLQT1* exons remain to be determined, we have designated this transcript *KvLQT1-AS* (*KvLQT1* antisense).

Imprinted Expression of *KvLQT1/Kvlqt1-AS*. Because of the proximity to *KvDMR1*, we wished to determine whether *KvLQT1-AS* was imprinted. However, no polymorphisms were detected in 12 individuals after single-strand conformation polymorphism scanning of 450 bp and restriction-endonuclease-fingerprinting analysis of 2,600 bp (data not shown). We therefore took advantage of a recently developed panel of single human chromosome 11 somatic cell hybrids that have been characterized with respect to their expression of the imprinted *H19* and *IGF2* genes and methylation at *KvDMR1* (47). Primers designed for ESTs 68627, 592241, and 435896 (Fig. 2a) were used in oligo(dT)-primed RT-PCR analysis of these hybrids, and, as illustrated for the EST 592241 primer pair (Fig. 4b), expression was observed only in the six hybrids shown to contain an unmethylated chromosome 11 (i.e., paternal). Identical results were obtained when this experiment was repeated with a primer designed for reverse transcription of the antisense RNA. By using an expressed sequence polymorphism, RT-PCR analysis with either strand-specific or oligo(dT)-primed cDNA of embryonic day-14.5 fetal liver from (C57BL/6J × PWK)_{F1} offspring identified exclusive paternal expression of the mouse antisense transcript (Fig. 4c), confirming the pattern of expression for the human transcript. Furthermore, we found that *Kvlqt1-AS* is also paternally expressed in embryonic day-14.5 mouse kidney, lung, gut, and heart (data not shown), the same fetal tissues shown in earlier studies (44–46) to have exclusive maternal expression of *Kvlqt1*.

Loss of Imprinting at *KvDMR1* in Patients with BWS. Because all BWS chromosome rearrangements in BWS breakpoint cluster 1 (*BWSC1*) are located within the *KvLQT1* gene (38, 39), it has been postulated that the disruption of the *KvLQT1* genomic region affects the imprinting of *IGF2* and perhaps other genes in the 11p15 domain (38). Because epigenetic changes at *KvDMR1* might be related to this deregulation, the methylation status of this locus was tested in several classes of patients with BWS. Reduced methylation at *KvDMR1* was observed in three patients with paternal UPD (Fig. 5a and not shown), reflecting the mosaic nature of UPD in BWS (28). Of 12 patients without UPD and with normal methylation at *H19* (31, 32), 5 showed complete loss of the methylated band, whereas all 4 patients with BWS and hypermethylation at *H19* (31, 32) showed normal methylation at *KvDMR1* (Fig. 5a and data not shown). Of the five patients with loss of methylation at *KvDMR1*, two were informative for the *ApaI/AvaII* polymorphism described in *IGF2* (48) and both showed LOI at *IGF2* (32). All seven samples with normal methylation at *KvDMR1* and *H19* were uninformative at *IGF2*, precluding assessment of imprinting in these patients. However, three of these have been shown to have mutations in the *p57^{KIP}* gene (A.C.S. and E.R.M., unpublished work). DNA from an aborted fetus with BWS, a maternally inherited *inv(11)(p13;p15.5)* (40), and LOI at *IGF2* also showed loss of methylation at *KvDMR1* (Fig. 5b), indicating that the *inv(11)* affected imprinted loci separated by 500 kb and on either side of the breakpoint. Two additional BWS translocations and one rhabdoid tumor translocation (40) showed normal methylation at *KvDMR1* (Fig. 5b); the allelic expression pattern of *IGF2*

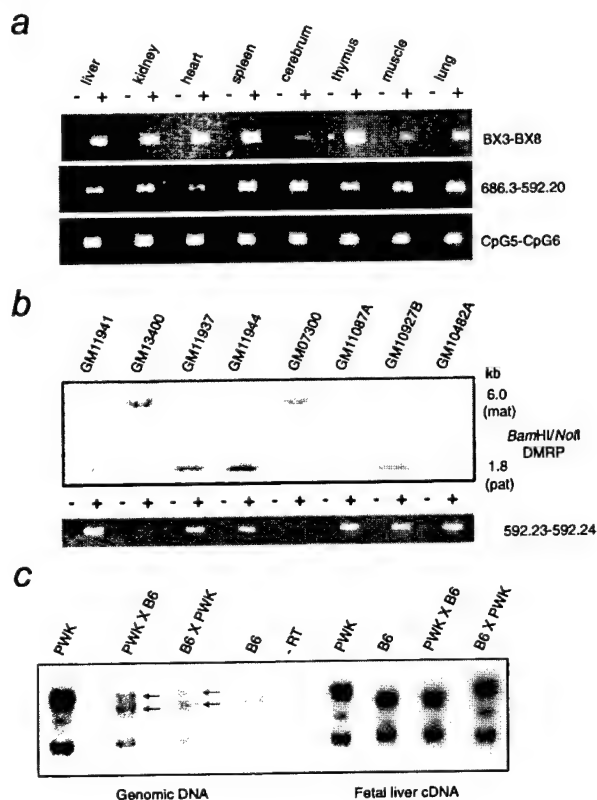


FIG. 4. Expression of an antisense transcript associated with *KvDMR1*. (a) RNA was isolated from human fetal tissues and analyzed by RT-PCR with the indicated primer pairs (see Fig. 2a for location of primers). Primers 686.3 and 592.20 were designed from EST 68627 and EST 592241, respectively, and were used to show the connection of these two ESTs. The + and - indicate that the PCR templates were from cDNA (+RT) or mock cDNA (-RT), respectively. (b, Upper) Southern blot of *Bam*HI/*Not*I-digested DNA from a panel of eight human chromosome 11 somatic cell hybrids (47) hybridized with DMRP. (b, Lower) RT-PCR analysis of same hybrids with primers specific for EST 592241. (c) Paternal-specific expression at the mouse *KvDMR1* locus. Arrows indicate the presence of both alleles in DNA from F₁ animals. In F₁ fetal liver RNA from a C57BL/6J × PWK mating, as well as in the reciprocal cross, only the paternal allele was detected. The weak bands in the -RT lane result from contaminating DNA in the RNA samples, because the PCR primers do not amplify across an intron.

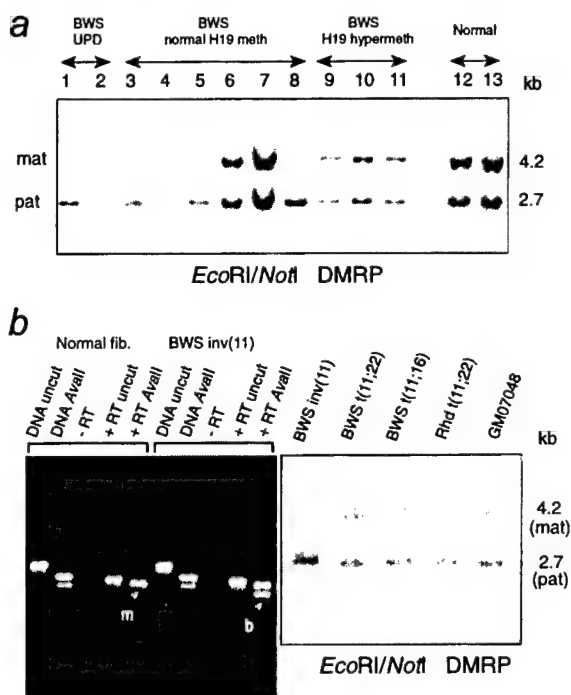


FIG. 5. (a) Southern blot of *EcoRI/NotI* digests of DNA from patients with nonrearrangement BWS and normal controls hybridized with DMRP. Densitometric analysis showed an increase in the cleaved unmethylated (paternal) band with respect to the uncleaved methylated (maternal) band in patients with BWS known to have paternal UPD (lanes 1 and 2) compared with normal individuals (lanes 12 and 13). Methylation at *KvDMR1* was absent in the patients with BWS shown in lanes 3, 5, and 8. (b) Loss of imprinting at *IGF2* and *KvDMR1* in a BWS-associated *inv(11)*. (Left) PCR and RT-PCR analysis at the *AvaII/ApaI* polymorphism in *IGF2* (48). The lane labeled DNA *AvaII* illustrates that the BWS *inv(11)* cells and normal skin fibroblast control cells are heterozygous for the *AvaII* site. The presence of both alleles in the RNA +RT *AvaII* lane indicates that *IGF2* is biallelically expressed. +RT and -RT indicate that the PCR templates were from cDNA (+RT) or mock cDNA (-RT). m, monoallelic; b, biallelic. (Right) Southern hybridization of the DMRP probe to *EcoRI/NotI* digests of DNA from individuals with BWS with the *inv(11)*, a *t(11;22)*, and *t(11;16)*, as well as a rhabdoid tumor with a *t(11;22)* (40), all of which disrupt *KvLQT1* (39). DNA from the *inv(11)* fetus with BWS showed an absence of the methylated allele.

could not be determined in these samples, because none were informative at *IGF2*. The BWS *t(11;22)* has, however, been shown to disrupt the asynchronous replication pattern at *IGF2* (28), suggesting that rearrangements in this domain might affect imprinting by additional mechanisms not connected to aberrant methylation at *KvDMR1*.

DISCUSSION

This work describes an imprinted CpG island in an intron of *KvLQT1* that is methylated on the active (maternal) allele of this gene and associated with an oppositely oriented RNA transcript expressed from the repressed (paternal) *KvLQT1* locus. This situation is reminiscent of the "imprinting box" in region 2 of the mouse *Igf2r* locus (8), which has recently been shown to be necessary for the correct imprinted expression of *Igf2r* transgenes (16). Moreover, transgenes showing repression of *Igf2r* after paternal transmission expressed an antisense transcript dependent on this CpG island (16). Thus, *KvLQT1* can be added to the increasing number of endogenous imprinted genes shown to overlap with imprinted antisense transcripts (13–17). Similar to the situation at the *Igf2r* and *UBE3A* loci, and unlike that at *Igf2* and *Zpf127/ZPF127* (13–15), *KvLQT1-AS/Kvlt1-AS* is imprinted in the opposite direction compared with the associated

protein-coding gene and therefore conforms to the expression competition model of genomic imprinting (19, 49). On the other hand, if the overlapping antisense transcripts associated with the similarly imprinted *Igf2* and *ZPF127/Zpf127* loci carry out regulatory functions, these functions may not be related to genomic imprinting and/or are likely to act through a different mechanism. It is interesting to note that the three oppositely imprinted antisense RNAs described to date are associated with maternally expressed imprinted genes (16, 17, and this study).

Based on expression analysis in *Dnmt1*^{-/-} mice, Caspary *et al.* (37) showed *Kvlt1* to be an indirect target of methylation and predicted the existence of a maternally methylated locus and associated paternally expressed RNA within *Kvlt1*, with the paternal transcript competing with *Kvlt1* for expression. One possibility is that *Kvlt1-AS* is an imprinting gene that competes with the target-imprinted gene (19) *Kvlt1* for expression and is silenced directly by DNA methylation. Down-regulation of *Kvlt1-AS* expression during developmental relaxation of *Kvlt1* imprinting (37, 44–46) would lend support to the notion of a functional role for the antisense RNA transcription in *Kvlt1* imprinting. A second possibility is that *KvDMR1* acts as an insulator or boundary element as recently suggested for the core element upstream of the *H19* gene (50, 51). In this model, *KvDMR1* would block the promoter of *Kvlt1* and/or other genes in the vicinity from interacting with enhancers, and antisense RNA transcript levels would not necessarily change during development. Although *Kvlt1* has maternal-specific expression during early embryonic growth in all mice tested, the developmental regulation of *Kvlt1* imprinting varies considerably between strains (37, 44–46). Whether this variability is related to differences in methylation at *KvDMR1* or elsewhere within the gene is unknown; however, consistent with *KvDMR1* being a imprinting control element, differential methylation is maintained (at least at the *EagI* sites tested; Fig. 3c) in adult kidney DNA where biallelic expression of *Kvlt1* is evident in the same tissue from (C57BL/6J × PWK)F₁ offspring (G.V.F. and M.J.H., unpublished work). In this respect, it will also be important to compare the expression of *KvLQT1* and *KvLQT1-AS* in BWS patients with and without methylation at *KvDMR1*.

The *H19* locus is not a domain-wide imprinting control element, because, unlike *Ins2* and *Igf2*, the imprinting of *p57^{Kip2}*, *Kvlt1*, and *Mash2* is unaffected in *H19* deletion mice (37). This finding supports earlier conclusions resulting from the observation that the majority of informative patients with BWS have LOI at *IGF2* (32) but retain normal methylation and monoallelic expression at *H19* (30–32). This lack of reciprocity was also noted for the BWS *inv(11)* reported by Brown *et al.* (35) as well as the *inv(11)* case described here. These observations suggest the existence of an *H19*-independent mechanism for the regulation of *IGF2* imprinting and, together with the results of the study of the *H19* knockout mouse (36, 37), predict the existence of a separately regulated imprinted domain and at least one additional cis-acting imprinting control element or center in 11p15.5 (and mouse distal 7). A subset of DMRs have been termed gametic imprints because of their establishment in the germ line and maintenance throughout development (2). Transgenic and targeted mutation analyses in the mouse have shown the importance of at least two of these sites in the regulation of genomic imprinting, namely the upstream DMR of *H19* and region 2 in *Igf2r* (16, 50). Furthermore, the maternally methylated DMR at exon 1 of the *SNRPN* gene is included in the smallest microdeletions found in patients with Prader-Willi syndrome showing imprinting-center defects (52). Although direct studies of purified oocytes are needed for confirmation, the lack of methylation at *KvDMR1* in sperm and its enrichment in ovaries suggest that this locus is also a gametic imprinting mark and could therefore represent a critical control element or imprinting center in 11p15.5 (and distal chromosome 7 in the mouse). The loss of methylation at *KvDMR1* in patients with BWS with normal *H19* methylation and biallelic expression of *IGF2* and the existence of

the associated paternally expressed antisense RNA suggest the hypothesis that this locus regulates the imprinted expression of *KvLQT1*, *IGF2*, and perhaps other imprinted genes in the domain. Functional disruption of *KvDMR1*, as evidenced by loss of methylation, may account for a majority (five of nine patients studied here) of non-UPD, nonrearrangement BWS cases without mutations at *p57^{KIP2}*. A limitation of this study is the general unavailability of patient tissues affected by overgrowth. It is formally possible that changes in methylation at *KvDMR1* in fibroblasts and lymphocytes from patients with BWS may reflect tissue-specific differences or occasional loss of methylation in these cell types, and may not accurately reflect the methylation status in affected tissues. However, in an analysis of 17 normal individuals (Fig. 3a and data not shown) including DNA from four lymphoblast and two fibroblast cell lines, three lymphocyte samples, and eight fetal hearts, no departure from the differentially methylated pattern shown in Fig. 3a has been observed. On the other hand, the proportion of patients with BWS and epigenetic changes at *KvDMR1* might even be greater if analysis of the tissues actually affected by overgrowth were available for molecular examination. Analysis of genomic sequence indicates the presence of multiple CpG islands within the 11p15.5 imprinted domain (C.D.D., G.V.F., and M.J.H., unpublished work). The assessment of methylation at these sites in both normal and patient DNA will help to determine whether their methylation patterns show allelic specificity and are as stringently controlled as the methylation pattern for *KvDMR1*. Definitive answers to questions regarding the function of *KvDMR1* and its associated paternal transcript await the generation of mouse models with specific mutations in this region and further detailed study of the molecular pathology of patients with BWS.

We would like to thank Paul Grundy and the National Wilms' Tumor Study Group Tissue Bank for supplying Wilms' tumor samples; Pamela Karnes for the rhabdoid tumor cell lines; Rosemary Elliott and the Roswell Park Cancer Institute animal facility for C57BL/6J and PWK mice; Paul Soloway, Ramsi Haddad, and Bill Held for critically reading the manuscript; and the Brain and Tissues Banks for Developmental Disorders for human fetal tissues. W.R., E.R.M., and P.N.S. acknowledge the support of the Wellcome Trust, and J.A.J. acknowledges the support of the Biotechnology and Biological Sciences Research Council (United Kingdom) and the Newton Trust. This work was funded by a grant to W.R. from the Cancer Research Campaign (United Kingdom) and National Institutes of Health Grant CA63333 to M.J.H. and T.B.S.

- Barlow, D. P. (1994) *Trends Genet.* **10**, 194–199.
- Constancia, M., Pickard, B., Kelsey, G. & Reik, W. (1998) *Genome Res.* **8**, 881–900.
- Surani, M. A. (1998) *Cell* **93**, 309–312.
- Li, E., Beard, C. & Jaenisch, R. (1993) *Nature (London)* **366**, 362–365.
- Olek, A. & Walter, J. (1997) *Nat. Genet.* **17**, 275–276.
- Tremblay, K. D., Duran, K. L. & Bartolomei, M. S. (1997) *Mol. Cell. Biol.* **17**, 4322–4329.
- Shibata, H., Ueda, T., Kamiya, M., Yoshiki, A., Kusakabe, M., Plass, C., Held, W. A., Sunahara, S., Katsuki, M., Muramatsu, M., *et al.* (1997) *Genomics* **44**, 171–178.
- Stoger, R., Kubicka, P., Liu, C. G., Kafri, T., Razin, A., Cedar, H. & Barlow, D. P. (1993) *Cell* **73**, 61–71.
- Shemer, R., Birger, Y., Riggs, A. D. & Razin, A. (1997) *Proc. Natl. Acad. Sci. USA* **94**, 10267–10272.
- Shibata, H., Yoda, Y., Kato, R., Ueda, T., Kamiya, M., Hiraiwa, N., Yoshiki, A., Plass, C., Pearsall, R. S., Held, W. A., *et al.* (1998) *Genomics* **49**, 30–37.
- Neumann, B., Kubicka, P. & Barlow, D. (1995) *Nat. Genet.* **9**, 12–13.
- Gabriel, J. M., Gray, T. A., Stubbs, L., Saitoh, S., Ohta, T. & Nicholls, R. D. (1998) *Mamm. Genome* **9**, 788–793.
- Moore, T., Constancia, M., Zubair, M., Bailleul, B., Feil, R., Sasaki, H. & Reik, W. (1997) *Proc. Natl. Acad. Sci. USA* **94**, 12509–12514.
- Jong, M. T. C., Carey, A. H., Caldwell, K. A., Lau, M. H., Handel, M. A., Driscoll, D. J., Stewart, C. L., Rinchik, E. M. & Nicholls, R. D. (1999) *Hum. Mol. Genet.*, in press.
- Jong, M. T. C., Gray, T. A., Glenn, C. C., Ji, Y., Saitoh, S., Driscoll, D. J. & Nicholls, R. D. (1999) *Hum. Mol. Genet.*, in press.
- Wutz, A., Smrzka, O., Schweifer, N., Schellanders, K., Wagner, E. & Barlow, D. (1997) *Nature (London)* **389**, 745–749.
- Rougeulle, C., Cardoso, C., Fontes, M., Colleaux, L. & Lalande, M. (1998) *Nat. Genet.* **19**, 15–16.
- Reik, W. & Constancia, M. (1997) *Nature (London)* **389**, 669–671.
- Barlow, D. P. (1997) *EMBO J.* **16**, 6899–6905.
- Cattanach, B. & Jones, J. (1994) *J. Inherited Metab. Dis.* **17**, 403–420.
- Surani, M. (1994) *Curr. Opin. Cell Biol.* **6**, 390–395.
- Morison, I. M. & Reeve, A. E. (1998) *Hum. Mol. Genet.* **7**, 1599–1609.
- Ledbetter, D. H. & Engel, E. (1995) *Hum. Mol. Genet.* **4**, 1757–1764.
- Lalande, M. (1996) *Annu. Rev. Genet.* **30**, 173–195.
- Issa, J. P. & Baylin, S. B. (1996) *Nat. Med.* **2**, 281–282.
- Reik, W. & Maher, E. R. (1997) *Trends Genet.* **13**, 330–334.
- Nicholls, R. D., Saitoh, S. & Horsthemke, B. (1998) *Trends Genet.* **14**, 194–200.
- Li, M., Squire, J. A. & Weksberg, R. (1998) *Am. J. Med. Genet.* **79**, 253–259.
- Weksberg, R., Shen, D. R., Fei, Y. L., Song, Q. L. & Squire, J. (1993) *Nat. Genet.* **5**, 143–150.
- Reik, W., Brown, K. W., Schneid, H., Le Bouc, Y., Bickmore, W. & Maher, E. R. (1995) *Hum. Mol. Genet.* **4**, 2379–2385.
- Catchpoole, D., Lam, W. W., Valler, D., Temple, I. K., Joyce, J. A., Reik, W., Schofield, P. N. & Maher, E. R. (1997) *J. Med. Genet.* **34**, 353–359.
- Joyce, J. A., Lam, W. K., Catchpoole, D. J., Jenks, P., Reik, W., Maher, E. R. & Schofield, P. N. (1997) *Hum. Mol. Genet.* **6**, 1543–1548.
- Rainer, S., Johnson, L. A., Dobry, C. J., Ping, A. J., Grundy, P. E. & Feinberg, A. P. (1993) *Nature (London)* **362**, 747–749.
- Taniguchi, T., Sullivan, M. J., Ogawa, O. & Reeve, A. E. (1995) *Proc. Natl. Acad. Sci. USA* **92**, 2159–2163.
- Brown, K., Villar, A., Bickmore, W., Clayton-Smith, J., Catchpoole, D., Maher, E. & Reik, W. (1996) *Hum. Mol. Genet.* **5**, 2027–2032.
- Leighton, P. A., Ingram, R. S., Eggenschwiler, J., Efstratiadis, A. & Tilghman, S. M. (1995) *Nature (London)* **375**, 34–39.
- Caspary, T., Cleary, M. A., Baker, C. C., Guan, X. J. & Tilghman, S. M. (1998) *Mol. Cell. Biol.* **18**, 3466–3474.
- Lee, M., Hu, R.-J., Johnson, L. & Feinberg, A. (1997) *Nat. Genet.* **15**, 181–185.
- Reid, L. H., Davies, C., Cooper, P. R., Crider-Miller, S. J., Sait, S. N., Nowak, N. J., Evans, G., Stanbridge, E. J., deJong, P., Shows, T. B., *et al.* (1997) *Genomics* **43**, 366–375.
- Sait, S., Nowak, N., Singh-Kahlon, P., Weksberg, R., Squire, J., Shows, T. & Higgins, M. (1994) *Genes Chromosomes Cancer* **11**, 97–105.
- Driscoll, D. J. & Migeon, B. R. (1990) *Somatic Cell Mol. Genet.* **16**, 267–282.
- Day, C. D., Smilnich, N. J., Fitzpatrick, G. V., deJong, P. J., Shows, T. B. & Higgins, M. J. (1999) *Mamm. Genome* **10**, 182–185.
- Wang, Q., Bowles, N. E. & Towbin, J. A. (1998) *Mol. Med. Today* **4**, 382–388.
- Gould, T. D. & Pfeifer, K. (1998) *Hum. Mol. Genet.* **7**, 483–487.
- Jiang, S., Hemann, M. A., Lee, M. P. & Feinberg, A. P. (1998) *Genomics* **53**, 395–399.
- Paulsen, M., Davies, K. R., Bowden, L. M., Villar, A. J., Franck, O., Fuermann, M., Dean, W. L., Moore, T. F., Rodrigues, N., Davies, K. E., *et al.* (1998) *Hum. Mol. Genet.* **7**, 1149–1159.
- Gabriel, J. M., Higgins, M. J., Gebuhr, T. C., Shows, T. B., Saitoh, S. & Nicholls, R. D. (1998) *Proc. Natl. Acad. Sci. USA* **95**, 14857–14862.
- Tadokora, K., Fujii, H., Inoue, T. & Yamada, M. (1991) *Nucleic Acids Res.* **19**, 6967.
- Bartolomei, M., Webber, A. L., Brunkow, M. E. & Tilghman, S. M. (1993) *Genes Dev.* **7**, 1663–1673.
- Thorvaldsen, J. L., Duran, K. L. & Bartolomei, M. S. (1998) *Genes Dev.* **12**, 3693–3702.
- Webber, A. L., Ingram, R. S., Levorse, J. M. & Tilghman, S. M. (1998) *Nature (London)* **391**, 711–716.
- Ohta, T., Gray, T. A., Rogan, P. K., Buiting, K., Gabriel, J. M., Saitoh, S., Muralidhar, B., Bilienska, B., Krajewska-Walasck, M., Driscoll, D. J., *et al.* (1999) *Am. J. Hum. Genet.* **64**, 397–413.

Thomas B. Shows, Ph.D.
Identifying and Isolating Breast Cancer-Associated
Genes on Chromosome 11

GENOMICS 46, 355-363 (1997)
ARTICLE NO. GE975061

Novel Transcribed Sequences within the BWS/WT2 Region in 11p15.5: Tissue-Specific Expression Correlates with Cancer Type

Shyra J. Crider-Miller,* Laura H. Reid,* Michael J. Higgins,† Norma J. Nowak,†
Thomas B. Shows,† P. Andrew Futreal,‡ and Bernard E. Weissman*,¹

*Department of Pathology & Lineberger Comprehensive Cancer Center, University of North Carolina, Chapel Hill, North Carolina 27599; †Department of Human Genetics, Roswell Park Cancer Institute, Buffalo, New York 14263; and ‡Department of Surgery, Duke University Medical Center, Duke University, Durham, North Carolina 27710

Received August 12, 1997; accepted September 9, 1997

Chromosome band 11p15.5 has proven to be an intriguing area of the human genome. Various studies have linked alterations in this region to growth-related disorders such as Beckwith-Wiedemann syndrome and a variety of human cancers. Furthermore, functional assays in G401 Wilms tumor cells and RD rhabdomyosarcoma cells support the existence of a tumor suppressor gene on 11p15.5, sometimes called WT2. In addition, several genes mapping to this region show imprinted expression, suggesting that 11p15.5 contains an imprinted domain. We have employed solution hybrid capture in combination with sequence analysis to identify 16 genes within the ~700-kb critical region of 11p15.5 between D11S601 and D11S1318. Two of these genes, NAP1L4 and KCNA9, had been previously reported. Ten novel transcripts were identified with partial cDNA sequences selected by solution hybrid capture. Sequence homology to known ESTs was used to identify the remaining gene transcripts. Interestingly, the tissue-specific mRNA expression of these genes correlates with the tumor types linked to this region. This work can be compiled into a transcript map, important in the elucidation of tumor suppressor activity on chromosome 11p15.5. © 1997 Academic Press

INTRODUCTION

Several lines of evidence suggest the involvement of one or more genetic element on chromosome 11p15.5 in growth regulation. Beckwith-Wiedemann Syndrome (BWS),² an overgrowth disorder with a predispo-

sition to pediatric tumor development, has been linked to this region (Ping *et al.*, 1989; Koufos *et al.*, 1989). In addition, chromosomal breakpoints in BWS patients and one rhabdoid tumor map to 11p15.5 (Mannens *et al.*, 1994; Sait *et al.*, 1994; Hoovers *et al.*, 1995; Reid *et al.*, 1996). Loss of heterozygosity (LOH) studies have reported alterations in this region in various tumor types, including the pediatric Wilms tumor and rhabdomyosarcoma sometimes associated with BWS (Seizinger *et al.*, 1991). Finally, functional studies have shown suppression of tumorigenicity in G401 Wilms tumor cells (Weissman *et al.*, 1987; Dowdy *et al.*, 1991; Reid *et al.*, 1996) and growth suppression in RD rhabdomyosarcoma cells (Loh *et al.*, 1992; Koi *et al.*, 1993) upon introduction of a portion of 11p15.5.

Our functional assay involved introducing t(X;11) chromosomes into G401 cells via microcell-mediated chromosome transfer and assaying for the ability of the hybrid cells to form tumors in nude mice. By transferring radiation-reduced t(X;11) chromosomes, we were able to localize the operative tumor suppressor gene in this G401 assay telomeric to D11S601 (Reid *et al.*, 1996). Using a similar method, Koi *et al.* (1993) identified a subchromosomal transfer fragment capable of suppressing growth in RD cells. Analysis of pulsed-field gel electrophoresis (PFGE) data suggests this fragment contains DNA from the β -globin (HBB) locus on 11p15.5 through D11S724, but not including D11S1318. Assuming a common genetic element is involved in tumor suppression in G401 and growth suppression in RD, we can narrow the critical region of suppressor activity in 11p15.5 to the smallest region of overlap, 700 kb of DNA between D11S601 and D11S1318 (Reid *et al.*, 1997).

To build a foundation for the isolation of genes in 11p15.5, we constructed a 1-Mb genomic contig that includes the critical region between D11S601 and D11S1318 (Reid *et al.*, 1997). Utilizing clones from our genomic contig, we have employed the solution hybrid capture technique to isolate several gene transcripts between D11S601 and D11S1318, including the pre-

¹ To whom correspondence should be addressed. Telephone: (919) 966-7533. Fax: (919) 966-3015.

² Abbreviations used: ASCL2, achaete-scute homolog-2; BWS, Beckwith-Wiedemann syndrome; CARS, cysteinyl-tRNA synthetase; EST, expressed sequence tag; HBB, β -globin; IGF2, insulin-like growth factor II; INS, insulin; IPL, imprinted in placenta and liver; KCNA9 (KVLAQT1), potassium voltage-gated channel, long QT syndrome; LOH, loss of heterozygosity; LOI, loss of imprinting; NAP1L4 (NAP2), nucleosome assembly protein 1-like 4; STS, sequence-tagged site; TAPA1, target of an antiproliferative antibody; TH, tyrosine hydroxylase.

viously reported NAP1L4 (Hu *et al.*, 1996) and KCNA9 (Wang *et al.*, 1996) genes. In addition, sequence analysis of P1 and PAC clones revealed EST clusters in this candidate region. Characterization of these genes will provide evidence for or against their role in tumor development.

MATERIALS AND METHODS

Preparation of selector DNA and target cDNA. Selector DNA includes PAC, BAC, and P1 genomic clones isolated and mapped to 11p15.5 as described (Reid *et al.*, 1997). PAC clones were isolated from the Roswell Park Cancer Institute libraries (P. deJong, unpublished). BAC clones were identified in a library constructed by Shizuya *et al.* (1992) obtained from Research Genetics. Assisted by Genome Systems, P1 clones were isolated from the DuPont Merck Pharmaceutical Human Foreskin Fibroblast Library (Shephard *et al.*, 1994). Selector genomic clones were digested with *Hae*III, ligated to a uniaamp adaptor (Clontech), and biotin-labeled by PCR amplification with uniaamp primers (Clontech) that had been synthesized using a biotin phosphoramidite as described (Futreal *et al.*, 1994).

Target cDNA was generated separately from normal human breast tissue, human fetal kidney, and the MCH 486.2L nontumorigenic G401 hybrid cell line (Reid *et al.*, 1996). Human tissues were collected from Duke Breast Cancer SPORE Center and University of North Carolina Tissue Distribution Laboratory. Poly(A)⁺ mRNA was isolated with an oligo(dT) kit (Collaborative Biomedical) and used as a template to synthesize double-stranded, blunt-ended cDNA (Gibco/BRL). Both oligo(dT) and random hexamer primers were used in first-strand synthesis. A custom uniaamp adaptor, gt10sal, was ligated to the cDNA after second-strand synthesis (Futreal *et al.*, 1994).

Solution hybrid capture of cDNA fragments. Prior to hybridization, both the biotin-labeled selector DNA and the target cDNA were purified on Wizard columns (Promega). Repeat sequences in genomic selector DNA were suppressed by annealing with CotI DNA (Gibco/BRL). Approximately 100 ng of preannealed selector DNA and 1 μ g of denatured target cDNA were hybridized in a small volume of hybridization mix at 65°C overnight.

Streptavidin-coated magnetic beads were used to capture the biotinylated hybrid molecules on a magnetic stand (Promega). Selected cDNA fragments that hybridized with genomic fragments from 11p15.5 were eluted from the beads in 50 mM NaOH and neutralized with 1 M Tris (pH 8). After purification and size selection via a Microspin S-400 column (Pharmacia), the eluate was amplified with the gt10sal primer. The entire amplified product was purified on a Wizard column (Promega) and recycled through a second round of selection for further enrichment.

Second-round selected cDNA fragments were also amplified and purified, then cloned into a TA vector (Promega). Cloned cDNA inserts were transformed into XL-1 Blue MRF-competent cells. DNA from approximately 200 colonies was amplified with vector-specific PCR primers flanking the cloning site. Sizes of the cDNA inserts were estimated on an ethidium bromide-stained agarose gel. The amplified cDNA inserts were purified on Wizard columns (Promega) for sequence analysis. Several purified cDNA inserts were used as probes for Southern and Northern analysis.

Sequence analysis. Amplified cDNA inserts were sequenced using a PRISM dye terminator kit on an ABI automated fluorescent sequencer (Applied Biosystems). Sequences of individual cDNA clones were assembled into contigs using the Sequencer 3.0 computer program (Gene Codes). Homology searches against GenBank, dbEST, and other databases were initially carried out using the FASTA program in the GCG package and later with the POWBLAST program (Zhang and Madden, 1997) distributed by the NCBI.

Genomic sequence of selector clones was generated at the McDermott Center at University of Texas Southwestern (<http://mcdermott.swmed.edu>) as described (C. Davies, manuscript in preparation). This sequence was also analyzed with the POWBLAST pro-

gram. In addition, GRAIL and GENSCAN programs were used to predict exon sequences.

ESTs. EST clones were purchased from Genome Systems and are described at the IMAGE website <http://www-bio.lnl.gov/bbrp/image/lib/info.html>. Once the identity of each EST clone was confirmed by sequence analysis, the insert was gel-purified and used as a probe in Northern analysis.

Southern analysis. Aliquots of genomic DNA (5 μ g) were digested with *Hind*III, separated on 1% agarose gels, and transferred to positively charged nylon membranes (Boehringer Mannheim). Southern blots were hybridized with ³²P-labeled cDNA inserts at 42°C overnight in a 50% formamide hybridization buffer. After hybridization, blots were washed to high stringency and exposed to X-ray film (Kodak) overnight.

Northern analysis. Poly(A)⁺ mRNA was isolated from G401, MCH 485.1, and MCH 486.1 cells using an oligo(dT) kit (Collaborative Biomedical). G401 is a tumor cell line derived from what was originally described as a Wilms tumor (Pecbles *et al.*, 1978) but may actually have been a rhabdoid tumor of the kidney (Garvin *et al.*, 1993). MCH 485.1 and MCH 486.1 are G401 hybrid lines that contain radiation-reduced t(X;11) chromosomes from XMCH 708.26 and XMCH 708.25, respectively. When injected into nude mice, MCH 485.1 cells form tumors whereas MCH 486.1 cells do not (Reid *et al.*, 1996). Poly(A)⁺ mRNA (2 μ g) was separated on 1% agarose/formaldehyde/Mops gels and transferred to positively charged nylon membranes (Boehringer Mannheim). Multiple tissue Northern blots contain 2 μ g of poly(A)⁺ mRNA from adult human pancreas, kidney, skeletal muscle, placenta, liver, lung, brain, and heart tissues or fetal human kidney, liver, brain, and lung (Clontech). Hybridization with cDNA or EST inserts proceeded as described in Southern analysis. Human β -actin or GAPDH was used as a control probe.

RESULTS

Selection of cDNA Fragments

To identify candidate tumor suppressor genes in 11p15.5, cDNA fragments were isolated in four rounds of solution hybrid capture with six genomic clones (Table 1), covering most of the proposed critical region between D11S601 and D11S1318. In the original solution hybrid capture experiments, the 120-kb PAC-23N20 was used as a selector to isolate cDNA fragments expressed in normal breast tissue and the MCH 486.2L G401-derived hybrid cell line. Normal human breast target cDNA served as a general source of normally expressed genes that had been successfully used in previous solution hybrid capture experiments to isolate gene fragments (Wooster *et al.*, 1995). In addition, because LOH at 11p15.5 has been observed in breast carcinoma (Ali *et al.*, 1987), normal breast tissue may express a putative tumor suppressor gene. MCH 486.2L is a G401-derived microcell hybrid that contains a t(X;11) chromosome from the donor cell line XMCH 708.25 (Reid *et al.*, 1996). MCH 486.2L cells do not form tumors when injected into nude mice, while the parental G401 cells and other G401 hybrids remain tumorigenic. We assume that these cells express the tumor suppressor gene that complements the G401 defect. Because DNA between D11S601 and D11S1318 is present on this introduced t(X;11) chromosome, it should contain any suppressive genetic elements contributing to this observation. Therefore, MCH 486.2L

TABLE 1
Summary of cDNA Clones Selected by Solution Hybrid Capture

Experiment	Selector DNA	Target cDNA	Contamination ^a	Known genes ^b	Novel cDNA sequences
1	PAC-23N20	MCH 486.2L	9	4 ^{c,d}	14 ^e
2	PAC-23N20	Breast	4	20 ^d	3
3	PAC-74K15, BAC-47G8, + P1-6960	MCH 486.2L + HFK	2	1	26
4	BAC-7016 + P1-6959	MCH 486.2L + HFK	4	3	14
Total			19 (18%)	28 (27%)	57 (55%)

^a Includes vector, ribosomal, mitochondrial, and repetitive sequences.

^b Four cDNA fragments from PAC-23N20 were homologous to NAP1L4 cDNA (Hu *et al.*, 1996). One cDNA fragment from PAC-74K15 and three cDNA fragments from BAC-7016 were homologous to KCNA9 (Wang *et al.*, 1996).

^c Two cDNA fragments identified in experiment 1 were also identified in experiment 2.

^d 19 cDNA fragments from experiments 1 and 2 are not homologous to NAP1L4 cDNA, but based upon their location and expression pattern may be previously undescribed exons of this gene.

^e One cDNA fragment identified in experiment 1 was also identified in experiment 2.

represented an excellent source of the operative tumor suppressor gene in the G401 functional assay.

Later solution hybrid capture experiments involved pooling of both the genomic selector DNA and the target cDNA. Pooling of the selectors provided greater coverage of the region, spanning ~350 kb. Two separate pools were created to minimize possible self-hybridization between overlapping genomic clones. The selector pool used in experiment 3 (Table 1) contained genomic DNA from PAC-74K15, BAC-47G8, and P1-6960. The pool of genomic clones used for selection in experiment 4 (Table 1) included BAC-7016 and P1-6959. (Figure 1 illustrates the location of these genomic clones on 11p15.5). Both selector pools were hybridized separately to the target cDNA, derived from both the MCH 486.2L cells and human fetal kidney. Because Wilms tumors are pediatric kidney tumors, it is possible that they develop after the inactivation of a tumor suppressor gene normally expressed in human fetal kidney. Therefore, human fetal kidney was included as an additional source of Wilms' tumor suppressor genes.

Identification of Novel Genes

Approximately 50 cDNA clones from each of the four solution hybrid capture experiments were sequenced. Many individual clones shared overlapping sequence and were assembled into cDNA clusters, representing a contiguous cDNA sequence. This analysis resulted in the identification of 104 distinct cDNA sequences between D11S601 and D11S1318. Database searches were used to detect homology with known genes and to eliminate contaminating sequences, such as vector, mitochondrial, ribosomal, and repetitive sequences. Identification of novel gene sequences was suggested by the absence of homology to known genes and supported by homology to expressed sequenced tags (ESTs). Furthermore, homology to specific genes could provide insight into the possible function of the newly identified cDNA. Overall (Table 1), 19 of the 104 cDNA sequences were considered contamination and were not

further characterized. Twenty-eight cDNAs were homologous to two known genes on 11p15.5, NAP1L4 and KCNA9. The remaining 57 clones appeared to represent novel genes and were characterized further by Northern analysis.

Because some of the PAC, BAC, and P1 clones used in our experiments had been sequenced as part of the Human Genome Project, we could localize the selected cDNA sequences within the 11p15.5 genomic sequence. Those cDNA sequences that did not share homology with the available genomic sequence on 11p15.5 were localized by Southern analysis and PCR. Figure 1 summarizes the locations of these sequences. Only five cDNA clones did not map back to 11p15.5. To identify true gene transcripts, cDNA clones were hybridized to mRNA from multiple adult or fetal tissues. Although the majority of these probes did not hybridize, 10 clones detected a message, each with a unique transcript size and pattern of expression. These results suggest that each clone may be part of a unique gene.

Six of the ten novel transcripts identified with cDNA sequences selected by solution hybrid capture were localized to the 120-kb PAC-23N20, revealing an unusually concentrated gene region. One cDNA clone selected with PAC-23N20, C2bBr, predominantly hybridized to a 7.5-kb transcript in kidney tissue (Fig. 2). Clone C2bBr is located between NAP1L4 and D11S648. Two clones, located just distal to p57 (Fig. 1), detected a message in all tissues but showed distinct muscle-specific expression (Fig. 2). Clone B4bBr hybridized to a 2.2-kb transcript in all tissues and an additional 1.2-kb transcript specifically in skeletal muscle, whereas clone E4c recognized a faint 4.5-kb band in all tissues and a 2.2-kb band in skeletal muscle only. Clones D3a and D5a represent pancreas-specific genes on PAC-23N20. These transcripts lie between the genes with muscle-specific expression described above. When hybridized with mRNA from multiple tissues, D3a recognized a single 2.4-kb message expressed only in pancreas (Fig. 2). D5a hybridized to a pancreas-specific message similar in size, 2.8 kb (Fig. 2). Due to their similar size and expression pattern, we are investi-

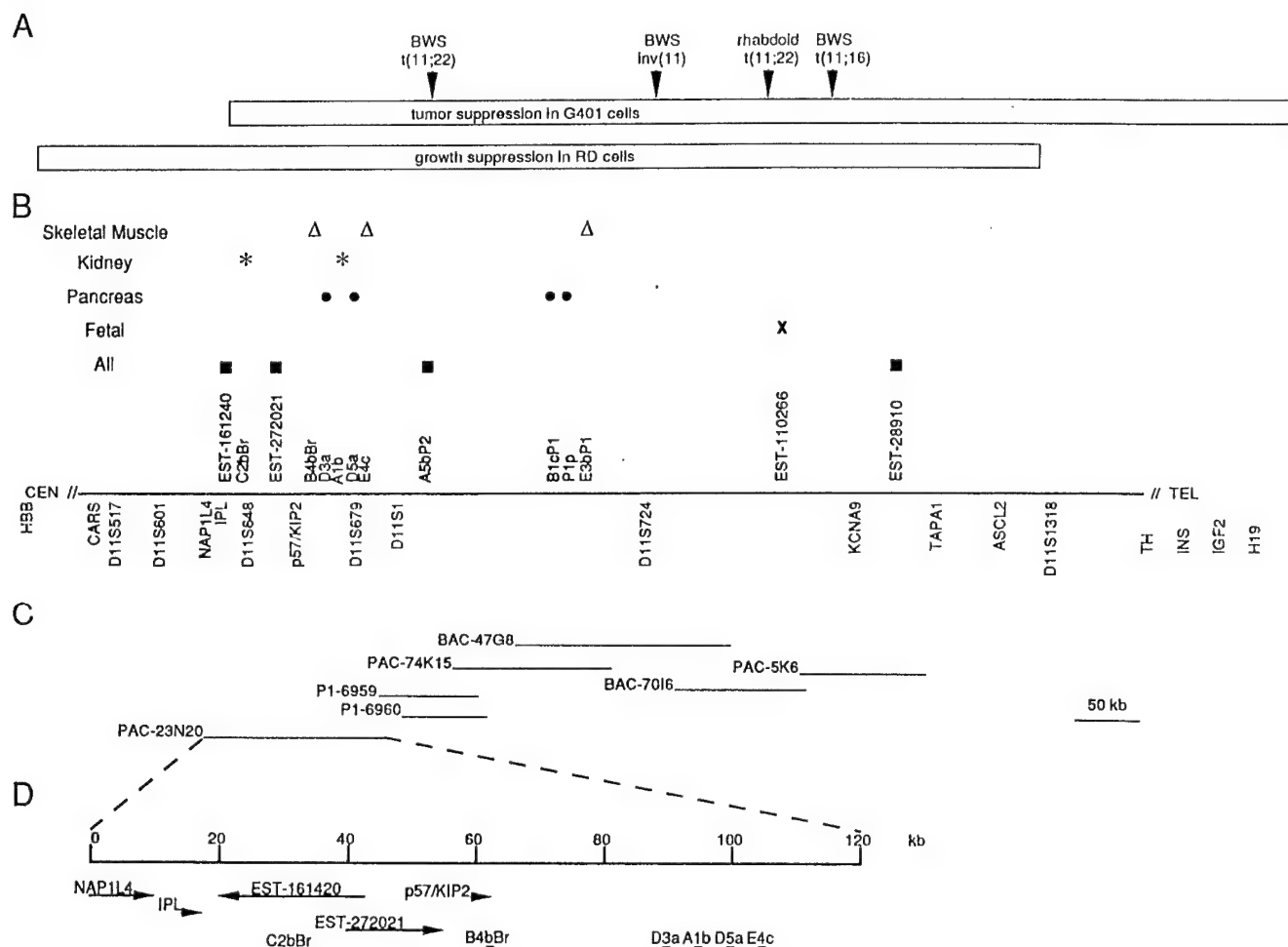


FIG. 1. Transcript map and partial contig of the BWS/WT2 region in 11p15.5. (A) Arrowheads mark the positions of chromosomal breakpoints identified in three BWS patients and one rhabdoid tumor (Mannens *et al.*, 1994; Sait *et al.*, 1994; Hoovers *et al.*, 1995; Reid *et al.*, 1997). Open bars represent DNA responsible for tumor suppression in G401 cells (Reid *et al.*, 1996) and growth suppression in RD cells (Koi *et al.*, 1993). The telomeric boundary of the DNA responsible for growth suppression in RD cells is not exact. PFGE analysis suggests it extends approximately 300 kb telomeric to D11S724, at most. (B) The horizontal line represents contiguous genomic DNA. STSs and known genes are positioned below this line at their location in 11p15.5. Similarly, the newly identified transcripts are positioned above this line. Expression data are indicated above each newly identified transcript: open triangle (Δ), skeletal muscle-specific expression; star (*), kidney-specific expression; solid circle (\bullet), pancreas-specific expression; cross (X), fetal-specific expression; solid box (\blacksquare), expression in most tissues. (C) Genomic clones are represented by horizontal lines. BAC-47G8 is a chimeric clone, resulting in an internal deletion of 11p15.5 DNA (Reid *et al.*, 1997). (D) PAC-23N20 genomic DNA is represented by the horizontal line. Distance is marked in intervals of 20 kb. Newly identified genes are indicated by horizontal bars or arrows, if transcriptional orientation is known.

gating the possibility that D3a and D5a may be part of the same gene. Finally, cDNA clone A1b recognized a 9.5-kb mRNA transcript mainly in pancreas and kidney with an additional kidney-specific transcript of 6.5 kb (Fig. 2).

The four remaining transcripts identified with selected cDNAs are scattered throughout the approximately 400-kb sequence telomeric to PAC-23N20. A single gene was localized to P1-6959. This gene produces a 2.5-kb message in all tissues analyzed and was identified with cDNA fragment A5bP2 (Fig. 3). Clone E3bP1 maps to PAC-74K15 and recognized a 1.2-kb transcript exclusively in skeletal muscle tissue (Fig. 3). The cloned sequence overlaps an excellent quality exon predicted by GRAIL to be transcribed from centromere to telomere, suggesting transcriptional orientation of

this gene. Just proximal to E3bP1 on PAC-74K15 there appears to be a cluster of pancreas-specific genes. Clone B1cP1 represents a 1.5-kb mRNA present only in pancreas (Fig. 3). A large pancreas-specific transcript, greater than 9.5 kb, has also been identified with a pool of cDNA clones (P1p) located between E3bP1 and B1cP1 (Fig. 3). The sizes of these transcripts distinguish them from one another and from the pancreas-specific genes on PAC-23N20, although alternative splicing cannot be eliminated. Several cDNA fragments were localized to BAC-70I6, but none produced a band in Northern analysis of multiple adult tissues.

ESTs

A powerful utility of sequence analysis is the identification of known ESTs within the region of interest.

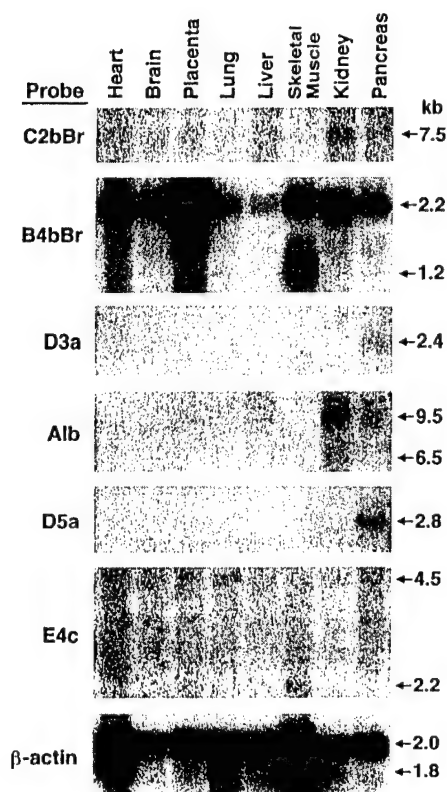


FIG. 2. mRNA expression pattern of novel genes in PAC-23N20. cDNA clones from PAC-23N20 were used as probes to screen multiple tissue Northern blots (Clontech) containing 2 μ g of poly(A)⁺ mRNA from adult tissues. The human β -actin probe was used as a control to demonstrate relative mRNA loading.

Many of the large-insert clones in our contig are being used as template to sequence this region of 11p15.5. At this time, complete sequence is available for PAC-23N20 and PAC-74K15. Preliminary sequence contigs are available for P1-6959, BAC-70I6, and PAC-5K6. Homology searches using the FASTA and POWBLAST programs identified a pseudogene of cytochrome c oxi-

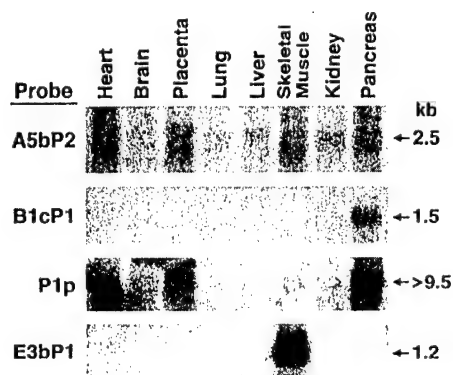


FIG. 3. mRNA expression pattern of novel genes telomeric to PAC-23N20. cDNA clones selected with PAC-74K15, P1-6960, BAC-47G8, BAC-70I6, and P1-6959 were used as probes to screen multiple tissue Northern blots (Clontech) containing 2 μ g of poly(A)⁺ mRNA from adult tissues. A representative multiple tissue Northern blot probed with human β -actin as a control to demonstrate relative mRNA loading is shown in Fig. 2.

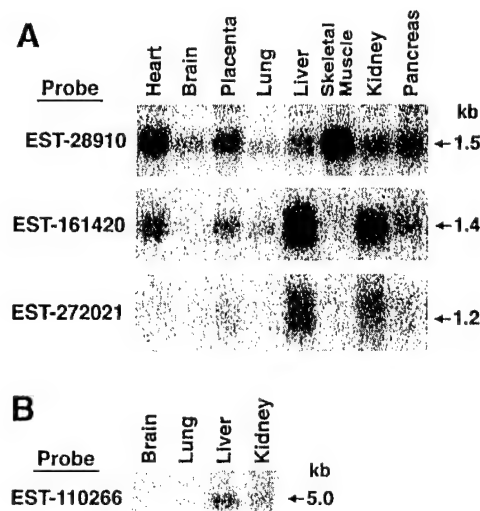


FIG. 4. mRNA expression pattern of ESTs in 11p15.5. EST clones were used as probes to screen multiple tissue Northern blots (Clontech) containing 2 μ g of poly(A)⁺ mRNA from (A) adult tissues or (B) fetal tissues. A representative adult multiple tissue Northern blot probed with human β -actin as a control to demonstrate relative mRNA loading is shown in Fig. 2.

dase subunit VIc in P1-6959 (L.H.R., manuscript in preparation) as well as two 11p15.5 polymorphic markers, D11S4088 (AFMa155te9) in PAC-74K15 and SHGC-14772 in PAC-5K6. Sequence analysis also detected several ESTs. As expected some of the EST clones were homologous to the previously isolated 11p15.5 genes, NAP1L4 (Hu *et al.*, 1996), IPL (GenBank Accession No. AF001294; Qian *et al.*, unpublished), p57/KIP2 (Lee *et al.*, 1995), and KCNA9 (Wang *et al.*, 1996). Others overlapped apparently transcribed *Alu* or L1 repeat sequences. However, many clones mapped into four predominant EST clusters. Such EST clusters can represent novel transcripts, sometimes referred to as "UniGenes" (Schuler *et al.*, 1996). Therefore, a representative cDNA clone from each EST cluster was hybridized to multiple tissue Northern blots as shown in Fig. 4.

EST-161420 (GenBank Accession Nos. H25530 and H25531) and EST 272021 (GenBank Accession Nos. N35348 and N44716) detected 1.4- and 1.2-kb transcripts, respectively, in most adult and fetal tissues but most predominantly in liver and kidney. These EST clusters were both located in PAC-23N20. In fact, further characterization has shown they are part of two overlapping genes that are transcribed in opposite orientations (Fig. 1D; M.J.H., manuscript in preparation). EST-110266 (GenBank Accession No. T71335 and T71490) was identified in BAC-70I6. It detected a 5.0-kb transcript in fetal liver and kidney mRNA, but did not hybridize to any of the adult mRNA samples. EST-28910 (GenBank Accession No. R40349) maps to PAC-5K6 and detected a 1.5-kb transcript in all adult tissues examined. PAC-74K15 contains two EST clusters. One group represented by EST-D205 (GenBank Accession No. T20200) overlaps a cDNA fragment isolated in solu-

tion hybrid capture experiment 3. This cDNA fragment did not detect a transcript in any of the adult tissues examined, although EST-D205 itself has not been tested. A second EST cluster is located near cDNA fragments B1cP1 and P1p, both of which hybridized exclusively to pancreatic mRNA. This cluster is represented by EST-592241 (GenBank Accession Nos. AA155639 and AA155694). Interestingly, EST-592241 and the other two clones in this cluster are all derived from pancreatic tissue. Therefore, it may be part of the B1cP1 or P1p transcripts. Alternatively, EST-592241 may represent another pancreas-specific gene. Unfortunately, a signal was not detected when this clone was used to probe a multiple tissue Northern blot.

Expression Analysis in G401

All cDNA and EST clones potentially representing novel genes in 11p15.5 were used as probes in Northern analysis to observe their expression patterns in G401 cells and G401-derived hybrid lines. Theoretically, any cDNA probe that recognized a transcript in a G401 hybrid suppressed for tumorigenicity but did not recognize the same transcript in tumorigenic G401 cells or G401 hybrid lines would have been considered a candidate tumor suppressor gene in this system. Unfortunately, none of the clones tested revealed this expression pattern. However, some cDNA probes recognized the same transcript in both tumorigenic and nontumorigenic cell lines (data not shown). The possibility that the G401 tumor suppressor gene may be mutated without affecting its transcript size is under investigation.

DISCUSSION

Fourteen novel transcripts in 11p15.5 were identified in the critical region between D11S601 and D11S1318 using cDNA fragments selected by solution hybrid capture and by homology searching of genomic DNA sequence. Interestingly, most showed a tissue-specific mRNA expression pattern related to tumors associated with this region. Although LOH in 11p15.5 has been detected in a variety of adult and pediatric tumors (Seizinger *et al.*, 1991), it is more frequently associated with two childhood cancers, Wilms tumor in kidney and rhabdomyosarcoma in skeletal muscle. In fact, a common region of LOH in Wilms tumor and rhabdomyosarcoma has been identified distal to D11S988 (Besnard-Guerin *et al.*, 1996). These findings suggest that a tumor suppressor gene(s) with kidney- or muscle-specific expression located in this region may be inactivated during tumor development. In our experiments, we identified three genes with skeletal muscle-specific transcripts (B4bBr, E4c, and E3bP1) and two genes with kidney-specific transcripts (C2bBr and A1b). It is possible that alterations in one or more of these genes may contribute to the development of rhabdomyosarcoma and Wilms tumor, respectively.

Several of the novel transcripts in 11p15.5 showed

pancreas-specific expression (D3a, D5a, B1cP1, and P1p). Because less than 40% LOH at 11p in pancreatic carcinoma had been reported (Hahn *et al.*, 1995), we were somewhat surprised by this observation. However, a review of the literature revealed the existence of pancreatoblastoma, a rare childhood cancer of the pancreas distinct from the more common adult pancreatic carcinoma. To our knowledge, LOH at 11p15.5 in pancreatoblastomas has not been examined, possibly because of the rarity of this tumor. Pancreatoblastoma is described as an embryonal tumor similar to Wilms tumor but consisting of pancreatic tissue. This neoplasm has also been observed in some BWS patients (Drut and Jones, 1988). Therefore, disruption of any or all of these pancreas-specific genes may result in yet another embryonal tumor linked to 11p15.5.

One might expect that tumor suppressor genes inactivated during the development of childhood cancers would be highly expressed in fetal tissues and reduced in adult tissues. Only EST-110266 fit the fetal-specific expression profile, recognizing transcripts in fetal liver and fetal kidney but not adult tissues. The pediatric Wilms tumor and hepatoblastoma associated with BWS could possibly result from the absence of this gene. However, some pediatric tumor suppressor genes are general regulators of cellular proliferation, such as the retinoblastoma gene, Rb (Weinberg 1995). Because Rb is important for general growth control, it is not surprising that it is widely expressed among tissues (Lee *et al.*, 1987). Four novel genes (EST-161420, EST-272021, A5bP2, and EST-28910) in 11p15.5 were expressed in all tissues tested with no tissue-specific transcripts. If they act as tumor suppressor genes, they too may be involved in regulating cell growth in all tissues.

Solution hybrid capture proved an efficient technique for identifying genes between D11S601 and D11S1318 on 11p15.5. By pooling genomic selector clones mapped to this region, we covered a large interval of genomic DNA. In addition, combining several cDNA target sources increased the number of expressed genes in the selection pool. Our solution hybrid capture experiments produced approximately 100 distinct cDNA sequences. Sequence analysis revealed a low frequency (18%) of contaminating sequences, such as vector, ribosomal, mitochondrial, and repetitive sequences, and most (94%) of the remaining cDNA sequences mapped back to 11p15.5. In general, solution hybrid capture experiments report that 70–75% of the selected cDNA clones map back to the region of interest, and up to 30% represent contamination (Lovett, 1994; Osborne-Lawrence *et al.*, 1995). Therefore, our data fall well within the expected values.

Many of the cDNA sequences selected in our solution hybrid capture experiments shared homology with the recently identified KCNA9 (Wang *et al.*, 1996) and NAP1L4 (Hu *et al.*, 1996) genes. One cDNA sequence fragment in PAC-74K15 and three in BAC-70I6 had homology to exons of KCNA9, and most of the cDNAs selected with PAC-23N20 localized to the NAP1L4 re-

gion (Table 1). This preferential selection of NAP1L4 sequence has also been observed in exon trapping experiments performed in other laboratories (J. Pelletier, J. Landers, personal communications). In addition, the majority of ESTs homologous to PAC-23N20 reside within this gene. NAP1L4 is highly expressed in many tissues. Although solution hybrid capture is designed to normalize transcript levels (Tagle *et al.*, 1993; Lovett, 1994), it appears that complete normalization was not achieved in our experiments, resulting in the selection of an overabundance of NAP1L4 cDNA fragments. NAP1L4 reportedly contains 14 exons (Hu *et al.*, 1996). Several of the cDNA fragments we isolated were localized to genomic regions surrounding these exons. Yet, these presumably intronic fragments hybridized to a 3.0-kb transcript in all tissues typical of NAP1L4 (data not shown). This result suggests the existence of previously unidentified NAP1L4 exons. Similar results have been observed in other laboratories (J. Pelletier, A. Buckler, personal communication). Interestingly, over half of the newly identified genes in 11p15.5 were also localized to PAC-23N20, creating a particularly gene-rich region. Moreover, the p57/KIP2 and IPL genes reside within this region, tallying 11 genes within approximately 100 kb (Fig. 1D).

Although solution hybrid capture has advantages over other methods of gene isolation, construction of a complete transcript map generally requires a combination of techniques. For example, characterization of the region surrounding BRCA1 (Brody *et al.*, 1995) utilized a combination of solution hybrid capture (referred to as direct selection), exon trapping, sequence analysis, island-rescue PCR, evolutionary conservation or "zoo blotting," and direct screening of cDNA libraries with genomic clones mapping to the region. Indeed, transcript maps of 11p15.5 have been constructed using other methods. Hoovers *et al.* (1995) have used evolutionary conservation, CpG island identification, and direct library screening to isolate 10 novel genes in this region. Although we cannot definitively determine the number of overlapping genes, a comparison of expression patterns and location of the genes identified by Hoovers *et al.* with our newly identified transcripts suggests we may have identified at least two common genes. Clone E3bP1 maps to the telomeric end of PAC-74K15 and recognized a 1.2-kb message in adult skeletal muscle only. Hoovers *et al.* (1995) isolated a clone, 5C, located approximately 150 kb distal to E3bP1, which showed a similar pattern of expression. In addition, clone 5C detected a message in all fetal tissues. The expression pattern observed with our cDNA clone A5bP2, a 2.5-kb transcript in all tissues, closely resembles that of clone 18-4 described by Hoovers *et al.* However, a higher level of expression of this gene in liver and kidney, observed by Hoovers *et al.*, was not evident in our analysis. A5bP2 maps to P1-6959, which appears to be a significant distance from clone 18-4, approximately 100 to 200 kb. Isolation of the full-length cDNA

sequences of these genes will be required to determine which clones truly represent the same gene.

The tissue-specific pattern of expression observed with many of the newly identified genes in 11p15.5 may simply reflect their distinct functions in cell differentiation. Yet, it is conceivable that the expression patterns also indicate a role for these genes in tumorigenesis. Rather than disruption of a single gene leading to all cancers linked to this chromosomal region, each tumor type may result from alteration in a unique tissue-specific tumor suppressor gene. For example, abolishing the function of a tumor suppressor gene expressed only in kidney may produce Wilms tumor, while inactivation of a skeletal muscle-specific transcript may lead to rhabdomyosarcoma. In this model, multiple tumor suppressor genes would exist in 11p15.5, but only one of these loci would need to be altered in each tumor type. An alternative, more complex, model might involve inactivation of more than one tissue-specific gene. For example, mutations or alteration in expression in two or all three of the genes with a skeletal muscle-specific transcript may lead to rhabdomyosarcoma. Recent evidence indicates that gene expression at multiple loci is frequently altered in 11p15.5-associated tumors. Loss of normal imprinting (LOI) at IGF2, H19, and p57/KIP2 has been detected in Wilms tumors, rhabdomyosarcomas, and BWS patients that apparently results in the simultaneous gain of growth promoting signals and loss of tumor suppressor activity (Ogawa *et al.*, 1993; Rainier *et al.*, 1993; Weksberg *et al.*, 1993; Moulton *et al.*, 1994; Pedone *et al.*, 1994; Steenman *et al.*, 1994; Zhan *et al.*, 1994; Reik *et al.*, 1995; Hatada *et al.*, 1996).

Defining tissue-specific expression by the presence of a transcript of unique size in a single tissue, three distinct categories of tissue-specific genes have emerged (skeletal muscle, kidney, and pancreas). However, the genes contained within each category are not tightly clustered in separate regions of the candidate domain. Furthermore, as shown in Fig. 1B, the three genes with skeletal muscle-specific transcripts and the four pancreas-specific genes are spread over at least 200 kb, while the two kidney-specific genes are approximately 75 kb apart. This arrangement predicts that microdeletions are an unlikely mechanism of inactivating multiple tissue-specific genes. However, physically separated genes throughout a chromosomal band may undergo changes in expression due to a common regulatory element, such as an imprinting center. The imprinted expression of 11p15.5 genes may be controlled by a common 11p15.5 imprinting center. Alternatively, multiple imprinting centers may exist to regulate related sets of genes. In this case, the maintenance of imprinting at pancreas-specific genes may be controlled by one imprinting center which is altered during pancreatoblastoma development, while the kidney- and skeletal muscle-specific genes may be controlled by separate and unique imprinting centers. Indeed, distinct regulation for the maintenance of imprinting in

11p15.5 has been suggested by the uncoupled LOI "mutations" at the p57/KIP2 locus and the IGF2/H19 cluster (Chung *et al.*, 1996; Matsuoka *et al.*, 1996).

In this report, we have employed solution hybrid capture and sequence analysis to identify 16 genes in a 700-kb interval of 11p15.5. Although none of these genes appeared to be responsible for tumor suppression in G401 cells, it is possible that the tumor suppressor gene is not expressed at a level detectable by Northern analysis. Furthermore, the tumor suppressor gene may only be expressed in the more physiologically relevant environment of the animal and not in cell culture. Regardless, the striking tissue-specific expression patterns observed with these genes correlate well with the cancer types associated with alterations in 11p15.5, suggesting the existence of multiple tumor suppressor genes within this region. Further characterization of these genes (e.g., expression in tumors, imprinting status, mutation screening) will result in significant progress toward the understanding of genetic alterations involved in BWS and human cancers.

ACKNOWLEDGMENTS

We thank Curtis Gumbs for assistance in sequencing; the UNC sequencing facility for sequencing services; Chris Davies, Glen Evans, and the McDermott Center for Human Growth and Development at the University of Texas Southwestern in Dallas for sequence of genomic clones; Tina Dennis for assistance localizing cDNA sequences; Judith Blasser for human fetal kidney supply; and John Landers, Jerry Pelletier, and Alan Buckler for personal communications concerning NAP1L4. This research is supported by NIH Grants CA63176 (B.E.W.), ES07017 (S.J.C.-M.), HG00333 (T.B.S.), and CA6333 (T.B.S.).

REFERENCES

- Ali, I. U., Lidereau, R., Theillet, C., and Callahan, R. (1987). Reduction to homozygosity of genes on chromosome 11 in human breast neoplasia. *Science* **238**: 185–188.
- Besnard-Guerin, C., Newsham, I., Winqvist, R., and Cavenee, W. K. (1996). A common loss of heterozygosity in Wilms' tumor and embryonal rhabdomyosarcoma distal to the D11S988 locus on chromosome 11p15.5. *Hum. Genet.* **97**(2): 163–170.
- Brody, L. C., Abel, K. J., Castilla, L. H., Couch, F. J., McKinley, D. R., Yin, G. Y., Ho, P. P., Merajver, S., Chandrasekharappa, S. C., Xu, J., Cole, J. L., Struwing, J. P., Valdes, J. M., Collins, F. S., and Weber, B. L. (1995). Construction of a transcription map surrounding the BRCA1 locus of human chromosome 17. *Genomics* **25**: 238–247.
- Chung, W. Y., Yuan, L., Feng, L., Hensle, T., and Tycko, B. (1996). Chromosome 11p15.5 regional imprinting: Comparative analysis of KIP2 and H19 in human tissues and Wilms' tumors. *Hum. Mol. Genet.* **5**(8): 1101–1108.
- Dowdy, S. F., Fasching, C. L., Araujo, D., Lai, K.-M., Livanos, E., Weissman, B. E., and Stanbridge, E. J. (1991). Suppression of tumorigenicity in Wilms' tumor by the p15.5–p14 region of chromosome 11. *Science* **254**: 293–295.
- Drut, R., and Jones, M. C. (1988). Congenital pancreatoblastoma in Beckwith–Wiedemann syndrome: An emerging association. *Pediatr. Pathol.* **8**: 331–339.
- Futreal, P. A., Cochran, C., Rosenthal, J., Miki, Y., Swenson, J., Hobbs, M., Bennett, L. M., Haugen-Strano, A., Marks, J., Barrett, J. C., Tavtigian, S. V., Shattuck-Eidens, D., Kamb, A., Skolnick, M., and Wiseman, R. W. (1994). Isolation of a diverged homeobox gene, MOX1, from the BRCA1 region on 17q21 by solution hybrid capture. *Hum. Mol. Genet.* **3**: 1359–1364.
- Garvin, A. J., Re, G. G., Tarnowski, B. I., Hazen-Martin, D. J., and Sens, D. A. (1993). The G401 cell line, utilized for studies of chromosomal changes in Wilms' tumor, is derived from a rhabdoid tumor of the kidney. *Am. J. Pathol.* **142**(2): 375–380.
- Hahn, S. A., Seymour, A. B., Hoque, A. T. M. S., Schutte, M., da Costa, L. T., Redston, M. S., Caldas, C., Weinstein, C. L., Fischer, A., Yeo, C. J., Hruban, R. H., and Kern, S. E. (1995). Allelotype of pancreatic adenocarcinoma using xenograft enrichment. *Cancer Res.* **55**: 4670–4675.
- Hatada, I., Inazawa, J., Abe, T., Nakayama, M., Kaneko, Y., Jinno, Y., Niikawa, N., Ohashi, H., Fukushima, Y., Iida, K., Yutani, C., Takahashi, S. I., Chiba, Y., Ohishi, S., and Mukai, T. (1996). Genomic imprinting of human p57/KIP2 and its reduced expression in Wilms' tumors. *Hum. Mol. Genet.* **5**(6): 783–788.
- Hoovers, J. M. N., Kalikin, L. M., Johnson, L. A., Alders, M., Redeker, B., Law, D. J., Blik, J., Steenman, M., Benedict, M., Wiegant, J., Lengauer, C., Taillon-Miller, P., Schlessinger, D., Edwards, M. C., Elledge, S. J., Ivens, A., Westerveld, A., Little, P., Mannens, M., and Feinberg, A. P. (1995). Multiple genetic loci within 11p15 defined by Beckwith–Wiedemann syndrome rearrangement breakpoints and subchromosomal transferable fragments. *Proc. Natl. Acad. Sci. USA* **92**: 12456–12460.
- Hu, R.-J., Lee, M. P., Johnson, L. A., and Feinberg, A. P. (1996). A novel human homologue of yeast nucleosome assembly protein, 65 kb centromeric to the p57/KIP2 gene, is biallelically expressed in fetal and adult tissues. *Hum. Mol. Genet.* **5**(11): 1743–1748.
- Koi, M., Johnson, L. A., Kalikin, L. M., Little, P. F. R., Nakamura, Y., and Feinberg, A. P. (1993). Tumor cell growth arrest caused by subchromosomal transferable DNA fragments from chromosome 11. *Science* **260**: 361–364.
- Koufos, A., Grundy, P., Morgan, K., Aleck, K. A., Hadro, T., Lampkin, B. C., Kalbakji, A., and Cavenee, W. K. (1989). Familial Wiedemann–Beckwith syndrome and a second Wilms' tumor locus both map to 11p15.5. *Am. J. Hum. Genet.* **44**: 711–719.
- Lee, M.-H., Reynisdottir, I., and Massague, J. (1995). Cloning of p57^{KIP2}, a cyclin-dependent kinase inhibitor with unique domain structure and tissue distribution. *Genes Dev.* **9**: 639–649.
- Lee, W.-H., Bookstein, R., Hong, F., Young, L.-J., Shew, J.-Y., and Lee, E. Y.-H. P. (1987). Human retinoblastoma susceptibility gene: Cloning, identification, and sequence. *Science* **235**: 1394–1399.
- Loh, W. E., Scrabble, H. J., Livanos, E., Arboleda, M. J., Cavenee, W. K., Oshimura, M., and Weissman, B. E. (1992). Human chromosome 11 contains two different growth suppressor genes for embryonal rhabdomyosarcoma. *Proc. Natl. Acad. Sci. USA* **89**: 1755–1759.
- Lovett, M. (1994). Fishing for complements: Finding genes by direct selection. *Trends Genet.* **10**: 352–357.
- Mannens, M., Hoovers, J. M. N., Redeker, E., Verjaal, M., Feinberg, A. P., Little, P., Boavida, M., Coad, N., Steenman, M., Blik, J., Niikawa, N., Tonoki, H., Nakamura, Y., deBoer, E. G., Slater, R. M., John, R., Cowell, J. K., Junien, C., Henry, I., Tommerup, N., Weksberg, R., Poeschel, S. M., Leschot, N. J., and Westerveld, A. (1994). Parental imprinting of human chromosome region 11p15.3–pter involved in the Beckwith–Wiedemann syndrome and various human neoplasia. *Eur. J. Hum. Genet.* **2**: 3–23.
- Matsuoka, S., Thompson, J. S., Edwards, M. C., Barletta, J. M., Grundy, P., Kalikin, L. M., Harper, J. W., Elledge, S. J., and Feinberg, A. P. (1996). Imprinting of the gene encoding a human cyclin-dependent kinase inhibitor, p57^{KIP2}, on chromosome 11p15. *Proc. Natl. Acad. Sci. USA* **93**: 3026–3030.
- Moulton, T., Crenshaw, T., Hao, Y., Moosikasuwan, J., Lin, N., Dembitzer, F., Hensle, T., Weiss, L., McMorris, L., Loew, T., Kraus, W., Gerald, W., and Tycko, B. (1994). Epigenetic lesions at the H19 locus in Wilms' tumor patients. *Nature Genet.* **7**: 440–447.
- Ogawa, O., Eccles, M. R., Szeto, J., McNee, L. A., Yun, K., Maw,

- M. A., Smith, P. J., and Reeve, A. E. (1993). Relaxation of insulin-like growth factor II gene imprinting implicated in Wilms' tumor. *Nature* **362**: 749-751.
- Osborne-Lawrence, S., Welsh, P. L., Spillman, M., Chandrasekharappa, S. C., Gallardo, T. D., Lovett, M., and Bowcock, A. M. (1995). Direct selection of expressed sequences within a 1-Mb region flanking BRCA1 on human chromosome 17q21. *Genomics* **25**: 248-255.
- Pedone, P. V., Tirabosco, R., Cavazzana, A. O., Ungaro, P., Basso, G., Luksch, R., Carli, M., Bruni, C. B., Frunzio, R., and Riccio, A. (1994). Mono- and bi-allelic expression of insulin-like growth factor II gene in human muscle tumors. *Hum. Mol. Genet.* **3**(7): 1117-1121.
- Peebles, P. T., Trisch, T., and Papageorge, A. G. (1978). Isolation of four unusual pediatric solid tumor cell lines. *Pediatr. Res.* **12**: 485.
- Ping, A. J., Reeve, A. E., Law, D. J., Young, M. R., Boehnke, M., and Feinberg, A. P. (1989). Genetic linkage of Beckwith-Wiedemann syndrome to 11p15. *Am. J. Hum. Genet.* **44**: 720-723.
- Rainier, S., Johnson, L. A., Dobry, C. J., Ping, A. J., Grundy, P. E., and Feinberg, A. P. (1993). Relaxation of imprinted genes in human cancer. *Nature* **362**: 747-749.
- Reid, L. H., West, A., Gioeli, D. G., Phillips, K. K., Kelleher, K. F., Araujo, D., Stanbridge, E. J., Dowdy, S. F., Gerhard, D. S., and Weissman, B. E. (1996). Localization of a tumor suppressor gene in 11p15.5 using the G401 Wilms' tumor assay. *Hum. Mol. Genet.* **5**: 239-247.
- Reid, L. H., Davies, C., Cooper, P., Crider-Miller, S. J., Sait, S. N. J., Nowak, N. J., Evans, G., Stanbridge, E. J., deJong, P., Shows, T. B., Weissman, B. E., and Higgins, M. J. (1997). A 1 Mb physical map and contig of the imprinted domain in 11p15.5 that contains TAPA1 and the BWSCR1/WT2 region. *Genomics* **43**: 366-375.
- Reik, W., Brown, K. W., Schneid, H., LeBouc, Y., Bickmore, W., and Maher, E. R. (1995). Imprinting mutations in the Beckwith-Wiedemann syndrome suggested by altered imprinting pattern in the IGF2-H19 domain. *Hum. Mol. Genet.* **4**(12): 2379-2385.
- Sait, S. N. J., Nowak, N. J., Singh-Kahlon, P., Weksberg, R., Squire, J., Shows, T. B., and Higgins, M. J. (1994). Localization of Beckwith-Wiedemann and rhabdoid tumor chromosome rearrangements to a defined interval in chromosome band 11p15.5. *Genes Chromosomes Cancer* **11**: 97-105.
- Schuler, et al. (1996). A gene map of the human genome. *Science* **274**: 540-546.
- Seizinger, B. R., Klinger, H. P., Junien, C., Nakamura, Y., Le Beau, M., Cavenee, W., Emanuel, B., Ponder, B., Naylor, S., Mitelman, F., Louis, D., Menon, A., Newsham, I., Decker, J., Kaelbling, M., Henry, I., and Deimling, A. V. (1991). Report of the committee on chromosome and gene loss in human neoplasia. *Cytogenet. Cell. Genet.* **58**: 1080-1096.
- Shephard, N. S., Pfrogner, B. D., Coulby, J. N., Ackerman, S. L., Vaidyanathan, G., Sauer, R. H., Balkenhol, T. C., and Sternberg, N. (1994). Preparation and screening of an arrayed human genomic library generated with the P1 cloning system. *Proc. Natl. Acad. Sci. USA* **91**: 2629-2633.
- Shizuya, H., Birren, B., Kim, U. J., Mancino, V., Slepak, T., Tachiiri, Y., and Simon, M. (1992). Cloning and stable maintenance of 300-kilobase-pair fragments of human DNA in *Escherichia coli* using an F-factor-based vector. *Proc. Natl. Acad. Sci. USA* **89**(18): 8794-8797.
- Steenman, M. J. C., Rainier, S., Dobry, C. J., Grundy, P., Horon, I. L., and Feinberg, A. P. (1994). Loss of imprinting of IGF2 is linked to reduced expression and abnormal methylation of H19 in Wilms' tumor. *Nature Genet.* **7**: 433-439.
- Tagle, D. A., Swaroop, M., Lovett, M., and Collins, F. C. (1993). Magnetic bead capture of expressed sequences encoded within large genomic segments. *Nature* **361**: 751-753.
- Wang, Q., Curran, M. E., Splawski, I., Burn, T. C., Millholland, J. M., VanRaay, T. J., Shen, J., Timothy, K. W., Vincent, G. M., deJager, T., Schwartz, P. J., Towbin, J. A., Moss, A. J., Atkinson, D. L., Landes, G. M., Connors, T. D., and Keating, M. T. (1996). Positional cloning of a novel potassium channel gene: *KCNQ9* mutations cause cardiac arrhythmias. *Nature Genet.* **12**: 17-23.
- Weinberg, R. A. (1995). The retinoblastoma protein and cell cycle control. *Cell* **81**: 323-330.
- Weissman, B. E., Saxon, P. J., Pasquale, S. R., Jones, G. R., Geiser, A. G., and Stanbridge, E. R. (1987). Introduction of a normal human chromosome 11 into a Wilms' tumor cell line controls its tumorigenic expression. *Science* **236**: 175-180.
- Weksberg, R., Shen, D. R., Fei, Y. L., Song, Q. L., and Squire, J. (1993). Disruption of insulin-like growth factor 2 imprinting in Beckwith-Wiedemann syndrome. *Nature Genet.* **5**: 143-150.
- Wooster, R., Bignell, G., Lancaster, J., Swift, S., Seal, S., Mangion, J., Collins, N., Gregory, S., Gumbs, C., Micklem, G., Barfoot, R., Hamoudi, R., Patel, S., Rice, C., Biggs, P., Hashim, Y., Smith, A., Connor, F., Arason, A., Gudmundsson, J., Ficenec, D., Keisell, D., Ford, D., Tonin, P., Bishop, D. T., Spurr, N. K., Ponder, B. A. J., Eeles, R., Peto, J., Devilee, P., Cornelisse, C., Lynch, H., Narod, S., Lenoir, G., Egilsson, V., Barkadottir, R. B., Easton, D. F., Bentley, D. R., Futreal, P. A., Ashworth, A., and Stratton, M. R. (1995). Identification of the breast cancer susceptibility gene BRCA2. *Nature* **378**: 789-792.
- Zhan, S., Shapiro, D. N., and Helman, L. J. (1994). Activation of an imprinted allele of the insulin-like growth factor II gene implicated in rhabdomyosarcoma. *J. Clin. Invest.* **94**(1): 445-448.
- Zhang, J., and Madden, T. L. (1997). PowerBLAST: A new network BLAST application for interactive or automated sequence analysis and annotation. *Genome Res.* **7**: 649-656.

Functional Characterization of Human Nucleosome Assembly Protein-2 (NAP1L4) Suggests a Role as a Histone Chaperone

Pedro Rodriguez,* David Munroe,† Dirk Prawitt,‡ Lee Lee Chu,* Eva Bric,† Jungho Kim,* Laura H. Reid,§ Chris Davies,|| Hitoshi Nakagama,|| Ralf Loebbert,‡ Andreas Winterpacht,‡ Mary-Jane Petruzzi,** Michael J. Higgins,** Norma Nowak,** Glen Evans,|| Tom Shows,|| Bernard E. Weissman,§ Bernhard Zabel,‡ David E. Housman,†† and Jerry Pelletier*,¹

*Department of Biochemistry, McGill University, 3655 Drummond Street, Montreal, Quebec, Canada H3G 1Y6; †Sequana Therapeutics, 11099 North Torrey Pines Road, Suite 160, La Jolla, California 92037; ‡Department of Pediatrics, University of Mainz, Langenbeckstrasse 1, D-55101 Mainz, Germany; §UNC Lineberger Comprehensive Cancer Center, University of North Carolina at Chapel Hill, Chapel Hill, North Carolina 27599-7295; ||The Eugene McDermott Center for Growth and Develop, University of Texas Southwestern Medical Center, Dallas, Texas 75235; ||National Cancer Research Institute, 5-1-1 Tsukiji Chuo-ku, Tokyo 104, Japan; **Roswell Park Memorial Institute, State University of New York at Buffalo, Buffalo, New York 14263; ††Center for Cancer Research, Massachusetts Institute of Technology, 40 Ames Street, Cambridge, Massachusetts 02139

Received March 13, 1997; accepted June 17, 1997

Histones are thought to play a key role in regulating gene expression at the level of DNA packaging. Recent evidence suggests that transcriptional activation requires competition of transcription factors with histones for binding to regulatory regions and that there may be several mechanisms by which this is achieved. We have characterized a human nucleosome assembly protein, NAP-2, previously identified by positional cloning at 11p15.5, a region implicated in several disease processes including Wilms tumor (WT) etiology. The deduced amino acid sequence of NAP-2 indicates that it encodes a protein with a potential nuclear localization motif and two clusters of highly acidic residues. Functional analysis of recombinant NAP-2 protein purified from *Escherichia coli* demonstrates that this protein can interact with both core and linker histones. We demonstrate that recombinant NAP-2 can transfer histones onto naked DNA templates. Deletion mutagenesis of NAP-2 demonstrates that both NH₂- and COOH-terminal domains are required for histone transfer activity. Subcellular localization studies of NAP-2 indicate that it can shuttle between the cytoplasm and the nucleus, suggesting a role as a histone chaperone. Given the potential role of the human NAP-2 gene (HGMW-approved symbol NAP1L4) in WT etiology, we have elucidated the exon/intron structure of this gene and have analyzed the mutational status of NAP-2 in sporadic WTs. Our results, coupled with tumor suppression assays in G401 WT cells, do not sup-

port a role for NAP-2 in the etiology of WT. A putative role for NAP-2 in regulating cellular differentiation is discussed. © 1997 Academic Press

INTRODUCTION

In eukaryotic chromosomes, DNA is packaged in the form of chromatin, a complex of DNA and histones organized into distinct regularly spaced structural units referred to as nucleosomes. The nucleosome core contains ~145 bp of DNA wrapped around a central histone octamer comprising two molecules each of the core histones (H2A, H2B, H3, and H4) (Arents and Moudrianakis, 1993; Richmond *et al.*, 1993) and represents the first level of compaction in the nucleus. Each class of core histone has been highly conserved in evolution. A less conserved fifth histone, histone H1, is thought to bind to DNA as it enters and exits the nucleosome core and to the DNA that links adjacent nucleosome cores. Not all H1 linker histones are essential for viability (Shen *et al.*, 1995; Sirotkin *et al.*, 1995). A number of studies have established a general global repressive effect of chromatin on transcription (Cullen *et al.*, 1993; Lu *et al.*, 1993; Marsolier *et al.*, 1995; Schild *et al.*, 1993; Thomas and Elgin, 1988), possibly mediated through excluding access of transcription factors to their cognate sequences. A better understanding of this process would yield insight into this fundamental aspect of gene regulation.

Biochemical analysis of chromatin assembly has led to the identification of core histone-binding proteins which may be involved in this process. These include proteins such as nucleoplasmin, N1/N2, and nucleosome assembly proteins (NAP) (Dilworth and Dingwall,

Sequence data from this article have been deposited with the GenBank Data Library under Accession No. U51281.

¹To whom correspondence should be addressed at the Department of Biochemistry, McGill University, Room 927, 3655 Drummond St., Montreal, Quebec, Canada, H3G 1Y6. Telephone: (514) 398-2323. Fax: (514) 938-7384.

1988; Svaren and Chalkley, 1990; van Holde, 1989; Wolffe, 1995) and DF-31, a sperm decondensation factor which can also facilitate loading of nucleosomes onto both decondensed sperm DNA and naked DNA templates (Crevel and Cotterill, 1995). Nucleoplasmin was discovered as a nucleosome assembly protein (Laskey *et al.*, 1978) and binds H2A and H2B histones; whereas N1/N2 protein is complexed with H3 and H4 histones in *Xenopus* eggs (Kleinschmidt *et al.*, 1985; Kleinschmidt and Franke, 1982; Dilworth *et al.*, 1987). Both complexes are thought to be required for maximal nucleosome assembly (Dilworth *et al.*, 1987), functioning as histone transfer proteins. Since polyanions, such as polyglutamic acid (Stein *et al.*, 1979) or RNA (Nelson *et al.*, 1981), can also function as negatively charged histone transfer molecules, stretches of acidic amino acids present within these histone-binding proteins may be involved directly in the assembly reaction. Although the functions of nucleoplasmin and N1/N2 have been extensively assessed in the *Xenopus* system, the relevance of these specific proteins to nucleosome assembly in mammalian cells is unknown.

Biochemical analysis of the yeast NAP gene product has led to the proposal that it functions in a manner similar to that of nucleoplasmin and N1/N2 to deposit histones onto DNA (Ishimi and Kikuchi, 1991; Fujii-Nakata *et al.*, 1992). NAP-1 is a 58-kDa polypeptide that has higher affinity for H2A and H2B than for H3 and H4 and can stimulate nucleosome assembly *in vitro* (Ishimi *et al.*, 1987). Related genes have been isolated from human (called nucleosome-assembly protein-1-related gene product; NRP) (Simon *et al.*, 1994), murine (Ishimi *et al.*, 1984), and *Drosophila* cells (Ito *et al.*, 1996). Recent experiments in *Drosophila* have demonstrated that NAP-1 is part of a multifactorial chromatin assembly machinery that mediates the ATP-facilitated assembly of regularly spaced nucleosomal arrays (Ito *et al.*, 1996). Experiments in yeast have suggested that nucleosome assembly proteins may also play a role in performing mitotic functions by interacting with B-type cyclins (Kellogg *et al.*, 1995; Kellogg and Murray, 1995). In humans, disruption of a human homologue of the NAP-1 protein, SET, is associated with a putative oncogenic fusion protein in myeloid leukemogenesis (von Lindern *et al.*, 1992).

Hu *et al.* (1996) have recently reported on the cloning of NAP-2² from a human placenta cDNA library. This gene was previously reported by us to reside at 11p15.5 (Prawitt *et al.*, 1996), a region showing loss of heterozygosity (LOH) in Wilms tumor (WT), as well as in a number of adult cancers (reviewed under Discussion). Hu *et al.* (1996) found that NAP-2 mRNA is ubiquitously expressed and biallelically expressed in fetal tissue. In this paper, we functionally characterize human NAP-2, demonstrating that recombinant NAP-2 protein is capable of interacting with both core and linker

histones, that it can transfer histones onto DNA templates, and that the subcellular location of NAP-2 is cell-cycle dependent. We have also elucidated the exon/intron boundaries of the NAP-2 gene and performed mutational scans in sporadic WT's. Our results, coupled with tumor suppression assays in G401 WT cells, do not support a direct role for NAP-2 in WT initiation or progression. Functional analysis of NAP-2 suggests that it may be involved in regulating gene expression by delivering histones from the cytoplasm to the chromatin assembly machinery.

MATERIALS AND METHODS

Isolation and nucleotide sequencing of human NAP-2 cDNA and genomic clones. Two exons (2A6, 1H11), isolated from an 11p15.5 cosmid and showing homology to human NRP (Simon *et al.*, 1994) (which we refer to as hNAP-1 throughout this article) (Fig. 1A), were used to screen HL60 cell, HeLa cell, kidney, and placenta cDNA libraries under conditions of high stringency (final wash: 0.5× SSC, 0.1% SDS at 65°C). DNA inserts from four positive phages were rescued into pBluescript II KS (') for restriction mapping and nucleotide sequencing. The complete nucleotide sequence of the hNAP-2 cDNA clones was carried out by the dideoxy chain termination method of Sanger *et al.* (1977), using modified T7 DNA polymerase and double-stranded DNA templates. Oligonucleotide primers used for sequencing were derived either from the plasmid sequences near the cloning site or from the cDNA insert sequence using a bidirectional walking strategy. The nucleotide sequence of the full-length hNAP-2 cDNA was obtained from both strands of all four clones presented in Fig. 1A. The sequence of cosmid cSRL-87f11, containing the entire NAP-2 coding region, was obtained using fluorescence-based high-throughput sequencing on an ABI 377 sequencer, essentially as described (Smith *et al.*, 1994). The sequence of cosmid cSRL-87f11 has been deposited with GenBank under Accession No. HSU51281.

Purification of recombinant NAP protein. A NAP-1 cDNA was obtained by polymerase chain reaction (PCR) amplification of cDNA generated by random priming of human kidney mRNA. The primers used in the PCR amplification flanked the ATG and TGA codons of the cDNA (Simon *et al.*, 1994) and introduced the influenza hemagglutinin (HA) epitope, YPYDVPDYAS, immediately upstream of the TGA codon (Field *et al.*, 1988). Using PCR-mediated mutagenesis, an HA epitope tag was also placed immediately upstream of the TAA codon of NAP-2 (Splice Form D). PCR products were cloned into pBluescript II KS (') and sequenced to ensure the absence of mutations arising as a result of the amplification process. Both NAP-1 and NAP-2 cDNAs were subcloned into the *Xho*I site of pET15b, resulting in an in-frame fusion with six histidine residues. A freshly transformed colony of pET15b/NAP-1 or pET15b/NAP-2(HA) in *Escherichia coli* BL21(DE3) was grown at 37°C in a volume of 6 liters to an A_{600} of ~0.7, and synthesis of NAP-1 and NAP-2 was induced by the addition of isopropyl- β -D-thiogalactopyranoside to a final concentration of 1 mM. The culture was incubated for an additional 50 min. The bacteria were harvested by centrifugation (Sorval GAS rotor: 4000 rpm for 20 min) and resuspended in 1/100 of the original volume in resuspension buffer (20 mM Tris-HCl [pH 8.0], 500 mM NaCl, 0.2% Tween 20, 1 mM DTT, 5% glycerol, 1 mM ethylenediaminetetraacetate [EDTA], 10 μ g/ml pepstatin, 1 mM phenylmethylsulfonyl fluoride [PMSF], 10 μ g/ml aprotinin). Cells were lysed by sonication, and the insoluble material was removed by centrifugation (Sorval SS-34 rotor: 10,000 rpm for 60 min). The supernatant was then incubated with Ni²⁺-agarose (Qiagen) with gentle mixing at 4°C for 2 h. The resin was collected by centrifugation (Sorval refrigerated RT6000B centrifuge: 2000 rpm for 10 min). The resin was washed with resuspension buffer containing 35 mM imidazole until no more protein could be detected in the wash. The NAP proteins were eluted in elution buffer (20 mM Tris-HCl [pH 8.0], 150 mM NaCl, 1 mM

² The HGMW-approved symbol for the gene described in this paper is NAP1L4.

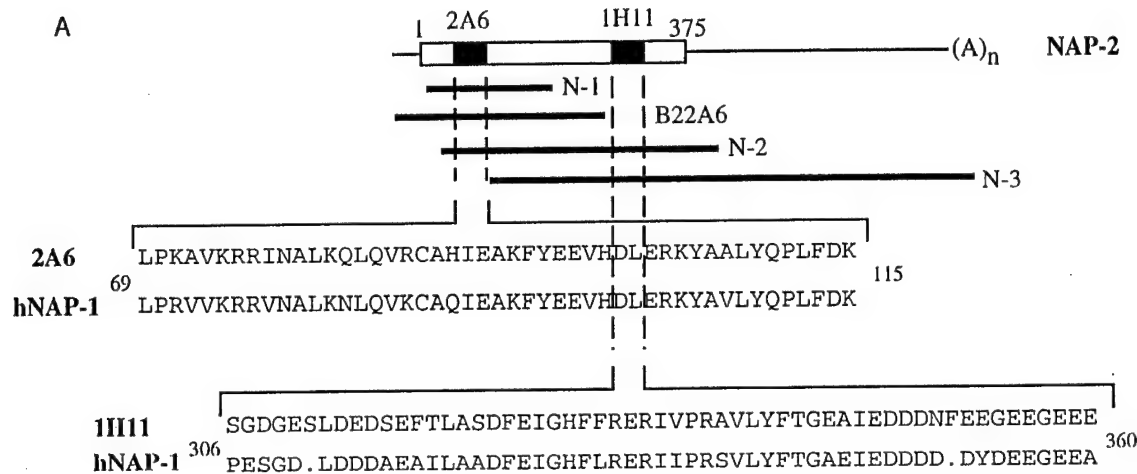


FIG. 1. Structure of the NAP-2 gene. (A) Schematic representation of the NAP-2 cDNA, identifying the coding region (open box) and the UTRs (thin line). Amino acid positions are indicated above the coding region. A schematic representation of the four cDNA clones used to elucidate the NAP-2 sequence in this study are shown immediately below. The relative positions and amino acid sequences of the trapped exons used to screen cDNA libraries for NAP-2 are illustrated. A comparison to the homologous regions of the human NAP-1 gene is illustrated. (B) Alignment of the amino acid sequences of NAP-2 to NAP-1 sequences from human (hNAP-1), mouse (mNAP-1), *Drosophila* (dNAP-1), and yeast (yNAP-1). Dashes between NAP-2 and hNAP-1 indicate identical amino acid residues, whereas + indicates a conserved charged amino acid residue. Amino acid differences between the murine and the human NAP-1 proteins are indicated by lowercase murine amino acids. Amino acids conserved among the NAP proteins are grouped within boxes. Stretches of acidic amino acids are indicated by an overline and the putative nuclear localization signal is indicated by a dashed overline. (C) Alternative splicing of the NAP-2 gene. The nucleotide sequence at the C-terminus of the predicted ORF of N-2 (Splice Form I) and N-3 (Splice Form II) are presented (right). An RT-PCR was performed from human placenta RNA with primers (NF-8, 5'GCTGTGCTGTAAGTCACTGGG3' and NAP-D, 5'CCACTGTACAAGTTAA3') that bracketed the alternatively spliced region and are predicted to generate products of 393 bp (Splice Form I) and 355 bp (Splice Form II). Complementary DNA was generated with SuperScript (Life Technologies) and random hexamers according to the manufacturer's protocol. Amplifications were performed with an annealing temperature of 55°C and for 40 cycles. Products were analyzed on a 10% polyacrylamide gel and visualized by staining with ethidium bromide (left, lane 2). Molecular weight markers are pBR322 digested with *MspI* (NEB) (left, lane 1).

EDTA, 10% glycerol) containing 300 mM imidazole. Proteins were dialyzed against elution buffer (lacking imidazole) overnight and stored at -80°C.

Enzyme-linked immunosorbent assay (ELISA). To quantitate NAP binding to histones, ELISA was performed by coating the wells of microtiter plates (Nunc) with individual, purified histones (Boehringer Mannheim Corp). Essentially 100 μ l of 3.5 μ M each histone (dissolved in PBS) was incubated with the microtiter plates overnight at 4°C. After incubation, plates were washed with PBS and pre-blocked overnight at 4°C with 100 μ l PBS containing 5% bovine serum albumin (BSA). One hundred microliters of purified NAP protein (0–60 ng/ml) (see Fig. 3B), resuspended in PBS containing 5% BSA and 0.2% Tween 20, was added to each microtiter well and incubated at 37°C for 1 h. The plates were washed three times with PBS/0.2% Tween 20, after which a rabbit polyclonal anti-NAP-2 antibody (diluted 1/700 in PBS containing 5% BSA) was added to each well and incubated for 1 h at 37°C. After three washes with PBS/0.2% Tween 20, a color reaction was developed using alkaline phosphatase-conjugated anti-rabbit antibodies and *p*-nitrophenylphosphate. Reactions were quantitated by recording the optical density at 405 nm.

Affinity selection of histones from nuclear extracts. Recombinant NAP-2 was coupled to cyanogen bromide-activated Sepharose (CNBr-Sepharose; Pharmacia) in 0.2 M phosphate buffer (pH 6.0), 0.5 M NaCl for 2 h at room temperature. The final concentration of hNAP-2 immobilized to CNBr-Sepharose was 10 mg/ml. The matrix was washed and treated as recommended by the manufacturer's instructions. HeLa nuclear extracts were prepared as previously described (Dignam *et al.*, 1983). Sixty milligrams of nuclear extract (0.3 mg/ml) was passed over 700 μ l NAP-2-Sepharose in binding buffer (20 mM *N*-2-hydroxyethylpiperazine-*N*'-2-ethanesulfonic acid [pH 7.6], 20% glycerol, 1 mM EDTA, 1 mM DTT, 120 mM NaCl, 1 mM PMSF, 10 μ g/ml pepstatin, 10 μ g/ml aprotinin) overnight at 4°C. The resin was then washed extensively with the same buffer until

no protein could be detected in the eluent by the Pierce Coomassie blue protein assay. Washes were then performed in binding buffer containing 250, 400, and 600 mM NaCl. In the case of Western blot analysis, an anti-H1 histone monoclonal antibody (Boehringer Mannheim) was utilized to detect H1. Although this antibody can specifically recognize all histones, it is weakly reactive and does not decorate well (Fig. 3B, lane 6; P.R., unpublished observations).

Histone transfer assays. Reactions were performed at 37°C in buffer containing 20 mM Tris-Cl [pH 8.0], 150 mM NaCl, 5 mM MgCl₂, 1 mM EDTA, and 2 mg/ml bovine serum albumin. Covalently closed circular DNA (0.4 μ g) of pKS II' was preincubated with 1 unit of topoisomerase I (Promega) for 40 min. HeLa core histones (0.6 μ g) were preincubated with various concentrations of hNAP-1, NAP-2, or deletions of NAP-2 on ice for 30 min in a total volume of 5 μ l. These two reactions were combined (final volume of 7 μ l) and incubated further at 37°C for 40 min. The reaction was terminated with the addition of 0.3 μ g of proteinase K in PK buffer (100 mM Tris-Cl [pH 7.5], 12.5 mM EDTA, 0.15 M NaCl, 1% SDS) and further incubated at 37°C for 30 min. The DNA was purified by phenol/chloroform extraction, precipitated with ethanol, and electrophoresed in 0.9% agarose gel (TAE) to determine the gain of negative supercoil by histone transfer. DNA was stained by ethidium bromide and visualized by ultraviolet light.

Immunofluorescence and cell cycle synchronization. Sterile coverslips (Chamber Slide System; Nunc) were placed in 100-mm tissue culture dishes and seeded with 2.5×10^4 COS-7 cells. Twenty-four hours later, the cells were transfected with calcium phosphate precipitates of a CMV-based eukaryotic expression vector driving synthesis of HA-tagged NAP-2. Twenty-eight hours after transfection, the coverslips were rinsed with PBS and cells were fixed for 5–10 min, at -20°C, with acetone/methanol (1/1, v/v). The coverslips were then briefly washed with PBS and rehydrated in PBS with 0.2% sodium azide (4°C). For staining, cells were preincubated for 45 min

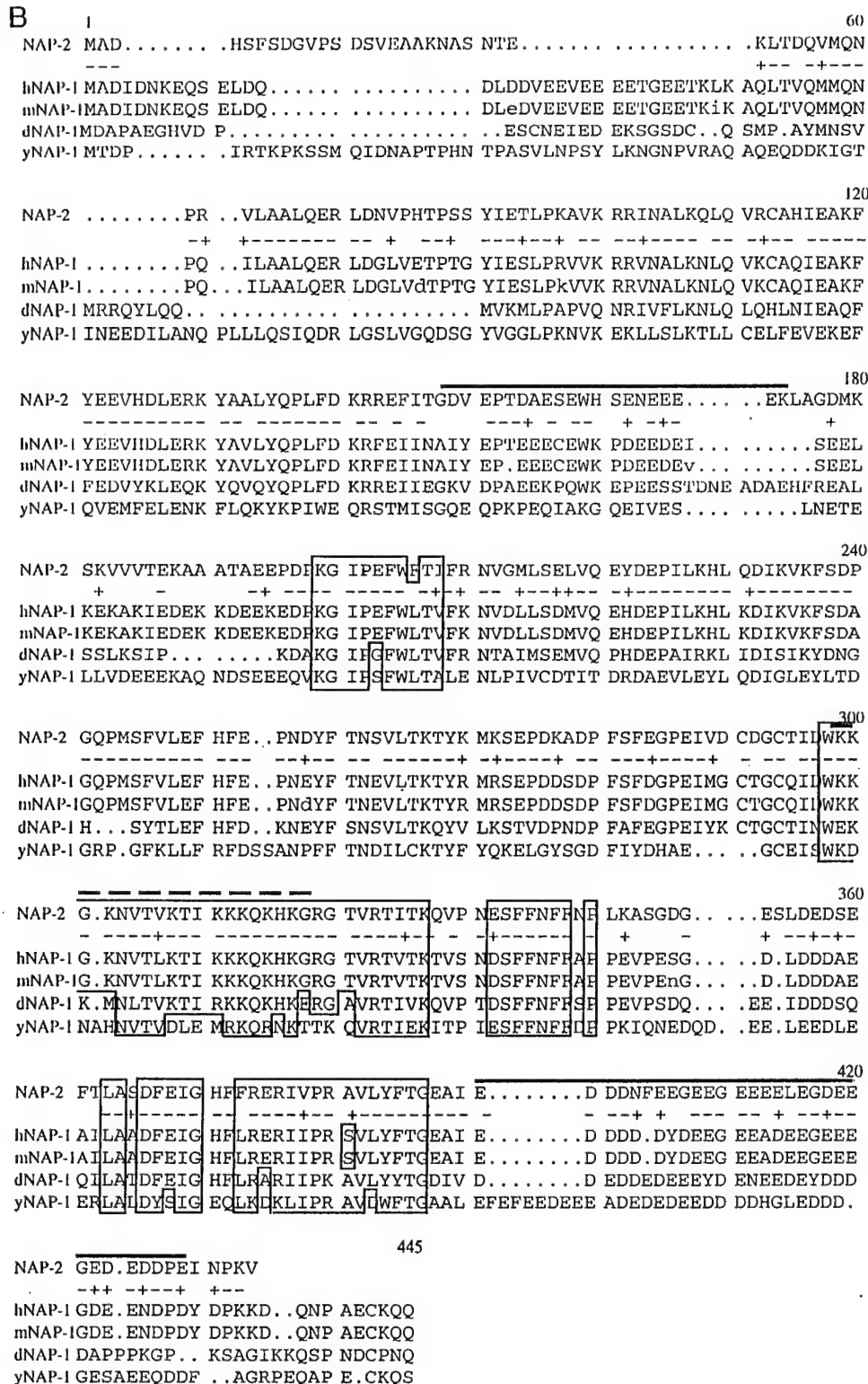


FIG. 1—Continued

in blocking solution (50% fetal bovine serum, 6% skim milk, 3% bovine serum albumin, 0.2% Tween 20, and 0.02% sodium azide in PBS), then incubated with primary antibody (12CA5) diluted in 3% bovine serum albumin, 0.2% Tween 20, 0.02% sodium azide in PBS for 1 h at room temperature. After several washes, secondary anti-mouse antibody conjugated with rhodamine (Pierce) was incubated

for 30 min at room temperature. Cells were rinsed in PBS with 0.2% Tween 20, mounted with 30% glycerol (v/v) in PBS, and examined using a fluorescence microscope (Nikon).

To arrest cells in G0 phase, transfected cells were washed extensively with serum-free medium 24 h after transfection. Complete medium containing 0.5% serum was then added, and cells were incu-

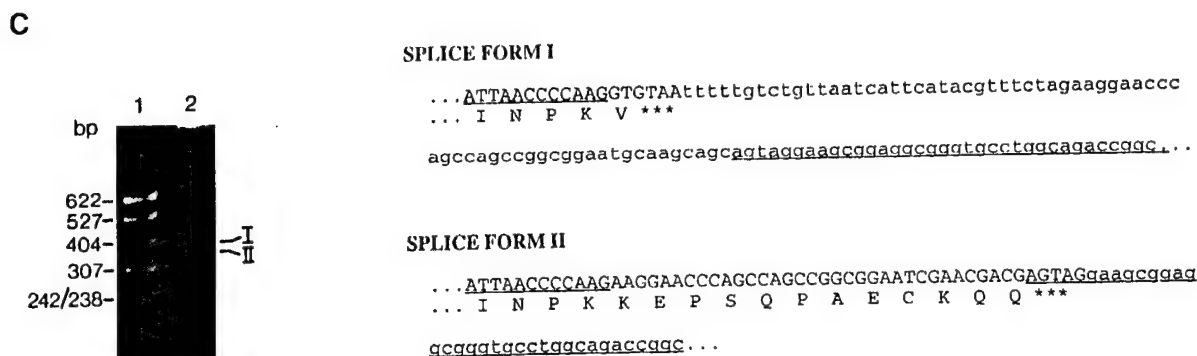


FIG. 1—Continued

bated in a CO₂ incubator at 37°C. After 48 h, fresh medium containing 0.5% serum was added and the incubation continued for another 24 h. For synchronizing cells in S phase, hydroxyurea (final concentration of 2 mM) was added to the culture medium, and cells were treated for 8 h.

RESULTS

The human chromosome 11p15.5 region has been the site of intensive investigation in light of genetic evidence suggesting the presence of a gene(s) involved in normal mammalian development as well as predisposing to several human cancers. Beckwith–Wiedemann syndrome (BWS), a fetal overgrowth syndrome showing predisposition to several embryonal cancers, including rhabdomyosarcoma and WT, maps to 11p15 by genetic linkage analysis (Koufos *et al.*, 1989; Ping *et al.*, 1989), and translocation breakpoints from several BWS individuals have been mapped to the 11p15.5 subband (Hoovers *et al.*, 1995). In addition, several embryonal and adult malignancies demonstrate LOH at 11p15.5 (Mannens *et al.*, 1988; Reeve *et al.*, 1989; Albrecht *et al.*, 1994; Baffa *et al.*, 1996; Bepler and Garcia-Blanco, 1994; Looijenga *et al.*, 1994; Sonoda *et al.*, 1995; Winqvist *et al.*, 1995), suggesting the existence of a tumor suppressor gene(s) in this region. Consistent with this idea are genetic complementation studies in which this DNA band has been shown to suppress tumorigenicity in G401 WT cells (Dowdy *et al.*, 1991; Reid *et al.*, 1996).

Isolation and Characterization of Human NAP2 cDNA Clones

During a physical and transcript mapping strategy aimed at identifying and characterizing genes within the chromosome 11p15.5 subband involved in tumor initiation or progression, a set of exons (2A6, 1H11) that showed significant homology to a family of genes encoding a group of proteins from mammals, *Drosophila*, and yeast, known as nucleosome assembly proteins, was isolated (Fig. 1A) (Ishimi and Kikuchi, 1991; Ito *et al.*, 1996; Simon *et al.*, 1994). These exons mapped between the human cysteinyl-tRNA synthetase gene (Cruzen *et al.*, 1993) and the p57^{KIP2} gene (Matsuoka

et al., 1995), an ~150-kb interval (Prawitt *et al.*, 1996). NAP-1 was originally defined as an activity in mammalian cells that could deposit core histones onto DNA in an ATP-independent fashion (Ishimi *et al.*, 1983, 1984). More recently, NAP-1 has been found to facilitate the binding of transcription factors to mononucleosomes (Walter *et al.*, 1995) and to function with other chromatin assembly activities from *Drosophila* in mediating ATP-facilitated assembly of regularly spaced nucleosome arrays (Ito *et al.*, 1996). Given the postulated role of NAPs in nucleosome assembly and possibly in regulating gene expression (see Discussion), exons 2A6 and 1H11 were further pursued and used as probes to isolate four corresponding cDNAs (Fig. 1A). When sequencing information from these clones was compiled, an open reading frame of 375 amino acids was obtained (Fig. 1A). The sequence of this gene was identical to that previously reported for hNAP-2, a clone obtained by screening a human placental cDNA library (Hu *et al.*, 1996).

The open reading frame encodes a predicted polypeptide of 42,764 Da. Examination of the primary amino acid sequence of NAP-2 (Fig. 1B) revealed that it contains two highly acidic segments, one at amino acids 113–132 and one at the C-terminus, encompassing amino acids 341–360 (overlined in Fig. 1B). In addition, there is a stretch of amino acid residues at position 255–274 (dashed overline in Fig. 1B) that has characteristics similar to those of nuclear localization signals (Dingwall and Laskey, 1991). Comparison of the primary amino acid sequences of NAP-2 to the human and murine hNAP-1 polypeptides revealed ~63% identity between hNAP-2 and the two mammalian NAP-1 genes. There is 41% identity between the primary amino acid sequences of dNAP-1 versus NAP-2 and 31% identity between yNAP and NAP-2 (Fig. 1B). This is similar to the identities between hNAP-1 and dNAP-1 (47%) and between hNAP-1 and yNAP (31%) (Ito *et al.*, 1996). The putative nuclear import signal is highly conserved among NAP-2, hNAP-1, and mNAP-1 (position 299–319 in Fig. 2). Three previously identified regions are well conserved among all NAP proteins: (i) KGIPXFWLTϕ situated at position 199–208 of Fig. 1B, (ii) cSFFNFFXP situated at position 332–340 of

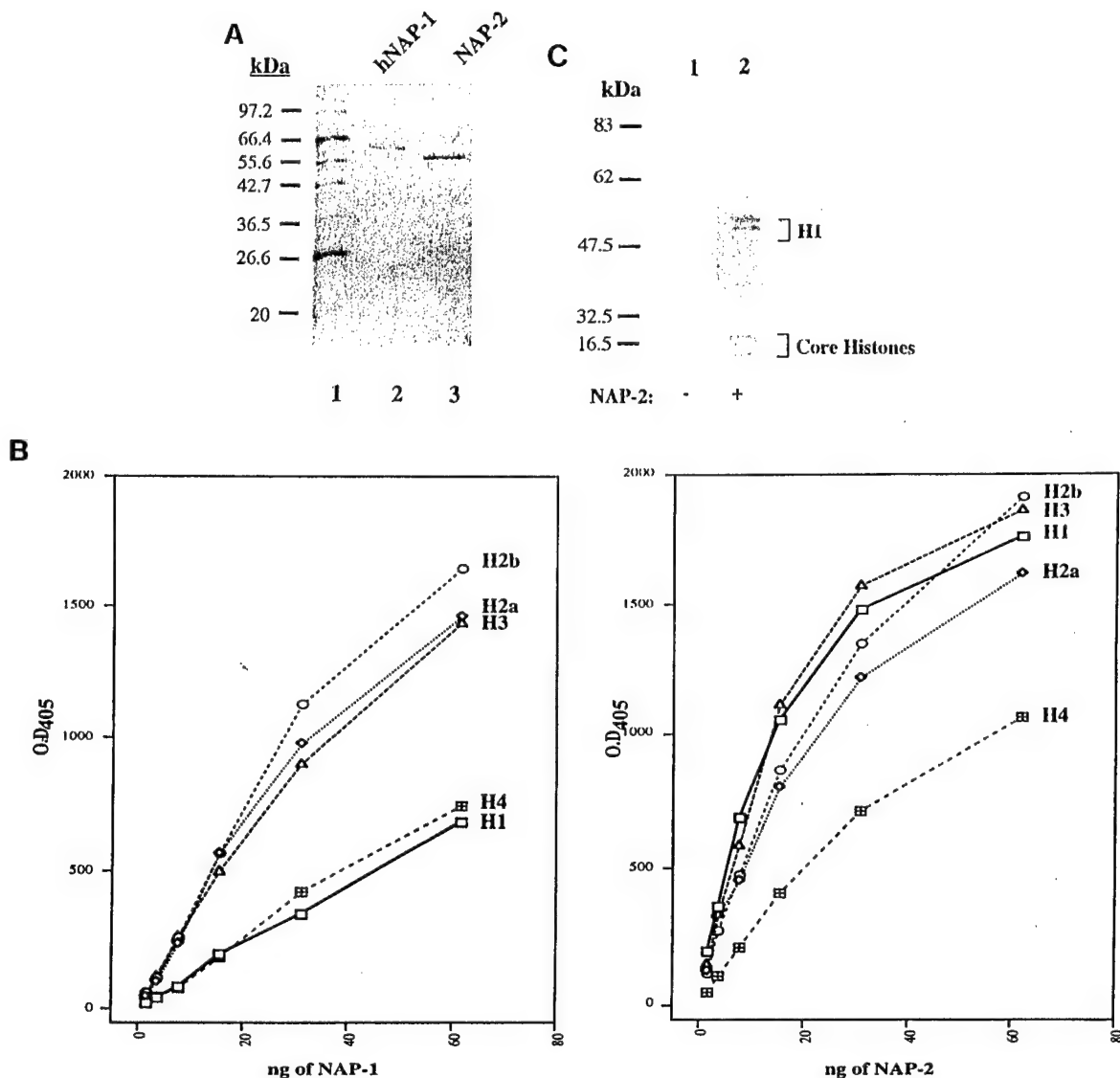


FIG. 2. Binding of hNAP-1 and NAP-2 to core and linker histones. (A) Analysis of *E. coli*-synthesized hNAP-1 and NAP-2. Recombinant proteins were analyzed by SDS-12.5% PAGE and stained with Coomassie blue R-250. Samples were loaded as follows: lane 1, molecular weight markers (Broad Range; New England Biolabs) (in kDa); lane 2, recombinant hNAP-1 protein; lane 3, recombinant NAP-2 protein. Both proteins migrate slower than expected from the predicted molecular weights. The basis for this difference is not known. (B) Binding of hNAP-1 and NAP-2 to core and linker histones. ELISA was performed as described under Materials and Methods. The OD₄₀₅ is presented on the y axis and the amount of NAP protein titrated into the ELISA indicated on the x axis. Histones used to coat the microtiter wells are indicated to the right of each graph. Each assay was performed in duplicate in two independent experiments. (C) Far-Western blot using NAP-2 as probe. Ten micrograms of H1 and core histones was fractionated on a 12% SDS-PAGE and blotted onto nitrocellulose. Following transfer, the membrane was washed three times in wash buffer (20 mM Tris-HCl [pH 7.5], 150 mM NaCl, 0.2% Tween 20, 1 mM EDTA, 1 mM β -mercaptoethanol). Blocking was performed in the same buffer containing 5% BSA overnight at 4°C. Recombinant NAP-2 (~0.1 μ g/ μ l) dissolved in wash buffer was incubated with the nitrocellulose filter at room temperature for 2 h. Following washing and staining with anti-HA antibodies, the blot was decorated using an anti-mouse alkaline phosphatase polyclonal antibody. Lane 1, negative control consisting of a nitrocellulose blot containing histones and processed as described above but to which recombinant NAP-2 was not added; lane 2, nitrocellulose blot containing histones and incubated in the presence of NAP-2. Molecular weight standards (pre-stained; New England Biolabs) are indicated to the left.

Fig. 1B, and (iii) LAXD Φ E/SIGXXF/L ρ X ρ ϕ ϕ P ρ S/AVX- Φ Φ TG situated at position 363–387 (X represents any amino acid, ϕ is A/V/I/L, Φ represents polar aliphatic amino acids, ϵ represents conserved negatively charged amino acids, and ρ represents conserved positively charged residues). The conserved nature of these domains from yeast to mammals suggests that they may

play important roles in NAP function. In addition, 3 cysteine residues present in NAP-2 are also present in the two other mammalian homologues, suggesting conservation of intra- and/or intermolecular disulfide bridge interaction. We also note the presence of nine predicted casein kinase II phosphorylation sites (S*/T*XXD/E, in which the asterisk denotes the phosphory-

lated serine or threonine and X is any nonbasic amino acid) (Allende and Allende, 1995), with only the site at Ser²²⁹ conserved among mammalian NAP homologues (Fig. 1B).

During nucleotide sequence characterization of our cDNAs, we noticed that clone N-3 displayed a primary nucleotide sequence around the termination codon different from that of clone N-2. The difference in sequence information implied that N-3 encoded a NAP-2 protein isoform differing from that present in Fig. 1B with an additional 12 amino acids at the C-terminus replacing the terminal valine residue (Splice Form II; Fig. 1C). This feature was also noticed by Hu *et al.* (1996), who found this difference in one of four clones, but did not define the molecular basis for this change. To determine if this was the result of alternative splicing, we performed RT-PCR to determine if we could detect both predicted mRNA isoforms from placenta RNA. The predicted molecular sizes of the two PCR products are 392 and 355 bp from Splice Forms I and II, respectively. Both products were obtained from placenta cDNA (Fig. 1C, left). These results indicate that the NAP-2 gene is alternatively spliced to produce two protein isoforms which differ at their C-termini. For the functional studies described below, we have restricted our analyses to characterization of Splice Form I.

Recombinant hNAP-2 Can Bind Core and Linker Histones

To characterize the biochemical properties of hNAP-2, we overexpressed hNAP-1 and NAP-2 in *E. coli* and purified the recombinant protein to greater than 95% homogeneity (Fig. 2A). This recombinant protein was then used in an ELISA to determine if it could bind to histones (Fig. 2B). Under physiological ionic conditions, both hNAP-1 and NAP-2 could complex with all four core histones (H2a, H2b, H3, and H4), as well as the H1 linker histone (Fig. 2B). One noticeable difference in the binding properties of the two proteins is the higher retention of NAP-2 by H1, compared to hNAP-1.

These results were extended in a Western blot overlay assay. In this approach, core (H2a, H2b, H3, H4) and linker (H1) histones were fractionated on a 12% polyacrylamide gel, transferred to nitrocellulose, and incubated with recombinant HA-tagged NAP-2. Following decoration with an anti-HA monoclonal antibody, it is clear that NAP-2 had been retained on the nitrocellulose by its interaction with both core and linker histones (Fig. 2C). Linker histone H1 often appears as several species on SDS-PAGE analysis due to the existence of several isoforms of this protein (Wolffe, 1995). In addition, using immobilized recombinant NAP-2-Sepharose affinity chromatography, we have also demonstrated retention of all four core and H1 linker histones by NAP-2 (P.R., data not shown). These experiments directly demonstrate that NAP-2 is capable of interacting with core and H1 linker histones.

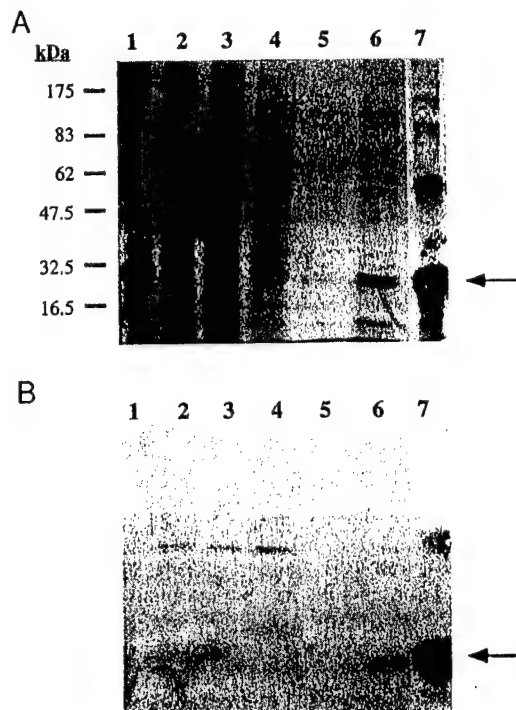


FIG. 3. Selection of the linker histone, H1, from HeLa nuclear extracts by immobilized NAP-2. Recombinant NAP-2 was immobilized to CNBr-activated Sepharose as described under Materials and Methods. A HeLa nuclear extract was loaded and fractionated on the NAP-2-Sepharose column as described under Materials and Methods. Protein fractions were analyzed directly by Coomassie staining (A) or by Western blotting using an anti-histone antibody (B) and consisted of lane 1, prestained molecular weight markers from New England Biolabs; lane 2, input crude nuclear extract (19 μ g); lane 3, flowthrough (19 μ g); lane 4, 250 mM NaCl eluent (50 μ l); lane 5, 400 mM NaCl eluent (50 μ l); lane 6, 600 mM NaCl eluent (50 μ l); lane 7, histone H1 (8 μ g) (Sigma).

The linker histone, H1, is present in crude preparations of nuclear extracts. To determine if H1/NAP-2 recognition could occur among a complex pool of proteins, immobilized NAP-2-Sepharose was incubated with nuclear extracts prepared from HeLa cells. Nuclear extract was loaded onto immobilized NAP-2-Sepharose and protein fractions obtained after washing the column were fractionated by SDS-PAGE and visualized by staining with Coomassie blue (Fig. 3A). A parallel analysis was performed in which the same samples were transferred to nitrocellulose paper following SDS-PAGE fractionation and decorated with an anti-histone monoclonal antibody (Fig. 3B). Coomassie blue analysis of proteins loaded onto immobilized hNAP-2 (Fig. 3A, lane 2), eluting in the flowthrough (lane 3), or stripped from the column with 250 mM NaCl (lane 4) revealed a complex profile. A small amount of H1 histone could be detected in the input nuclear extract preparation when stained with an anti-histone monoclonal antibody (Fig. 3B, lane 2). However, no H1 histone was detectable in the flowthrough (Fig. 3B, lane 3) or in the 250 mM wash (Fig. 3B, lane 4), suggesting that the majority of H1 was retained by immobilized NAP-2. Washing NAP-2-

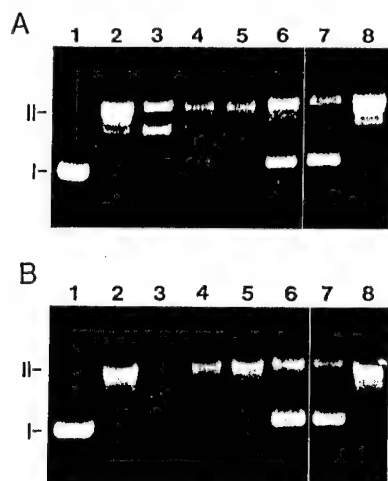


FIG. 4. Supercoiling assay for hNAP-1 and NAP-2. Recombinant hNAP-1 (A) or NAP-2 (B) was added to relaxed DNA, and histone transfer reactions were performed as detailed under Materials and Methods. Lane 1 contains 0.4 μ g of supercoiled pKS II⁺ as marker for Form I DNA, and lane 2 contains relaxed circular DNA prepared with topoisomerase I. A fixed amount of core histones (0.8 μ g) (lane 3–7) was incubated with increasing amounts of NAP-1 (A) or NAP-2 (B): lane 3, 0 μ g; lane 4, 0.4 μ g; lane 5, 0.8 μ g; lane 6, 1.6 μ g; lane 7, 6.4 μ g. Lane 8 contains relaxed circular DNA incubated with 1.6 μ g of recombinant NAP protein in the absence of core histones.

Sephacrose with 400 mM NaCl did not result in the elution of any new proteins, as assessed by Coomassie blue (Fig. 3A, lane 5), nor did any H1 histones elute at this salt concentration (Fig. 3B, lane 5). However, when the hNAP-2–Sephacrose column was washed with 600 mM NaCl, the eluent clearly contained a protein doublet that comigrated with purified histone H1 (compare lane 6 to 7). The identity of this protein doublet as histone H1 was revealed by immunoblotting with anti-histone antibodies (Fig. 3B, lane 6). These results indicate that NAP-2 can specifically recognize H1 histone from a complex mixture of macromolecules.

Histone Transfer Assays

We assessed the ability of NAP-2 to transfer histones onto naked DNA in a supercoiling assay. In this assay, hNAP-1 and NAP-2 were preincubated with histones followed by the addition of relaxed DNA to the reaction mixture. When the DNA was recovered as a negatively supercoiled form, this indicated that nucleosomes were formed, otherwise the DNA remained relaxed. The histone transfer reaction was dependent on the presence of both core histones and either hNAP-1 (Fig. 4A) or NAP-2 (Fig. 4B), since in the absence of either of these proteins, no supercoiling is observed (Fig. 4, lanes 2–4 and lane 8). Addition of increasing amounts of hNAP-1 (Fig. 4A) or NAP-2 (Fig. 4B) resulted in the formation of progressively greater amounts of supercoiled DNA (lanes 5–7). These results indicate that NAP-2 has a nucleosome assembly activity comparable to that of hNAP-1.

In an attempt to map the region necessary for histone

transfer, various regions of the NAP-2 coding region were deleted (Fig. 5A) and expressed in *E. coli*. We deleted a conserved motif at amino acid position 157–165, KGIPXFWLT ϕ , found in yeast, *Drosophila*, and mammalian NAP proteins [Δ (157–165)]. In addition, we eliminated the C-terminal acidic domain [Δ (330–375)] or amino-terminal sequences [Δ (1–35)]. Larger deletions removed the C-terminal half of the protein, while retaining [Δ (159–375)] or losing [Δ (108–375)] the first acidic domain. Each polypeptide was purified by Ni²⁺-chelate chromatography to greater than 90% homogeneity (Fig. 5B). All deletions abolished histone transfer activity of NAP-2 (Fig. 5C, compare lanes 6–11 to lane 5). These results indicate that N- and C-terminal regions, as well as the internal conserved motif (KGIPXFWLT ϕ) of NAP-2, are necessary for its histone transfer activity.

Subcellular Localization of NAP-2

The above experiments suggest a role for NAP-2 in chromatin assembly. It has recently been demonstrated that *Drosophila* NAP-1 can shuffle between the cytoplasm and the nucleus, possibly acting as a histone chaperone to bring histones from their site of synthesis (cytoplasm) to their site of action (nucleus) (Ito *et al.*, 1996). We therefore determined the subcellular localization of NAP-2 in two groups of COS cells transfected with a CMV-based expression vector synthesizing HA-tagged NAP-2. In these experiments, cells were either arrested in S phase by treatment with hydroxyurea (Fig. 6A) or blocked at the G0/G1 boundary by serum starvation (Fig. 6B). Visualization of NAP-2 with anti-HA staining demonstrated that NAP-2 is present in the cytoplasm and excluded from the nucleus during G0/G1 (Fig. 6B), then relocates to the nucleus by the time cells are in S phase (Fig. 6A). These results demonstrate that the subcellular localization of NAP-2 is cell-cycle dependent and that this protein may play a role in shuttling histones from the cytoplasm to the nucleus.

Analysis of NAP-2 in Wilms Tumors

The chromosomal location of the NAP-2 gene at 11p15.5 and its putative role in nucleosome assembly (and hence in regulating gene expression) suggested it might be a candidate for the second WT suppressor gene mapping to this region. To perform PCR–single-stranded conformational polymorphism (SSCP) analysis of the NAP-2 gene in WT, we elucidated the exon/intron structure of NAP-2 by comparing genomic and cDNA sequences (Fig. 7). The coding region of the NAP-2 gene consists of 14 exons and spans ~30,500 bp. Fourteen pairs of PCR primers were designed to amplify each individual NAP-2 coding exon from DNA from a total of 100 sporadic WTs (P.R. and L.L.C., data not shown) and 28 individuals with Beckwith–Wiedemann syndrome (D.M., data not shown). No evidence for nonsense, frameshift, or deletion mutations was ob-

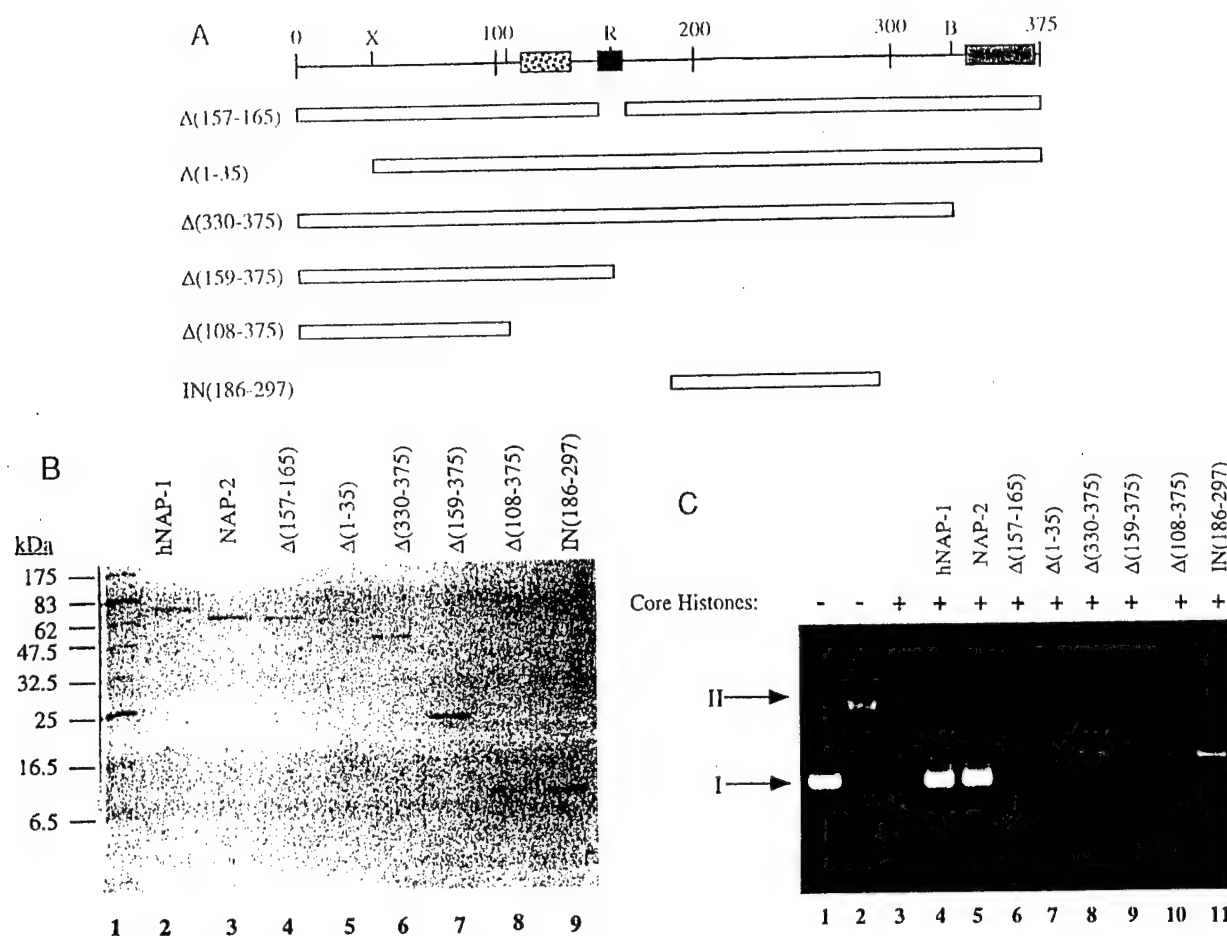


FIG. 5. Deletion analysis of NAP-2. (A) Schematic representation of NAP-2 deletion mutants. PCR-mediated mutagenesis was used to generate the NAP-2 deletion mutants illustrated, and details as to plasmid construction can be obtained from the authors upon written request. All products generated by PCR were sequenced to verify the integrity of the coding region. (B) Analysis of *E. coli*-synthesized NAP-2 deletion mutants. Recombinant proteins were analyzed by SDS-12.5% PAGE and stained with Coomassie blue R-250. Samples were loaded as follows: lane 1, molecular weight markers (broad range; New England Biolabs) (in kDa); lane 2, recombinant NAP-2 protein; lane 3, $\Delta(157-165)$; lane 4, $\Delta(1-35)$; lane 5, $\Delta(330-375)$; lane 6, $\Delta(159-375)$; lane 7, $\Delta(108-375)$; lane 8, $\Delta(186-297)$. (C) Supercoiling assay for NAP-2 derivatives. A fixed amount of core histones (0.6 μ g) (lanes 3-11) was incubated with relaxed DNA (0.3 μ g) (lane 2) and the following recombinant NAP proteins for 2 h at 37°C: lane 3, no NAP protein; lane 4, 3.2 μ g NAP-1; lane 5, 3.2 μ g NAP-2; lane 6, 3.2 μ g $\Delta(157-165)$; lane 7, 3.2 μ g $\Delta(1-35)$; lane 8, 3.2 μ g $\Delta(330-375)$; lane 9, 1.6 μ g $\Delta(159-375)$; lane 10, 1 μ g $\Delta(108-375)$; lane 11, 1 μ g $\Delta(186-297)$. Lane 1 contains supercoiled plasmid as a marker.

tained by this analysis. To eliminate the possibility that we had missed a mutational hotspot by PCR-SSCP (i.e., false negatives), we analyzed the complete coding region of NAP-2 by directly sequencing the cDNA obtained by RT-PCR from 5 sporadic WT specimens. No mutations were found in these 5 sporadic WT samples (L.L.C. and J.P., data not shown).

We used G401 cells to functionally assess whether NAP-2 could suppress tumorigenicity in this cell line (Table 1). G401 cells form tumors when injected subcutaneously into nude mice. They have a pseudodiploid karyotype with two cytogenetically normal copies of chromosome 11 but presumably lack expression of an 11p15 tumor suppressor gene. In our assay, we introduced NAP-2 into G401 cells under control of the constitutive CMV viral promoter (G401/NAP-2), as well as a control vector (G401/pSV2neo) lacking the NAP-2 coding region. The tumorigenic potential of these cell

lines was analyzed in nude mice. The results indicate that NAP-2 had no influence on the tumorigenicity of G401 cells (Table 1). Taken together, these results suggest that mutations in NAP-2 are not associated with initiation or progression of WT and that this gene does not function as a tumor suppressor gene in G401 cells.

DISCUSSION

The identification of a family of related histone-binding proteins demonstrating sequence conservation from humans to yeast suggests that aspects of chromatin assembly have been evolutionarily conserved. The protein we characterize in this report, NAP-2, represents a new member of the nucleosome assembly protein family. Comparison of NAP-2 with other mammalian, yeast, and *Drosophila* NAP proteins revealed



FIG. 6. Cell-cycle-dependent subcellular localization of NAP-2. Following transfection of COS-7 cells with a CMV-based expression vector driving synthesis of HA-tagged NAP-2, cells were treated with hydroxyurea for 8 h (A) or starved for fetal calf serum for 72 h (B). The protein was visualized by indirect immunofluorescence using the anti-HA antibody, 12CA5, and rhodamine-conjugated secondary antibody.

several regions of interesting similarity (Fig. 1B). Polyacidic stretches of the kind found in NAP proteins may facilitate binding of these molecules to histones or to other basic proteins (Stein *et al.*, 1979; Jantzen *et al.*, 1990). Clusters of negatively charged regions are also found in N1, nucleoplasmin, and high-mobility-group protein-1 (Lapeyre *et al.*, 1987; Schmidt Zachmann *et al.*, 1987; Wen *et al.*, 1989). Not all polyacidic domains are essential for NAP-stimulated histone transfer to DNA, as assessed by deletion mutagenesis of the yeast NAP-1 homologue (Fujii-Nakata *et al.*, 1992). However, these may be required for other aspects of NAP function. Interestingly, fusion of a polyacidic domain from a NAP-related protein, *set*, to the *can* gene has been associated with myeloid leukemogenesis (von Lindern *et al.*, 1992), although the mechanism of transformation has not been elucidated for this fusion protein. Unlike other mammalian NAP proteins, which have three acidic domains, NAP-2 has only two such domains (Fig. 1B). Like NAP-1, NAP-2 can transfer histones to naked DNA, albeit with lower efficiency (Fig.

4). Whether this decreased efficiency is the result of having only two acidic domains remains to be experimentally addressed. Deletion mutagenesis of the C-terminal acidic region abolishes the histone transfer activity of NAP-2, demonstrating the essential nature of this domain for NAP-2 activity (Fig. 5).

Three regions are well conserved among all NAP proteins, (i) KGIPXFWLT ϕ (position 199–208 in Fig. 1B), (ii) ϵ SFFNFFXP (position 332–340 in Fig. 1B), and (iii) LAXD ϕ E/SIGXXF/L ρ X ρ ϕ ϕ P ρ S/AVX ϕ GTG (position 363–387), suggesting functionally important domains. Consistent with this interpretation, deletion of the KGIPXFWLT ϕ region resulted in a NAP-2 polypeptide that was not capable of nucleosome assembly (Fig. 5). NAP-2 has a large number of potential casein kinase II phosphorylation sites, and consequently, its activity may be regulated by this enzyme. Such is the case for nucleoplasmin for which it has been shown that the phosphorylated protein binds to histones more effectively and is more active in histone transfer than the unphosphorylated protein (Schmidt Zachmann *et al.*, 1987).

Northern blot analysis of NAP-2 mRNA expression demonstrated that NAP-2 is expressed as a 2.6- to 3.0-kb transcript in all tissues analyzed (Hu *et al.*, 1996). Analysis of NAP-2 protein expression profile using anti-NAP-2 antibodies indicates that it is also ubiquitously expressed (P.R. and J.P., data not shown). In our hands, NAP-2 was able to bind to core histones as well as to H1 linker histones (Fig. 2). NAP-1 was also capable of binding to H1 linker histones, although it did so less effectively than NAP-2 (Fig. 2B). It has been suggested that, *in vivo*, H3/H4 histones are rapidly deposited onto newly replicated DNA followed by binding of H2A/H2B histones (Worcel *et al.*, 1978). NAP-1 has been shown to have higher affinity for H2A/H2B than for H3/H4 histones and may therefore act at the second stage of H2A/H2B histone transfer to DNA (Ishimi *et al.*, 1987). Elucidating the relative affinities of NAP-2 for the core histones may help determine at which step it plays a role in histone transfer.

We have found that NAP-2 protein is present in the cytoplasm of cells at the G0/G1 boundary, then proceeds to translocate to the nucleus where the majority of protein can be found in S phase. These results are similar to those obtained for dNAP-1, demonstrating that this factor is present in the nucleus during S phase and is predominantly cytoplasmic during G2 phase (Ito *et al.*, 1996). Ito and co-workers (1996) proposed that dNAP-1 may therefore function as a chaperone to deliver histones from their site of synthesis (cytoplasm) to their site of utilization (nucleus). Taken together, our results demonstrating (i) NAP-2 binding to core and linker histones, (ii) cell-cycle-dependent localization of NAP-2, and (iii) the histone transfer activity of NAP-2, suggest that NAP-2 functions in a manner similar to that of dNAP-1 to transfer core and linker histones from the cytoplasm (site of synthesis) to the nucleus, where they are then incorporated into nucleo-

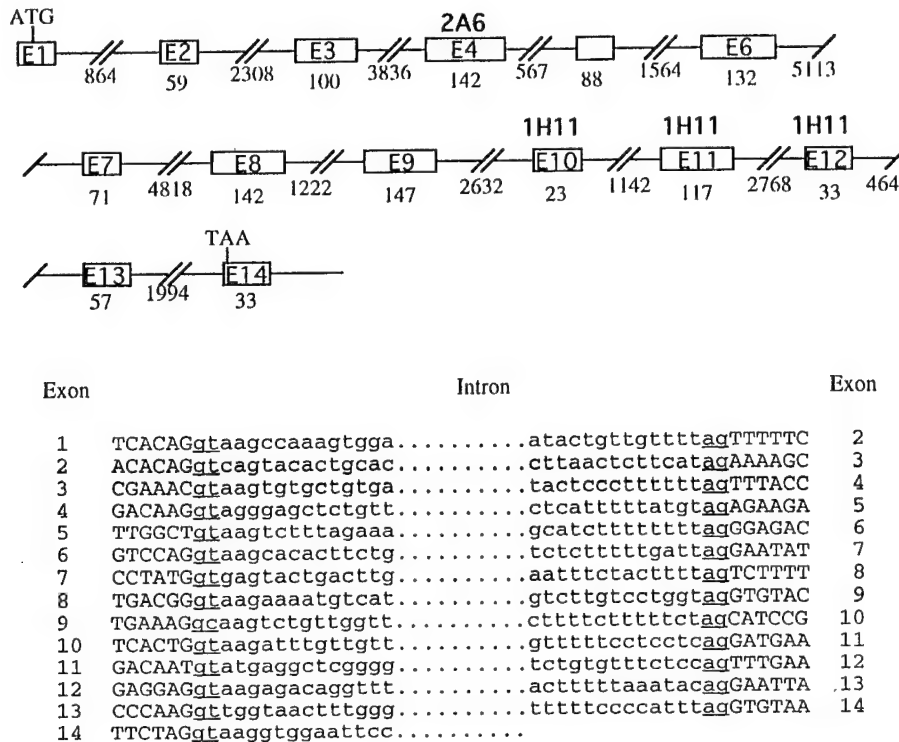


FIG. 7. Genomic organization of NAP-2. The exon/intron structure of NAP-2 was elucidated by comparing genomic and cDNA sequence information and is schematically shown. Numbers below individual exons (illustrated by boxes) or introns (broken lines) refer to the size (in basepairs) of each unit. The sequences of the individual exon/intron boundaries are shown. Exon sequence information is in uppercase while intron sequence is in lowercase. Splice donor and acceptor sites are underlined.

somes. A putative nuclear import signal, KKKGKNV-TVKTIKKKQKHKGR, is highly conserved among NAP-2, hNAP-1, and mNAP-1 (position 299–319 in Fig. 1B). This motif is present in a number of other nuclear proteins, and whether this signal is necessary and/or sufficient to confer nuclear localization to NAP-2 remains to be determined (Dingwall and Laskey, 1991). Whether this signal motif is the target of posttranslational modifications to regulate subcellular localization of NAP-2 remains to be experimentally addressed.

The NAP-2 gene maps to 11p15.5 (Prawitt *et al.*, 1996; Hu *et al.*, 1996), a region in which LOH has been observed in several embryonal and adult tumors (Mannens *et al.*, 1988; Reeve *et al.*, 1989; Albrecht *et al.*,

1994; Baffa *et al.*, 1996; Bepler and Garcia-Blanco, 1994; Looijenga *et al.*, 1994; Sonoda *et al.*, 1995; Winqvist *et al.*, 1995). These genetic studies indicate the presence of one or more tumor suppressor genes in this region. Since 50% of WTs show LOH restricted to 11p15.5 (Mannens *et al.*, 1988; Reeve *et al.*, 1989), we elucidated the exon/intron structure of the NAP-2 gene (Fig. 7) and examined its structural integrity in 100 WT specimens by PCR–SSCP. We have also directly sequenced the entire NAP-2 coding region from five sporadic WTs and found no evidence for inactivating mutations (L.L.C. and J.P., data not shown). NAP-2 was also unable to suppress tumorigenesis in the G401 tumor suppression assay (Table 1). The functional data we present herein are consistent with the idea that this novel protein acts as a histone chaperone, in an activity related to chromatin assembly and/or in DNA replication. Further characterization of this protein will provide a framework for understanding the putative role of NAP-2 in these processes.

ACKNOWLEDGMENTS

P.R. and J.K. were supported by student fellowships from the McGill Cancer Center. D.M. and D.P. contributed equally to the work presented herein. J.P. is an MRC scientist. This work was supported by a grant from the Deutsche Forschungsgemeinschaft to A.W. and B.Z., by NIH Grant CA63176 to B.W., by grants from the National Center for Human Genome Research to G.A.E. and C.D. and from the Department of Energy to G.A.E., by NIH Grant PO1 CA42063

TABLE 1

Results of Tumorigenicity Tests

Cell line	Tumor take ^a
G401.6GTG.c6	6/6
G401/pSV2neo.2	4/4 ^b
G401/pSV2neo.3	6/6
G401/NAI ² .1	5/6
G401/NAI ² .3	6/6
G401/NAP2.6	6/6

^a Each line was injected into three nude mice, two sites per animal, for a total of six sites.

^b One animal died soon after injection so there are only four sites for this line.

to D.H., by NIH Grants CA63333 and HG00333 and Army Grant DAMD17-94-J-4417 to T.S., and by grants from the National Cancer Institute of Canada, the Medical Research Council of Canada, and the Kidney Foundation of Canada to J.P.

REFERENCES

- Albrecht, S., von Schweinitz, D., Waha, A., Kraus, J. A., von Deimling, A., and Pietsch, T. (1994). Loss of maternal alleles on chromosome arm 11p in hepatoblastoma. *Cancer Res.* **54**: 5041–5044.
- Allende, J. E., and Allende, A. C. (1995). Protein kinases. IV. Protein kinase CK2: An enzyme with multiple substrates and a puzzling regulation. *FASEB J.* **9**: 313–323.
- Arents, G., and Moudrianakis, E. N. (1993). Topography of the histone octamer surface: Repeating structural motifs utilized in the docking of nucleosomal DNA. *Proc. Natl. Acad. Sci. USA* **90**: 10489–10493.
- Baffa, R., Negrini, M., Mandes, B., Rugge, M., Ranzani, G. N., Hirohashi, S., and Croce, C. M. (1996). Loss of heterozygosity for chromosome 11 in adenocarcinoma of the stomach. *Cancer Res.* **56**: 268–272.
- Bepler, G., and Garcia-Blanco, M. A. (1994). Three tumor-suppressor regions on chromosome 11p identified by high-resolution deletion mapping in human non-small-cell lung cancer. *Proc. Natl. Acad. Sci. USA* **91**: 5513–5517.
- Crevel, G., and Cotterill, S. (1995). DF 31, a sperm decondensation factor from *Drosophila melanogaster*: Purification and characterization. *EMBO J.* **14**: 1711–1717.
- Cruzen, M. E., Bengtsson, U., McMahon, J., Wasmuth, J. J., and Arfin, S. M. (1993). Assignment of the cysteinyl-tRNA synthetase gene (CARS) to 11p15.5. *Genomics* **15**: 692–693.
- Cullen, K. E., Kladde, M. P., and Seyfred, M. A. (1993). Interaction between transcription regulatory regions of prolactin chromatin. *Science* **261**: 203–206.
- Dignam, J. D., Lebovitz, R. M., and Roeder, R. G. (1983). Accurate transcription initiation by RNA polymerase II in a soluble extract from isolated mammalian nuclei. *Nucleic Acids Res.* **11**: 1475–1488.
- Dilworth, S. M., Black, S. J., and Laskey, R. A. (1987). Two complexes that contain histones are required for nucleosome assembly in vitro: Role of nucleoplasmin and N1 in *Xenopus* egg extracts. *Cell* **51**: 1009–1018.
- Dilworth, S. M., and Dingwall, C. (1988). Chromatin assembly in vitro and in vivo. *Bioessays* **9**: 44–49.
- Dingwall, C., and Laskey, R. A. (1991). Nuclear targeting sequences—A consensus? *Trends Biochem. Sci.* **16**: 478–481.
- Dowdy, S. F., Fasching, C. L., Araujo, D., Lai, K.-M., Livanos, E., Weissman, B. E., and Stanbridge, E. J. (1991). Suppression of tumorigenicity in Wilms tumor by the p15.5–p14 region of chromosome 11. *Science* **254**: 293–295.
- Field, J., Nikawa, J.-I., Broek, D., MacDonald, B., Rodgers, I. A., Wilson, I. A., Lemer, R. A., and Wigler, M. (1988). Purification of a RAS-responsive adenyl cyclase complex from *Saccharomyces cerevisiae* by use of an epitope addition method. *Mol. Cell. Biol.* **8**: 2159–2165.
- Fujii-Nakata, T., Ishimi, Y., Okuda, A., and Kikuchi, A. (1992). Functional analysis of nucleosome assembly protein, NAP-1. *J. Biol. Chem.* **267**: 20980–20986.
- Hoovers, J. M. N., Kalikin, L. M., Johnson, L. A., Alders, M., Redeker, B., Law, D. J., Bliet, J., Steenmen, M., Benedict, M., Wiegant, J., Lengauer, C., Taillon-Miller, P., Schlessinger, D., Edwards, M. C., Elledge, S. J., Ivens, A., Westerveld, A., Little, P., Mannens, M., and Feinberg, A. P. (1995). Multiple genetic loci within 11p15 defined by Beckwith-Wiedemann syndrome rearrangement breakpoints and subchromosomal transferable fragments. *Proc. Natl. Acad. Sci. USA* **92**: 12456–12460.
- Hu, R.-J., Lee, M. P., Johnson, L. A., and Feinberg, A. P. (1996). A novel human homologue of yeast nucleosome assembly protein, 65 kb centromeric to the p57^{KIP2} gene, is biallelically expressed in fetal and adult tissues. *Hum. Mol. Genet.* **5**: 1743–1748.
- Ishimi, Y., Hirosumi, J., Sato, W., Sugawara, K., Yokota, S., Hanaoka, F., and Yamada, M. (1984). Purification and initial characterization of a protein which facilitates assembly of nucleosome-like structure from mammalian cells. *Eur. J. Biochem.* **142**: 431–439.
- Ishimi, Y., and Kikuchi, A. (1991). Identification and molecular cloning of yeast homolog of nucleosome assembly protein 1 which facilitates nucleosome assembly in vitro. *J. Biol. Chem.* **266**: 7025–7029.
- Ishimi, Y., Kojima, M., Yamada, M., and Hanaoka, F. (1987). Binding mode of nucleosome-assembly protein (AP-1) and histones. *Eur. J. Biochem.* **162**: 19–24.
- Ishimi, Y., Yasuda, H., Hirosumi, J., Hanaoka, F., and Yamada, M. (1983). A protein which facilitates assembly of nucleosome-like structures in vitro in mammalian cells. *J. Biochem.* **94**: 735–744.
- Ito, T., Bulger, M., Kobayashi, R., and Kadonaga, J. T. (1996). *Drosophila* NAP-1 is a core histone chaperone that functions in ATP-facilitated assembly of regularly spaced nucleosomal arrays. *Mol. Cell. Biol.* **16**: 3112–3124.
- Jantzen, H.-M., Admon, A., Bell, S. P., and Tjian, R. (1990). Nucleolar transcription factor hUBF contains a DNA-binding motif with homology to HMG proteins. *Nature* **344**: 830–836.
- Kellogg, D. R., Kikuchi, A., Fujii-Nakata, T., Turck, C. W., and Murray, A. W. (1995). Members of the NAP/SET family of proteins interact specifically with B-type cyclins. *J. Cell Biol.* **130**: 661–673.
- Kellogg, D. R., and Murray, A. W. (1995). NAP1 acts with Clb2 to perform mitotic functions and to suppress polar bud growth in budding yeast. *J. Cell Biol.* **130**: 675–685.
- Kleinschmidt, J. A., Fortkamp, E., Krohne, G., Zentgraf, H., and Franke, W. W. (1985). Coexistence of two different types of soluble histone complexes in nuclei of *Xenopus laevis* oocytes. *J. Biol. Chem.* **260**: 1166–1176.
- Kleinschmidt, J. A., and Franke, W. W. (1982). Soluble acidic complexes containing histones H3 and H4 in nuclei of *Xenopus laevis* oocytes. *Cell* **29**: 799–809.
- Koufos, A., Grundy, P., Morgan, K., Aleck, K. A., Hadro, T., Lampkin, B. C., Kalbakji, A., and Cavenee, W. K. (1989). Familial Wiedemann-Beckwith syndrome and a second Wilms' tumor locus both map to 11p15.5. *Am. J. Hum. Genet.* **44**: 711–719.
- Lapeyre, B., Bourbon, H., and Amalric, F. (1987). Nucleolin, the major nucleolar protein of growing eukaryotic cells: An unusual structure revealed by the nucleotide sequence. *Proc. Natl. Acad. Sci. USA* **84**: 1472–1476.
- Laskey, R. A., Honda, B. M., Mills, A. D., and Finch, J. T. (1978). Nucleosomes are assembled by an acidic protein which binds histones and transfers them to DNA. *Nature* **275**: 416–420.
- Looienga, L. H., Abraham, M., Gillis, A. J., Saunders, G. F., and Oosterhuis, J. W. (1994). Testicular germ cell tumors of adults show deletions of chromosomal bands 11p13 and 11p15.5, but no abnormalities within the zinc-finger regions and exons 2 and 6 of the Wilms' tumor 1 gene. *Genes Chromosomes Cancer* **9**: 153–160.
- Lu, Q., Wallrath, L. L., Granok, H., and Elgin, S. C. R. (1993). (CT)_n (GA)_n repeats and heat shock elements have distinct roles in chromatin structure and transcriptional activation of the *Drosophila* hsp26 gene. *Mol. Cell. Biol.* **13**: 2802–2814.
- Mannens, M., Slater, R. M., Heyting, C., Bliet, J., de Kraker, J., Coad, N., de Pagter-Holthuisen, P., and Pearson, P. L. (1988). Molecular nature of genetic changes resulting in loss of heterozygosity of chromosome 11 in Wilms' tumors. *Hum. Genet.* **81**: 41–48.
- Marsolier, M.-C., Tanaka, S., Livingstone-Zatchej, M., Grunstein, M., Thoma, F., and Sentenac, A. (1995). Reciprocal interferences between nucleosomal organization and transcriptional activity of the yeast SNR6 gene. *Genes Dev.* **9**: 410–422.

- Matsuoka, S., Edwards, M. C., Bai, C., Parker, S., Zhang, P., Baldini, A., Harper, J. W., and Elledge, S. J. (1995). p57^{KIP2}, a structurally distinct member of the p21CIP1 Cdk inhibitor family, is a candidate tumor suppressor gene. *Genes Dev.* **9**: 650–662.
- Nelson, T., Wiegand, R., and Brutlag, D. (1981). Ribonucleic acid and other polyanions facilitate chromatin assembly in vitro. *Biochemistry* **20**: 2594–2601.
- Ping, A. J., Reeve, A. E., Law, D. J., Young, M. R., Boehnke, M., and Feinberg, A. P. (1989). Genetic linkage of Beckwith–Wiedemann syndrome to 11p15. *Am. J. Hum. Genet.* **44**: 720–723.
- Prawitt, D., Munroe, D. J., Pelletier, J., Loebbert, R., Bric, E., Hermanns, P., Housman, D., Winterpacht, A., and Zabel, B. U. (1996). Identification of a NAP related gene in the Wilms' tumor candidate region at 11p15.5. *Am. J. Hum. Genet.* **59**: A79.
- Reeve, A. E., Sih, S. A., Raizis, A. M., and Feinberg, A. P. (1989). Loss of allelic heterozygosity at a second locus on chromosome 11 in sporadic Wilms' tumor cells. *Mol. Cell. Biol.* **9**: 1799–1803.
- Reid, L. H., West, A., Gioeli, D. G., Phillips, K. K., Kelleher, K. F., Araujo, D., Stanbridge, E. J., Dowdy, S. F., Gerhard, D. S., and Weissman, B. E. (1996). Localization of a tumor suppressor gene in 11p15.5 using the G401 Wilms' tumor assay. *Hum. Mol. Genet.* **5**: 239–247.
- Richmond, T. J., Rechsteiner, T., and Luger, K. (1993). Studies on nucleosome structure. *Cold Spring Harbor Symp. Quant. Biol.* **58**: 265–272.
- Sanger, F., Nicklen, S., and Coulson, A. R. (1977). DNA sequencing with chain-terminating inhibitors. *Proc. Natl. Acad. Sci. USA* **74**: 5463–5467.
- Schild, C., Claret, F. X., Wahli, W., and Wollfe, A. P. (1993). A nucleosome-dependent static loop potentiates estrogen-regulated transcription from the Xenopus vitellogenin B1 promoter in vitro. *EMBO J.* **12**: 423–433.
- Schmidt Zachmann, M. S., Hugle-Dorr, B., and Franke, W. W. (1987). A constitutive nucleolar protein identified as a member of the nucleoplasmin family. *EMBO J.* **6**: 1881–1890.
- Shen, X., Yu, L., Weir, J. W., and Gorovsky, M. A. (1995). Linker histones are not essential and affect chromatin condensation in vivo. *Cell* **82**: 47–56.
- Simon, H.-U., Mills, G. B., Kozlowski, M., Hogg, D., Branch, D., Ishimi, Y., and Siminovich, K. A. (1994). Molecular characterization of hNRP, a cDNA encoding a human nucleosome-assembly-protein-1-related gene product involved in the induction of cell proliferation. *Biochem. J.* **297**: 389–397.
- Sirotkin, A. M., Edelmann, W., Cheng, G., Klein-Szanto, A., Kucheralapati, R., and Skoultschi, A. I. (1995). Mice develop normally without the H1(0) histone. *Proc. Natl. Acad. Sci. USA* **92**: 6434–6438.
- Smith, M. W., Holmsen, A. L., Wei, Y. H., Peterson, M., and Evans, G. A. (1994). Genomic sequence sampling: A strategy for high resolution sequence-based physical mapping of complex genomes. *Nature Genet.* **7**: 40–47.
- Stein, A., Whitlock, J. P. Jr., and Bina, M. (1979). Acidic polypeptides can assemble both histones and chromatin in vitro at physiological ionic strength. *Proc. Natl. Acad. Sci. USA* **76**: 5000–5004.
- Sonoda, Y., Iizuka, M., Yasuda, J., Makino, R., Ono, T., Kayama, T., Yoshimoto, T., and Sekiya, T. (1995). Loss of heterozygosity at 11p15 in malignant glioma. *Cancer Res.* **55**: 2166–2168.
- Svaren, J., and Chalkley, R. (1990). The structure and assembly of active chromatin. *Trends Genet.* **6**: 52–56.
- Thomas, G. H., and Elgin, S. C. R. (1988). Protein/DNA architecture of the DNase I hypersensitive region of the Drosophila hsp26 promoter. *EMBO J.* **7**: 2191–2201.
- van Holde, K. E. (1989). "Chromatin," Springer-Verlag, New York.
- von Lindern, M., van Baal, S., Wiegant, J., Raap, A., Hagemeijer, A., and Grosveld, G. (1992). *can*, a putative oncogene associated with myeloid leukemogenesis, may be activated by fusion of its 3' half to different genes: characterization of the *set* gene. *Mol. Cell. Biol.* **12**: 3346–3355.
- Walter, P. P., Owen-Hughes, T. A., Coté, J., and Workman, J. L. (1995). Stimulation of transcription factor binding and histone displacement by nucleosome assembly protein 1 and nucleoplasmin requires disruption of the histone octamer. *Mol. Cell. Biol.* **15**: 6178–6187.
- Wen, L., Huang, J.-K., Johnson, B. H., and Reeck, G. R. (1989). A human placental cDNA that encodes nonhistone chromosomal protein HMG-1. *Nucleic Acids Res.* **17**: 1197–1214.
- Winqvist, R., Hampton, G. M., Mannermaa, A., Blanco, G., Alavaikko, M., Kiviniemi, H., Taskinen, P. J., Evans, G. A., Wright, F. A., Newsham, I., and Cavenee, W. K. (1995). Loss of heterozygosity for chromosome 11 in primary human breast tumors is associated with poor survival after metastasis. *Cancer Res.* **55**: 2660–2664.
- Wollfe, A. P. (1995). "Chromatin: Structure and Function," Academic Press, San Diego.
- Worcel, A., Han, S., and Wong, M. L. (1978). Assembly of newly replicated chromatin. *Cell* **15**: 969–977.

Thomas B. Shows, Ph.D.
Identifying and Isolating Breast Cancer-Associated
Genes on Chromosome 11

The Human Transaldolase Gene (TALDO1) Is Located on Chromosome 11 at p15.4-p15.5

BEST AVAILABLE COPY

Katalin Baraki,* Roger L. Eddy,† Thomas B. Shows,† David L. Halladay,‡ Florencia Bullrich,§
Carlo M. Croce,§ Vesna Jurecic,|| Antonio Baldini,|| and Andras Perl†¹

‡Department of Medicine, †Department of Microbiology and Immunology, and *Department of Pathology, State University of New York Health Science Center, College of Medicine, 750 East Adams Street, Syracuse, New York 13210; ||Department of Molecular and Human Genetics, Baylor College of Medicine, Houston, Texas 77030; †Department of Human Genetics, Roswell Park Cancer Institute, Buffalo, New York 14263; and §Kimmel Cancer Institute, Thomas Jefferson University, Philadelphia, Pennsylvania 19107

Received May 27, 1997; accepted July 25, 1997

Transaldolase (TAL) is a key enzyme of the pentose phosphate pathway, which is responsible for generation of reducing equivalents to protect cellular integrity from reactive oxygen intermediates. While exons 2 and 3 are highly repetitive, the complete TAL-H gene is mapped to a single genomic locus (TALDO1²) by several independent approaches. Southern blot hybridization of a 827-bp 3' *EcoRI* fragment of the TAL-H cDNA to human-mouse somatic cell hybrid DNA localized TALDO1 to the p13 → pter region of chromosome 11. Fluorescence *in situ* hybridization with a 15-kb genomic fragment harboring exons 1 and 2 mapped TALDO1 to 11p15.4-p15.5. A truncated and mutated segment of TAL-H exon 5 terminating with a poly(A) tail was identified in a pseudogene locus (TALDOP1) on chromosome 1. Reverse transcriptase-PCR studies of human-mouse somatic cell hybrids revealed the presence of the functional TAL-H gene on chromosome 11 and its absence on human chromosome 1. Mapping of radiation hybrids placed TALDO1 between markers WI-1421 and D11S922 on 11p15. © 1997 Academic Press

Transaldolase (TAL) is an enzyme of the reversible nonoxidative branch of the pentose phosphate pathway (PPP). This metabolic pathway provides d-ribose 5-phosphate for the synthesis of nucleic acids and NADPH to maintain glutathione at a reduced state (GSH) and, thus, to protect cellular integrity from reactive oxygen intermediates (ROIs) (14). Enzymatic activity of TAL is regulated in a tissue-specific (11, 16) and developmentally specific manner (6). In the brain, TAL is expressed selectively in oligodendrocytes at high levels (2). This is particularly interesting because myelin sheaths are formed by oligodendrocytes, and lesions in the most common demyelinating disease of the CNS, multiple sclerosis (MS), are characterized by

a progressive loss of oligodendrocytes and demyelination. Oligodendrocytes are exquisitely sensitive to damage by ROI, nitric oxide, and tumor necrosis factor- α (TNF) released by activated macrophages and astrocytes (15). Overexpression of TAL is accompanied by a decrease in glucose 6-phosphate dehydrogenase (G6PD) and 6-phosphogluconate dehydrogenase (6PGD) activities, a concomitant depletion in NADPH and GSH levels, and increased sensitivity to apoptosis provoked by serum deprivation, H₂O₂, nitric oxide (NO), TNF, and anti-Fas monoclonal antibody. In contrast, suppression of TAL activity increased G6PD and 6PGD activities, augmented GSH levels, and inhibited cell death. Susceptibility to apoptosis could be regulated by TAL through control of the balance between the two branches of the PPP and its overall output as measured by NADPH and GSH production (3). Thus, high levels of TAL expression may sensitize oligodendrocytes to apoptotic signals. MS lesions are characterized by a concurrent loss of oligodendrocytes and staining with TAL-specific antibodies (8). There is a robust antibody and T-cell-mediated autoimmunity to TAL in patients with MS (2, 4, 8).

The major difficulties in mapping the TAL-H gene stem from the presence of a high-copy-number transaldolase-associated repetitive element (TARE) in the coding sequence (5). TARE comprises exons 2 and 3 with a 474-bp 5' *EcoRI* fragment (4/2 probe) and a 1.1-kb length TAL-H cDNA. Nevertheless, in accordance with our earlier findings (5), a 3' 827-bp *EcoRI* fragment of the TAL-H cDNA (4/1 probe) hybridizes to a 11.1-kb *EcoRI* fragment in genomic DNA. To determine the chromosomal origin of TAL-H, a panel of human cell hybrids derived from 22 unrelated human cell lines and 4 mouse cell lines (19, 20) was analyzed. The human cell hybrids have been characterized by cytogenetic analysis, enzyme marker mapping, and hybridization with mapped DNA probes (19, 20). DNA from the hybrids was digested with *EcoRI* restriction enzyme and hybridized to the 3' 4/1 fragment of the TAL-H cDNA under high-stringency conditions. Chromosome assignment has been based on the segregation of the

¹ To whom correspondence and reprint requests should be addressed at SUNY HSC, 750 East Adams Street, Syracuse, NY 13210.

² In distinction from the TAL1 locus harboring a T-cell lymphocytic acute leukemia-associated gene, the transaldolase-containing genomic locus has been designated TALDO1.

TABLE 1

Segregation of TAL-H with Human Chromosomes in *Eco*RI-Digested Human-Mouse Cell Hybrid DNA

		Human Chromosomes																								Translocations	
DNA no.	Hybrid	TAL-H	1	2	3	4	5	6	7	8	9	10	11	12	13	14	15	16	17	18	19	20	21	22	X		
1274	20L-7	-	-	-	+	-	+	-	+	+	-	-	-	-	-	-	-	-	+	-	-	+	+	-	-	1/17	
1285	20L-9	+	t	-	+	+	+	+	+	+	+	+	+	+	+	-	+	+	+	+	+	+	+	+	+		17/1
1287	20L-17	-	t	-	-	-	-	-	-	-	-	-	-	-	-	-	-	-	t	-	-	-	-	-	-	1/17	
1304	20L-33	-	-	-	-	-	-	-	-	-	-	-	-	-	-	-	-	-	+	-	-	+	+	-	-		
1277	20L-37	-	t	-	+	+	+	+	+	+	-	+	-	+	-	-	-	-	+	+	-	+	-	-	+	1/17	
1273	31L-6	-	-	-	+	-	-	+	-	-	-	+	-	+	+	+	-	-	+	+	-	-	+	-	-		
1281	31L-37	+	-	-	+	-	+	+	+	+	+	-	+	-	-	-	+	-	+	-	+	+	+	-	+	1/17	
1243	35R-14	+	+	+	+	-	+	+	+	+	-	+	+	+	+	+	+	+	-	-	-	-	+	+	+		
1151	38L-27	-	-	-	-	-	-	-	-	-	-	-	-	-	-	-	-	-	+	-	-	-	-	-	-	1/17	
845	38L-33	+	-	-	+	-	-	-	+	-	-	-	+	-	-	-	-	-	+	-	-	-	+	-	-		
1238	55R-16	-	+	+	+	t	+	+	+	+	-	+	t	+	+	-	+	+	-	-	+	-	+	+	+	11-4, 7q-	
1246	55R-33	-	+	+	+	+	+	+	+	+	+	-	t	+	+	+	+	+	+	-	-	-	+	+	+		11-4
48	ATR-13	-	+	+	+	+	+	+	+	+	+	+	-	+	+	+	+	+	+	+	+	+	-	-	-	5X	
1211	DUA-3BSAGA	-	-	+	-	-	-	-	+	+	-	-	-	-	+	+	-	-	+	-	-	-	-	-	-	X 15, 15X X 11	
186	DUM-13	+	+	+	+	-	+	+	+	+	-	+	+	+	-	+	t	+	+	+	+	+	+	+	t		
82	EXR-5CSAz	-	+	+	+	+	+	+	+	+	+	+	t	+	+	+	+	+	-	+	+	+	+	+	+	7-9	
1185	GAR-1	-	-	-	+	-	+	-	+	-	+	-	+	+	+	-	+	+	-	-	-	+	-	-	+		
1178	JSR-17S	+	+	+	+	+	+	-	t	+	t	+	+	+	+	+	+	+	+	+	+	-	+	+	+	2-1	
653	JWR-22H	+	t	t	-	+	-	+	-	+	-	+	+	+	+	+	+	+	+	+	-	+	+	-	-		
187	JWR-26C	+	t	+	+	+	+	+	+	+	+	+	+	+	+	+	+	+	+	+	+	+	+	+	+	1-2	
830	KER-3	+	-	-	-	-	-	-	-	-	-	-	+	-	+	+	+	+	+	-	-	-	-	-	-		
40	NSL-5	-	+	-	-	-	-	-	-	-	+	t	+	-	+	-	+	-	+	t	+	-	+	-	-	17-9, 12q+	
1146	NSL-9	-	-	-	-	-	+	-	-	+	t	+	-	+	+	+	+	+	+	+	+	-	+	+	+	17-9	
192	NSL-16	-	-	-	+	+	+	-	+	+	t	+	-	+	-	+	+	+	+	+	+	-	+	+	+	17-9	
42	REW-11	+	-	-	-	+	-	-	+	-	-	-	+	+	+	-	+	+	-	-	-	-	+	+	+	17-9	
184	REX-11BSAgB	-	-	-	+	-	-	-	-	-	-	-	+	-	-	-	+	+	-	+	-	-	-	-	-		
1162	RSR-3	+	-	-	-	+	-	-	+	-	-	+	+	-	-	+	-	+	+	-	-	-	+	-	-	17-9	
665	SIR-11	-	-	+	-	-	-	-	-	-	+	-	-	-	-	+	-	-	-	-	-	-	-	+	-		
643	TSL-1	+	-	+	+	+	-	-	-	-	-	-	+	+	-	+	-	-	+	+	+	-	+	+	-	17-9	
53	TSL-2	-	-	+	t	-	+	+	-	-	-	+	-	+	-	-	-	-	t	+	-	+	+	-	-		
395	VTL-6	+	-	+	-	-	-	+	+	+	-	+	+	-	-	-	+	-	+	-	-	+	+	+	+	17-9	
407	VTL-17	+	-	-	-	-	+	-	+	-	-	+	+	-	+	+	-	-	+	-	+	+	+	+	-		
1098	VTL-23	+	-	-	-	-	+	-	+	+	-	+	+	+	+	+	+	+	+	+	+	+	+	+	+	17-9	
559	W12	+	-	+	-	-	+	-	-	-	-	-	+	-	+	-	+	-	+	-	-	+	+	+	+		
212	WIL-2	-	-	-	-	-	-	-	-	+	-	+	-	+	-	-	+	-	+	-	+	-	+	+	-	17-9	
794	WIL-8Y	+	-	-	+	-	-	+	+	+	-	+	+	-	-	+	-	-	+	+	-	+	+	+	+		
1144	WIL-13	-	-	-	-	-	+	-	-	-	-	-	-	-	-	-	-	-	+	+	-	-	-	-	-	17-9	
347	WIL-14	-	+	-	+	-	+	-	+	+	-	+	-	+	-	+	+	-	+	-	-	-	-	-	-		
25	WIL-15	+	-	+	+	+	-	+	+	-	-	+	+	+	+	+	+	+	-	+	+	-	+	+	-	17-9	
1320	WTR-15	+	+	+	+	-	+	-	+	-	+	+	+	-	+	t	+	-	-	-	-	-	+	+	+		
640	XER-7	-	+	+	+	+	+	+	+	+	+	+	+	+	+	+	+	+	-	-	+	+	-	+	-	17-9	
Chromosome:			1	2	3	4	5	6	7	8	9	10	11	12	13	14	15	16	17	18	19	20	21	22	X		
Concordant no.			(+/+)	4	9	11	8	10	9	14	8	4	14	19	9	10	12	9	9	15	9	5	14	18	9	1	17-9
of hybrids			(-/-)	13	14	9	15	9	14	12	8	15	8	18	8	12	11	11	15	5	11	18	13	9	17	11	
Discordant no.			(+/-)	12	9	8	11	9	10	4	11	14	5	0	10	9	6	9	10	4	10	14	5	1	10	1	17-9
of hybrids			(-/+)	7	8	12	6	13	8	10	14	4	14	0	14	10	11	11	7	14	11	4	9	13	5	10	
% Discordancy				53	43	50	43	54	44	35	61	49	46	0	59	46	42	50	41	47	51	44	34	34	37	16	

Note. Southern blot hybridization of somatic cell hybrid DNA samples to the nonrepetitive 3' 4/1 (827-bp *Eco*RI) fragment of full-length TAL-H cDNA as described in the legend to Fig. 1. Concordant hybrids have either retained (+/+) or lost (-/-) sequence together with a specific human chromosome. Discordant hybrids have either retained the sequence but not a specific chromosome (+/-) or the reverse (-/+). Percentage discordancy indicates the degree of discordant segregation for TAL-H and a particular chromosome. A 0% discordancy is the basis for chromosome assignment. The TAL-H probe mapped to human chromosome 11.

*Eco*RI fragment with human chromosomes in human-mouse cell hybrid DNA samples. A 0% discordancy indicated a matched segregation of the probe with a chromosome. Table 1 demonstrates that TALDO1 is present on human chromosome 11. All other chromosomes

segregated discordantly. Among the hybrids, four carried translocations involving chromosome 11. Chromosomal translocations with no intact chromosome present were not counted for the percentage discordancy. All four translocation hybrids

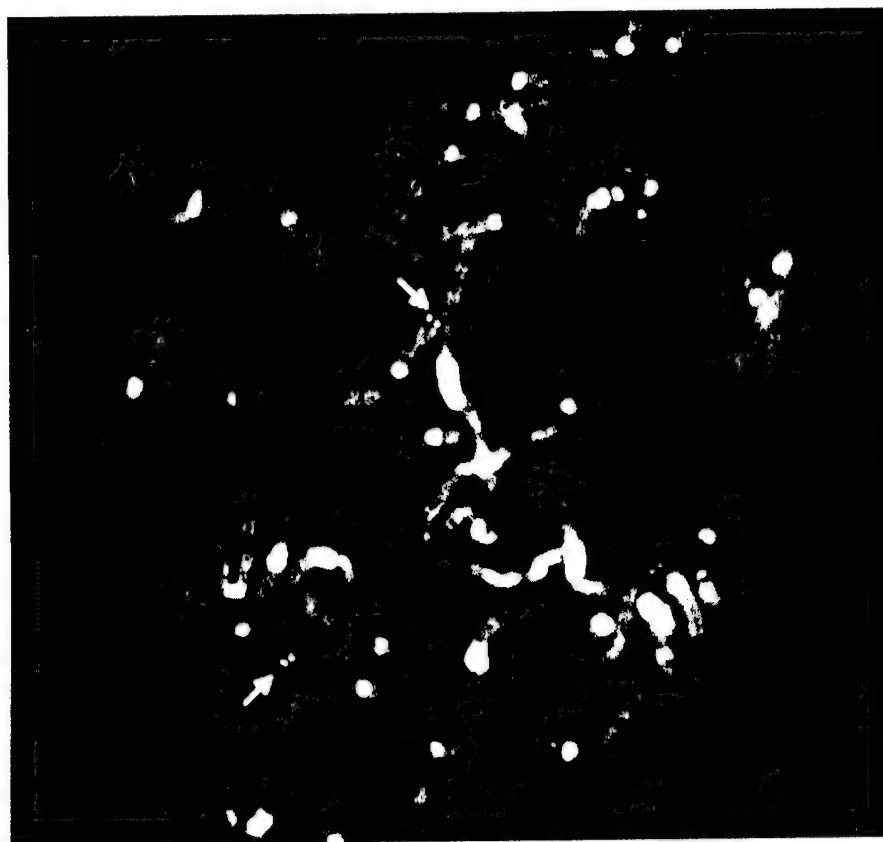


FIG. 1. Fluorescence *in situ* hybridization on human metaphase chromosomes using two adjacent *Eco*RI fragments harboring exons 1 (clone 276 containing an 8-kb *Eco*RI fragment) and 2 (clone 281 containing a 7-kb *Eco*RI fragment) as probe. The hybridizing dots present on each chromatid of both chromosomes 11 are indicated with arrows.

55R-33 with the 11qter \rightarrow 11p13::4q25 \rightarrow 4qter, EXR-5CSAz with the Xpter \rightarrow Xq22::11q13 \rightarrow 11qter, and XER-7 with the 11qter \rightarrow 11p11::Xq11 \rightarrow Xqter, scored negative for TALDO1. These data localized TALDO1 to the p13 \rightarrow pter region of chromosome 11.

TALDO1 was independently mapped to chromosome 11 by fluorescence *in situ* hybridization (FISH; Fig. 1). Metaphase spreads were prepared from peripheral blood lymphocytes of a male donor. Two adjacent genomic DNA fragments harboring exons 1 (clone 276 containing an 8-kb *Eco*RI fragment) and 2 (clone 281 containing a 7-kb *Eco*RI fragment) were labeled with biotin-14-dATP (Life Technologies, Gaithersburg, MD), hybridized to chromosome spreads under suppression conditions, and then detected by fluorescein-conjugated avidin as earlier described (1). Chromosome identification was performed by simultaneous DAPI staining, which produces a Q-banding pattern (1). Fluorescent signals were detected at 11p15.4–p15.5 on both chromatids of each of the two chromosomes 11 retained in 20 metaphases. No hybridization signal was detected on other sites.

The data obtained by the Southern blot hybridizations of somatic cell hybrids with the 827-bp 3' cDNA fragment and FISH analysis with human genomic clones containing intact exons 1 and 2 of the TAL-H

gene clearly mapped the TALDO1 locus to chromosome 11 at p15.4–p15.5. In addition, we have isolated a phage clone, designated 1/3A, from a λ DASH genomic library with the 4/1 probe (5), which contained a truncated and mutated segment of TAL-H exon 5 (Fig. 2A). Bases 439–712 in clone 1/3 (GenBank Accession No. AF003890) correspond to bases 960–1233 in the coding sequence of human transaldolase cDNA (GenBank Accession No. L19437, last update May 8, 1997). While the exon 5-related domain of clone 1/3A begins at position 960, it terminates early at position 1233, and, furthermore, directly continues into an 8-nucleotide-long poly(A) tail (Figs. 2A and 2B), thus suggesting that this locus represents a pseudogene (TALDOP1). This possibility was supported by the presence of 11 point mutations (single-base substitutions) with respect to the functional cDNA capable of encoding enzymatically active recombinant protein (4). One of the point mutations, a C \rightarrow T substitution at position 520 of clone 1/3A, results in a TGA stop codon and truncation of the coding region. The genomic locus corresponding to clone 1/3A was mapped to human chromosome 1p32–p33 by FISH analysis (data not shown). The DNA sequence flanking the exon 5-related segment of clone 1/3A was found to be identical at both its 5' and 3' ends to that of clone λ TAG8, previously mapped to chro-

A

Clone 4/2-4/1 451 CTGGGATCAGCAAGGACCGAATTCCTTATAAAGCTGTCATCAACCTGGGAA 500
 Clone 1/3A 1GAATTCAGGATA 12
 501 GGAAATTCAGGCTGGAAAGGAGCTCGAGGAGCAGCACGGCATCCACTGCAA 550
 13 GTGATTCCTCGGGATGAGATGGGAGAGAAATATTGGTAGATTAAATTT 62
 551 CATGACGTTACTCTTCTCTCTCGCCAGGCTGTGGCCTGTGCCGAGGCGG 600
 63 GTCAGTGATGCTATACAATTTGGTGGTAGGTTACAGATCTTCAATTACA 112
 601 GTGTGACCCCTCATCTCCCAATTGTTGGGCGCATCCTTGATTGGCATGTG 650
 113 TTATTAATAAATAAGTGGGGCTGGGTGTGGTGGTTATGCCGTGAATTCGA 162
 651 GCAACACCCGACAAGAAATCCATATGAGCCCTTGAAGACCTGGGGTAAA 700
 163 GCATTTTGGGAGGCCAGGTGGGAGGATCACCTGAAGCCAGGAGTTTGGAG 212
 701 GAGTGTCACTAAAATCTACAATACTACAAGAAGTTAGCTACAAAACCA 750
 213 ACCAGCCTGGACAACATAGTGAGACCTGTCTTTATAAAAAATAAAAAAT 262
 751 TTGTCAATGGGCGCCCTCCCTTCCGCAACACGGCGAGATCAAAAGCACTGGCC 800
 263 TAGCTGGGTGTGGTGGTGTGTGCTGTAGTCTCAGCTGCTCGGGAGGCTG 312
 801 GGCCTGTGACTTCTCTACCACTCTCACCAAGCTCCTGGGAGAGCTGCTGCA 850
 313 AGGTGGGAAAATCACCTGAGGCTGGGAGATTGAGTCTACA 352
 851 GGACAACGCCAAGCTGGTGGCTGTGCTCTCAGCCAAGCGGGCCCAAGCCA 900
 353 GTGAATCTGCCCTCCAGCTAGGACAACAGAGTGAGACCTTGTCTCAAAAAA 402
 901 GTGACCTGGAAAAAATCCACCTGGATGAGAAGTCTTCCGTGGGTGAC 950
 403 TAAATAAATAAATAAATATGAAAAAT 429
 951 AACGAGGACAGATGGCTGTGGAGAAGCTCTCTGACGGGATCCGCAAGTT 1000
 430 AAATGGATGCAGATGGCTGTGGAGAAGCTCTCTGATGGGATCCGCAAGTC 479
 1001 TGCCGCTGATGCAGTGAAGCTGGAGCGGATGCTGACAGAACGAATGTTCA 1050
 480 TGCCGCTGATGCAGTGAAGCTGGAGCGGATGCTGACAGAACGAATGTTCA 529
 1051 ATGCAGAGAATGGAAAGTAGCGCATCCCTGAGGCTGGAGTCCAGATCTGC 1100
 530 ATGCAGAGAATGGAAAGTAGTGACGATGAGGCTGGAGTCCAGATCTGC 579
 1101 ACCGCCGGCCAGCTGGGATCTGACTGCACGTGGCTTCTGATGAATCTTGC 1150
 580 ACTGCTGGCCAGCTGGGCTGACTGCACATGGCTTCTGATGAATCTTGC 629
 1151 GTTTTATTACAAATGGAGCAGGACAGATCATAGATTTCTGATTTTATGT 1200
 630 GTTTTATTACAAATCGGAGCAGGACAGATCATAGATTTCTGATTTTATGT 679
 1201 AAAATTTTGCCTAATACATTAAAGCAGTCACCTTCTCTGTGCTGTTTCAA 1250
 680 AAAATTTTGCCTAATACATTAAAGCAGTCACCTTAAAAAATGGATGTTT 729
 1251 AA 1300
 730 GTTAAACCCATAGAATGTATACGAATGAACCTAATGTAAGCTATGGAC 779
 1301 AAAAAAAAAAAAAAAAAAAAAAAAAAAGGAATTC 1332
 780 TTTAATTAATAGTATATCAGTATTGGCTCATCAGTTGAACAAATGCCCC 829

B

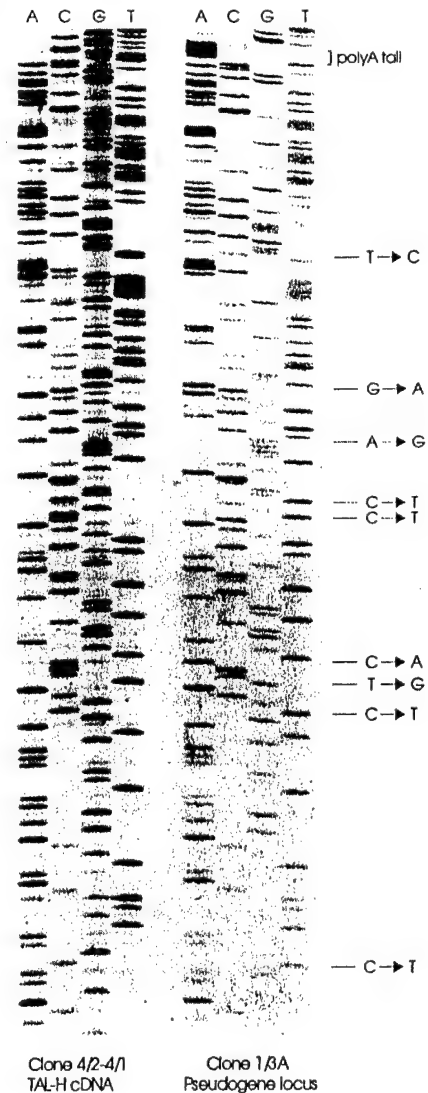


FIG. 2. (A) Nucleotide sequence of TAL-H cDNA clone 4/2-4/1 and of genomic DNA clone 1/3A. Bases 439-712 in clone 1/3A, which correspond to bases 960-1233 of clone 4/2-4/1, are underlined. A C → T substitution at position 520 of clone 1/3A results in a TGA stop codon (boldface) and truncation of the coding region. The TAL-related region in clone 1/3A terminates early and continues into an 8-nucleotide-long poly(A) tail (italicized). (B) Visualization of 9/11 point mutations at nucleotides 520, 550, 554, 557, 582, 585, 597, 609, and 643 (from bottom to top of gel) and early polyadenylation in genomic clone 1/3A (marked at the top of gel) in comparison to cDNA clone 4/2-4/1.

mosome 1p33-34.1 (13). Since clones λ TAG8 and 1/3A contain the same truncated segment of exon 5 terminating in a poly(A) tail, they are likely to represent the same pseudogene locus (TALDOP1). The presence of the functional TAL-H gene on chromosome 11 was confirmed by reverse transcriptase-PCR-mediated amplification of the entire coding sequence (bases 57-1244) from RNA extracted of human-mouse hybrid GM10927B (NIGMS/Coriell Cell Repository, Camden, NJ) harboring human chromosome 11 only. TAL-H ex-

pression could not be detected in mouse cells and human-mouse hybrid GM13139A containing human chromosome 1 alone (Fig. 3).

PCR amplification of bases 669-948 of the TAL-H coding sequence from a radiation hybrid panel (Genebridge 4 panel, Research Genetics, Huntsville, AL) utilizing an STS-based map of the human genome (12) available at the Whitehead Institute Center for Genome Research Server (<http://www-genome.wi.mit.edu>) mapped transaldolase at a LOD > 3.0 between mark-

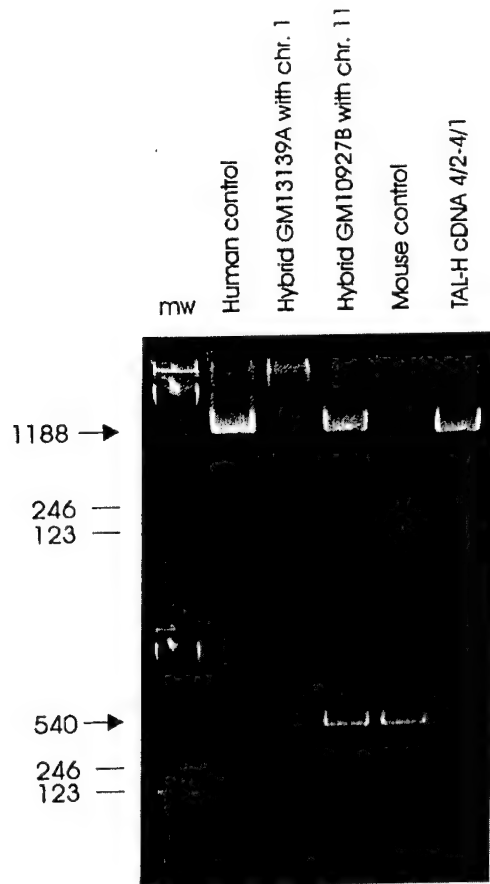


FIG. 3. RT-PCR analysis of TAL-H expression in human–mouse hybrid cell lines. Total cellular RNA was isolated from cultured cells by the RNazol method (7). Three micrograms of RNA was reverse transcribed into cDNA with oligo(dT) primer by 200 U of Superscript reverse transcriptase according to the manufacturer's protocol (GIBCO-BRL). For analysis of TAL-H expression, cDNA aliquots were subjected to PCR using TAL-H sense (bases 57–74) and antisense oligonucleotides (bases 1225–1244) (5), which resulted in an 1188-bp amplicon (indicated by the arrow in the upper panel). As a control, a 540-bp region of β -actin (indicated by the arrow in the lower panel) conserved between mouse and human was amplified using sense (5'-GTGGGCGCTCTAGGCACCAA-3') and antisense oligonucleotides (5'-CTCTTTGATGTCACGCACGATTTC-3') (Clontech, Palo Alto, CA). Lanes are: mw, 123-bp molecular weight marker; human control RNA from Jurkat cells (3), human–mouse hybrid GM13139A containing human chromosome 1 only; human–mouse hybrid GM10927B containing human chromosome 11 only; mouse control RNA from NIH-3T3 cells; and TAL-H cDNA 4/2-4/1 (used with TAL-H primers only).

ers WI-1421 (GenBank Accession No. M17887; 5.45 cR toward the telomere from TALDO1) and D11S922 (WICGR database No. AFM217YB10; 6.2 cR toward the centromere from TALDO1). WI-1421 is located 17.1 cR from the telomere of 11p. Based on the resolution of the map (3.7 cR/Mb), TALDO1 is located 22.6 cR or 6.1 Mb from the end of 11p. D11S922, the nearest marker, located 6.2 cR or 1.7 Mb from TALDO1 toward the centromere, has been mapped to 11p15.5 (18).

The present study clearly assigns the TALDO1 locus to 11p15.4–p15.5. This region of chromosome 11 has been implicated in a number of developmental disor-

ders and tumor suppression. Loss of heterozygosity at 11p15 has been documented in solid tumors, including breast, bladder, ovarian, and testicular carcinomas and malignant gliomas (21). This led to its designation as multiple tumor associated chromosome region 1 (MTACR1) (17). Existence of a tumor suppressor gene in this region was supported by chromosome transfer experiments (9). Because of its role in regulating programmed cell death (3), transaldolase may indeed correspond to a tumor suppressor gene. In addition, 11p15 has been identified as one of eight loci linked to MS at relatively high lod scores in a large-scale linkage study of MS families using 443 markers on all chromosomes with an average spacing of 9.6 cM (10). TAL-H is a prominent target of both cell- and antibody-mediated autoimmunity in patients with MS (2, 8). PCR mapping of radiation hybrids placed TALDO1 6.2 cR or 1.7 Mb or approximately 1.7 cM from D11S922, the marker of 11p15 that has been associated with MS (10). These results suggest that TALDO1 may correspond to a susceptibility gene influencing development of MS.

ACKNOWLEDGMENTS

This work was supported in part by Grant RO1 DK 49221 (A.P.), HG-00333 (T.B.S.), and CA-63333 (T.B.S.) from the National Institutes of Health, Grant DAMD17-94-J-4417 (T.B.S.), and Grant RG 2466A1/3 from the National Multiple Sclerosis Society (A.P.).

REFERENCES

1. Baldini, A., Ross, M., Nizetic, D., Vatcheva, R., Lindsay, E. A., Lehrach, H., and Siniscalco, M. (1992). Chromosomal assignment of human YAC clones by fluorescence *in situ* hybridization: Use of single yeast colony PCR and multiple labeling. *Genomics* 14: 181–184.
2. Banki, K., Colombo, E., Sia, F., Halladay, D., Mattson, D., Tatum, A., Massa, P., Phillips, P. E., and Perl, A. (1994). Oligodendrocyte-specific expression and autoantigenicity of transaldolase in multiple sclerosis. *J. Exp. Med.* 180: 1649–1663.
3. Banki, K., Hutter, E., Colombo, E., Gonchoroff, N. J., and Perl, A. (1996). Glutathione levels and sensitivity to apoptosis are regulated by changes in transaldolase expression. *J. Biol. Chem.* 271: 32994–33001.
4. Banki, K., and Perl, A. (1996). Inhibition of the catalytic activity of human transaldolase by antibodies and site-directed mutagenesis. *FEBS Lett.* 378: 161–165.
5. Banki, K., Halladay, D., and Perl, A. (1994). Cloning and expression of the human gene for transaldolase: A novel highly repetitive element constitutes an integral part of the coding sequence. *J. Biol. Chem.* 269: 2847–2851.
6. Baquer, N. Z., Hothersall, J. S., McLean, P., and Greenbaum, A. L. (1977). Aspects of carbohydrate metabolism in developing brain. *Dev. Med. Child Neurol.* 19: 81–104.
7. Chomczynski, P., and Sacchi, N. (1987). Single step method of RNA isolation by acid guanidinium-isothiocyanate–phenol–chloroform extraction. *Anal. Biochem.* 162: 156–159.
8. Colombo, E., Banki, K., Tatum, A. H., Daucher, J., Ferrante, P., Murray, R. S., Phillips, P. E., and Perl, A. (1997). Comparative analysis of antibody and cell-mediated autoimmunity to transaldolase and myelin basic protein in patients with multiple sclerosis. *J. Clin. Invest.* 99: 1238–1250.
9. Dowdy, S. F., Fasching, C. L., Araujo, D., Lai, K., Livanos, E., Weisman, B. E., and Stanbridge, E. J. (1991). Suppression of

- tumorigenicity in Wilms' tumor by the p15.5-p14 region of chromosome 11. *Science* **254**: 293-295.
10. Haines, J. L., Ter-Minassian, M., Bazyk, A., Gusella, J. F., Kim, D. J., Terwedow, H., Pericak-Vance, M. A., Rimmmler, J. B., Haynes, C. S., Roses, A. D., Lee, A., Shaner, B., Menold, M., Seboun, E., Fitoussi, R., Gartioux, C., Reyes, C., Ribierre, F., Gyapay, G., Weissenbach, J., Hauser, S. L., Goodkin, D. E., Lincoln, R., Usuku, K., Garcia-Merino, A., Gatto, N., Young, S., and Oksenberg, J. R. (1996). A complete genomic screen for multiple sclerosis underscores a role for the major histocompatibility complex. *Nature Genet.* **13**: 469-471.
 11. Heinrich, P. C., Morris, H. P., and Weber, G. (1976). Behavior of transaldolase (EC 2.2.1.2.) and transketolase (EC 2.2.1.1.) in normal neoplastic, differentiating, and regenerating liver. *Cancer Res.* **36**: 3189-3197.
 12. Hudson, T. J., Stein, L. D., Gerety, S. S., Ma, J., Castle, A. B., Silva, J., Slonim, D. K., Baptista, R., Kruglyak, L., Xu, S., Hu, X., Colbert, A. M. E., Rosenberg, C., Reeve-Daly, M. P., Rozen, S., Hui, L., Wu, X., Vestergaard, C., Wilson, K. M., Bae, J. S., Maitra, S., Ganiatsas, S., Evans, C. E., DeAngelis, M. M., Ingalls, K. A., Nahf, R. W., Horton, L. T., Jr., Anderson, M. O., Collymore, A. J., Ye, W., Kouyoumjian, V., Zemsteva, I. S., Tam, J., Devine, R., Coutney, D. F., Renaud, M. T., Nguyen, H., O'Connor, T. J., Fizames, C., Faure, S., Gyapay, G., Dib, C., Morissette, J., Orlin, J. O., Birren, B. W., Goodman, N., Weissenbach, J., Hawkins, T. L., Foote, S., Page, D. C., and Lander, E. S. (1995). An STS-based map of the human genome. *Science* **270**: 1945-1954.
 13. Kusuda, J., Hirai, M., Toyoda, A., and Hashimoto, K. (1997). Localization of the human transaldolase gene (TALDO) to chromosome 1p33-p34.1 by fluorescence *in situ* hybridization and PCR analysis of somatic cell hybrids. *Genomics* **40**: 378-381.
 14. Mayes, P. (1993). The pentose phosphate pathway & other pathways of hexose metabolism. In "Harper's Biochemistry" (R. Murray, D. Granner, P. Mayes, and V. Rodwell, Eds.), pp. 201-211. Appleton & Lange, Norwalk, CT.
 15. Merrill, J. E., Ignarro, L. J., Sherman, M. P., Melinek, J., and Lane, T. E. (1993). Microglial cell cytotoxicity of oligodendrocytes is mediated through nitric oxide. *J. Immunol.* **151**: 2132-2141.
 16. Novello, F., and McLean, P. (1968). The pentose phosphate pathway of glucose metabolism. Measurements of the nonoxidative reactions of the cycle. *Biochem. J.* **107**: 775-791.
 17. Seizinger, B., Klinger, H. P. J., Junien, C., Nakamura, Y., LeBeau, M., Cavenee, W., Emmanuel, B., Ponder, B., Naylor, S., Mittelman, F., Louis, D., Menon, A., Newsham, I., Decker, J., Kneibling, M., Henry, I., and Deimling, A. V. (1991). Report of the committee on chromosome and gene loss in human neoplasia. *Cytogenet. Cell Genet.* **58**: 1080-1096.
 18. Shows, T. B., Alders, M., Bennett, S., Burbee, D., Cartwright, P., Chandrasekharappa, S., Cooper, P., Courseaux, A., Davies, C., Devignes, M.-D., Devilee, P., Elliot, R., Evans, G., Fantes, J., Garner, H., Gaudray, P., Gerhard, D. S., Gessler, M., Higgins, M., Hummerich, H., James, M., Lagercrantz, J., Litt, M., Little, P., Mannens, M., Munroe, D., Nowak, N., O'Brien, S., Parker, N., Perlin, M., Reid, L., Richard, C., Sawicki, M., Swallow, D., Thakker, R., van Heyningen, V., van Schothorst, E., Vorechovsky, I., Wadelius, C., Weber, B., and Zabel, B. (1996). Report of the fifth international workshop on human chromosome 11 mapping (1996). *Cytogenet. Cell Genet.* **74**: 1-56.
 19. Shows, T. B., Eddy, R., Haley, L., Byers, M., Henry, M., Fujita, T., Matsui, H., and Taniguchi, T. (1984). Interleukin 2 (IL-2) is assigned to human chromosome 4. *Somat. Cell. Mol. Genet.* **10**: 315-318.
 20. Shows, T. B., Sakaguchi, A. Y., and Naylor, S. L. (1982). Mapping the human genome, cloned genes, DNA polymorphisms, and inherited diseases. In "Advances in Human Genetics" H. Harris and K. Hirschhorn, Eds.), pp. 341-452. Plenum New York/London.
 21. Sonoda, Y., Iizuka, M., Yasuda, J., Makino, R., Ono, T., Kiyama, T., Yoshimoto, K., and Sekiya, T. (1995). Loss of heterozygosity at 11p15 in malignant glioma. *Cancer Res.* **55**: 2166-2168.

A model system to study genomic imprinting of human genes

(Beckwith–Weidemann syndrome/gene expression/imprinting/methylation/Prader–Willi syndrome)

J. M. GABRIEL^{*†}, M. J. HIGGINS[‡], T. C. GEBUHR^{*†}, T. B. SHOWS[‡], S. SAITOH^{*†§}, AND R. D. NICHOLLS^{*†¶}

^{*}Department of Genetics, Case Western Reserve University School of Medicine, and [†]Center for Human Genetics, University Hospitals of Cleveland, 10900 Euclid Avenue, Cleveland, OH 44106-4955; and [‡]Department of Human Genetics, Roswell Park Cancer Institute, Elm and Carlton Streets, Buffalo, NY 14263

Edited by Francis H. Ruddle, Yale University, New Haven, CT, and approved October 2, 1998 (received for review December 19, 1997)

ABSTRACT Somatic-cell hybrids have been shown to maintain the correct epigenetic chromatin states to study developmental globin gene expression as well as gene expression on the active and inactive X chromosomes. This suggests the potential use of somatic-cell hybrids containing either a maternal or a paternal human chromosome as a model system to study known imprinted genes and to identify as-yet-unknown imprinted genes. Testing gene expression by using reverse transcription followed by PCR, we show that functional imprints are maintained at four previously characterized 15q11–q13 loci in hybrids containing a single human chromosome 15 and at two chromosome 11p15 loci in hybrids containing a single chromosome 11. In contrast, three γ -aminobutyric acid type A receptor subunit genes in 15q12–q13 are nonimprinted. Furthermore, we have found that differential DNA methylation imprints at the *SNRPN* promoter and at a CpG island in 11p15 are also maintained in somatic-cell hybrids. Somatic-cell hybrids therefore are a valid and powerful system for studying known imprinted genes as well as for rapidly identifying new imprinted genes.

The process of genomic imprinting differentially marks genes in the germ line such that gene expression in the embryo and adult depends on the sex of the transmitting parent. This unequal parental contribution to offspring was first demonstrated by pronuclear transplantation studies in the mouse (1) and was further supported by breeding experiments giving rise to mice with uniparental disomy (UPD) for portions of their genome (2). Imprinting effects were shown for 10 regions on 6 different chromosomes, with phenotypes ranging from embryonic lethality to more subtle growth abnormalities (1, 2). To date, most of the imprinted genes in the mouse have been shown to have imprinted homologs in humans. Based on results from mice generated to have UPD for portions of their genome (2), one may expect 10 or more imprinted domains in humans, each containing multiple imprinted loci.

Recently, genomic imprinting has been shown to be involved in the etiology of human disease. Prader–Willi syndrome (PWS) and Angelman syndrome (AS) are clinically distinct disorders caused by the lack of expression of genes in chromosome 15q11–q13 (3). Most commonly, PWS arises from a paternally inherited *de novo* 4-Mb deletion of this region ($\approx 75\%$ of cases) or from a maternally inherited UPD ($\approx 25\%$ of cases). Conversely, AS most frequently results from the maternal inheritance of an identical deletion, and paternal UPD has been shown in approximately 2% of cases. Some AS and PWS patients have mutations in the imprinting process (3, 4). Most recently, about 5% of AS patients have been shown to have mutations in the *UBE3A* gene (5), although the basis for AS in the remaining 10–15% of patients is unclear. Similarly, Beckwith–Weidemann syndrome, a fetal overgrowth syndrome associated with a high incidence of Wilms

tumors, is caused both by maternal chromosome 11p15 loss or rearrangement and paternal isodisomy (6). Furthermore, mutations in the imprinted *p57^{KIP2}* (*CDKN1C*) gene have been discovered in some patients with Beckwith–Weidemann syndrome (7), and the maternal (expressed) copy of this gene has been shown to be preferentially deleted in many lung cancers (8) and down-regulated in Wilms tumors (9, 10). Although the aforementioned phenotypes are readily discernible, it is likely that many more genes are subject to genomic imprinting, defects in which may lead to more subtle phenotypes.

With the importance of genomic imprinting in human disease and the relative frequency with which genes in imprinted domains are being discovered in both the mouse and human, there is a critical need for a general model system with which to identify novel imprinted genes in humans and to further characterize and potentially manipulate known imprinted genes. Currently, cell lines from patients with UPD or deletions of specific parental origins are available for very few chromosomes (11). In contrast, the availability of interspecific backcrosses makes determination of allele specificity of expression relatively easy in the mouse (12–14). However, because not all genes may show conserved imprinting, e.g., *IGF2R* (15), it is important to test each candidate human gene.

Previously, it has been demonstrated (16) that somatic-cell hybrids produced by fusing human erythroid cells expressing an embryonic, fetal, or adult β -like globin gene with mouse erythroleukemia cells, an adult cell type, retain expression of the appropriate human globin gene, indicating that the chromosomal state of the β -globin locus is transferred intact in these hybrid cells. Somatic-cell hybrids also have been shown to faithfully maintain the active or inactive state of the X chromosome and thus have been instrumental in determining which genes are subject to and which genes escape from X inactivation (17). Combined, these data suggest that the epigenetic state of a chromosome can be stably transferred into cells of a different developmental and/or differentiation stage and maintain its initial pattern of gene expression. Based on these results, and to provide a general model system for assaying novel imprinted genes, we have tested somatic-cell hybrids containing individual human chromosomes for the maintenance of characteristics of imprinted genes, including monoallelic expression and differential DNA methylation of maternal and paternal alleles. Here we show that imprinted gene expression and DNA methylation of critical CpG islands are faithfully maintained in somatic-cell hybrids. We also demonstrate that the γ -aminobutyric acid type A (GABA_A) receptor genes in 15q12–q13 are not imprinted, contrary to a recent report (18).

This paper was submitted directly (Track II) to the *Proceedings* office. Abbreviations: AS, Angelman syndrome; PWS, Prader–Willi syndrome; RT-PCR, reverse transcription-PCR; UPD, uniparental disomy.

[§]Present address: Department of Pediatrics, Hokkaido University School of Medicine, Kita 15 Nishi 7, Kita-ku, Sapporo 060, Japan.

[¶]To whom reprint requests should be addressed at: Department of Genetics, Case Western Reserve University, 10900 Euclid Avenue, Cleveland, OH 44106. e-mail: rxn19@po.cwru.edu.

The publication costs of this article were defrayed in part by page charge payment. This article must therefore be hereby marked “advertisement” in accordance with 18 U.S.C. §1734 solely to indicate this fact.

© 1998 by The National Academy of Sciences 0027-8424/98/9514857-6\$2.00/0 PNAS is available online at www.pnas.org.

MATERIALS AND METHODS

Cell Culture and Hybrids. Standard tissue-culture techniques were used to propagate the hybrid cell lines (Tables 1 and 2) used in this study. Chromosome 11 hybrids (Table 2) were obtained from the NIGMS Coriell Cell Repositories (Camden, NJ). It is important to note that hybrid cell lines may be karyotypically unstable and should be regularly assessed for chromosome content by either cytogenetic or molecular methods. Drug selection used in tissue culture may help to stabilize the genotype of cell lines; in particular, the chromosomes 15 in hybrids A15 and A9+15 confer neomycin resistance on those hybrids (19, 20).

DNA Methylation Analysis. DNA extraction and Southern hybridizations were performed by using standard procedures (21). For *SNRPN*, genomic DNA from cell lines was digested with *Xba*I and the methyl-sensitive *Not*I restriction enzymes, electrophoresed on a 0.8% gel, analyzed by Southern blotting, and hybridized with a *SNRPN* exon 1 probe (21). For *D15S63* and *ZNF127*, DNA was digested with *Bgl*II and *Hha*I or *Eco*RI and *Hpa*II and probed with PW71B or a 1.3-kb *Taq*I/*Eco*RI fragment of DN34, respectively. For the chromosome 11p15 region, genomic DNA was digested with *Bam*HI and *Not*I, blotted as above, and hybridized with a probe for a differentially methylated CpG island that maps to an intron of *KVLQTI* (*KCN49*). The image was exposed by using a PhosphorImager (Molecular Dynamics).

RNA Extraction and Reverse Transcription-PCR (RT-PCR). Total RNA was extracted from fibroblast cell lines twice (to remove DNA contamination) by using RNeasy (Qiagen/Biotech Laboratories, Friendswood, TX), and 5 μ g was reverse-transcribed by using SuperScriptII (GIBCO/BRL) with random hexamers as a primer, and 1/25 of the RT reaction was used for subsequent 50- μ l PCR amplifications. Primers and conditions for PCR were as described: 60A and 60B for *IPW* (22); RN85 and RN133 for *SNRPN* (21); *PAR5* (23); P1 and P2 followed by P3 and P4 (nested) for *H19* (24). For *IGF2*, primers used were RN245, 5'-CTCGTGCTGCATTGCTGC-3' and RN246, 5'-GGACTGCTTCCAGGTGTC-3'. The following conditions were used: denaturation for 30 sec at 94°C, annealing for 30 sec at 58°C, and extension for 1 min at 72°C for 35 cycles. For *RPS12*, primers were F, 5'-ATTGAGCTTACCCGTAACC-3' and R, 5'-CAACCACTTTACGGGGATTTC-3'. The following conditions were used: 30 sec at 94°C, 30 sec at 56°C, and 30 sec at 72°C for 35 cycles. For *WT1*, primers were W1, 5'-ATCCTCTGCGGAGCCCAATA-3'

and W3, 5'-ACTGTGCTGCCTGGGACA-3', and the following conditions were used: 30 sec at 94°C, 30 sec at 55°C, and 30 sec at 72°C. For *NDN* (*NECDIN*), primers were RN700, 5'-AGCC-CCAAAAGAACTCGTATT-3' and RN709, 5'-CAGAAGGC-GCAGGAGTC-3', and the following conditions were used: 30 sec at 94°C, 30 sec at 60°C, 30 sec at 72°C. *GABRA5* primers were RN786, 5'-GAGAACATCAGCACCAGCACAG-3' and RN787, 5'-AAGACGAAGGCATAGCACACAG-3'; *GABRB3* primers were RN788, 5'-AGAATCACCACGACAGCAGC-AT-3' and RN789, 5'-CCAGAAGGACACCCACGACAGA-3'; *GABRG3* primers were RN790, 5'-TCACCATTGACAGACAT-CAATCC-3' and RN791, 5'-CATCAGACACTCATCGCCA-CA-3'. Cycling conditions for the *GABA_A* receptor genes were 35 cycles of 95°C for 30 sec, 62°C for 30 sec, and 72°C for 30 sec. Primers for *TAPA1* (*CD81*) were TAPA1a, 5'-ACTGACTGCTTTGACCACC-3' and TAPA1b, 5'-TCCACTCATACACGC-CACC-3' and cycling conditions as for *IGF2*, above. *GABRA5* and *GABRB3* were expressed at sufficiently high levels such that RT-PCR products could be seen directly on ethidium bromide-stained agarose gels, whereas RT-PCR products for *GABRG3* had to be blotted and hybridized with a cDNA probe.

Microsatellite Marker Analysis and Expressed Polymorphisms. Dinucleotide repeat alleles of *D15S123* (Genome Data-Base, Baltimore) were amplified by using 50 ng of DNA and a [γ -³²P]dATP-end-labeled forward primer. PCR was carried out in a 15- μ l reaction volume that included 200 mM each dATP, dCTP, dGTP, and dTTP and 1.5 μ l of 10 \times reaction buffer, reverse primer, and 0.5 units of *Taq* polymerase (Boehringer Mannheim). Samples were amplified in a thermocycler for 30 cycles (95°C, 30 sec; 55°C, 30 sec; 72°C, 30 sec) followed by a 6-min 72°C incubation. Before loading, 1.5 vol of 95% formamide loading buffer was aliquoted to each sample, which was electrophoresed on a 6% polyacrylamide gel (National Diagnostics). The gel was then transferred to 3M Whatman paper, dried, and exposed to autoradiographic film (Biomax) for 16 hr. Expressed polymorphisms in *IPW* (22) and *SNRPN* (25) were analyzed as described.

RESULTS

Strategy for a Somatic-Cell Hybrid Model to Study Genomic Imprinting. Genomic imprinting results in predominant-gene expression from one parental allele in somatic cells, although this may be subject to temporal and/or tissue-specific regulation. To test the fidelity of genomic imprints in somatic-cell hybrids, cell

Table 1. Somatic-cell hybrids used for analysis of chromosome 15

Hybrid	Rodent background	Origin of human donor cell	Chromosomes present	Chromosome 15 imprint	Source (reference)
A15	Mouse A9	GM01604 Fibroblast	15	pat	R. Schultz (19)
A9 + 15	Mouse A9	fetal lung Fibroblast	15	pat	NIGMS (20)
A59-3az	Mouse A9	Fibroblast	1, 4, 8, 10, 13, 15, 22	pat	H. F. Willard
t60-14	Mouse tsA-1S9	Fibroblast	4, 8, 11, 13, 14, 15, 18, 21, 22, X	pat	H. F. Willard (54)
20L-28	LM/TK	GM00291A Fibroblast	t(17;1), 3, 4, 5, 6, 7, 8, 11, 13, 14, 15, 16, 20, 21	mat	T.B.S.
ALA-8	Mouse A9	Fibroblast	1, 2, 3, 4, 5, 6, 7, 8, t(X;9), 10, 11, 12, 13, 14, 15, 16, 17, 18, 19, 20, 21, 22, X	mat	T.B.S. (55)
GAR-1	RAG	GM00806 Fibroblast	3, 5, 8, 10, 12, 13, 15, 16, 20, X	mat	T.B.S.
t75-2maz-34-4a	Mouse tsA-1S9	Fibroblast	X, 3, 6, 7, 12, 14, 15, 16, 17, 19, 20, 21	mat	H. F. Willard
15A	CHO-K1	AML Lymphocyte	15 + 2-3 non-random human	mat (+ pat frag. in ~10% of cells)	NIGMS
55R-16	RAG	GM05519 Fibroblast	1, 2, 3, t(4;11), 5, 6, 7, 8, 10, 12, 13, 15, 16, 19, 21, 22, X	mat/pat	T.B.S. (56)
DUA-1A	Mouse 1R	skin Fibroblast	t(X;15) (p11;q11)	pat	T.B.S. (28)
2-3-4	Mouse A9	skin Fibroblast	t(15;19) (q12;q13.41)	pat	R.D.N.
t86-B1-maz1b-3a	Mouse tsA-1S9	Fibroblast	X, 15	pat	H. F. Willard (57)

AML, Acute myelogenous leukemia; CHO, Chinese hamster ovary; frag., fragment; mat, maternal; pat, paternal; NIGMS, National Institute of General Medical Sciences.

Table 2. Somatic-cell hybrids used for analysis of chromosome 11

Somatic-cell hybrid	Rodent background	Origin of human donor cell	Chromosomes present	Chromosome 11 methylation imprint
GM10482A	Mouse A9	Fibroblast	der (11) t (X;11) (q26;q23),7	pat
GM10927B	CHO-K1	Amniotic fibroblast	11	pat
GM11087A	Mouse 3T3	Foreskin fibroblast	11	pat
GM07300	CHL	N/A	6,8,11,X	mat
GM11944	CHO-K1	Amniotic fibroblast	11pter>cen. translocated to a CH chromosome	pat
GM11941	Mouse L-1R	Lymphocyte	11, Xp translocated to a mouse chromosome	pat
GM13400	CHO a3	Ewing sarcoma	der 11t(11;22)(q24;q12)	mat
GM11937	CHO a3	Lymphocyte	der(11)t(4;11)(q21;q23)	pat

Abbreviations: pat, paternal; mat, maternal; cen, centromere; CHO, Chinese hamster ovary; CHL, Chinese hamster lung.

lines were grown to near confluency and DNA and total RNA were isolated. These lines were assayed for gene expression by using RT-PCR and for DNA methylation by using Southern blot analysis. In all cases, PCR primer pairs are specific for human sequence and are unable to amplify the orthologous rodent gene. Thirteen hybrids believed to contain a single human chromosome 15 were used for analysis of genes in the PWS/AS-critical region (Fig. 1a), and eight hybrids containing a single human chromosome 11 were used to assay genes in 11p15 (Fig. 1b). It is worth noting that our hybrid cell lines were generated by using various rodent backgrounds in the fusion process and that some hybrids contain a single human chromosome, whereas others contain a large complement of human chromosomes (Tables 1 and 2). However, neither of these variables appears to have had any effect on our assays.

Expression and Methylation Imprints in Chromosome 15q11-q13. We first tested hybrids containing chromosome 15 for maintenance of methylation and expression imprints at the *SNRPN* locus. *SNRPN* encodes the small nuclear ribonuclear protein N, a polypeptide believed to be involved in tissue-specific splicing of mRNAs. Previous studies (21, 23, 26) have established that the *SNRPN* transcript is expressed only from the paternal allele and that this allele is unmethylated at the *SNRPN* promoter. Eleven of 13 hybrids showed only a single methylated or unmethylated allele (Fig. 2a; Table 1), and seven of these expressed the *SNRPN* transcript (Fig. 3a; Table 1). Importantly, expression and methylation patterns were concordant, so that hybrids that were unmethylated at the *SNRPN* promoter expressed the transcript, whereas those that were methylated did not express the transcript. All hybrids expressed the nonimprinted chromosome 15 control gene *RPS12* (Fig. 3d).

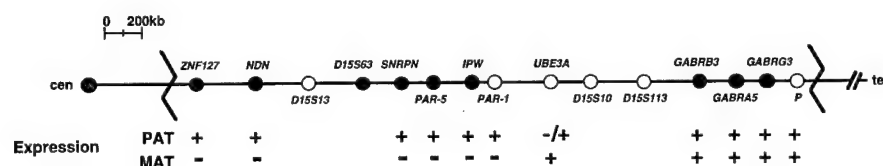
In two hybrids, 15A and 55R-16, both a methylated and an unmethylated allele were detected (Fig. 2a; data not shown), and both hybrids express the *SNRPN* transcript (Fig. 3a), suggesting either a relaxation of the imprint in tissue culture or the presence of both a maternal and a paternal chromosome in these cell lines. To distinguish between these possibilities, we PCR-amplified

across a previously described *HphI* polymorphism in exon 3 of the *IPW* gene (ref. 22; see Fig. 1) and digested the products to show the presence of two alleles in the DNA of each hybrid, only one of which is present in the cDNA from each hybrid (Fig. 4a; data not shown). Furthermore, fluorescence *in situ* hybridization using a commercial *SNRPN* cosmid and cells from hybrid 15A confirmed the presence of an intact chromosome 15 in most cells and a second human fragment containing *SNRPN* in about 10% of cells (National Institute of General Medical Sciences catalog, 1995; J. M. Amos-Landgraf and R.D.N., unpublished data). These data prove the presence of two chromosomes 15 in hybrids 15A and 55R-16. Therefore, monoallelic gene expression has been maintained in the entire panel of chromosome-15 hybrids, some of which are more than 10 yr old and have endured more than 100 passages in tissue culture.

Designating chromosomes in the hybrids as either maternal or paternal was initially done on the basis of previously established imprinting patterns; however, it was a formal possibility that during the process of fusing cell lines, or after many passages in tissue culture, genomic imprints might have been reversed. To address this possibility, an informative microsatellite marker was typed in the hybrid cell line GAR-1 as well as in the hybrid cell line donor and the parents of the hybrid cell line donor (Fig. 4b). The haplotype analysis shows that the chromosome 15 contained in the GAR-1 hybrid is of maternal origin, corroborating the methylation and expression data. A second hybrid cell line containing a t(15;19) translocation previously determined to be of paternal origin (27) likewise was shown to maintain the correct paternal methylation pattern (Fig. 2a; Table 1). Therefore, it is likely that all of the hybrids that are unmethylated and express *SNRPN* contain a single human chromosome 15 of paternal origin, whereas all of the hybrids that are methylated at *SNRPN* and do not express the transcript contain a single human chromosome 15 of maternal origin.

Additionally, as methylation at the *SNRPN* CpG island is strictly maintained in all tested somatic-cell hybrids, we were able to use this assay to assign a parental origin to a *de novo*

(a)



(b)



FIG. 1. Imprinted-gene maps of chromosomes 15q11-q13 (a) and 11p15 (b). The gene positions and loci assayed in somatic-cell hybrids (●) are shown. Jagged lines in a represent the common deletion breakpoints in PWS and AS patients. Symbols are: +, gene expression; -, lack of gene expression. PAT, paternal; MAT, maternal; cen, centromere; tel, telomere. The -/+ in a indicates that *UBE3A* is not expressed from the paternal allele in certain regions of the brain. Figure adapted from refs. 3 and 6.

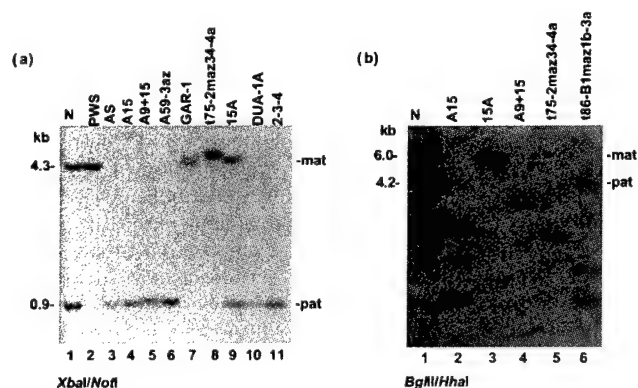


FIG. 2. DNA methylation analysis in chromosome-15 hybrids. (a) Maintenance of methylation imprints at *SNRPN* in somatic-cell hybrids. Normal individuals (lane 1) have both a methylated (4.3-kb) allele corresponding to the maternally inherited chromosome and an unmethylated (0.9-kb) allele corresponding to the paternally inherited chromosome. PWS deletion patients (lane 2) lack a paternal contribution, whereas AS deletion patients (lane 3) lack a maternal contribution. Most hybrids show either a completely methylated band, indicating the presence of only a maternal chromosome, or a completely unmethylated band, indicating the presence of only a paternal chromosome. Hybrids with both a methylated and an unmethylated band [15A and 55R-16 (latter data not shown)] were shown to contain both a maternal (mat) and a paternal (pat) human chromosome 15 (see Fig. 4a and Results). Lane 1, normal human lymphoblast; lane 2, lymphoblast from a PWS deletion patient; lane 3, lymphoblast from an AS deletion patient; lanes 4–11 contain DNAs from a subset of the chromosome-15 hybrid panel. (b) Methylation patterns are not maintained at *D15S63*, with most hybrids being hypomethylated. Hybrid 15A is hypermethylated, despite containing a proportion of cells with a paternally derived chromosome 15. Lane 1, normal human lymphoblast; lanes 2–6 contain DNAs from a subset of the chromosome-15 hybrid panel.

translocation chromosome in one cell line. Thus, the t(X;15) chromosome in hybrid DUA-1a (28), which is unmethylated at the *SNRPN* promoter, is likely of paternal origin (Fig. 2a).

To further characterize the panel of hybrids, RT-PCR was performed for the imprinted, paternally expressed *IPW* gene (22), the *PAR5* expressed sequence tag (23), and the recently identified *NDN* gene (29, 30). In each hybrid, expression of *IPW*, *PAR5*, and *NDN* (Fig. 3) correlated with the assigned paternal or maternal origin of each chromosome 15, as inferred from the *SNRPN* expression and methylation data (Table 1), confirming our finding that imprinted gene expression is strictly maintained in these somatic-cell hybrids. However, methylation of *D15S63*, a locus previously shown to be unmethylated on the paternal allele and methylated on the maternal allele (31), was not maintained in the hybrids, with most hybrids being hypomethylated (Fig. 2b). Similarly, DNA methylation was not maintained at the *ZNF127* CpG island (data not shown).

Nonimprinted Genes in Chromosome 15q11–q13. Recently, it was reported that the human GABA_A receptor genes in 15q12–q13 were imprinted and expressed exclusively from the paternal chromosome in hybrid cell lines generated by using microcell-mediated chromosome transfer (18). Because studies in the mouse suggested that these genes are not imprinted (32–34), we investigated the imprinted status of the human GABA_A receptor genes in our panel of hybrids by using RT-PCR. All three genes were amplified equally well for hybrids containing either a maternal or a paternal chromosome 15 (Fig. 3f and g; data not shown). Thus, in our system, the GABA_A receptor genes are not imprinted.

Expression and Methylation Imprints in 11p15. Maintenance of a methylation imprint in chromosome 11p15 was assayed at a CpG island in an intron of the *KVLQT1* gene previously shown to be unmethylated on the paternal chromosome and methylated on the maternal chromosome (M.J.H., unpublished data). In each hybrid containing an individual human chromosome 11, a single

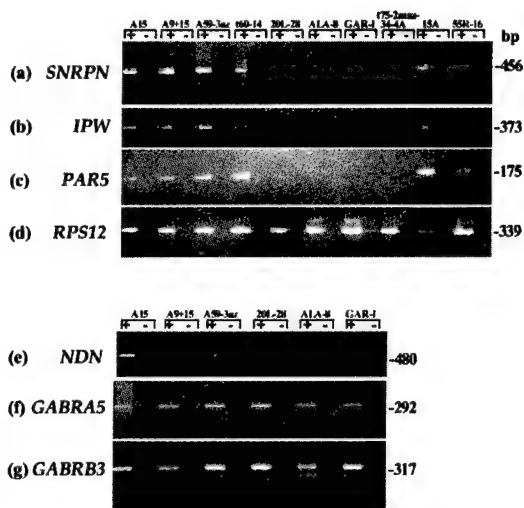


FIG. 3. Gene expression in hybrids containing human chromosome 15. Expression of *SNRPN* (a), *IPW* (b), *PAR5* (c), and *NDN* (e) as determined by RT-PCR correlates with the *SNRPN* methylation data. Only those hybrids that are unmethylated at the *SNRPN* promoter express each of these four transcripts. The *GABRA5* (f) and *GABRB3* (g) receptor subunit genes are expressed in hybrids containing either a maternal or a paternal chromosome 15. For *GABRG3* (data not shown), hybrid A9+15 (containing a paternal chromosome 15) and hybrid 20L-28 (containing a maternal chromosome 15) consistently showed high levels of expression. Additionally, one paternal (A59–3az2 maz) and two maternal (ALA-8, GAR-1) hybrids showed low levels of expression, whereas expression in A15 (paternal) was not detected in multiple experiments. The control gene *RPS12* (d) is expressed in all hybrids. PCR was performed with (+) or without (–) reverse transcriptase.

unmethylated allele or methylated allele was present, consistent with retention of methylation imprints at this locus (Fig. 5a; Table 2).

Further studies were performed to characterize the reciprocally imprinted *IGF2* and *H19* genes in the hybrid cell lines carrying a single human chromosome 11. *H19* is primarily expressed from the maternal allele only (24), whereas *IGF2* is expressed only from the paternal allele (35). Though neither gene was highly expressed, RT-PCR data revealed that *IGF2* was expressed in four hybrids and *H19* was expressed in the remaining two hybrids derived from human fibroblasts (Fig. 5b; Table 2). Hybrids derived from human lymphoblasts did not express reproducibly detectable levels of *IGF2* or *H19* mRNA. For five of the six hybrids, the *H19/IGF2* expression and *KVLQT1* intronic methylation data were concordant; however, hybrid GM10927B was unmethylated at the 11p15 *NoI* site but expressed *H19*. In repeated RT-PCR experiments, weak *IGF2* expression also was occasionally seen in this hybrid (data not shown). Because hybrid GM10927B was derived from amniotic fibroblasts and imprinting

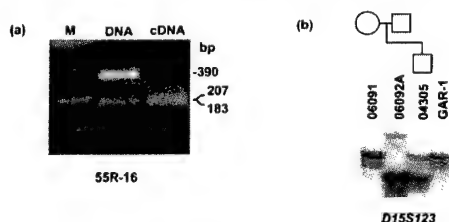


FIG. 4. Polymorphism studies of chromosome-15 hybrids. (a) Mono-allelic imprinted gene expression in hybrid 55R-16 with biallelic *SNRPN* DNA methylation. Primers amplify an *HphI* polymorphism in the *IPW* gene in exon 3. Digestion of amplified genomic DNA (lane 2) reveals the presence of two alleles in hybrid 55R-16, only one of which is expressed (lane 3). Lane 1 contains the 123-bp ladder size marker. (b) Microsatellite analysis of hybrid cell line GAR-1 and lineage. GAR-1 contains a maternal chromosome 15 from cell line GM04305, in accordance with complete methylation at the *SNRPN* promoter (see Fig. 2a).

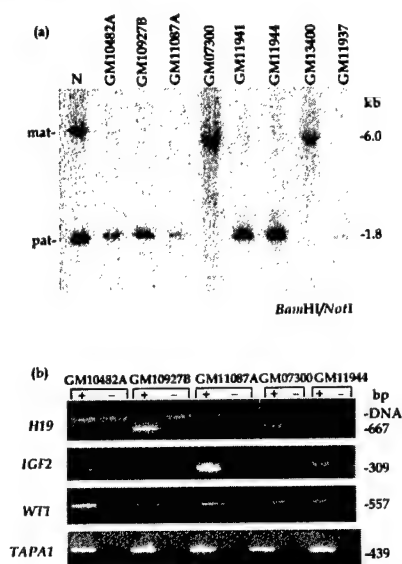


FIG. 5. Methylation and gene expression analyses of hybrids containing a single human chromosome 11. (a) DNA methylation imprints are monoallelic at an intronic *KVLQTI* intronic *NotI* site. Normal individuals have both a methylated (6.0-kb) allele corresponding to the maternally inherited chromosome (mat) and an unmethylated allele (1.8-kb) corresponding to the paternally inherited chromosome (pat). Each hybrid shows either the presence of a methylated or an unmethylated chromosome, suggesting that methylation imprints at this site are maintained in somatic-cell hybrids. (b) Each hybrid expressed either the maternal-only *H19* or paternal-only *IGF2* gene but never both, consistent with maintenance of functional imprints in chromosome 11p15. The primers used for *H19* RT-PCR span a small intron, giving a smaller-sized product in cDNA (667 bp) compared with amplification from genomic DNA (24). Although *TAPA-1* maps within the imprinted domain in 11p15, it is expressed from both maternal and paternal chromosomes, consistent with knockout studies in the mouse. The control gene, *WT1*, is expressed in all hybrid cell lines. + and - are as for Fig. 3.

of *H19* in the placenta has been shown to depend on developmental stage and cell type (36), fusion of a cell with biparental *H19* expression could result in expression from a paternally derived chromosome. Alternatively, in this cell, *H19* may be regulated independently of *IGF2* (37) or the domain containing the *KVLQTI* intronic *NotI* site; the latter is suggested by mouse studies (38). Expression of *KVLQTI* was not detectable in any of the chromosome 11 hybrids. The control gene, *WT1* (39), demonstrates polymorphic imprinting in preterm placentae and fetal brain (40) but generally shows biallelic expression, consistent with its expression in all somatic-cell hybrid lines. Also, *TAPA1*, a gene mapping between the imprinted *KVLQTI* and *ASCL2* genes (41) and which can be inferred from knockout experiments in the mouse not to be imprinted (42) was expressed from both chromosomes in our hybrid panel (Fig. 5b).

DISCUSSION

With the increased interest in the phenomenon of genomic imprinting and the rapid discovery of new transcripts in imprinted domains, there is a great need for a model system to study imprinted genes. Current methods for proving the imprinted status of a gene rely on finding a sequence polymorphism as well as informative families and can be very time consuming. Our approach for overcoming these obstacles is to assay for monoallelic gene expression from somatic-cell hybrids containing individual human chromosomes. By using this powerful system, it is possible to test for expression from one parental chromosome simply by performing RT-PCR on a panel of well-characterized hybrids. We have demonstrated that somatic-cell hybrids do maintain functional (expression) imprints with high fidelity. This has been shown for four known imprinted genes in chromosome 15q11–q13, as well as for two oppositely imprinted genes in

chromosome 11p15. The single chromosome-11 hybrid that demonstrated potentially discordant results may be readily explained by the cell type used in generating this hybrid (36, 37). Indeed, this is further testament to the evidence that the transcriptional state of the chromosome at the time of fusion is retained in somatic-cell hybrids. Combined, these data suggest that somatic-cell hybrids can be used as a powerful reagent to assess whether any human gene is imprinted and to describe from which parental allele it is expressed.

By using a panel of chromosome-15 hybrids, we were able to independently demonstrate that the *NDN* gene is imprinted and expressed only from the paternal chromosome, as recently reported by others (29, 30). This is of particular interest with respect to the sensitivity of this method, as mouse *Ndn* has been shown to be expressed only in neurons by Northern blot analysis and is undetectable in other tissues by these measures (43), yet is easily detectable by RT-PCR in somatic-cell hybrids containing a paternal human chromosome 15.

Our data also refute a recent report that the three GABA_A receptor subunit genes in chromosome 15q12–q13 are imprinted with exclusive expression from the paternal allele only (18). In an earlier study (44), *GABRB3* was suggested to show exclusive maternally derived expression based on differential expression between hydatidiform moles (paternal genome only) and ovarian teratomas (maternal genome only); however, these tumors represent highly differentiated tissues that are not true models for genomic imprinting studies (21, 45, 46). In the mouse, all three GABA_A receptor subunit genes, *Gabrb3*, *Gabra5*, and *Gabrg3*, show equal levels of expression in brain and other tissues after paternal or maternal inheritance of deletions spanning these genes, suggesting that none of these genes is imprinted (32, 33). Regional specific imprinting is unlikely, at least for *Gabrb3*, as ≈ 90 –95% of homozygous deleted mice die as neonates, most with an associated cleft-palate phenotype (34, 47). Heterozygous *Gabrb3* knockout mice also show intermediate values for mRNA levels as well as electrophysiological and electroencephalogram recording abnormalities compared with wild-type and *Gabrb3*-null mice (34). Although there may be cases of imprinted mouse genes in which the human gene appears not to be imprinted (e.g., *IGF2R*), studies on the mouse homologs of human 15q11–q13 genes have shown that all are conserved in relative chromosome position, structure, sequence, and imprinting status (3). Therefore, it is likely that the human GABA_A receptor genes are nonimprinted, as shown here.

Of interest, we have found that somatic-cell hybrids are often, but not always, a reliable resource for assaying DNA methylation imprints. We were able to demonstrate faithful retention of a methylation imprint in all hybrids tested only at the *SNRPN* and *NDN* (T.G.G., J.M.G., and R.D.N., unpublished data) promoters in 15q11–q13 and at a *KVLQTI* intronic CpG island in 11p15. The strict retention of the *SNRPN* methylation imprint could be indicative of its central importance in imprinting in this region. *SNRPN* is located in the middle of the 15q11–q13 imprinted domain and has been proposed to be an important component of the imprinting center involved in germ-line switching of the imprint for all imprinted genes in 15q11–q13 (3, 4). The *SNRPN* promoter methylation imprint, assayed here, is maintained in all somatic tissues tested to date (21). In contrast, differential methylation at *ZNF127* is maintained only in the brain, with leukocytes and fibroblasts showing partial methylation on both alleles (M. T. C. Jung, C. C. Glenn, D. J. Driscoll, R.D.N., unpublished data). Thus, individual cells fused in generating the hybrids may show different methylation levels at these and other loci. Sites in which DNA methylation is not maintained may not represent the critical CpG residues involved in regulating imprinted-gene expression in this system. Alternatively, it is possible that the particular chromatin state associated with maternally and paternally imprinted chromosomes, perhaps in concert with specific trans factors, is sufficient to maintain imprinted-gene expression. This would then be analogous to the maintenance of

the developmental state of β -globin gene expression (16) discussed earlier.

It is important to note that this system is constrained by the limitations imposed by imprinted genes subject to temporal and/or tissue-specific regulation. Although we generally have met with success in assaying imprinted-gene expression, we were not able to consistently detect expression of the *ZNF127* transcript, presumably because of low levels of expression and/or mRNA instability in the cell types used to generate our hybrid cell lines. The corollary to this may also be true; that is, because of the relative sensitivity of RT-PCR, one may detect expression of a transcript in both maternal and paternal chromosome containing hybrids when in fact, expression is predominantly silenced on one chromosome. This type of "leaky" expression has been shown for *p57^{KIP2}* (6) and *IMPT1/ORCTL2* (48, 49).

The fact that imprinted-gene expression is maintained in somatic-cell hybrids is important not only for its scientific utility but from an evolutionary point of view. Once replicated, the human chromosomes contained in the hybrid cell lines are remodeled using rodent proteins. The perpetuation of expression imprints strongly supports the existence of evolutionarily conserved factors involved in maintenance of genomic imprinting, perhaps including cis DNA elements and/or chromatin proteins, and is consistent with the maintenance of developmental globin-gene expression (16) and X chromosome inactivation (17) states in somatic-cell hybrids. One use of this system may be to analyze molecular mechanisms involved in the maintenance of genomic imprints in somatic cells; for example, by testing the efficacy of various chemicals to activate genes normally silenced by genomic imprinting. It has been shown that treatment of cells with 5-azacytidine can demethylate promoters and induce transcriptional activation (50), including reactivation of X-linked genes in somatic-cell hybrids containing a previously inactive X chromosome (51). Similarly, histone H4 acetylation has been associated with transcriptional activation (52), so that treatment of cell lines with sodium butyrate or Trichostatin A, inhibitors of histone deacetylase, also may have direct effects on imprinted gene activity (53).

At present, however, we envision this model system being most useful in rapidly determining the imprinted status of transcripts. This will be particularly true as the Human Genome Project identifies a large number of genes mapping within or near regions thought to be imprinted. A panel of somatic-cell hybrids containing a maternal or paternal homolog of each human chromosome suspected to contain imprinted genes would be an invaluable resource for such imprinting assays.

We thank Dr. Huntington F. Willard for cell lines, as well as for critical input on experimental design and writing of this manuscript. We also thank Dr. Andrew Miller for mapping the *RPS12* gene to chromosome 15, Stacey Bolk for help with microsatellite analysis, Dr. Bryan Williams for primers to *WT1*, James Amos-Landgraf for technical assistance, and Dr. Roger Schultz for cell line A15. This research was supported by the National Institutes of Health (Grant HD31491 to R.D.N. and CA63333 to T.B.S. and M.J.H.) and Pew Scholars Program in Biomedical Sciences (R.D.N.). J.M.G. was supported by National Institutes of Health Training Grant GM08613.

- Solter, D. (1988) *Annu. Rev. Genet.* **22**, 127–146.
- Cattanach, B. M. & Beechey, C. V. (1990) *Development (Cambridge, U.K.) Suppl.* **63**–72.
- Nicholls, R. D., Saitoh, S. & Horsthemke, B. (1998) *Trends Genet.* **14**, 194–200.
- Dittrich, B., Buiting, K., Korn, B., Rickard, S., Buxton, J., Saitoh, S., Nicholls, R. D., Poustka, A., Winterpacht, A., Zabel, B., *et al.* (1996) *Nat. Genet.* **14**, 163–170.
- Malzac, P., Webber, H., Moncla, A., Graham, J. M., Kukulich, M., Williams, C., Pagon, R. A., Ramsdell, L. A., Kishino, T. & Wagstaff, J. (1998) *Am. J. Hum. Genet.* **62**, 1353–1360.
- Reik, W. & Maher, E. R. (1997) *Trends Genet.* **13**, 330–334.
- Hatada, I., Ohashi, H., Fukushima, Y., Kaneko, Y., Inoue, M., Komoto, Y., Okada, A., Ohishi, S., Nabetani, A., Morisaki, H., *et al.* (1996) *Nat. Genet.* **14**, 171–173.
- Kondo, M., Matsuoka, S., Uchida, K., Osada, H., Nagatake, M., Takagi, K., Harper, J. W., Takahashi, T., Elledge, S. & Takahashi, T. (1996) *Oncogene* **12**, 1365–1368.
- Thompson, J. S., Reese, K. J., DeBaun, M. R., Perlman, E. J. & Feinberg, A. P. (1996) *Cancer Res.* **56**, 5723–5727.
- Hatada, I., Inazawa, J., Abe, T., Nakayama, M., Kaneko, Y., Jinno, Y., Niikawa, N., Ohashi, H., Fukushima, Y., Iida, K., *et al.* (1996) *Hum. Mol. Genet.* **5**, 783–788.
- Ledbetter, D. H. & Engel, E. (1995) *Hum. Mol. Genet.* **4**, 1757–1764.
- Kuroiwa, Y., Kaneko-Ishino, T., Kagitani, F., Kohda, T., Li, L. L., Tada, M., Suzuki, R., Yokoyama, M., Shiroishi, T., Wakana, S., *et al.* (1996) *Nat. Genet.* **12**, 186–190.
- Plass, C., Shibata, H., Kalcheva, I., Mullins, L., Kotelevtseva, N., Mullins, J., Kato, R., Sasaki, H., Hirotsune, S., Okazaki, Y., *et al.* (1996) *Nat. Genet.* **14**, 106–109.
- Hayashizaki, Y., Shibata, H., Hirotsune, S., Sugino, H., Okazaki, Y., Sasaki, N., Hirose, K., Imoto, H., Okuizumi, H., Muramatsu, M., *et al.* (1994) *Nat. Genet.* **6**, 33–40.
- Kalscheuer, V. M., Mariman, E. C., Schepens, M. T., Rehder, H. & Ropers, H. H. (1993) *Nat. Genet.* **5**, 74–78.
- Stanworth, S. J., Roberts, N. A., Sharpe, J. A., Sloane-Stanley, J. A. & Wood, W. G. (1995) *Mol. Cell. Biol.* **15**, 3969–3978.
- Brown, C. J., Carrel, L. & Willard, H. F. (1997) *Am. J. Hum. Genet.* **60**, 1333–1343.
- Meguro, K., Mitsuya, K., Sui, H., Shigenami, K., Kugoh, H., Nakao, M. & Oshimura, M. (1997) *Hum. Mol. Genet.* **6**, 2127–2133.
- McDaniel, L. D. & Schultz, R. A. (1992) *Proc. Natl. Acad. Sci. USA* **89**, 7968–7972.
- Ning, Y., Lovell, M., Taylor, L. & Pereira-Smith, O. M. (1992) *Cytogenet. Cell Genet.* **60**, 79–80.
- Glenn, C. C., Saitoh, S., Jong, M. T. C., Filbrandt, M. M., Surti, U., Driscoll, D. J. & Nicholls, R. D. (1996) *Am. J. Hum. Genet.* **58**, 335–346.
- Weyrick, R., Kerns, J. A. & Francke, U. (1994) *Hum. Mol. Genet.* **3**, 1877–1882.
- Sutcliffe, J. S., Nakao, M., Christian, S., Orstavik, K. H., Tommerup, N., Ledbetter, D. H. & Beaudet, A. L. (1994) *Nat. Genet.* **8**, 52–58.
- Zhang, Y. & Tycko, B. (1992) *Nat. Genet.* **1**, 40–44.
- Giaccone, J. & Francke, U. (1994) *Hum. Mol. Genet.* **3**, 379.
- Glenn, C. C., Porter, K. A., Jong, M. T. C., Nicholls, R. D. & Driscoll, D. J. (1993) *Hum. Mol. Genet.* **12**, 2001–2005.
- Sun, Y., Nicholls, R. D., Butler, M. G., Saitoh, S., Hainline, B. E. & Palmer, C. G. (1996) *Hum. Mol. Genet.* **5**, 517–524.
- Solomon, E., Bobrow, M., Goodfellow, P. N., Bodmer, W. F., Swallow, D. M., Povey, S. & Noel, B. (1976) *Somatic Cell Genet.* **2**, 125–140.
- MacDonald, H. R. & Weyrick, R. (1997) *Hum. Mol. Genet.* **6**, 1873–1878.
- Philippe, J., Rougeulle, C., Massacrier, A., Moncla, A., Mattei, M.-G., Malzac, P., Roeckel, N., Taviaux, S., Lefranc, J.-L. B., Cau, P., *et al.* (1997) *Nat. Genet.* **17**, 357–361.
- Dittrich, B., Buiting, K., Grob, S. & Horsthemke, B. (1993) *Hum. Mol. Genet.* **12**, 1995–1999.
- Nicholls, R. D., Gottlieb, W., Russell, L. B., Davda, M., Horsthemke, B. & Rinchik, E. M. (1993) *Proc. Natl. Acad. Sci. USA* **90**, 2050–2054.
- Culiat, C. T., Stubbs, L. J., Montgomery, C. S., Russell, L. B. & Rinchik, E. M. (1994) *Proc. Natl. Acad. Sci. USA* **91**, 2815–2818.
- Homanics, G. E., DeLorey, T. M., Firestone, L. L., Quinlan, J. J., Handforth, A., Harrison, N. L., Krasowski, M. D., Rick, C. E., Korpi, E. R., Makela, R., *et al.* (1997) *Proc. Natl. Acad. Sci. USA* **94**, 4143–4148.
- Giannoukakis, N., Cheri, D., Paquette, J., Goodyer, C. G., Polychronakos, C. (1993) *Nat. Genet.* **4**, 98–101.
- Adam, G. I., Cui, H., Miller, S. J., Flam, F. & Ohlsson, R. (1996) *Development (Cambridge, U.K.)* **122**, 839–847.
- Brown, K. W., Villar, A. J., Bickmore, W., Clayton-Smith, J., Catchpoole, D., Maher, E. R. & Reik, W. (1996) *Hum. Mol. Genet.* **5**, 2027–2032.
- Caspari, T., Cleary, M. A., Baker, C. C., Guan, X. J. & Tilghman, S. M. (1998) *Mol. Cell. Biol.* **18**, 3466–3474.
- Little, M. H. (1992) *Oncogene* **7**, 635–641.
- Jinno, Y., Yun, K., Nishiwaki, K., Kubota, T., Ogawa, O., Reeve, A. E. & Niikawa, N. (1994) *Nat. Genet.* **6**, 305–309.
- Reid, L. H., Davies, C., Cooper, P. R., Crider-Miller, S. J., Sait, S. N., Nowak, N. J., Evans, G., Stanbridge, E. J., de Jong, P., Shows, T. B., *et al.* (1997) *Genomics* **43**, 366–375.
- Maecker, H. T., Do, M. S. & Levy, S. (1998) *Proc. Natl. Acad. Sci. USA* **95**, 2458–2462.
- Aizawa, T., Maruyama, K., Kondo, H. & Yoshikawa, K. (1992) *Brain Res. Dev. Brain Res.* **68**, 265–274.
- Kubota, T., Niikawa, N., Jinno, Y. & Ishimura, T. (1994) *Am. J. Med. Genet.* **49**, 452–453.
- Mutter, G. L., Stewart, C. L., Chaponot, M. L. & Pomponio, R. J. (1993) *Am. J. Hum. Genet.* **53**, 1096–1102.
- Mowery-Rushton, P. A., Driscoll, D. J., Nicholls, R. D., Joseph, L. & Urvashi, S. (1996) *Am. J. Hum. Genet.* **61**, 140–146.
- Culiat, C. T., Stubbs, L., Woychik, R. P., Russell, L. B., Johnson, D. K. & Rinchik, E. M. (1995) *Nat. Genet.* **11**, 344–346.
- Dao, D., Frank, D., Qian, N., O'Keefe, D., Vosatka, R. J., Walsh, C. P. & Tycko, B. (1998) *Hum. Mol. Genet.* **7**, 597–608.
- Cooper, P. R., Smilnich, N. J., Day, C. D., Nowak, N. J., Reid, L. H., Pearsall, R. S., Reece, M., Prawitt, D., Landers, J., Housman, D. E., *et al.* (1998) *Genomics* **49**, 38–51.
- Robertson, K. D., Hayward, D., Ling, P. D., Samid, D. & Ambinder, R. F. (1995) *Mol. Cell. Biol.* **15**, 6150–6159.
- Mohandas, T., Sparkes, R. S. & Shapiro, L. J. (1981) *Science* **211**, 393–396.
- Loidl, P. (1994) *Chromosoma* **103**, 441–449.
- Jeppeson, P. & Turner, B. M. (1993) *Cell* **74**, 281–289.
- Brown, C. J., Powers, V. E., Munroe, D. L., Sheinin, R. & Willard, H. F. (1989) *Somatic Cell Genet.* **15**, 173–178.
- Shows, T. B. & Brown, J. A. (1975) *Proc. Natl. Acad. Sci. USA* **72**, 2125–2129.
- Schneider, R., Higgins, M. J., Kieninger, D., Schneider-Scherzer, E., Hirsch-Kauffmann, M., Schweiger, M., Eddy, R. L., Shows, T. B. & Zabal, B. U. (1992) *Cytogenet. Cell Genet.* **59**, 264–267.
- Brown, C. J. & Willard, H. F. (1994) *Nature (London)* **368**, 646–648.

Thomas B. Shows, Ph.D.
Identifying and Isolating Breast Cancer-Associated
Genes on Chromosome 11

The imprinted domain in mouse distal Chromosome 7: reagents for mutagenesis and sequencing

Colleen D. Day, Nancy J. Smilnich, Galina V. Fitzpatrick, Pieter J. deJong, Thomas B. Shows, Michael J. Higgins

Department of Cancer Genetics, Roswell Park Cancer Institute, Buffalo, New York 14263, USA

Received: 18 August 1998 / Accepted: 1 October 1998

Several lines of evidence suggest that human Chromosome (Chr) band 11p15.5 contains genes involved in tumor suppression and embryonic growth (reviewed in Reid et al. 1997 and Cooper et al. 1998). First, rare chromosomal breakpoints in Beckwith-Wiedemann syndrome (BWS) patients and pediatric tumors map to 11p15.5. Since BWS patients suffer from a variety of overgrowth disorders and predisposition to embryonic tumors including Wilms' tumor (WT) and rhabdomyosarcoma, the breakpoints may disrupt developmental genes or their regulation. Second, loss of heterozygosity (LOH) in 11p15.5 has been detected in BWS and sporadic WT cases. LOH in the same region of 11p15.5 is also observed in a variety of adult tumors, suggesting the presence of a common tumor suppressor gene or a cluster of cancer-related genes. Third, 11p15.5 contains at least seven imprinted genes (IPL, ORCTL2/IMPT1, p57^{KIP2}, KvLQT1, ASCL2, IGF2, and H19) that are normally expressed primarily from one, parent-specific allele. Loss of imprinting (LOI) mutations have been detected at H19, IGF2, and to a lesser extent p57^{KIP2} in WT and BWS patients. The resulting abnormal expression of these genes may contribute to BWS and sporadic tumor development. Finally, studies involving the transfer of regions of 11p15.5 into mammalian cells demonstrate tumor suppressor activity in the G401 WT cell line and growth arrest in the RD rhabdomyosarcoma cell line.

To study this complex genomic region, we have previously constructed a 1 mb P1-artificial chromosome (PAC) clone contig through the relevant part of 11p15.5 (Reid et al. 1997), identified several novel transcripts in this domain (Crider-Miller et al. 1997), and shown that at least one of these transcripts represents a new imprinted gene, ORCTL2 (Organic cation transporter-like 2; Cooper et al. 1998). Compared with human, the laboratory mouse provides many advantages for the study of tumor development and genomic imprinting. These include relatively easy access to tissue samples at various developmental stages, sophisticated tools and methods for genetic analysis, and the feasibility to carry out studies in experimental tumorigenesis. To allow investigation in the mouse, we have now constructed a complete PAC clone map through the segment of mouse distal Chr 7 syntenic to the known imprinted domain in human 11p15.5. Constituent clones provide ready access to genomic subclones necessary for targeted mutagenesis as well as large-insert clones that carry a selectable marker in mammalian cells to facilitate transgenic and complementation studies. Furthermore, now that the sequencing of PACs in the human region (Reid et al. 1997) is near completion (McDermott Center for Human Growth and Development; <http://gestec.swmed.edu/>), the availability of the corresponding mouse PAC clones will provide reagents for large-scale sequencing of the

mouse imprinted domain for comparative studies. We also report the mapping of the *Orctl2*, the mouse orthologue of ORCTL2, a novel murine gene represented by several expressed sequence tags (ESTs), as well as 10 new sequence tagged sites (STSs) corresponding to ends of PAC clone inserts.

The RPCI-21 mouse (129/SvEvTACfBr) PAC library consisting of more than 125,000 clones (avg. size, 127 kb) and representing 5.3 fold coverage (<http://bacpac.med.buffalo.edu/mousepac.html>) was screened by hybridization of high-density colony filters (18,000 clones each) with two pools of PCR or RT-PCR products. These probes corresponded to portions of *Orctl2/Impt1*, p57^{KIP2}, *Kvlt1* (exons 8 and 9–11), *Mash2*, *Igf2*, and *H19* (Table 1). Following tertiary screening by Southern blot, probe content was analyzed by SEGMAP (Green and Green 1991), resulting in the generation of two contigs, the smaller of which contained only *Igf2* and *H19*. To join these two contigs, ends were isolated from PACs 196D11 (*Mash2*-positive) and 235M8 (*Igf2*-positive) by ligation-mediated PCR (Reid et al. 1997) and used to rescreen the library. The T7 ends of 235M8 and 196D11, respectively, identified four and five clones, two of which (231E13 and 295M8) were in common between the probes, thereby merging the contigs (Fig. 1). To confirm overlaps, and to increase resolution and clone depth, additional PAC ends were isolated and used to probe Southern blots of the existing contig and to rescreen the library. Ten of these PAC ends were cloned and sequenced; primer pairs were then designed and tested by colony PCR on individual clones in the contig to confirm hybridization results and to provide novel STSs in this region (Fig. 1, Table 1).

The positions of other known genes were mapped in the contig by the use of "overgo" probes (J.D. McPherson, personal communication; Table 1). With the exception of that corresponding to *Nap114*, all overgo probes hybridized to constituent PAC clones including EST 671070, the likely mouse homolog of human EST 28910 (Crider-Miller et al. 1997). Finally, an additional PAC clone, 145B13, was identified with the *Nap114* overgo and shown to overlap with two *Ipl*-containing PAC clones (Fig. 1).

The lengths of all PAC inserts were determined by CHEF gels and, along with the additional probe content data, were analyzed by SEGMAP to generate the contig presented in Fig. 1. The 1100-kb contig consists of 42 clones and 32 markers for an average resolution of one marker every 34 kb. The mean number of clones "hit" per marker was 4.3, somewhat lower than expected from a 5.3-fold library. This discrepancy is probably due to the relative paucity of clones in the centromeric one-third of the contig. We noted a similar under-representation of clones at the corresponding human IGF2 and H19 loci (Reid et al. 1997), possibly indicating that this region is refractory to cloning. A set of 11 PAC clones (boxed clone names in Fig. 1), comprising a complete tiling path through the contig, was mapped by fluorescence in situ hybridization (FISH). To allow unambiguous identification of mouse Chr 7,

Correspondence to: M.J. Higgins

The sequences reported in this paper have been assigned GenBank accession numbers AF093705–AF093715.

Table 1. Probes and novel STSs used in construction of mouse distal chromosome 7 contig.

Locus	Accession Number	Probe type	Primer 1 (5' --- 3')	Primer 2 (5' --- 3')	PCR product size (bp)
<i>Nap114</i>	W50655	Overgo ^d	AGGCGTTTCAGATGGCAGAAAACAG	GCCTCCATCTGAAAGACTGTTTTTC	
295F16.T7 ^a	AF093713	PAC end	GATTAAACATCGAAGAAGGG	AGGAAGTAGACAGCAAAG	138
210N7.T7 ^a	AF093705	PAC end	CTTTTATGTTCCAGACC	CTTCCTCTCTGTTTATCC	227
<i>Ipl</i>	AF002708	Overgo ^d	CAGAGCGAGCGCATTTGGTGAAC	GAAGCCATTTGAAAGGTTGCACC	
30B5.T7 ^a	AF093714	PAC end	CTGGTCATTTTGTTCACAGG	ATTAAGAATGTGCTCTAGGG	142
<i>Orct12</i>	AF037065	PCR product	AGCCGCCAGATGGTCATC	GAAAACATCACCAGAAGAGTCC	375
23H6.SP6 ^a	AF093711	PAC end	ATGTATCCAGTATGGAACC	ATCCTACCAAGTGAGTAAC	102
<i>p57^{KIP2} (Cdkn1c)</i>	U20553	PCR product	GGACGATGGAAGAACTCTG	GAGAGCGAGTAGAGATTAAAC	212
<i>Kvlt1</i> (ex 13) ^b	U70068	Overgo ^d	AGCAAAGACCGTGGCAGTAACACC	TCAGACGGGCACCGATGGGTTC	
<i>Kvlt1</i> (ex 9–11) ^b	U70068	RT-PCR product	CTCCATTGATGGCTATGAC	TGCTGGAATTTCTCTTGCTAC	225
23H6.sc34 ^c		PAC subclone			
23H6.T7 ^a	AF093710	PAC end	GAACACGAGAGAAAGAAAG	TGGAATGGGAACCTTAGAG	125
332115.SP6 ^a		PAC end			
245A8.T7 ^a	AF093707	PAC end	GTAAGAAAGTGGGCAAG	GAATGGAGGAAACTTGTG	113
<i>Kvlt1</i> (ex 8–9) ^b	U70068	RT-PCR product	CGGAGTCACACGCTTCTG	CATCAATGGAGAAATGGTCTG	178
<i>Kvlt1</i> (ex 2) ^b	U70068	Overgo ^d	CCGCAGCAAGTACGTGGGCATCTG	AAACGTAGCCGGCCAGATGCC	
<i>Kvlt1</i> (ex 1) ^b	U70068	Overgo ^d	CTCATTGTTCTGGTCTGCCTCATC	TGGACAGGACACTGAAGATGAGGC	
<i>Kvlt1</i> (ex 1c) ^b	U70068	Overgo ^d	AGTCTACACATCTCTCGAGCGCCC	ACACTTCCAACCGTGGGGCGCTC	
EST671070	AA241958	Overgo ^d	AGTCCCTGACTATGTGTACACCC	TTGGTCCAACGCTCAGGGTGTGAC	
<i>Tapal</i> (cd81) 5'	X59047	Overgo ^d	ACCTGCTCTTCTGCTTCAATTTG	CCAGCCAGCCAGAAGCAAAATTG	
332115.T7 ^a	AF093715	PAC end	CTTCACTTTGTTACGCTCTC	TCCATTGAGCAGCAATAG	140
<i>Mash2</i>	U77628	PCR product	GTAAGAAAGGAGGCGGTGG	GGTGGGAAGTGGACGTTTG	260
273G21.T7 ^a	AF093708	PAC end	GAAGGTCCACCAATCTTAG	CTTGTTGTTGCTTAGTTTC	146
<i>Th</i>	M69200	Overgo ^d	GGATGGTCTGCTGCTCTCTG	AGAATACAGCATGAAGGGCAGGAG	
196D11.T7 ^a	AF093709	PAC end	TGCAGAATAGCATTAGGG	TGAGAAGCAAGCAAAGTC	102
235M8.T7 ^a		PAC end			
254L6.T7 ^a	AF093712	PAC end	GCTCTGTGGAATATTCAGCTCTGG	AATCTTGGGAATGCCTTGGG	254
<i>Igf2</i>	U71085	PCR product	GGGTGAGCCATTCTCTGGG	GTCAACAAGCTCCCTCCGC	197
235M8.SP6 ^a		PAC end			
<i>H19</i>	AF049091	PCR product	GTCGATTGCAGCTGTTTGG	GACTGTAAGTGTATTATTGATGG	289
<i>Rpl23l</i>	U84902	RT-PCR product	GACCTTCGGAATTACCTTG	GAATTTTATTGGGCTTGTCAGAAC	359

^a End probes were derived from PACs (Reid et al. 1997) from either the SP6 and/or T7 ends as indicated.

^b Mouse *Kvlt1* exons determined by alignment with human (Lee et al. 1997).

^c 1.1 kb PstI subclone derived from PAC 23H6.

^d Overgo probes consisted of two oppositely orientated 24-bp oligonucleotides (8 bp

overlap) designed from 40 bp of sequence from a given locus. Design criteria included approximately 50% GC-content and 3'-termination with a G or C (J. McPherson, personal communication). The two oligonucleotides were combined at a concentration of 1.7 μ M each, heated to 80° for 5 min and annealed at 37° for 10 min.

bacterial artificial chromosome (BAC) 287P4, which has been shown to contain the tubby locus (Kleyn et al. 1996), was hybridized simultaneously with each of the 11 PACs with a two-color FISH strategy (data not shown).

The overall length of 1.1 mb determined by SEGMAP is very similar to that found by restriction mapping of the human contig (Reid et al. 1997). As noted in reports of partial contigs of this domain (Caspary et al. 1998; Gould and Pfeifer 1998; Paulsen et al. 1998), the relative map positions of *Nap114*, *Ipl*, *p57^{KIP2}*, *Kvlt1*, *Mash2*, *Th*, *Ins2*, *Igf2*, and *H19* are conserved. The present report extends this observation of synteny by including the *Orct12/Impt1* and EST 671070 loci (for mapping in human see Crider-Miller et al. 1997; Cooper et al. 1998) as well as a novel differentially methylated CpG-island (23H6.sc34-DMCpG in Fig. 1) in an intron of the *Kvlt1* gene (unpublished data). However, we have not yet identified a murine homolog for the antisense transcript that overlaps with the human ORCTL2 gene (that is, ORCTL2S; Cooper et al., 1998). As also noted in previous reports, *Kvlt1* is over 300 kb in both human and mouse; however, the intergenic distance of *Th* and *Igf2* is much greater in mouse than in human.

The contig shown in Fig. 1 represents the first complete coverage, comprised of bacterial based clones, of the known imprinted domain in mouse distal Chr 7 (assuming boundaries defined by *Nap114* [Hu et al. 1996] and *Rpl23l* [Yuan et al., 1996]). Unlike YACs, bacterial-based clones tend to faithfully represent genomic DNA, are relatively easy to propagate, and can be easily subcloned in phagmid sequencing vectors. Thus, PACs and BACs are the cloning vehicles of choice for large-scale genomic sequencing projects. With the exception of *Nap114*, each of the markers present in the telomeric two-thirds (that is, from *Nap2* to *Th*) of the contig is present in an average of 5.75 clones, a depth of coverage deemed

adequate for clone verification by fingerprinting prior to sequencing (McPherson 1997). This region contains the entirety of the *Kvlt1* genomic locus, the human counterpart of which has been implicated in the regulation of genomic imprinting (Lee et al. 1997). Thus, the availability of a "sequence-ready" map of the region for comparative sequence analysis should expedite the identification of important *cis*-acting regulatory elements involved in the mechanism of imprinting.

Although other bacterial-based clones are available for portions of the imprinted domain in mouse distal Chr 7 (Caspary et al. 1998; Gould and Pfeifer 1998; Paulsen et al. 1998), their usefulness is limited owing to the vector from which they were constructed. Unlike clones using the vectors pADSacBII and pBelo-BAC11, RPCI-21 PAC clones were constructed in pPAC4, a vector that contains the blasticidin-S-methylase gene, which confers resistance to blasticidin in mammalian cells (<http://bacpac.med.buffalo.edu/mouse-pac.html>). This precludes the need to retrofit large-insert clones with drug resistance markers or to employ cotransfection strategies for selection following introduction into mammalian cells in culture. Furthermore, the pPAC4 vector also contains loxG and loxP511 sites which, in principle, can be used for the insertion of entire PACs into mammalian cells at a genomic site previously targeted with wild-type loxP or loxP511, respectively. Thus, the constituent PAC clones of this contig will also serve as useful reagents in the construction of transgenic cell lines and mice, as well as providing genomic fragments for the generation of constructs for targeted mutagenesis.

Acknowledgments. We thank Linda Haley for carrying out the FISH mapping. This work was funded by National Institutes of Health grant CA63333 and U.S. Army Grant DAMD17-94-J-4417.

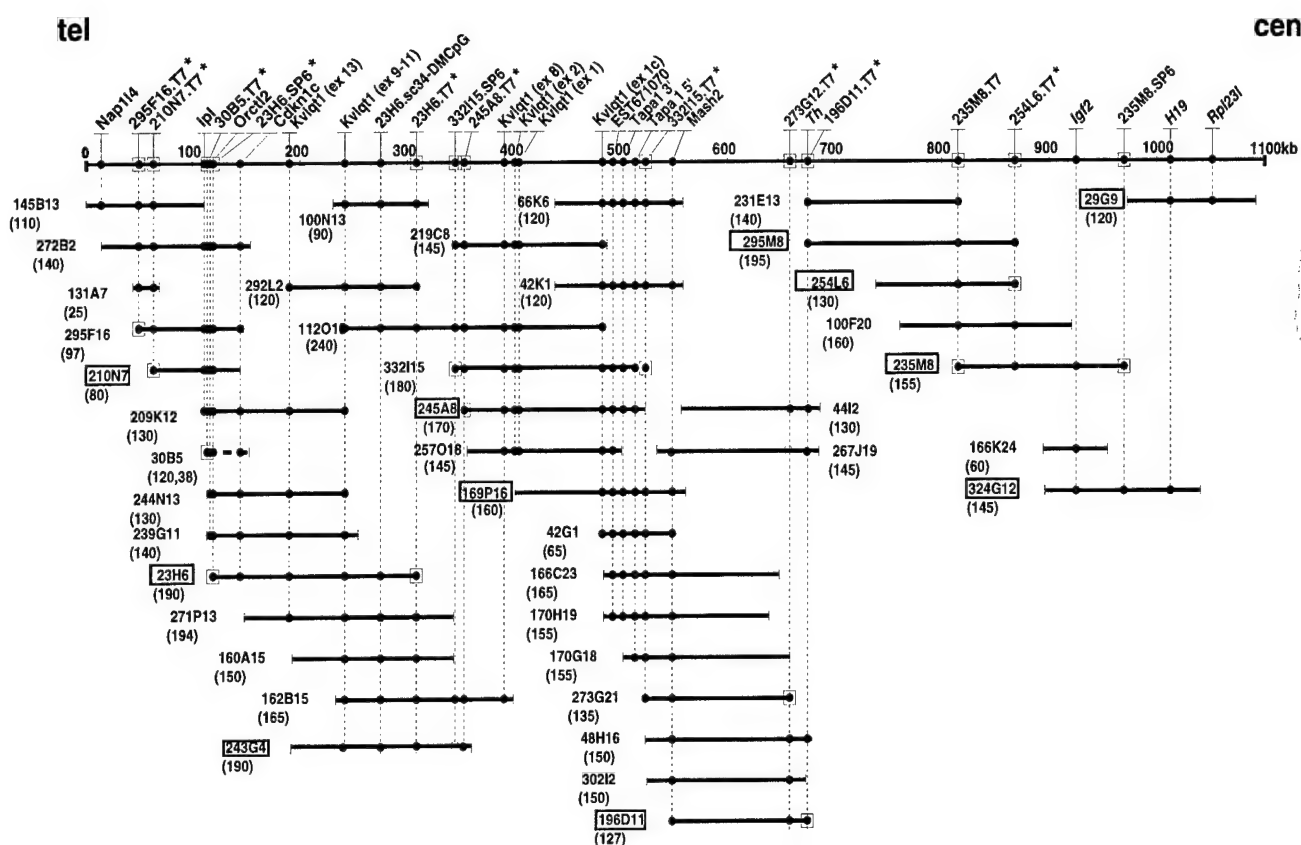


Fig. 1. PAC contig of mouse distal Chr 7. High-density colony filters (18,000 clones each) for the RPCI-21 Female (129/SvEvTACfBr) Mouse PAC Library (BAC PAC Resources, Roswell Park Cancer Institute), representing 5.3-fold coverage, were screened by hybridization with pools of radiolabeled probes. Positive clones were grown in 96-well plates, transferred to filter replicates, and hybridized to individual probes as described (Ioannou et al. 1994). A variety of hybridization probes were used to detect mouse distal 7 clones including PCR and RT-PCR products, end-fragments isolated from PACs (Reid et al. 1997) and "overgo" probes (J.D. McPherson, personal communication). Novel STSs (indicated with asterisks) were generated from PAC ends by cloning end-fragments into pCR-TOPOII (Invitrogen) and sequencing. Except for overgos, probes were labeled by random-priming of gel-isolated fragments (Feinberg and Vogelstein 1983). Overgo labeling was carried out in a 25- μ l reaction that included 6 μ l annealed overgo (see Table 1), 20 uCi 32 P-TTP (3000 Ci/mmol), 1 \times oligonucleotide labeling buffer (OLB; Feinberg and Vogelstein 1983) and 2 units Klenow; the reaction was incubated at 37°C for 10 min. Hybridization conditions for the majority of probes was at 65°C as described

(Reid et al. 1997). Southern hybridization and washings for overgos were done at 60°C as described (Church and Gilbert 1984) with one 30-min wash in each of solutions A, then B, followed by a rinse in 0.5 \times SSC, 0.1% SDS for 1 min. Following secondary screening, PAC DNA was isolated from positive clones by an alkaline lysis protocol, followed by phenol-chloroform extraction and isopropanol precipitation as recommended by Genome Systems. Tertiary screening was carried out by Southern analysis with DNA digested with *Eco*RI and *Not*I (New England Biolabs), hybridized with individual probes. PAC clone inserts were sized (in parentheses below clone name) by digesting DNA with *Not*I and separating in 1.0% agarose 0.5 \times TBE CHEF gels (BioRad) for 22 h at an 8-s switch time. The uppermost horizontal line represents the contiguous genomic map. The positions of STSs and genes are shown immediately above their location in this map. Dashed vertical lines intersect with PAC clones that are positive (closed circle) for a given STS or gene. Boxed circles indicate the position of an end probe or STS. Names of clones comprising a minimal tiling path and mapped by FISH are enclosed in boxes. The orientation of the contig with respect to the centromere (cen) and telomere (tel) is indicated.

References

- Caspari T, Cleary MA, Baker CC, Guan XJ, Tilghman SM (1998) Multiple mechanisms regulate imprinting of the mouse distal chromosome 7 gene cluster. *Mol Cell Biol* 18, 3466–3474
- Church GM, Gilbert W (1984) Genomic sequencing. *Proc Natl Acad Sci USA* 81, 1991–1995
- Cooper PR, Smilnich NJ, Day CD, Nowak NJ, Reid LH, et al. (1998) Divergently transcribed overlapping genes expressed in liver and kidney and located in the 11p15.5 imprinted domain. *Genomics* 49, 38–51
- Cridder-Miller SJ, Reid LH, Higgins MJ, Nowak NJ, Shows TB, et al. (1997) Novel transcribed sequences within the BWS/WT2 region in 11p15.5: tissue-specific expression correlates with cancer type. *Genomics* 46, 355–363
- Feinberg AP, Vogelstein B (1983) A technique for radiolabeling DNA restriction and endonuclease fragments to high specific activity. *Anal Biochem* 132, 6–13
- Gould TD, Pfeifer K (1998) Imprinting of mouse *Kvlqt1* is developmentally regulated. *Hum Mol Genet* 7, 483–487
- Green ED, Green P (1991) Sequence-tagged site (STS) content mapping of human chromosomes: theoretical considerations and early experiences. *PCR Methods Appl* 1, 77–90
- Hu RJ, Lee MP, Johnson LA, Feinberg AP (1996) A novel human homologue of yeast nucleosome assembly protein, 65 kb centromeric to the *p57KIP2* gene, is biallelically expressed in fetal and adult tissues. *Hum Mol Genet* 5, 1743–1748
- Ioannou PA, Amemiya CT, Ganes J, Kroisel PM, Shizuya H, et al. (1994) A new bacteriophage P1-derived vector for the propagation of large human DNA fragments. *Nat Genet* 6, 84–89
- Kleyn PW, Fan W, Kovats SG, Lee JJ, Pulido JC, et al. (1996) Identifi-

- cation and characterization of the mouse obesity gene *tubby*—a member of a novel gene family. *Cell* 85, 281–290
- Lee MP, Hu RJ, Johnson LA, Feinberg AP (1997) Human *KVLQT1* gene shows tissue-specific imprinting and encompasses Beckwith-Wiedemann syndrome chromosomal rearrangements. *Nat Genet* 15, 181–185
- Mcpherson JD (1997) Sequence ready—or not. *Genome Res* 7, 1111–1113
- Paulsen M, Davies KR, Bowden LM, Villar AJ, Frank O, et al. (1998) Syntenic organization of the mouse distal chromosome 7 imprinting cluster and the Beckwith-Wiedemann syndrome region in chromosome 11p15.5. *Hum Mol Genet* 7, 1149–1159
- Reid LH, Davies C, Cooper PR, Crider-Miller SJ, Sait SN, et al. (1997) A 1-Mb physical map and PAC contig of the imprinted domain in 11p15.5 that contains *TAPA1* and the *BWSCR1/WT2* region. *Genomics* 43, 366–375
- Yuan L, Qian N, Tycko B (1996) An extended region of biallelic gene expression and rodent-human synteny downstream of the imprinted *H19* gene on chromosome 11p15.5. *Hum Mol Genet* 5, 1931–1937

Appendix 9

Thomas B. Shows, Ph.D.
Identifying and Isolating Breast Cancer-Associated
Genes on Chromosome 11

Presented at: Department of Defense, U.S. Army Breast Cancer Meeting, "An Era of Hope", October 30–November 3, Washington, D.C., 1997.

IDENTIFYING AND ISOLATING BREAST CANCER-ASSOCIATED GENES ON CHROMOSOME 11

Thomas B. Shows, Michael J. Higgins and Norma J. Nowak

Department of Human Genetics, Roswell Park Cancer Institute
Elm & Carlton Streets, Buffalo, NY 14263

The molecular basis for the development of cancer is generally considered to involve a cascade of genetic alterations, such as the activation of cellular oncogenes or the inactivation of tumor suppressor genes. Breast cancer presents as a heterogeneous disorder, the severity of which is thought to be a result of an accumulation of these types of mutations at multiple sites controlling growth and proliferation. For example, the oncogenes, *c-myc*, *c-erbB*, and *HER-2/neu* and the tumor suppressor genes *p53* and *RB1* have been implicated in the development and the progression of the breast cancer phenotype. By comparison to colon and brain cancer, a subset of these alterations may prove to occur in breast cancer in a disease stage defined manner with specific alterations occurring early and others occurring as the disease progresses. Breast cancer displays differences in age of onset patterns, disease progression and histologies of the various categories of breast tumors reflecting considerable heterogeneity.

Two genes have already been identified (*BRCA1* and *BRCA2*) and shown to account for the 10-15% of the familial form of breast cancer. Loss of heterozygosity (LOH), a hallmark indicator for tumor suppressor genes was observed in the regions encoding these two genes in both the familial and sporadic breast tumors suggestive that these regions harbored tumor suppressor genes. This loss of genetic material may be as large as loss of an entire chromosome with reduplication of the remaining chromosome carrying the mutated tumor suppressor gene or the loss may be limited to a small region around the tumor suppressor locus. LOH in breast cancer at several other loci indicated that other tumor suppressor genes participate in the progression of this disease perhaps by a mechanism analogous to LOH at

Keywords: Breast cancer, metastasis, chromosome 11, gene cloning, prognostic markers

This work was supported by the U.S. Army Medical Research and Materiel Command under DAMD17-94-J-4417.

Appendix 10

Thomas B. Shows, Ph.D.
Identifying and Isolating Breast Cancer-Associated
Genes on Chromosome 11

Presented at: Human Genome Meeting (HGM '97), March 6-8, Toronto, Ontario, Canada, 1997.

A 1 mb transcription map of the imprinted BWSCR1/tumor suppressor region in 11p15.5. MJ Higgins¹, LH Reid², PR Cooper¹, BE Weissman², EJ Stanbridge³, SNJ Sait¹, NJ Nowak¹, PJ deJong¹, JM Gabriel⁴, RD Nicholls⁴, C Davies⁵, GA Evans⁵, K. Gross¹, J. Rommens⁶, J. Pelletier⁷, J. Landers⁸, B. Zabel⁹ and TB Shows¹. Roswell Park Cancer Institute, Buffalo NY¹, University of North Carolina, Chapel Hill², NC, University of California, Irvine³, CA, Case Western Reserve University, Cleveland, OH⁴, University of Texas, Southwestern Medical Center, Dallas⁵, TX, Hospital for Sick Children, Toronto, ON⁶, McGill University, Montreal, PQ⁷, Center for Cancer Research, MIT, Cambridge⁸, MA, University of Mainz⁹, Mainz, Germany.

Loss of heterozygosity (LOH) analysis in adult and childhood tumors suggest the presence of one or more tumor suppressor genes in 11p15.5. Chromosome fragment-mediated gene transfer studies indicate that the potential tumor suppressor lies between D11S601 and IGF2. A cluster of chromosome rearrangements (BWSCR1) in patients with Beckwith-Wiedemann syndrome (BWS), an overgrowth/tumor predisposition condition, disrupt the identical interval. This same region contains four genes (IGF2, H19, p57-KIP2, and ASCL2) known to be regulated by genomic imprinting in human and/or mouse.

In order to identify genes potentially involved in tumor development and/or BWS, and to study the 11p15.5 imprinted domain, we have constructed a contig through this region consisting of P1, PAC, and BAC clones. Established libraries were screened using STS-based PCR as well as hybridization with Alu-PCR probes and whole YAC inserts. The contig extends approximately 1000 kb from D11S601 to H19 and, at present, contains one gap (estimated to be <100 kb) just centromeric to IGF2. FISH analysis confirmed the relative order of clones and mapped three Beckwith-Wiedemann syndrome (BWS) breakpoints and a rhabdoid tumor breakpoint in the contig.

The contig has been used to precisely map an additional four known 11p15.5 genes (p57KIP2, KVLQT1, TAPA1, ASCL2) and to identify 10 new transcripts by direct cDNA selection and sequencing of the large insert bacterial clones. Together, these results describe a transcript map containing 18 loci distributed over approximately 1 mb. Since many of these genes are near or interspersed among known imprinted loci, cDNAs are being tested for monoallelic versus biallelic expression using a newly developed somatic cell hybrid "imprinting assay". Two of these novel genes overlap in a divergent orientation, and are expressed predominantly in fetal and adult liver and kidney by Northern blot analysis. The developmental expression patterns of these two loci are being studied in human fetal kidney and mouse embryos by *in situ* hybridization. Mutation analysis is being carried out to assess these loci as tumor suppressor genes in Wilms' tumor. This detailed physical and gene map should facilitate the study of this interesting and complex genomic region.

Appendix 11

Thomas B. Shows, Ph.D.
Identifying and Isolating Breast Cancer-Associated
Genes on Chromosome 11

Presented at: American Society for Human Genetics Meeting (ASHG), October 28-
November 2, Baltimore, MD, 1997.

Amer. J. Hum. Genet. 61: A78 (Abstract #428)

428

Characterization of transcripts expressed in kidney and derived from 11p15.5, a region linked to Beckwith-Wiedemann-syndrome and Wilms' tumor formation. D. Prawitt¹, B. Gaertner¹, M. Higgins³, T.B. Shows³, J. Landers⁴, D.E. Housman⁴, J. Pelletier², A. Winterpacht¹, and B. Zabel¹. ¹Childrens Hospital, University of Mainz, Germany ²McGill Cancer Center, McGill University, Montreal, Canada ³Roswell Park Cancer Institute, Buffalo NY, USA ⁴Center for Cancer Research, MIT, Cambridge MA, USA

Beckwith-Wiedemann syndrome (BWS), a congenital overgrowth syndrome with increased risk to develop embryonal tumors, such as Wilms' tumor (WT) has been linked to the chromosomal sub-band 11p15.5. Imprinted genes (IGF2/H19) located in this region have already been implicated in a subset of BWS cases and tumorigenesis. The only mutations found up to now are in p57^{Kip2}, an imprinted negative regulator of cell proliferation. Our analysis of 150 WTs and in 20 BWS patients however, revealed no mutations. To identify other tumor suppressor - (WT2) and BWS candidate genes, we focused on a subregion of this gene-rich terminal chromosome 11p band. Sequence analysis of exon clones obtained from this genomic area revealed several matches with expressed sequence tags (ESTs) from fetal brain or liver in the databases. These ESTs were used to isolate three novel transcripts (A6, 272, D7), located close to p57^{Kip2}. The gene A6 had high homologies to a previously described Nucleosome-Assembly-Protein (NAP1) gene, and was therefore called NAP2. Intensive screening of WTs and BWS patient DNA failed to detect mutations that would allow the implication of NAP2 in tumor formation. The two other cDNAs have no significant homology on DNA/protein level to entries of the available databases, but are transcribed in (fetal) kidney. This we took as a first assumption for genes possibly involved in WT / BWS development. In situ hybridization of cDNA 272 shows a similar expression pattern as observed for WT1 and PAX8 genes, supporting the idea, that it plays an important role in kidney development. The PAC clones that contain 272 and D7 are now being sequenced. The data enable us to analyse exon/intron structures of both genes. We are currently doing an extensive mutation screening on genomic and RNA level to obtain informations concerning functional mutations and imprinting.

Appendix 12

Thomas B. Shows, Ph.D.

Identifying and Isolating Breast Cancer-Associated
Genes on Chromosome 11

Presented at: American Association for Cancer Research (AACR Annual Meeting),
March 28-April 1, New Orleans, LA, 1998.

Proc. AACR 39: 133 (Abstract #910).

Identifying Breast Cancer-Associated Genes on Human Chromosome 11. Shows, T.B., Higgins, M.J. and Nowak, N.J. Department of Human Genetics, Roswell Park Cancer Institute, Buffalo, NY 14263.

Loss of heterozygosity (LOH) in a region of the genome is considered to be a hallmark for the presence of a tumor suppressor gene. Human chromosome 11 at band p15.5 has been shown to frequently lose genetic material in adult tumors of the breast, particularly those exhibiting the metastatic phenotype. This region has also been associated with embryonal pediatric tumors such as Wilms' tumor of the kidney and rhabdomyosarcoma. We have cloned, in overlapping DNA fragments, this region of 11p15.5 and performed LOH studies to narrow the region to about 300-400 kb. A gene hunt has identified a number of new genes in this region which may be responsible for the association of poor survival. These genes are being analyzed and the future will emphasize mutation analysis in breast cancer patients to conclusively identify the gene(s) involved. These studies should provide insights into the genetic mechanisms involved in breast cancer development, and diagnostic tools for identifying patients at risk for metastatic disease.

Thomas B. Shows, Ph.D.
Identifying and Isolating Breast Cancer-Associated
Genes on Chromosome 11

Presented at Gordon Research Conference on Epigenetics,
Plymouth, NH, August 10-15, 1997.

Loss of imprinting at IGF2 and a novel CpG-island in a BWS fetus with an inversion chromosome 11. Michael J. Higgins¹, Paul R. Cooper¹, Norma J. Nowak¹, Laura H. Reid², Shyra J. Crider-Miller³, Chris Davies³, Jamie M. Gabriel⁴, Robert D. Nicholls⁴, Pieter deJong¹, Glen Evans³, Bernard E. Weissmann², and Thomas B. Shows¹

¹Roswell Park Cancer Institute, Buffalo, NY; ²Lineberger Comprehensive Cancer Center, University of North Carolina, Chapel Hill, NC; ³McDermott Center for Human Growth & Development, Southwestern Medical Center, Dallas, TX; ⁴Case Western Reserve University, Cleveland, OH.

Several genes regulated by genomic imprinting have been identified in human chromosome band 11p15.5 including IGF2, H19, p57^{KIP2}, and KvLQT1. Changes in the expression of one or more of these loci and/or of additional unidentified imprinted genes are believed to contribute to the phenotype of the overgrowth condition Beckwith-Weidemann syndrome (BWS) and sporadic Wilms tumor. We are studying this interesting and complex region of the genome on multiple fronts: (1) a complete bacterial clone contig and physical map of the known imprinted domain has been constructed; (2) three chromosome rearrangements associated with BWS have been precisely positioned within this map; (3) novel transcripts are being identified by cDNA selection, exon-trapping, and large-scale genomic sequencing; (4) we have begun examining BWS patients and Wilms tumors for alterations in gene expression and epigenetic modification.

A CpG-island was identified in a large intron of the KvLQT1 gene that exhibits differential allelic methylation when assessed by methylation-sensitive restriction endonucleases. Pulsed-field gel mapping of BWS rearrangement breakpoints and methylation analysis of Wilms tumors showing loss of heterozygosity at 11p15 indicates that at least three rare-cutter restriction sites within the CpG-island are monoallelically methylated on the maternal chromosome. The island also contains a direct repeat structure reminiscent of those found at most other imprinted loci. We have recently isolated mouse PAC clones that should encompass the murine locus on distal chromosome 7 and are attempting to identify the corresponding mouse sequence to test in interspecific crosses. Although this CpG-island may be associated with KvLQT1, sequence analysis has identified an expressed sequence tag (EST) encoded on the opposite strand within 1 kb of the island. We are currently attempting to obtain the full length cDNA and to test this transcript for imprinted expression using a novel somatic cell hybrid imprinting assay as well as more conventional methods.

Although differential methylation at this CpG-island was observed in DNA samples from eight normal individuals (3 lymphoblast, 3 peripheral blood lymphocyte, 1 foreskin fibroblast, one fetal lung fibroblast), no methylated allele was detected in fibroblasts derived from a fetus with suspected BWS and an inversion in the short arm of chromosome 11 [inv(11)(p13;p15.5)]. Furthermore, using expressed polymorphisms, we have shown that these cells express IGF2 biallelically while maintaining monoallelic expression at IPW(chromosome 15). Thus, this chromosome rearrangement may represent an "imprinting mutation" affecting more than one locus at considerable distances (100 kb for the CpG-island and 400 kb for IGF2). Expression and methylation analyses are underway at other known 11p15.5 imprinted loci in these cells to determine if this relaxation of imprinting is even more widespread.

Thomas B. Shows, Ph.D.
Identifying and Isolating Breast Cancer-Associated
Genes on Chromosome 11

Presented at: American Society for Human Genetics Meeting (ASHG), October 28-
November 2, Baltimore, MD, 1977.

Amer. J. Hum. Genet. 61: A78 (Abstract #429).

429

Loss of replicative asynchrony at the imprinted region on 11p15.5 in embryonal rhabdomyosarcoma EA Preisinger¹, MJ Higgins², SD Morgenbesser¹, F Baas³, S Dasgupta¹, JE Landers¹, TB Shows², and DE Housman¹. ¹MIT Center for Cancer Research, Massachusetts Institute of Technology, Cambridge, MA; ²Department of Human Genetics, Roswell Park Cancer Institute, Buffalo, NY, and ³Neurozintuigen Laboratory, AMC, Amsterdam, The Netherlands

Chromosome subband 11p15.5 is implicated in several human disease states including the Beckwith-Wiedemann syndrome, which is a developmental overgrowth syndrome of childhood, and in pediatric malignancies associated with the BWS including Wilms' tumor and embryonal rhabdomyosarcoma. A 1000kb region of 11p15.5 extending from CARS to H19 is the site of both a cluster of breakpoints in BWS chromosome rearrangements and of LOH in embryonal rhabdomyosarcoma. This region is known to contain a cluster of genes shown to be imprinted and monoallelically expressed, including H19, IGF-2, ASCL-2, KVLQT1 and p57. Early replication of a particular locus within S phase has been shown to correlate generally with expression at that locus, and in imprinted genes, asynchronous replication is associated with monoallelic expression. We have used replication timing assays by FISH to show that the entire 1000kb region containing imprinted genes on 11p15.5 is replicated asynchronously in lymphocytes, and that a lesser degree of replicative asynchrony is observed several megabases away from the imprinted gene cluster. In several embryonal rhabdomyosarcoma cell lines likely to have lost heterozygosity at these loci, replicative asynchrony is lost. We are currently investigating the interrelationships between loss of normal replicative asynchrony, control of gene expression for imprinted genes within the region, and the etiology of rhabdomyosarcoma and the Beckwith-Wiedemann syndrome.

Appendix 15

Thomas B. Shows, Ph.D.
Identifying and Isolating Breast Cancer-Associated
Genes on Chromosome 11

Presented at: American Society for Human Genetics Meeting (ASHG), October 28-
November 2, Denver, CO, 1998.

Amer. J. Hum. Genet. 63: A328 (Abstract #1898).

1898

A maternally methylated CpG-island in KvLQT1 is associated with a paternally expressed transcript and loss of imprinting in Beckwith-Wiedemann syndrome. M. J. Higgins¹, N. J. Smilnich¹, C. D. Day¹, A. V. Smallwood², A. Lossie³, P. R. Cooper¹, G. M. Caldwell¹, D. J. Driscoll³, E. R. Maher², T. B. Shows¹. 1) Roswell Park Cancer Institute, Buffalo, NY; 2) U. of Birmingham, Birmingham, United Kingdom; 3) U. Florida College of Medicine.

Changes in the expression of 11p15.5 genes can result in Beckwith-Wiedemann syndrome (BWS) and tumors. We have identified a CpG-island exhibiting maternal specific methylation in an intron of the KvLQT1 gene. Sequence identity with ESTs and RT-PCR indicated the presence of a transcript including the CpG-island and oriented in the opposite direction (i.e. antisense) with respect to KvLQT1. This transcript is at least 3.2 kb long and shows no evidence of introns or a significant ORF. SSCP and RFLP failed to detect polymorphisms over the transcribed region suggesting a high degree of conservation. The likely murine homologue was sequenced and exhibits 74-98% identity over 400 bp with the human transcript. SSCP analysis using F1 fetal liver cDNA from interspecific crosses suggests that the mouse transcript is expressed exclusively from the paternal allele. This transcript is analogous to the antisense RNA initiating from an intronic CpG-island in the IGF2 receptor (Igf2r) gene, the expression of which was found to be necessary for the imprinting of Igf2r itself. Although differential methylation at the human CpG-island was observed in DNA samples from 18 normal individuals, absence or reduction in the methylated allele was observed in DNA from cytogenetically normal BWS patients that show normal methylation and expression at H19. Furthermore the methylated allele was absent in fibroblasts derived from a fetus with suspected BWS, an inv(11)(p13p15.5), and loss of imprinting (LOI) at IGF2. However, normal methylation was preserved in BWS patients with H19 hypermethylation and IGF2 LOI. These findings suggest two distinct imprinting control centers in 11p15.5. These results will be presented in the context of the expression competition model of genomic imprinting and BWS as a model disorder for elucidating the mechanisms of IGF2 imprinting. Funded by CA63333.

Appendix 16

Thomas B. Shows, Ph.D.

Identifying and Isolating Breast Cancer-Associated Genes on Chromosome 11

The Great Lakes Mammalian Development Meeting,
Presented at: 18th Annual Samuel Lunenfeld Research Institute, Mt. Sinai Hospital,
Toronto, Ontario, Canada, 1998.

Towards the molecular dissection of the imprinted domains in human chromosome band 11p15.5 and mouse distal chromosome 7. Paul R. Cooper¹, Laura H. Reid², Shyra J. Crider-Miller², Jerry Pelletier¹, R. Scott Pearsall¹, Bernhard U. Zabel⁴, Bernard E. Weissmann², Thomas B. Shows¹, and Michael J. Higgins¹, ¹Roswell Park Cancer Institute, Buffalo, NY; ²Lineberger Comprehensive Cancer Center, Chapel Hill, NC; ³McGill Cancer Centre, Montreal, PQ; ⁴University of Mainz, Germany

Several genes regulated by genomic imprinting have been identified in human chromosome band 11p15 including *IGF2*, *H19*, *p57^{KIP2}*, *IPL*, *ASCL2* and *KvLQT1*. Changes in the expression of one or more of these loci and/or additional unidentified imprinted genes, brought about by disruption of imprinting, are believed to contribute to the overgrowth condition Beckwith-Wiedemann syndrome (BWS) and sporadic Wilms tumor. To facilitate the study of this interesting and complex region, we constructed a 1 mb PAC contig of this region, constituent clones of which have been used for cDNA selection and as templates for large-scale genomic sequencing. This work resulted in a comprehensive transcript or gene map containing nine previously identified genes and more than 10 EST clusters or potential genes.

Two of the genes identified by these ESTs map between *IPL* and *p57^{KIP2}* and encode transcripts of 1-1.1 kb with predominant expression in fetal and adult liver and kidney. Full length cDNA sequences predict ORFs encoding putative proteins of 253 and 424 amino acids, with the amino acid sequence of the larger transcript showing homology to integral membrane organic cation transporters; hence we designate this gene as *ORCTL2* (Organic Cation Transporter Like 2). *ORCTL2* exhibits "leaky" imprinting in both human fetal kidney and liver while *Orctl2* (the mouse orthologue) demonstrated nearly exclusive expression from the maternal allele in fetal liver from interspecific F1 mice. The predicted protein of the smaller gene showed no significant similarity in the database. Northern and RACE analysis suggests that this gene may have multiple transcription start sites. Preliminary results using single nucleotide primer extension (SNuPE) suggest that at least one isoform exhibits allelic expression bias or partial imprinting although its direction has yet to be determined. The genomic structure in humans indicates that the two 5'-exons of this transcript overlap in divergent orientation with the first two exons of *ORCTL2*, suggesting a possible role for antisense regulation of one gene by the other. We therefore provisionally call this second transcript *ORCTL2S* (*ORCTL2*-antisense). The expression pattern of these genes and the imprinted expression of *ORCTL2* are suggestive of their possible role in the development of Wilms' tumor (WT) and hepatoblastoma. Although SSCP analysis of 62 WT samples and 10 BWS patients did not result in the identification of any mutations in *ORCTL2* or *ORCTL2S*, it will be important to examine their expression pattern in tumors and BWS patients since epigenetic alteration at these loci may play a role in the etiology of these diseases.

A PAC contig has also been constructed encompassing the syntenic domain on mouse chromosome 7. For each case tested, the order and transcriptional orientation appears to be maintained between mouse and human suggesting a high degree of conservation between species, perhaps reflecting a requirement for regional regulation of imprinting. This contig will provide excellent reagents for the development of targeted deletions and for comparative sequencing, both of which should contribute to our understanding of genomic imprinting.

Thomas B. Shows, Ph.D.
Identifying and Isolating Breast Cancer-Associated
Genes on Chromosome 11

Presented at: American Society for Human Genetics Meeting (ASHG), October 19-23,
San Francisco, CA, 1999

Amer. J. Hum. Genet. 65: A104 (Abstract #549).

549

A putative imprinting control region in 11p15.5 and its loss of methylation in Beckwith-Wiedemann syndrome. C.D. Day¹, N.J. Smilnich¹, G.V. Fitzpatrick¹, N. Diaz-Meyer¹, R.L. Titus¹, G.M. Caldwell¹, A.C. Lossie², A.C. Smallwood³, J.A. Joyce³, P.N. Schofield³, W. Reik³, R.D. Nicholls⁴, R. Weksberg⁵, D.J. Driscoll², E.R. Meyer¹, P.R. Cooper¹, T.B. Shows¹, M.J. Higgins¹. 1) Roswell Park Cancer Institute, Buffalo, NY; 2) University of Florida College of Medicine; 3) Universities of Birmingham and Cambridge, and Babraham Institute, UK; 4) Case Western Reserve University School of Medicine, Cleveland, OH; 5) Hospital for Sick Children, Toronto, ON, Canada.

Imprinting control elements are proposed to exist within the *KvLQT1* locus since multiple chromosome rearrangements associated with Beckwith-Wiedemann syndrome (BWS) disrupt this gene. We have identified an evolutionarily conserved CpG island (*KvDMR1*) in an intron of the *KvLQT1* gene which is methylated in the ovary, unmethylated in sperm, and exhibits differential methylation in all human and mouse somatic tissues tested. Strand-specific RT-PCR analysis of the human and syntenic mouse loci demonstrated the presence of a *KvDMR1*-associated RNA transcribed exclusively from the paternal allele and in the opposite orientation with respect to the maternally expressed *KvLQT1* gene. Loss of imprinting at *IGF2*, generally through an *H19*-independent mechanism, is associated with a large percentage of patients with BWS. Among twelve cases of BWS with normal *H19* methylation, five showed demethylation of *KvDMR1* in fibroblast or lymphocyte DNA, while in four cases of BWS with *H19* hypermethylation, methylation at *KvDMR1* was normal. Thus, inactivation of *H19* and hypomethylation at *KvDMR1* represent distinct epigenetic anomalies associated with biallelic expression of *IGF2*. We propose that *KvDMR1* and/or its associated antisense RNA (*KvLQT1-AS*) represents an additional imprinting control element or center in the human 11p15.5 and mouse distal 7 imprinted domains. To test this hypothesis we are carrying out targeted mutagenesis of *KvDMR1* in the mouse and assessing the expression of 11p15.5 imprinted genes in BWS patients with and without loss of methylation at *KvDMR1*. Supported by CA63333.